Vegetation dynamics during the Late Triassic (Carnian-Norian):

Response to climate and environmental changes inferred from palynology

Viktória Baranyi

Dissertation for the degree of Philosophiae Doctor (Ph. D)

Department of Geosciences

Faculty of Mathematics and Natural Sciences

University of Oslo

Norway

2018

Series of dissertations submitted to the
Faculty of Mathematics and Natural Sciences, University of Oslo
No. 1994

ISSN 1501-7710

Cover: Hanne Baadsgaard Utigard.
Print production: Reprosentralen, University of Oslo.

“Research is to see what everybody else has seen and to think what nobody else has thought”

by Albert Szent-Györgyi

Table of Contents

Preface and scope of the thesis ii

List of publications vii

Oral presentations vii

Poster presentations viii

Peer reviewed articles and poster abstracts as co-author viii

Acknowledgements ix

1. General introduction 1

1.1 Palaeoenvironmental and palaeoclimatic implications of palynology and palynofacies 1

1.2. Late Triassic paleogeography and palaeoclimate 5

1.2.1. Carnian Pluvial Episode 8

1.2.2. Mid-Norian Climate Shift in SW equatorial Pangea 11

1.3 Late Triassic (Carnian-Norian) palynostratigraphy in Europe and North America 16

2. Study areas 18

2.1 Geological setting of the Mercia Mudstone Group ("British Keuper"), SW England 18

2.2 Geological setting of the Transdanubian Range (western Hungary) 21

2.3 Chinle geological setting 24

3. Methodology 27

4. Summary of the research articles 34

4.1. Paper 1 34

4.2. Paper 2 37

4.3. Paper 3 40

4.4. Paper 4 43

4.5 CPCP core (Colorado Plateau Drilling Project, core PF 1) 45

Synthesis and concluding remarks 47

Potential for future work and limitations 51

References 55

Systematic palynology 71

Photoplates 89

Scientific papers 1-4 .....

Supplements .....

Preface and scope of the thesis

This thesis has been submitted to the Department of Geosciences University of Oslo (UiO) in accordance with requirements for dissertation for the degree of Philosophiae Doctor. The outcomes of this study are presented here in this thesis, comprising four scientific papers preceded by an introduction, summary of the research papers, synthesis and a systematic palynology chapter with 14 photoplates.

The purpose of the research project was to reconstruct the impact of environmental changes on terrestrial ecosystems during the Late Triassic (Carnian-Norian) (Fig. 1). The project focuses on climate variations, palaeoenvironmental changes and biostratigraphy inferred form palynology and stable carbon isotope analysis during two fascinating periods of the Late Triassic: the Carnian Pluvial Episode and the Mid Norian Climate Shift.

Globally, terrestrial floras diversified during the Triassic following the end Permian mass-extinction, with low-diversity somewhat uniform floras in the Early Triassic developing into more complex vegetation types towards the Late Triassic (Willis & McElwain 2002; Kustatscher et al. 2018). Many plant groups such as the Gnetales, Bennettitales and several modern conifer families like the Cupressaceae (Mao et al. 2012) diversified during the Late Triassic, and later became important elements of the Jurassic and Cretaceous floras (Kustatscher et al. 2018). Moreover, the Triassic marks the time when the first dinosaurs evolved (Benton et al. 2014). The global palaeogeography was marked by the maximum aggregation of the continents forming the supercontinent Pangea (see chapter 1.2.) and the global climate was quite different from that of the present-day situation with broad arid belts and a monsoon regime (see chapter 1.2.).

The Late Triassic period is marked by severe environmental perturbations, floral and faunal turnovers that culminated in the End-Triassic extinction, which represents one of the "Big Five" extinction events during the Phanerozoic (Raup & Sepkoski 1982). The End-Triassic extinction event has been extensively studied in the last decades (e.g., Fowell et al. 1994; Benton 1995; Hallam & Wignall 1999; Hallam 2002; Olsen et al. 2002; Kiessling et al. 2007; Kuerschner et al. 2007; Pálfy et al. 2007; Mander et al. 2008; Götz et al. 2009; McElwain et al. 2009; van de Schootbrugge et al. 2009; Mander et al. 2010; Bonis & Kürschner 2012; Mander et al. 2013). Yet our knowledge on the biotic events preceding the End-Triassic mass

extinction is rather limited. For instance, in the terrestrial realm in NW and Central Europe enhanced extinctions occurred during the entire Late Triassic with more than 60% loss in diversity during the late Carnian and Norian before the End-Triassic diversity decline of about 20% (Kürschner & Herngreen 2010). The Carnian has recently received more attention as it records an episode in the late Julian with increased precipitation. This interval, known as Carnian Pluvial Episode (further referred to as CPE) represents so far the most pronounced climate shift within the Triassic (see chapter 1.2.1). Since the onset of the CPE studies (Simms & Ruffell 1989, 1990; Visscher et al. 1994) the interest for Carnian palynological assemblages has steadily increased as the pollen and spore record can be an excellent indicator of past climate changes. On the contrary, Norian palynological assemblages are still lesser known than Carnian or Rhaetian assemblages (Cirilli 2010; Kürschner & Herngreen 2010). In Europe, the main limitation is due to the dearth of complete and well-dated sections and the limited number of suitable section for palynology as the majority of the successions are red beds with evaporites in the Germanic Realm or dolomite formation in the Alpine Realm (e.g., Berra et al. 2010; Preto et al. 2010; Haas et al. 2012).

Two locations were selected for the study of the CPE. **Paper 1** describes the palynological assemblages from the Carnian terrestrial series of the Mercia Mudstone Group in the Wessex Basin, SW England. The British Carnian successions were among the first locations where evidence had been found for a significant environmental change during the Carnian (Simms & Ruffell, 1989, 1990). The British Carnian successions were deposited in a predominantly lacustrine setting in a sabkha environment (Porter & Gallois 2008). A clear humidity signal related to the CPE in the late Julian is not found in the palynological record. Despite the assumed more humid conditions seasonally, the prevailing "background" climate in the studied area was perhaps still too dry to support the proliferation of a "permanent" hygrophyte vegetation. Secondly, the overrepresentation of the predominantly xerophyte regional pollen might have masked the humid signal. This taphonomical bias is common in modern lake settings where the proportion of regional pollen increases with increasing size of the sampling site and catchment area. Palynostratigraphy integrated with bulk organic carbon isotope chemostratigraphy enabled the correlation to other Carnian successions (**Paper 1**).

The second location for the study of the CPE was a marine, mixed carbonate-clastic Carnian succession of the Veszprém Marl Formation, in the Transdanubian Range, western Hungary. The palaeogeographical setting of this area shows close affinity to the Southern Alps and the

Dolomites as they all formed the western Tethys margin during the Late Triassic. Like in the well-studied Alpine successions, an abrupt change from carbonate-dominated sedimentation to calcareous and clayey marls is recorded in the late Julian. **Paper 2** describes the results of the palynological analysis that was extended with a comparison to clay mineralogy (Rostási et al. 2011) and weathering indices (α^{Al}_{K}, α^{Al}_{Na}, α^{Al}_{Ba}) of the sedimentary rocks from the unpublished data of Rostási (2011) to gain a better view on potential climate variations affecting the vegetation and the continental weathering. The sedimentology and palynological record indicates the presence of multiple shifts between wetter and drier conditions during the CPE in agreement with other studies from the Alpine Realm (e.g., Roghi et al. 2010). Palynostratigraphy enabled the correlation to the siliciclastic pulses known from the Dolomites, Julian Alps and Northern Calcareous Alps, which are associated with the relatively wetter climate. However, the clay minerals and weathering indices suggest that enhanced continental weathering related to higher precipitation rates is only present in the early Julian 2, in the early stages of the CPE.

Unlike the CPE, the Mid Norian Climate Shift (Nordt et al. 2015) recorded in the Chinle Formation in western equatorial Pangea marks a shift from seasonally wet conditions to more pronounced seasonality and a long-term, gradual transition to drier climate. So far, the Mid Norian Climate Shift is thought to be a more regional climate change, which affected primarily the terrestrial ecosystems in western equatorial Pangea and in the eastern part of North America in the Newark Basin (Olsen & Kent 2000).

There is a notable link between the CPE and the Mid Norian Climate Shift. Previously, the Norian series of Chinle Formation in the SW USA, which record the climate shift, were considered to be Carnian-Norian (Litwin et al. 1991; Heckert et al. 2007). The lower part of the formation contains hygrophyte palynoflora similar to that of the CPE successions in the Alpine and Germanic Realms from Europe (Roghi et al. 2010). The hygrophyte palynoflora together with paleosol characteristics led to the conclusion that the lower part of the Chinle might record the CPE, and the shift to drier climate might be equivalent to the return to drier climatic condition in the late Tuvalian and Norian after the CPE (Prochnow et al. 2006). Since then, radiometric dating and magnetostratigraphy have suggested a much younger age for the Chinle Formation implying that the recorded shift to drier climate is not related to the termination of the CPE (Riggs et al. 2003; Muttoni et al. 2004; Irmis et al. 2011; Olsen et al. 2011; Ramezani et al. 2011, 2014).

In the mid-Norian around 215 Ma the western part of Pangea experienced a series of environmental perturbations besides the climate change, such as volcanism (Atchley et al. 2013; Nordt et al., 2015), pCO_2 variations (Cleveland et al. 2008a, b; Atchley et al., 2013; Nordt et al. 2015; Schaller et al. 2015; Whiteside et al. 2015) and presumably the effects of an impact event (Manicouagan impact, Ramezani et al. 2005) are recorded during the Norian. Previous palaeontology and palynology suggested a significant faunal turnover roughly simultaneously with a floral turnover around 215 Ma in the middle of the Chinle Formation (SW USA) (Parker & Martz 2011; Reichgelt et al. 2013). The palynological assemblages of the Chinle Formation were analysed from the Petrified Forest National Park (PEFO), Arizona to reconstruct the plant communities and vegetation changes through the Norian (**Paper 3**). Bulk carbon isotope ratios were applied to reveal variations in the composition of the sedimentary organic matter.

The floral changes are associated with a long-term increase in the abundance of xerophyte pollen types and successive peaks of certain palynomorphs e.g., *Klausipollenites gouldii*, aberrant pollen grains of *K. gouldii*, the enigmatic *Froelichsporites traversei* and the *Patinasporites* group. The gradual climate change was interrupted by at least two relatively more humid episodes during the Norian. The palaeoenvironmental changes in the middle Norian led to the reorganisation of the riparian forests in the lowland areas opening niches for new plant groups such as the Cupressaceae and Cupressaceae-related conifers. The age range of the floral turnover at the PEFO is very close to the date of the Manicouagan impact event at 215 Ma, but the existing data are unable to demonstrate direct causality. The climate deteriorated during the Norian, it became drier and the seasonality increased resulting in a younger more pronounced floral turnover *ca.* 4 Ma later recorded by Whiteside et al. (2015) and Lindström et al. (2016).

Froelichsporites traversei is one of the lesser-known elements of Norian palynofloras known almost exclusively from the Norian sediments of the USA (Litwin et al. 1991; Litwin & Ash 1993). Its most striking morphological features are the occurrence as permanent tetrads, one well-developed distal pore (ulcus) on each grain and the annulus-like exine thickening around the pores (Litwin et al. 1993). The abundance of the species arose during the Norian environmental perturbations, but its botanical affinity has been uncertain. The conducted wall-ultrastructure analysis with transmission electron microscopy (TEM) described in **Paper 4** aimed at revealing its botanical affinity and contributing to its ecological significance. The wall ultrastructure of *F. traversei* suggests that it represents gymnosperm pollen, but the

botanical affinity could not be determined more precisely, as there is no other known gymnosperm pollen type with the exact same ultrastructure pattern. The occurrence as permanent tetrads may be related to polyembryony or polyploidy, and they probably provided an adaptive advantage to the parent plant during the Norian environmental crisis in North America.

Environmental changes and climate change in particular, represent major environmental factors shaping diversity and vegetation patterns. The presented research has implications for documenting the interaction between past climate changes and vegetation. It contributes to our understanding how terrestrial ecosystems respond to environmental stress factors in the past and what can be expected in the future. The interaction between climate and the biosphere has gained vast public interest as global climate change in the 20th and 21st century has already had observable effects on the environment and is present in the day-to-day life of humanity.

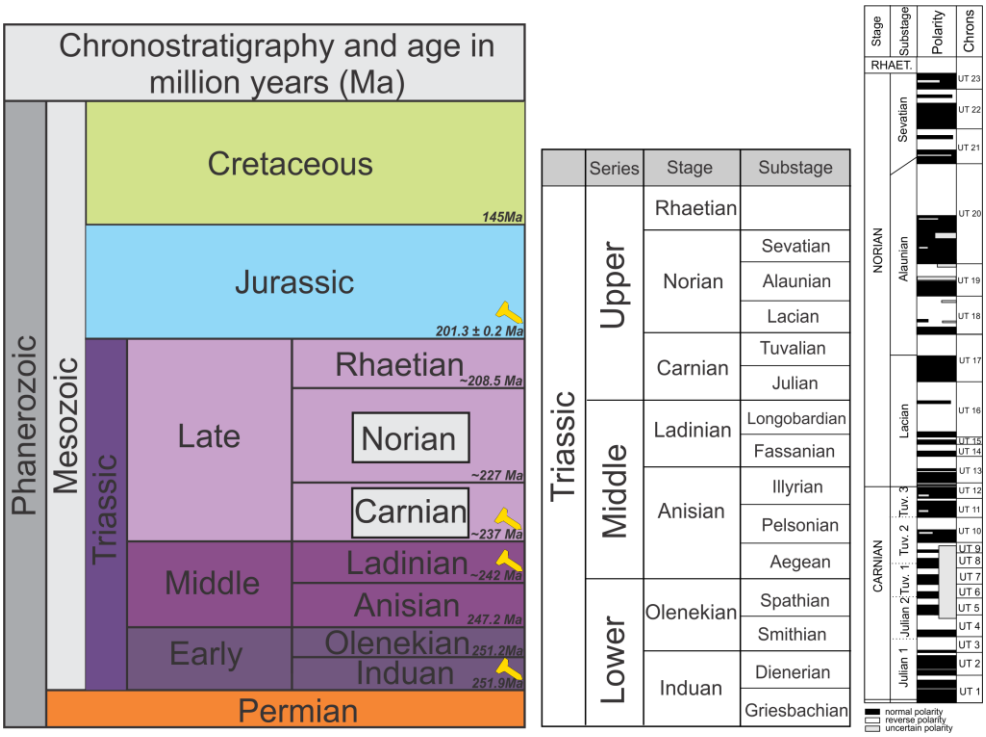

Figure 1 Chronostratigraphic chart of the Mesozoic (International Chronostratigraphic Chart 2016), Triassic chronostratigraphic scheme from Lucas (2018) and summary of the magnetostratigraphic timescale for the Carnian-Norian from (Hounslow & Muttoni 2010). Tuv. = Tuvalian.

List of publications

The project resulted in four scientific contributions (two accepted, one submitted and one in preparation (hereafter referred to as Paper 1 to 4) presented subsequent to the introduction. In addition, several talks and poster presentations have been given at international conferences and meetings.

Paper 1: Baranyi, V., Miller, C.S., Ruffell, A., Hounslow, M.W. & Kürschner, W.M. A continental record of the Carnian Pluvial Episode (CPE) from the Mercia Mudstone Group: palynology and climatic implications. *Submitted to the Journal of the Geological Society*

Paper 2: Baranyi, V., Rostási, Á., Raucsik, B. & Kürschner, W.M. Climatic fluctuations during the Carnian Pluvial Episode (CPE) in marine successions from the Transdanubian Range (western Hungary) inferred from palynology. *In preparation, to be submitted.*

Paper 3: Baranyi, V., Reichgelt, T., Olsen, P.E., Parker, W.G. & Kürschner, W.M. 2017. Norian vegetation history and related environmental changes: New data from the Chinle Formation, Petrified Forest National Park (Arizona, SW USA). GSA Bulletin, Published Online First, https://doi.org/10.1130/B31673.1

Paper 4: Baranyi, V., Wellmann, C.H. & Kürschner, W.M. 2017. Ultrastructure and probable botanical affinity of the enigmatic sporomorph *Froelichsporites traversei* from the Norian (Late Triassic) of North America. International Journal of Plant Sciences, 179, 100–114, https://doi.org/10.1086/694762

Oral presentations

Baranyi, V., Wellmann, C.H. & Kürschner, W.M. 2015. Morphology and wall-ultrastructure of *Froelichsporites traversei*, an enigmatic sporomorph from the Late Triassic in North America. Palynology Specialist Group Meeting of The Linnean Society, 24th November 2015, London

Baranyi, V., Kürschner, W.M., Olsen, P.E., Parker, W.G. 2016. Vegetation dynamics of riparian plant communities in the Norian on the western margin of Pangea (Chinle Formation, Petrified Forest National Park, Arizona, SW USA). XIV International Palynological Congress, Salvador, Brasil, Abstract Book, 204

Baranyi, V., Reichgelt, T., Olsen, P.E., Parker, W.G. & Kürschner, W.M. 2017. Correlation and provincialism among Late Triassic (Norian) low and high latitude plant assemblages: an example from the Chinle Formation (Petrified Forest National Park, Arizona, USA). Vinterkonferansen 2017 32nd Winter Meeting of the Norwegian Geological Society, NGF Abstracts and Proceedings, 1, 12-13.

Baranyi, V., Miller, C.S., Ruffell, A. & Kürschner, W.M. 2017. Continental record of the Carnian Pluvial Episode (CPE) from the British Keuper (Mercia Mudstone Group, southwestern United Kingdom). The Golden Anniversary Meeting of the AASP – The Palynological Society, Nottingham, UK, Abstract Book, 23.

Baranyi, V. & Kürschner, W.M. 2017. Palynological characterization of the the Carnian Pluvial Episode in the British Keuper (Late Triassic). FORCE Seminar "Predictive Stratigraphy", Stavanger, Norway, Abstracts, 14

Poster presentations

Baranyi, V., Wellmann, C.H., Kürschner, W.M. 2016. Morphology and wall-ultrastructure of *Froelichsporites traversei*, an enigmatic sporomorph from the Triassic in North America. XIV International Palynological Congress, Salvador, Brasil, Abstract Book, 261.

Baranyi, V. 2017. Quantifying past climates based on vegetation: an example from the Late Triassic (237-201 Ma) Chinle Formation (SW USA). PhD Day 2017, The Faculty of Mathematics and Natural Sciences, UiO, Oslo

Baranyi, V., Raucsik, B., Kürschner, W.M. 2017. Palynological investigation of Carnian succesions from the Transdanubian Range, western Hungary. The Golden Anniversary Meeting of the AASP – The Palynological Society, Nottingham, UK, Abstract Book, 69.

Peer reviewed articles and poster abstracts as co-author

Miller, C.S., Peterse, F., da Silva, A-C., Baranyi, V., Reichart, G.J. & Kürschner, W.M. 2017. Astronomical age constraints and extinction mechanisms of the Late Triassic Carnian crisis. Scientific Reports, 7:2557, https://doi.10.1038/s41598-017-02817-7

Olsen, P.E., Geissman, J.W., Kent, D.V., Gehrels, G.E., Mundil, R., Irmis, R.B., Lepre1,C., Rasmussen, C., Giesler, D., Parker, W.G., Zakharova, N., Kürschner, W.M., Miller, C.S., Baranyi, V., Schaller, M.F., Whiteside, J.H., Schnurrenberger, D., Noren, A., Shannon, K.B. ,O'Grady, R., Colbert, M.W., Maisano, J., Edey, D., Kinney, S.T. and the CPCP Team. Colorado Plateau Coring Project, Phase I (CPCP-I): A continuously cored, globally exportable chronology of Triassic continental environmental change from Western North America. *Submitted to Scientific Drilling*

Miller, C., Kürschner, W., Peterse, F., Barnyi, V. & Reichart, G-J. 2016. The Carnian (Late Triassic) carbon isotope excursion: new insights from the terrestrial realm. Geophysical Research Abstracts Vol. 18, EGU2016-6899, EGU General Assembly 2016

N. B. As the chapters of this thesis are, or will be published as separate papers in scientific journals, some repetition of the statements could not be avoided.

Acknowledgements

My first acknowledgment goes to my principal supervisor Professor Dr. Wolfram M. Kürschner. I am very grateful to him for putting his faith in me and accepting me as a PhD student. He has guided and supported me through the four years at UiO and imparted a great deal of scientific knowledge. He always believed in my abilities even when I doubted myself and he challenged my thinking for finding the answers to my own questions. I hope that I will be eligible for the "palynological driving licence".
Thank you to Professor Dr. Paul Olsen who helped in the USA case study and contributed with his knowledge on the American Triassic.
I would like to thank Professor Dr. Henning Dypvik for taking over the role as co-supervisor.
I would like to acknowledge my co-authors of the papers which form this thesis. I learnt a great deal from each and I am thankful for their academic contribution and the useful discussions that we had. Special thanks go to Tammo Reichgelt and Ágnes Rostási who provided some of their unpublished data and agreed on publishing them together as a comparison to my palynological data.

I thank the colleagues at the Department of Geosciences for their help and assistance. Mufak Said Naoroz is especially thanked for his assistance in the processing of the palynological samples. Thanks to his help we could save plenty of lab hours that could be spent on microscopy work and manuscripts. Berit Løken Berg and Siri Simonsen are thanked for their help with the SEM. Tusen hjertelig takk!

My special thank goes to Silvia Hess and Stefan Rothe for their friendship, who welcomed me into the Norwegian system, for helping me get to know the Norwegian way of life better, dinners, game nights, trips together, cross-country ski lessons and for supporting my German language practice.
I thank Els van Soelen, Anouk Klootwijk and Lottie Miller for the fun and cheerful office hours, coffee breaks, lunches and occasional gym classes where we could absolutely discuss everything: from foraminifers to cats, life in general… but mainly cats…

At last but by all mean not least I sincerely thank my family, especially my mother (Anya) and grandmother (Mami) and all other members of the family (with two or four legs) for their love, caring and support through the long years of studies and a life abroad.

1. General introduction

1.1 Palaeoenvironmental and palaeoclimatic implications of palynology and palynofacies

Palynology is the study of the organic-walled microfossils that are found in the maceration residue of sedimentary rocks after dissolving the carbonate and silicate fraction respectively. The term palynology originates from the Greek word: ***παλυνω*** ("I sprinkle"), suggestive of „fine meal", „fine flour" or „dust" (Traverse 2007). The organic-walled microfossils labelled as palynomorphs contain terrestrial and aquatic (marine-freshwater) forms, elements related to plants (pollen and spores), green algae, dinocysts, animal remains (e.g., scolecodonts), the inner chitinous test linings of the foraminifera and organisms of unknown biological affinity (acritarchs, chitinozoa) as well[1]. The terrestrially derived pollen grains represent the male reproductive organ of seed plants (gymnosperms and angiosperms) (Traverse 2007). Spores refer to meiospores that give rise to a male gametophyte in liverworts, mosses, ferns, and lycophytes (Punt et al. 2007; Traverse 2007). The megaspores containing the female gametophyte in heterosporous plants are differentiated and treated separately in palynological studies. The term "sporomorphs" is often used to designate spores and pollen grains (Traverse 2007).

The main component of the sporomorph wall is sporopollenin, a chemically resistant material, which enables the preservation of sporomorphs in sedimentary rocks in non-oxidizing environments and the survival of the rigorous acid treatment of palynological processing techniques (see chapter 3). Sporopollenin consists of highly cross-linked biopolymers of carbon, hydrogen and oxygen comprising branched aliphatic chains, aromatic chains and phenolic compounds (e.g., Mackenzie et al. 2015).

In sedimentary environments, palynomorphs behave as clastic particles during transport and sedimentological processes. Their size varies between 5-500 µm, in the size range of silt-fine sand, but due to their lower specific gravity they tend to be deposited together with smaller sedimentary particles (Traverse 2007).

Spores and pollen are present in non-oxidized sedimentary rocks since the Silurian (Traverse 2007). The sporomorphs are identifiable to various taxonomic levels due to characteristic morphological features (Moore et al. 1991, Punt et al. 2007). Their abundance and morphological changes through time makes the palynomorphs potential candidates for biostratigraphy and the development of zonations. Spores and pollen are important tools in the biostratigraphical subdivision of terrestrial successions where no marine age-diagnostic fossils (e.g., ammonoids, nannoplankton, plankton foraminifers or conodonts) are present. As spores and pollen can be present in both terrestrial and marine successions they can be used for land-sea correlation and correlation of various depositional environments. Palaeozoic acritarchs and chitinozoans have been widely used in biostratigraphy, and in the Mesozoic and Cenozoic numerous dinocyst-based zonations have been developed for marine successions (Bolli et al. 1989). Prasinophytes and freshwater algae have no stratigraphical value, but they are

[1] This study focuses primarily on the terrestrial palynomorphs. Detailed description is only provided for them.

important environmental indicators and can be present in rock forming amount and contribute to hydrocarbon generation (Tyson 1995).

The quantitative distribution of palynomorphs and their spatial and temporal distribution can reflect relationship to various environmental gradients e.g., climate, nutrient availability, salinity, hydrodynamic conditions (e.g., Traverse 2007). It complements sedimentological or geochemical methods to better understand palaeoenvironmental or climatic changes. The advantage of studying pollen and spore assemblage is that unlike plant megafossils, which represent predominantly local vegetation, the palynological assemblages record plant communities of different habitats, as well as local and regional vegetation types (Jacobson & Bradshaw 1981; Demko et al. 1998). Spores and pollen can be used to trace the source vegetation and reveal climate, which started with the pioneering work of Swedish geologist Lennart von Post. In 1916 Von Post showed his results of pollen abundance as stratigraphical diagrams today known as pollen diagrams, which gave a temporal dimension to the vegetation data. One of the earliest applications of pollen analysis has been the palaeoclimatological and palaeoecological study of Quaternary deposits (e.g., Iversen 1944; Prentice 1986). Here modern-day observations are used as a model or analogue for past conditions (Birks & Seppä 2004). The vegetation data inferred from palynology is also a common method for climate reconstruction in deep time. A widespread method is assigning the dispersed spores and pollen to a hygrophyte or xerophyte group according to the method of Visscher & van der Zwan (1981) based on the ecology of the known or presumed parent plants. Though, this method is only approximation of climate trends. The main concerns are that many Mesozoic palynomorphs have uncertain botanical affinity and their exact ecological needs are unknown. Despite the limitations, this method has been widely applied in numerous Triassic palynological studies (e.g., Hochuli & Vigran 2010; Kustatscher et al. 2010; Roghi et al. 2010; Kustatscher et al. 2012; Dal Corso et al. 2015b; Mueller et al. 2016a, b). However, differences in pollen productivity and dispersion type pose a significant problem for vegetation reconstruction because the relative abundances of pollen grains in a deposit cannot be directly interpreted in terms of species abundance in the study area (Moore et al. 1991). Wind-blown pollen types from the hinterland (e.g., conifers) have generally higher pollen production rates than the insect-pollinated palynomorph types (e.g. Cycadales pollen, *Cycadopites* sp., *Aulisporites astigmosus* in the Late Triassic) or spores (e.g., Fægri & van der Pijl 1966).

Abbink (1998) and Abbink et al. (2004) introduced a palaeocommunity model termed as sporomorph ecogroup model (SEG) to recognize and reconstruct co-existing plant communities from the dispersed spore-pollen record. The method can be used to detect sea-level changes from shifts in a successive assemblage of the various SEGs and from quantitative or compositional changes within each SEG climate related changes can be inferred (Abbink et al. 2004).

The distribution of the various sporomorph types e.g., spores or bisaccates can be informative about proximal-distal trends on a cross-shelf transect described by the Neves effect (Chaloner & Muir 1968). Triassic sporomorphs relied mainly on wind- and water dispersal. Among them, the bisaccate pollen can be transported over longer distances as airbags attached to their main body provide them with higher buoyancy and is consequently usually the dominant

sporomorph further from the shoreline in marine assemblages. By contrast, spores, especially thick-walled and ornamented morphotypes, tend to settle out closer to their terrestrial source.

The stratigraphical distribution of the various palynomorph types, marine and terrestrial fossils, can yield information on cyclic sedimentation patterns and therefore can be effective tools in sequence stratigraphy (e.g., Gorin & Steffen 1991; Gregory & Hart 1992; Tyson 1995; Helenes & Somoza 1999). By grouping the marine palynomorphs according to their environmental affinities (e.g., coastal, open marine) and with the continental *vs*. marine palynomorph ratio, the changes in the depositional conditions can be detected and transgressive-regressive trends inferred. An increase of outer neritic to oceanic taxa is interpreted to indicate a sea level rise, whereas increasing abundances of neritic to coastal taxa were interpreted to denote a regressive trend. For instance in the case of dinocysts, minimum species numbers occurred in the lowstand system tracts (LST) (e.g., Sluijs et al. 2005). All palynomorphs are often poorly preserved due to mechanical and biological degradation with many reworked forms in the LST (Gregory & Hart 1992). The terrigenous component of the palynoflora will contain wide spectrum of habitats from the shoreline (swamps, deltaic, lowlands) to pollen of the hinterland vegetation (Gregory & Hart 1992). In transgressive systems tracts (TST) offshore, the marine component of the palynoflora is predominant both in frequency and diversity. Much of the terrestrial palynomorphs are expected to be trapped in near-shore environments (Gregory & Hart 1992). In the highstand system tract (HST), proximal settings will experience an increase in the terrestrial component as progradation continues. Locations more distal to the delta will experience continued marine dominance in the palynoflora (Gregory & Hart 1992).

Palynology has gained commercial significance in the petroleum industry and coal mining as one of major tools for biostratigraphy, correlation and environmental reconstruction. The advantage of the method is that small sample amount is required and therefore it can be performed on cuttings as well although the core sample provide more reliable results due to downfall, mixing or reworking.

Prior to the widespread application of vitrinite reflectance, spores and pollen grains had been widely utilized in hydrocarbon exploration as thermal maturity proxies. With increasing burial the organic matter undergoes thermal alteration and gradually becomes darker. The coloration of the spore/pollen wall formed the basis for several indices to evaluate the grade of thermal maturity such as the SCI (Spore Coloration Index) of Batten (2002).

A more recent approach in the study of spores and pollen is the study of the spore-pollen wall chemistry and the concentrations of phenolic pigment with FTIR (Fourier transform infrared spectroscopy) (e.g., Jardine et al. 2017). These compounds protect the cytoplasm and organelles from high levels of UV-B damage (Rozema et al. 2001). Environmental perturbations associated with presumably high UV radiation are also known in deep time (e.g., end-Permian, Visscher et al. 2004). However, the major limitation of the sporopollenin-based UV-B proxy is its longevity in the geological record (Fraser et al. 2014). Already low-grade diagenetic processes can alter the chemical structure of sporopollenin rendering the proxy unsuitable for reconstructing UV-B flux (Fraser et al. 2014). Therefore, its use will probably be widespread only in young associations.

Outside earth-and life sciences palynology is applied in forensics (Mildenhall et al. 2006), pollen grains are investigated in melissopalynology (Louveaux et al. 1970), allergy studies and archeology to trace the environment of pre-historical human habitats and man`s effect on nature (e.g., Bryant & Holloway 1983).

1.2. Late Triassic paleogeography and palaeoclimate

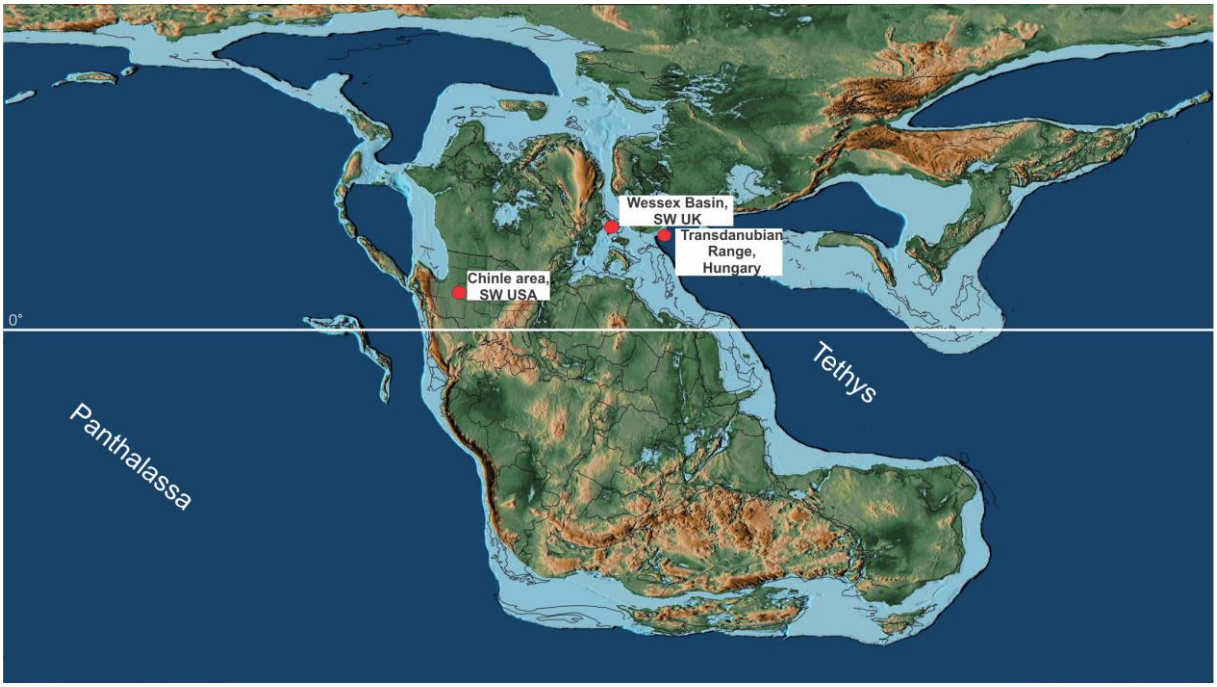

Figure 2 Global palaeogeography during Late Triassic (Norian) with the studied localities. Map modified from the PALEOMAP project (Scotese 2001).

The Triassic was an exceptional period in Earth`s history as all the continents were assembled into a single supercontinent, Pangea extending from about 85°N to 90°S (Ziegler et al. 1993; Golonka 2007) (Fig. 2). Pangea came into being in the Carboniferous with the collision of Laurasia and Gondwana and the aggregation culminated in the Triassic with the addition of Kazakhstan, Siberia, China and southern Asia (Ziegler et al. 1993; Golonka 2007). The exposed land was divided more or less symmetrically about the palaeoequator between the northern and southern hemispheres (Golonka 2007). The continent was surrounded by Panthalassa and in low-mid latitudes (between 30°N and 30°S) the Tethys formed a warm seaway extending eastward (Ziegler et al. 2003). The poles were ice-free (Frakes & Francis 1988; Golonka 2007). Rifting and break-up of Pangaea was initiated during the Late Permian-Early Triassic, intensified at the beginning of the Norian and culminated in the CAMP volcanic activity (McHone 2000; Marzoli et al. 2011).

The Triassic climate is transitional from the harsh hot-house climate at the end Permian to the greenhouse climate in the Jurassic with climatic fluctuations locally or on a regional scale. The interval is marked by the global occurrence of red beds and evaporite deposits in numerous locations world-wide (Dubiel et al. 1991) as it was probably the most arid and

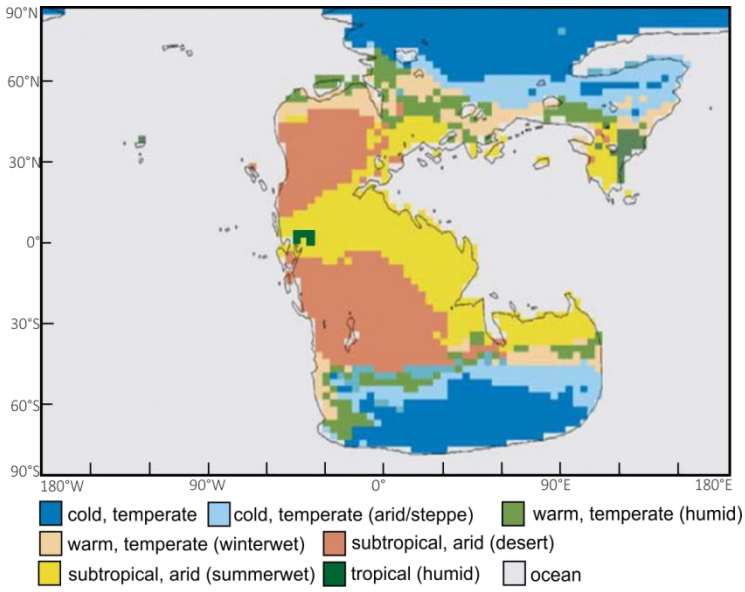

Figure 3 *Walter biome zones for the Late Triassic based on the predicted temperatures and precipitation. Modified from Sellwood & Valdes (2006).*

hottest period during the Phanerozoic (Wilson et al. 1994). The concentration of exposed land at low-mid latitudes and the warm Tethys seaway would have maximized the summer-heating in the circum-Tethyan region (Parrish 1993; Preto et al. 2010) with hot summers and relatively cold winters. This continent-ocean configuration imposed strong subtropical trade winds and strong monsoonal circulation with cross-equatorial flow and non-zonal climate pattern (Crowley et al. 1989; Kutzbach & Gallimore 1989; Mutti & Weissert 1995; Sellwood & Valdes 2006). The shape of Pangea enhanced the seasonally alternating circulation that occurred due to the thermal and pressure contrast between the two hemispheres (Crowley et al. 1989). This thermal contrast would have been comparable to that occurring now during the summer monsoon in Asia, but greater as both hemispheres were land (Crowley et al. 1989). Consequences of the "mega-monsoonal" climate were: small annual temperature fluctuation in low latitudes, abundant but extremely seasonal rainfall concentrated mainly in the summer in the northern hemisphere (Dubiel et al. 1991; Parrish 1993). The inside of Pangea was characterized by extreme continentality and arid climate (Kutzbach & Gallimore 1989; Dubiel et al. 1991) (Fig. 3). In the Late Triassic, during the strongest monsoon regime, the monsoonal circulation in western Pangea probably resulted in the reversal of cross-equatorial flow and drew moisture along the equator from the west (Parrish & Peterson 1988; Parrish 1993; Loope et al. 2004). As a result, the western margin of the Pangea received higher, but highly seasonal rainfall, while eastern and central Pangea and the western Tethys were most likely arid throughout the year (Parrish & Peterson 1988, Parrish 1993; Loope et al. 2004) (Fig. 3). The eastern costs of Laurasia and Gondwana experienced seasonality and alternate wet-dry seasons (Parrish & Peterson 1988; Kutzbach & Gallimore 1989; Dubiel et al. 1991; Parrish 1993; Preto et al. 2010) (Fig. 3). The high latitudes were probably marked by wet climate (Fig. 3) due to westerlies and polar easterlies

(Dubiel et al. 1991; Preto et al. 2010). Climatic oscillations were superimposed on the general monsoonal climatic pattern with a pronounced climate change and increased humidity in the middle Carnian (e.g., Preto et al. 2010; Ruffell et al. 2016).

During the Triassic the amount of atmospheric CO_2 was several times higher than today (e.g., Retallack 2009). The oceans were in "aragonite sea mode" (Mg/Ca>2) where the equilibrium abiotic carbonate precipitate form the sea is aragonite or high Mg-calcite like today (Adabi 2004).

The palaeoclimate variations resulted in macro- and microfloral provincialism (e.g., summarised in Kustatscher et al. 2018, more references therein). In the Southern Hemisphere, two major phytogeographic realms are distinguished with corresponding microfloras: the Onslow and Ipswich provinces (Dolby & Balme 1976; Césari & Colombi 2013) (Fig. 4). The Onslow microflora throughout northwestern Australia, northwestern Madagascar, East Africa and the northern part of Southern America hosts a mixture of Gondwanan and equatorial Tethyan taxa (e.g., *Aulisporites, Camerosporites, Enzonalasporites, Infernopollenites, Minutosaccus, Ovalipollis* and *Samaropollenites*) (Dolby & Balme 1976; Buratti & Cirilli 2007; Césari & Colombi 2013) and it reflects vegetation of warm temperate climates (Césari & Colombi 2013). The Ipswich microflora developed in southern and eastern Australia, Southern America and Antarctica representing cool temperate plant communities (Césari & Colombi 2013). In the Northern Hemisphere the vegetation was more heterogenous resulting in several smaller provinces (Fig. 4) (e.g., summarised in Kustatscher et al. 2018, more references therein).

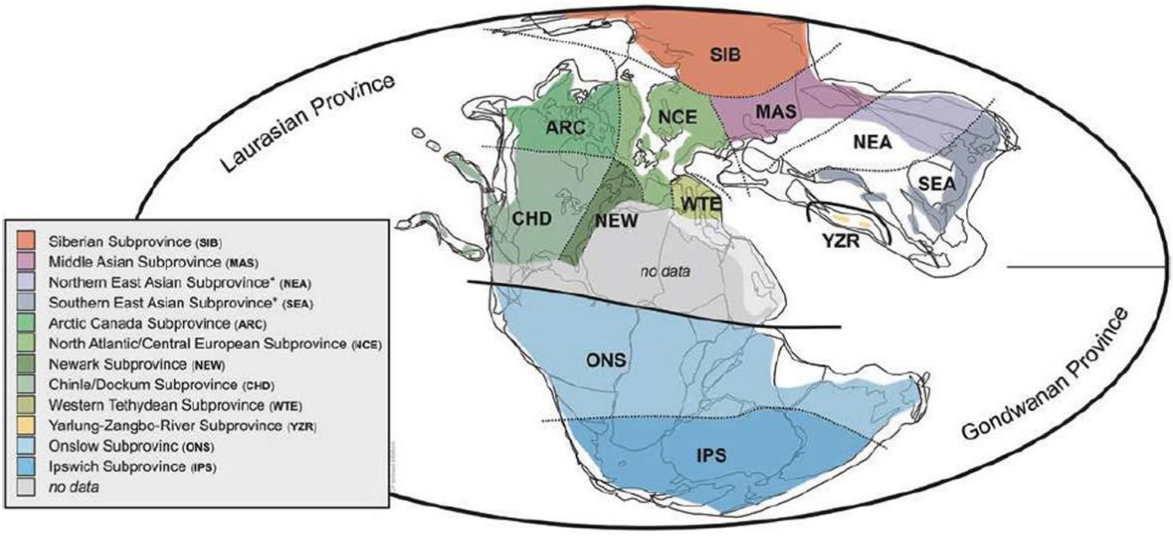

Figure 4 Palaeogeographic map showing floral provinces in the Late Triassic. Figure from Kustatscher et al. (2018).

1.2.1. Carnian Pluvial Episode

In the late early Carnian numerous sedimentary successions show significant changes in depositional style and biotic changes. The western Tethys areas experienced a significant change in depositional style and an increase in the terrestrial influx within the marine sedimentary basins (e.g., Roghi et al. 2010; Rostási et al. 2011; Haas et al. 2012). This episode is recognized within the Germanic Basin as the interval where the playa lake deposits were temporarily interrupted by sandy fluvial channels and overbank deposits of the Schilfsandtstein (Stuttgart Formation) during the late early Carnian (e.g., Bachmann et al. 2010; Shukla et al. 2010). The increase in clastic input has been related to a substantial climate change towards more humid climate (Simms & Ruffell, 1989, 1990; Ruffell et al. 2016) which appears to start in the late early Carnian close to the early to late Julian boundary in the Alpine realm (Dal Corso et al. 2012, 2015a; Mueller et al. 2016a, b). This unusual climate episode in the late Julian has been known as "Rheingraben turnover" (Schlager & Schöllnberger 1974), "Raibl Event" (Kozur 1991), "Carnian Crisis" (Hornung et al. 2007a), "Middle Carnian Wet Intermezzo" (Kozur & Bachmann 2010), "Carnian Pluvial Event" (Simms & Ruffell 1989, 1990). Recently, the most commonly used terms are Carnian Pluvial Episode (CPE) (e.g., Lukeneder et al. 2012; Muller et al. 2016a, b). In May 2017 at the international workshop: "The Carnian Pluvial Episode (Late Triassic) Climate Change and Evolutionary Innovations" the term "Mid Carnian Episode" was suggested as new name designating the mid Carnian climate-environmental perturbations. The new term is currently under consideration for publication (pers. comm. with Jacopo Dal Corso 2017).

The global nature of the CPE has been debated, but evidence from European successions (e.g., Schlager & Schöllnberger 1974; Simms & Ruffell 1989, 1990; Visscher et al. 1994), from the Middle East (Bialik et al. 2013), Asia (Hornung et al. 2007a, b; Nakada et al. 2014; Sun et al. 2016) and South America (Colombi & Parrish 2008) suggest that the CPE wet conditions had global extent (Ogg 2015; Ruffell et al. 2016). However, Visscher et al. (1994) rejected the presence of a wetter climatic phase during the Carnian based on palynological evidence from the Schilfsandstein. They explained the facies changes by the establishment of a large river system in an overall dry floodplain, but with locally wet environments near the river banks, with the present-day Nile Valley as an analogue.

The CPE was accompanied by sea level changes, global warming (Trotter et al. 2015; Sun et al. 2016) increased continental weathering (Rostási et al. 2011), demise of carbonate platforms (Keim et al. 2006; Breda et al. 2009; Lukeneder et al. 2012; Arche & López-Gómez

2014) and deepening of the carbonate compensation depth (CCD) in the oceans (Rigo et al. 2007; Lukeneder et al. 2012; Nakada et al. 2014). The enhanced terrigenous input lasted from the late Julian (Julian 2) to the early Tuvalian in low palaeolatitudes (Roghi et al. 2010; Rostási et al. 2011). The CPE is characterized by wet-dry cycles and multiple humid pulses; before the climate returned to persistent aridity in the late Carnian or Norian (Breda et al. 2009; Preto et al. 2010; Lukeneder et al. 2012; Bialik et al. 2013; Mueller et al. 2016b; López-Gómez et al. 2017).

The onset of the CPE in the mid Julian is associated with a negative carbon isotope excursion in the marine realm that suggests the injection of a significant amount of ^{13}C-depleted CO_2 into the atmosphere (Dal Corso et al. 2012, 2015a). Miller et al (2017) provided the first evidence of a negative carbon isotope excursion from a fully terrestrial realm, correlated to the onset of the CPE from the Carnian succession of the Mercia Mudstone Group, SW England. There the initial carbon isotope excursion is followed by four other negative C-isotope excursions (Miller et al. 2017). Since then multiple negative carbon isotope excursions are also recorded from the Alpine realm, from the Transdanubian Range, western Hungary (pers. comm. with Jacopo Dal Corso 2017). The isotope excursion lasted for *ca*. 0.8-1.2 Ma (Zhang et al. 2015; Miller et al. 2017). The origin of the ^{13}C-depleted CO_2 and the carbon isotope excursion is likely linked to enhanced volcanic activity and the associated feedbacks (warming, dissociation of methane clathrates, reductions in marine primary productivity) (Simms & Ruffell 1990; Hornung et al. 2007a, b). The emplacement of the Wrangellia Large Igneous Province basalts is the most likely trigger of the CPE (Furin et al. 2006; Dal Corso et al. 2012). However, the timing of the volcanism is not exactly contrained and Greene et al. (2010) and Xu et al. (2014) showed that the Wrangellia eruptions started earlier than the Carnian. Other causal mechanisms can be the changes in atmospheric and oceanic circulation driven by plate tectonics (Hornung & Brandner 2005) or peak of the Pangean mega-monsoon due to the maximum aggregation of the supercontinent (Parrish 1993; Colombi & Parrish 2008). Hornung & Brandner (2005) proposed the Cimmerian orogeny and the uplift of the Fennoscandian High built landmasses that enhanced the monsoonal circulation over the Tethys.

The CPE had significant effects both on terrestrial and marine organisms (Ruffell et al. 2016): The first occurrence of calcareous nannoplankton coincided with the Wrangellia eruptions (Furin et al. 2006). Calcispheres became abundant shortly after the CPE (Preto et al., 2013). Palynological analyses of the CPE typically show a shift towards hygrophyte vegetation with

increases of ferns, equisetaleans and cycadaleans (Roghi 2004; Hochuli & Vigran 2010; Roghi et al. 2010; Mueller et al. 2016a, b).

1.2.2. Mid-Norian Climate Shift in SW equatorial Pangea

During the Late Triassic, western equatorial Pangea, in the present-day American Southwest was unusually humid due to the monsoonal circulation (Parrish & Peterson 1988; Parrish 1993). During northern hemisphere summers, low pressure from continental heating in the north would draw south-easterly wind across the equator and into western equatorial Pangea similar to the situation in present day west Africa (Loope et al. 2004). This cross-equatorial summer air flow penetrated into western equatorial Pangea bringing abundant but highly seasonal rainfall (Parrish & Peterson 1988; Parrish 1993; Loope et al. 2004; Nordt et al. 2015). The Chinle depositional area in SW part of Pangea was situated at tropical latitudes within the Intertropical Convergence Zone (ITCZ) (Nord et al. 2015). Monsoonal seasonality indicators are inferred from occasional pedogenic carbonate nodules and complex drainage features in the sediments (Dubiel 1987; Dubiel & Hasiotis 2011). The palaeoclimatic aspect of the Chinle flora has been controversially discussed: Daugherty (1941) and Gottesfeld (1972) suggested seasonal climate with periodic drying based on the palynological assemblages and the presence of irregular growth rings in petrified tree trunks. By contrast, the plant macro remains suggested warm end ever-wet climate based on comparison of nearest living relatives, leaf morphology and the large size of the fossil tree trunks (e.g., Ash 1969; 1972; Dubiel et al. 1991; Parrish 1993; Ash 2001, 2005). The contrast between macroflora and palynological assemblages is explained by the more local nature of the macro remains. The palynological record can provide information on regional scale vegetation in contrast to the macrofossil record that can be biased to local vegetation elements and often shows the floral elements in localized wet habitats (Demko et al. 1998). Ash & Creber (1992) considered the irregular growth interruptions in the fossil wood (Fig. 5) similar to the growth patterns of trees which live in the tropics. They suggested that the interruptions are most likely caused by endogenous hormonal effects or occasional fluctuations in local water supply (Ash & Creber 2000). However, more recently, similar growth interruptions were found in Cretaceous silicified wood and they were interpreted as the evidence of seasonal droughts (Falcon-Lang 2003) (Fig. 5). Similar growth interruptions are present in trees from East Africa (e.g., Uganda, Somalia, Tanzania) (Jacoby 1989) and Australia (Schweingruber 1992) with highly seasonal rainfall. Lungfish burrows and teeth are characteristic elements of the fauna in the Chinle Formation during the Norian (Parrish 1993). At present, lungfish live in typical monsoonal environments with seasonality and periodic drying (Parrish 1993). Growth banding in mollusc shells also

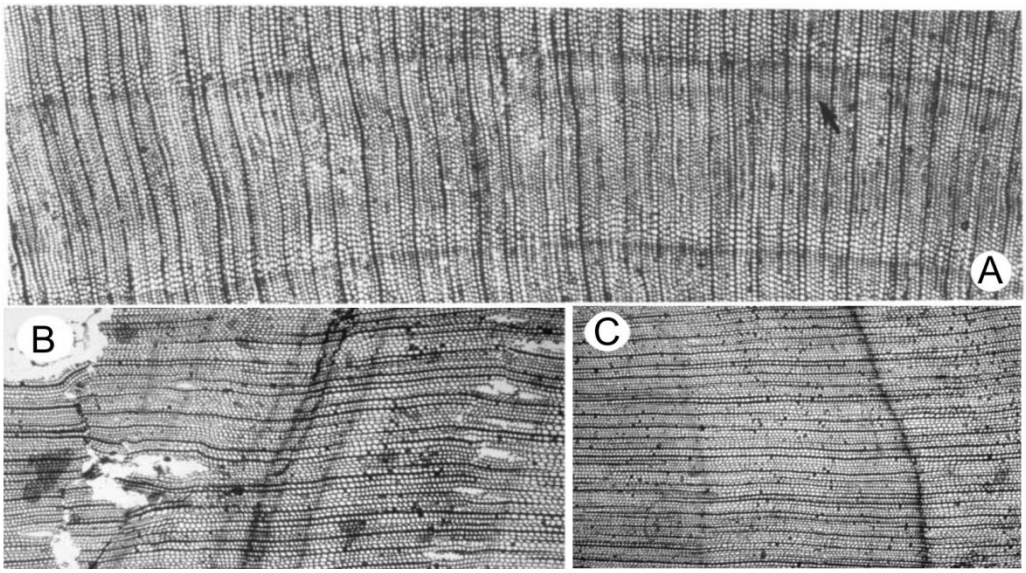

Figure 5 Growth interruptions in fossil wood from the Late Triassic Chinle Formation, Arizona and the Late Cretaceous Two Medicine Formation, Montana. A Growth interruption marked by arrow (about 1.5 mm wide) consisting of a broad band of generally large cells bounded on the exterior by a narrow, somewhat incomplete band of small cells having a maximum width of 3 cells. The band of small cells in the underlying interruption is also narrow and somewhat incomplete, magnification X20. From Ash & Creber (1992). B-C Examples of growth interruptions in Cupressinoxylon/Taxodioxylon from the Two Medicine Formation from Falcon-Lang (2003). B Closely spaced zones of variably persistent growth interruptions, magnification X12. C Variably developed interruptions, magnification X12.

indicates seasonal variations in growing rate most likely linked to seasonal wet conditions (Dubiel et al. 1991).

A trend from seasonally humid monsoonal climate to drier conditions labelled as "Mid Norian Climate Shift "(Nordt et al. 2015) and enhanced seasonality is observed in the Chinle area during the Norian (Dubiel 1987; Dubiel et al. 1991; Parrish 1993; Dubiel & Hasiotis 2011; Atchley et al. 2013; Nordt et al. 2015). Subsequently by the Triassic-Jurassic boundary, the region had become significantly more arid (Nordt et al. 2015). The transition from a fluvial-alluvial to eolian environment in the Chinle during the Norian-Rhaetian reflects this long-term climatic change from humid monsoonal climate to drier conditions (Dubiel & Hasiotis 2011). The increase in pedogenic carbonate formation beginning in the mid Norian has been interpreted as evidence of a shift from poorly drained wetlands to well-drained soils in agreement with the shift to drier climate (Martz & Parker 2010; Atchley et al. 2013; Nordt et al. 2015). A significant drop in mean annual precipitation (MAP) calculated from paleosols was shown by Atchley et al. (2013) and Nordt et al. (2015) indicating rapidly declining rainfall from the middle Norian. The main cause of the transition to drier and warmer climate was believed to be the northward movement of the North America continent from the equator

into the drier mid-latitudes (Dubiel et al. 1991; Kent & Tauxe 2005). Alternatively, the uplift of the Cordilleran Arc could have caused an increasing rain shadow over the Chinle sedimentary basin blocking the influx of moist tropical air from the west (Atchley et al. 2013; Nordt et al. 2015).

This climate change is expected to be a stress on the terrestrial ecosystems including plants and animals (e.g., Whiteside et al. 2015). The previous paleontological studies showed a significant turnover in the tetrapod fauna in the middle Norian (*ca*. 217-213 Ma) known as Adamanian/Revueltian faunal turnover (e.g., Benton 1995; Parker & Martz 2010) (Fig. 6). Phytosaurs, '*Leptosuchus'*, *Calyptosuchus* and dycnodonts disappear at the turnover coinciding with the lowest occurrence of the phytosaur *Pseudopalatus* and a dramatic increase in the abundance of the aetosaur *Typothorax* (Parker & Martz 2011). Large metoposaurs are far more common in the Adamanian than after the faunal turnover and several animal groups show signs of a more terrestrial lifestyle (Parker & Martz 2011) (Fig. 6). The flora inferred form the palynological assemblages experienced a roughly synchronous turnover with the vertebrate faunas in the middle Norian (Litwin et al. 1991; Reichgelt et al. 2013) indicating serious changes in the terrestrial ecosystems.

In addition to the climate change, other environmental perturbations e.g., volcanism (Atchley et al. 2013; Nordt et al. 2015) and pCO_2 variations (Cleveland et al. 2008a, b; Atchley et al. 2013; Nordt et al. 2015; Schaller et al. 2015; Whiteside et al. 2015) are recorded during the Norian which could have contributed to the biotic turnover. In the Norian, an increase in pCO_2 was reported by Cleveland (2008a, b), Atchley et al. (2013), Nordt et al. (2015), Schaller et al. (2015) and Whiteside et al. (2015) from 212 Ma, but the pCO_2 trends are not entirely clear between 215 Ma and 212 Ma around the age range of the faunal and floral turnover. Schaller et al. (2015) and Atchley et al. (2013) and Knobbe & Schaller (2018) showed a decline in the pCO_2 values between 215 Ma and 212 Ma, while the data of Nordt et al. (2015) indicate a slight increase in the pCO_2 values between 214 Ma and 215 Ma. The previously proposed long-term increase in pCO_2 was most likely driven by the transformation of the soils and biome after the shift to arid climate and due to the arc volcanism related to the uplift of the Cordilleran Arc (Nordt et al. 2015).

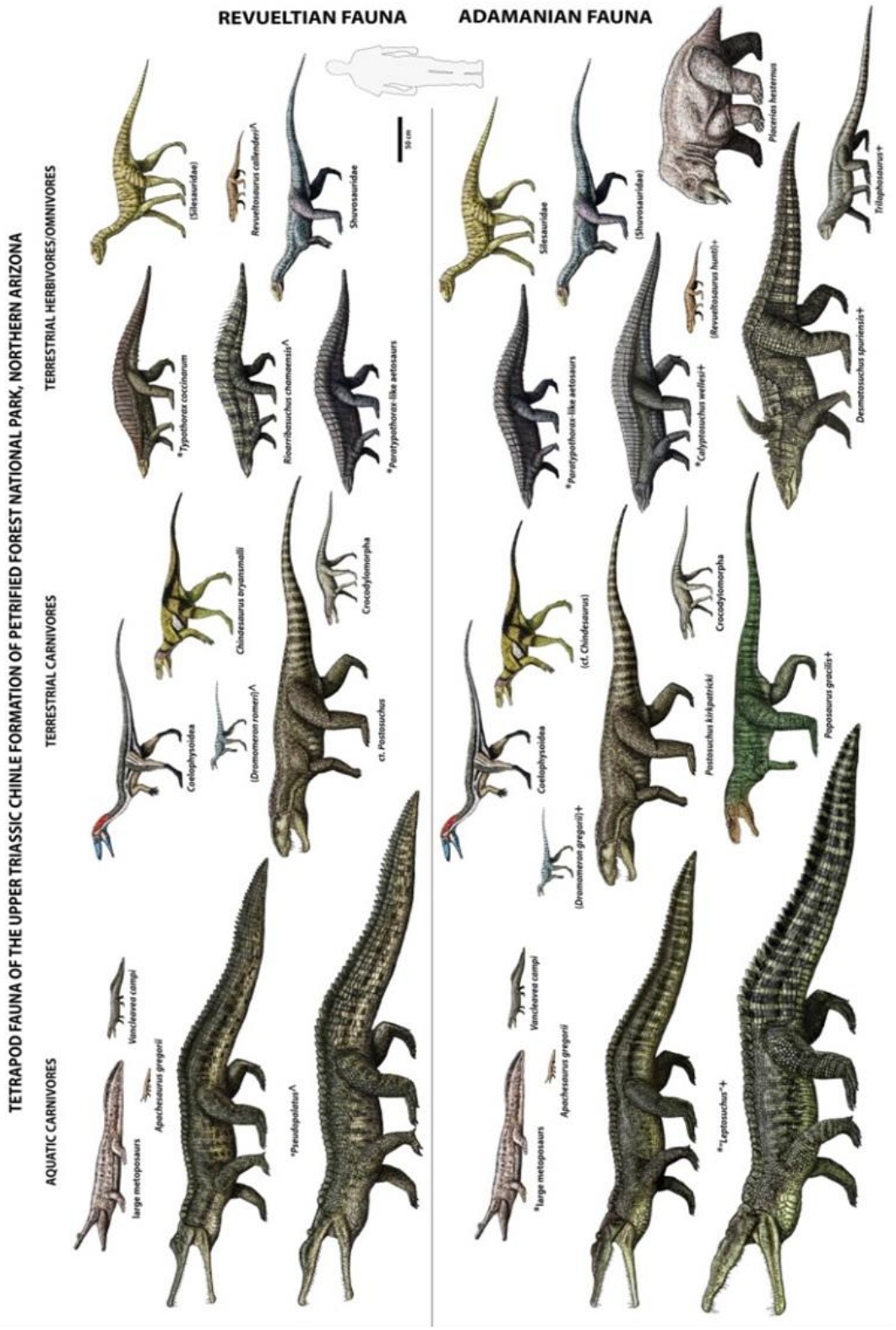

Figure 6 Adamanian/Revueltian faunal turnover. With the courtesy of W.P. Parker.

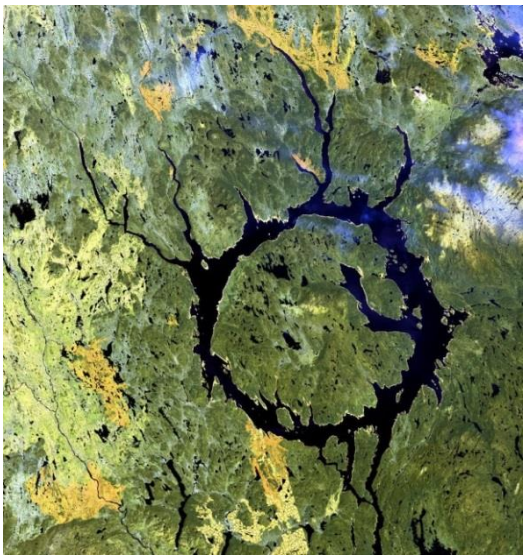

Figure 7 Eye of Québec" The Manicouagan impact crater. Courtesy of Landsat NASA.

The Mid Norian Climate Shift and the faunal/floral turnover dated to near the same time as the Manicouagan impact crater in Québec, Canada (N 51°23°, W 68°42°) (Fig. 7) at 214-215 Ma (Walkden et al. 2002; Ramezani et al. 2005; Jourdan et al. 2009; Parker & Martz 2011). This impact structure with a diameter of 85-100 km is the third largest of the Phanerozoic (Clutson et al. 2018). Preliminary radiometric ages for the stratigraphic interval containing the Adamanian/Revueltian transition in the Chinle Formation at the Petrified Forest National Park in Arizona, compare favourably with the age of the Manicouagan impact (Dunlavey et al. 2009; Ramezani et al. 2011). However, the existing data are unable to demonstrate direct causality between biotic changes and the impact event. The correlation of the imapct event and the biotic turnover will be tested by the ongoing CPCP (Colorado Plateau Drilling Project) project (*Olsen et al. submitted to Scientific Drilling*).

1.3 Late Triassic (Carnian-Norian) palynostratigraphy in Europe and North America

The extent of terrestrial depositional setting in the Late Triassic requires a suitable palynostratigraphical scheme, which can also enable the correlation of marine and non-marine sediments (e.g., Feist-Burkhardt et al. 2008; Cirilli 2010). Numerous previous palynological studies have contributed to our understanding of the Late Triassic palynostratigraphy of European and North American successions. The geographical and temporal variations in the palynological assemblages have necessitated the development of numerous regional zonation schemes (e.g., Feist-Burkhardt et al. 2008; Kustatscher et al. 2018). For the Alpine Triassic, the biostratigraphical evaluation of the palynomorph assemblages and zonations are known from e.g., Klaus (1960), Kavary (1972); Planderová (1972), Dunay & Fisher (1978), Planderová (1980), Visscher & Brugman (1981), van der Eem (1983), Blendinger (1988); Hochuli & Frank (2000), Roghi (2004); Roghi et al. (2010). From Central European Germanic Basins (mainly Germany, Poland), e.g., Orłowska-Zwolińska (1983, 1985), Fijałkowska (1994), Heunisch (1999), Fijałkowska-Mader et al. (2015) described the palynostratigraphy. Warrington (1967, 1970) and Warrington et al. (1980) tried to correlate the British Late Triassic successions to European palynostratigraphical schemes. In the Boral realm e.g., van Veen (1985), Vigran et al. (1998), Hochuli & Vigran (2010), Vigran et al. (2014), Paterson & Mangerud (2015) attempted to provide a palynostratigraphical framework. Palynostratigraphy of the North American succession was provided by Cornet (1977), Litwin et al. (1991), Cornet (1993) and Fowell (1993).

Cirilli (2010) and Kürschner & Herngreen (2010) compiled the available zonations from the northern and southern hemispheres with the attempt to correlate them to marine stages. Currently, the biostratigraphical resolution based on Late Triassic palynomorph assemblages is rather low (Cirilli 2010). One of the main limitations is the scarcity of suitable sections, especially in the Norian, due to the unfavourable depositional setting for the preservation of palynomorphs (e.g., red beds, evaporites, dolomites) and the semi-arid, arid climate in the western Tethys region (e.g., Preto et al. 2010). Many taxa have relatively long ranges, and changes in assemblages may often represent local environmental shifts or climate changes rather than useful temporal markers (Gradstein & Ogg 2012). Important taxa often lack well-calibrated stratigraphic ranges and the assemblages are often not dated independently with other fossils (e.g., ammonoids, conodonts) or other geochronological methods (e.g., radiometric dating) (Cirilli 2010). The stratigraphical ranges are often diachronous in different

regions (e.g., between Germanic Basin and Alpine realm, or Europe and North America) (Cirilli 2010). This microfloral provincialism is strongly controlled by climate variations on Pangea during the Late Triassic (Cirilli 2010; Kustatscher et al. 2018).

The comparison of European and North American Norian palynomorph assemblages showcases the limitations of the wider regional correlation (Lindström et al. 2016; **Paper 3**). Many palynomorphs (e.g., *Lagenella martinii*, *Brodispora striata*) have their last occurrence in the Tuvalian substage of the Carnian in Europe (Kürschner & Herngreen 2010), but these taxa are still present in the Norian Chinle Formation (Litwin et al. 1991; Lindström et al. 2016, **Paper 3**). The significant offset between the European and American palynofloras is the result of the generally hot and semiarid climate in the eastern part of Pangea and the western Tethyan realm (e.g., Preto et al. 2010), while the seasonal precipitation in western equatorial Pangea perhaps supported vegetation to thrive longer (e.g., Dubiel et al. 1991; Parrish 1993).

2. Study areas

2.1 Geological setting of the Mercia Mudstone Group ("British Keuper"), SW England

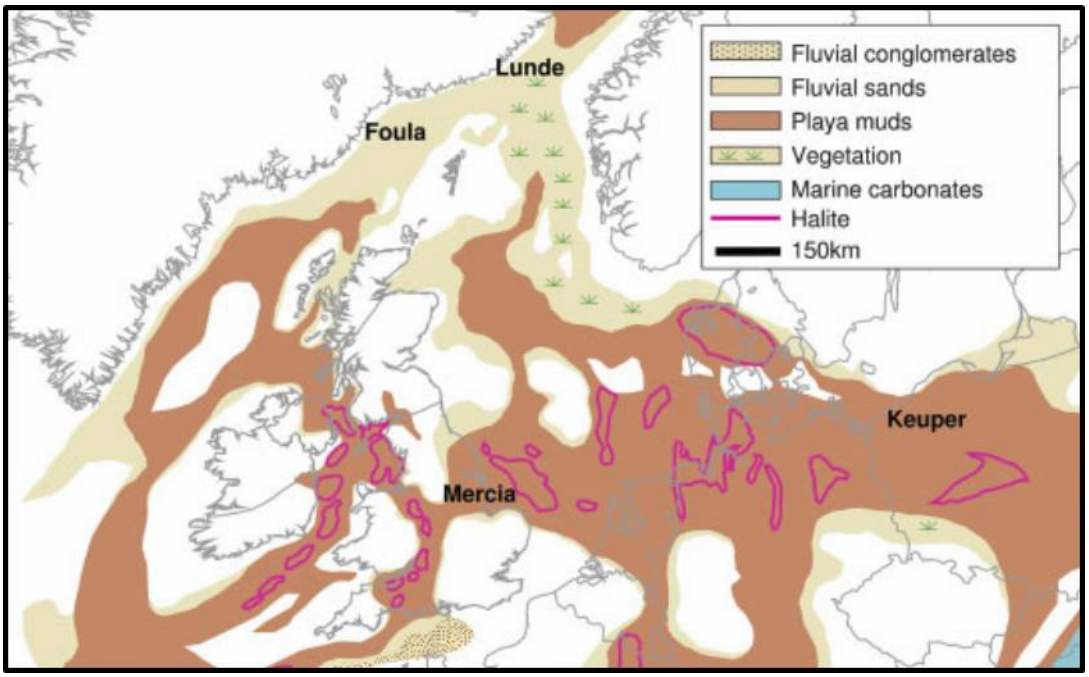

Figure 8 Carnian palaeogeographic reconstruction of north western Europe with the position of the Wessex Basin (asterisk). Modified from McKie & Williams (2009).

The Triassic in Europe is developed in two major facies domains, the mixed continental-marine facies of the north western European and central European Germanic realm and the mainly marine facies in the Alpine realm (Feist-Burkhardt et al. 2008). NW Europe was located at *ca*. 30°N in the arid continental interior of Pangea (Feist-Burkhardt et al. 2008). In the region, large fluvio-lacustrine systems were deposited in dry land within a collage of linked rift basins in the Late Triassic (McKie & Williams 2009) (Fig. 8). The streams were draining off the catchments of Greenland, Fennoscandia, the Scottish Highlands and the remnants of the Variscan mountains (McKie & Williams 2009). Fluvial drainage was dominantly endorheic in character, and terminated in playa, aeolian dune, sabkha or marsh settings (McKie & Williams 2009). The Central European Triassic basins are characterized by a tripartite facies evolution represented by the continental siliciclastic, Buntsandstein, the mostly marine carbonate unit, the Muschelkalk and the mixed marine-terrestrial Keuper with siliciclastics, carbonates and evaporites (McKie & Williams 2009 and references therein). In the UK, thick packages of fluvial-lacustrine sediments accumulated during the Triassic in fault-bounded basins extending from the Wessex Basin in the south to the east Irish Sea Basin

in the north (Ruffell & Shelton, 1999; Howard et al. 2008; McKie & Williams 2009; Hounslow et al. 2012). Unlike the Germanic Basin in Central Europe, the facies evolution in the UK region has a twofold subdivision: The Early-Middle Triassic fluvial-eolian Sherwood Sandstone is overlain by the Middle-Late Triassic (Ladinian-Rhaetian) Mercia Mudstone Group (Howard et al. 2008; McKie & Williams 2009; Hounslow et al. 2012). In the Wessex Basin, the Mercia Mudstone Group (MMG) consists of *ca*. 450 m of predominantly red mudstones and locally evaporites that were deposited in a low-relief sabkha environment in a hot desert (Gallois & Porter 2006; Hounslow & Ruffell, 2006; Hounslow et al. 2012) (Figs 8-9). The presence of evaporites is indicative of hydrologically closed basins and the fluvial systems were most likely terminal or endorheic (McKie & Williams 2009). The MMG is divided into the Sidmouth Mudstone Formation (Ladinian-Carnian), Arden Sandstone Formation (ASF) (Carnian), Branscombe Mudstone Formation (Carnian-Norian) and the Blue Anchor Formation (Norian-Rhaetian) (Howard et al. 2008) (Fig. 9). The Sidmouth and Branscombe Mudstone Formations comprise predominantly structureless red-brown mudstones and siltstones with anhydrite and gypsum veins and nodules that were deposited in playa lakes (Gallois 2001; Hounslow & Ruffell 2006; Gallois 2007). In the Wessex Basin, the Dunscombe Mudstone Formation (DMF) has been used more widely to distinguish the green to grey to purple predominantly mudstone unit between the red mudstones of the under-and overlying Sidmouth and (Jeans 1978) Branscombe Mudstone Formations (Jeans 1978; Porter & Gallois 2008). However, the DMF is not an official lithostratigraphical term according to the national nomenclature of the MMG (Howard et al. 2008). The DMF represents a fluvial–lacustrine succession with shallow freshwater lakes in low-relief topography that were fed by shallow distributary channels (Gallois & Porter 2006; Porter & Gallois 2008). Some cryptic marine indications have been detected in the Mercia Mudstone Group e.g., marine fossils including acritarchs, bivalves, shark teeth, but there is no direct evidence of a marine influence in the MMG depositional basins.

The significant lithological shift from red to greenish-grey mudstone at the boundary of the Sidmouth and Dunscombe Mudstone Formations in the Wessex Basin coincides with a significant negative carbon isotope excursion recorded in bulk organic carbon and plant lipids correlated to the onset of the Carnian Pluvial Episode (Miller et al. 2017).

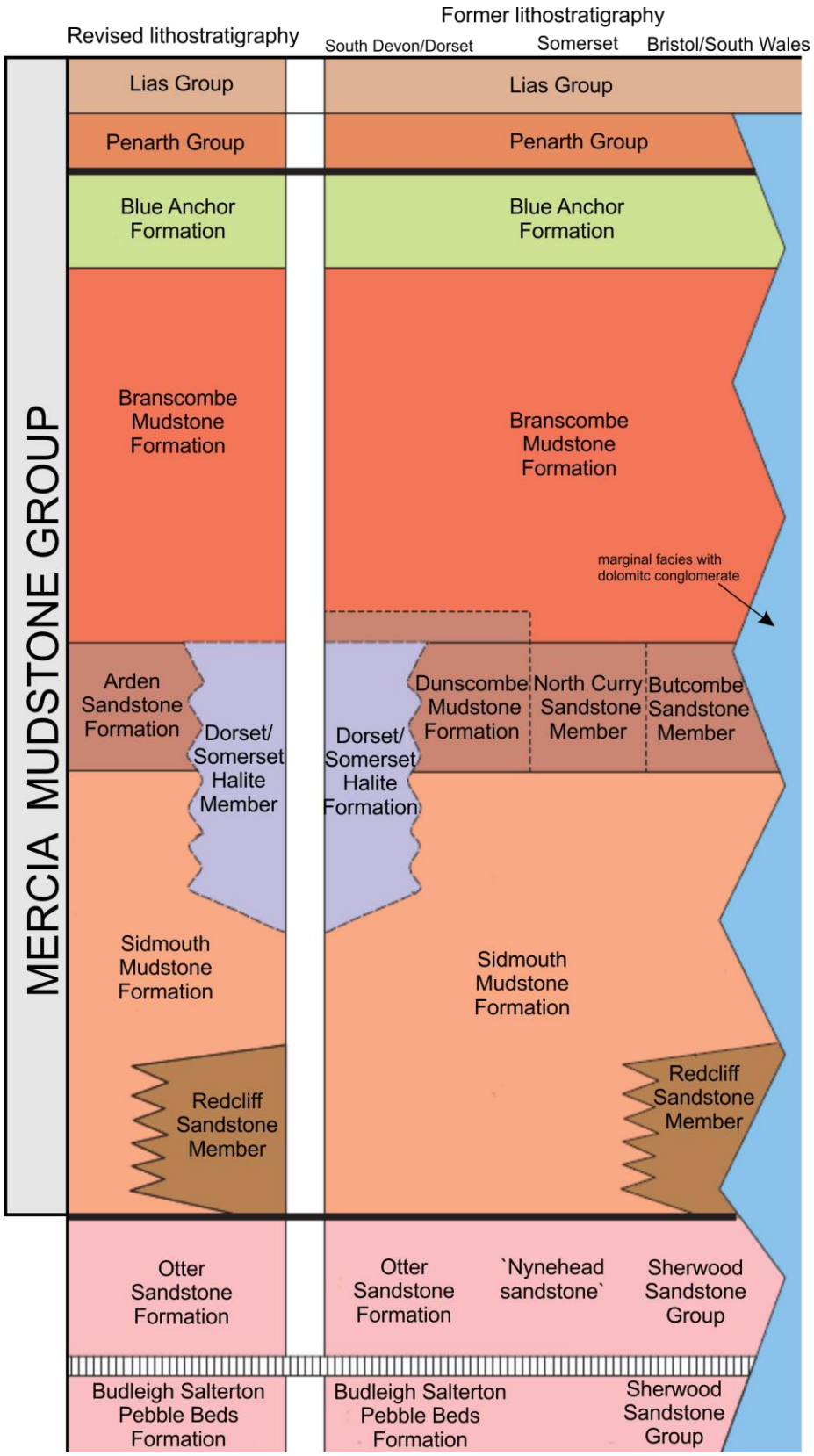

Figure 9 Lithostratigraphy of Middle and Late Triassic formations and the subdivision of the Mercia Mudstone Group in the SW UK. After Horward et al. (2008).

2.2 *Geological setting of the Transdanubian Range (western Hungary)*

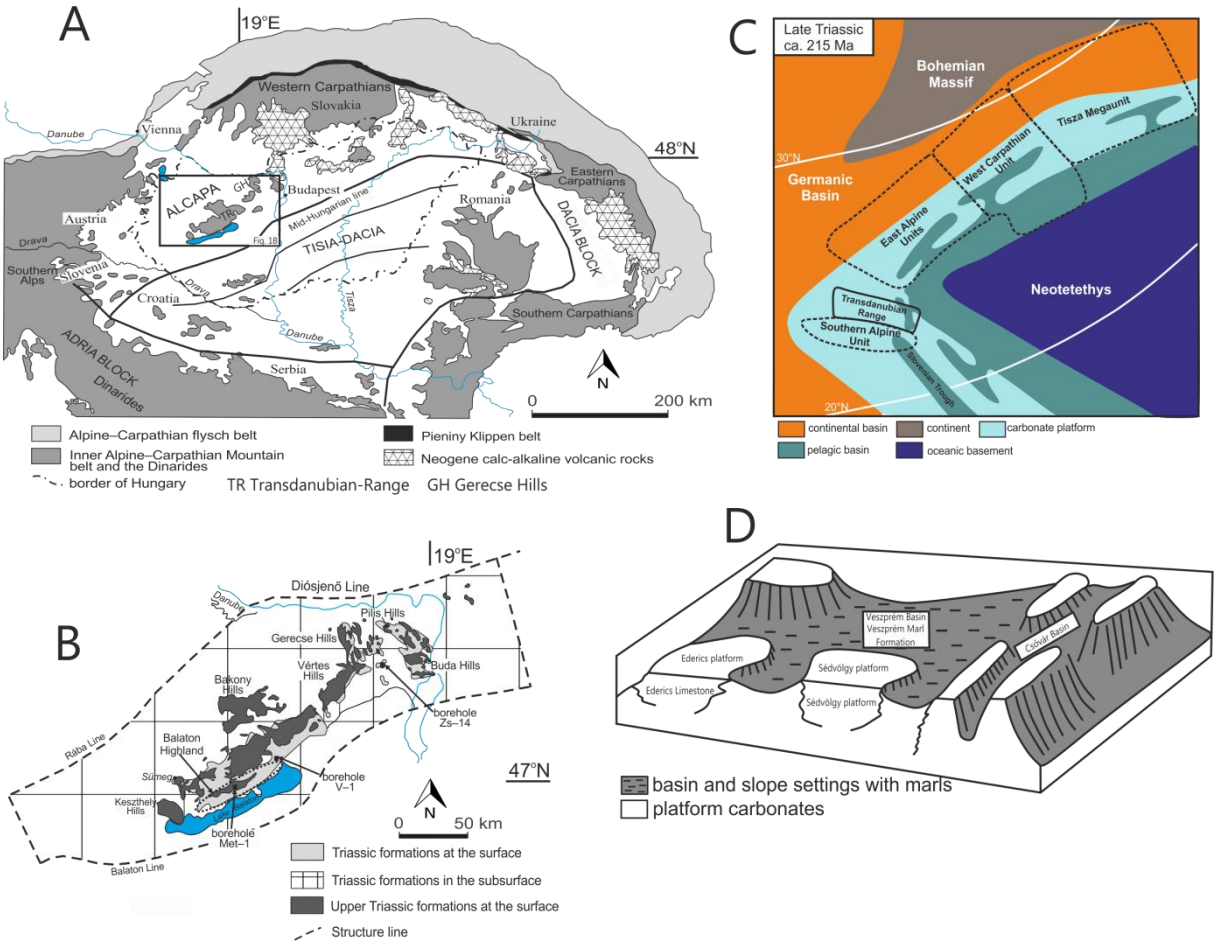

Figure 10 Geographical, geological and palaeographical setting of the Transdanubian Range (TR). A Geological framework and the major tectonic units of the Carpathian–Pannonian Basin (after Csontos & Vörös, 2004). The box indicates the area shown in 1B. B Generalized geological map of the Transdanubian Range modified after Haas (2002) and Rostási et al (2011) showing the locality of the three studied boreholes. C Palaeogeographic al setting of the Transdanubian Range in the western Neotethys during the Late Triassic. Modified after Haas et al. (1990, 2016). C Schematic palaeogeographical model for the depositional area of the Veszprém Marl Formation in the late Julian. Modified from Haas & Budai (1995).

The Transdanubian Range (TR) is situated in the western and north-western part of the Carpathian-Pannonian Basin extending 250 km in NE–SW (Fig. 10). The Palaeozoic and Mesozoic basement of the Carpathian-Pannonian Basin consists of two tectonic blocks of completely different origin; the ALCAPA and the Tisza block divided by the Mid-Hungarian Line (Csontos & Vörös 2004) (Fig. 10). The ALCAPA terrane (Alpine–West Carpathian–Pannonian) to the north includes the Transdanubian Range structural unit. The Permo-Mesozoic stratigraphy and facies evolution of the Transdanubian Range show close affinity to the central and western parts of the Southern Alps (Haas & Budai 1995; Budai & Haas 1997;

Haas & Budai, 1999; Haas et al. 2013). During the Late Triassic, it was part of the passive western Neotethys margin and was situated between the Northern Calcareous Alps and the Southern Alps (Haas & Budai 1995) (Fig. 10). By contrast, the Tisza block show similarities to the Northwest European and Germanic facies during the Triassic (Csontos & Vörös 2004) and it was at the northern Tethyan shelf margin east of the dry lands of the Bohemian Massive and Vindelician High (e.g., Kovács et al. 2011) (Fig. 10). The present-day setting of the Transdanubian Range is a result of complicated plate-tectonic rearrangements in the Cainozoic, the eastward escape of the ALCAPA terrane from the Alpine sector in the Palaeogene-early Miocene (mainly Oligocene) (e.g., Kázmér & Kovács 1985; (Csontos et al. 1992; Fodor et al. 1999) and a significant counter-clockwise rotation (e.g., Márton & Fodor 2003).

The Transdanubian Range is characterised by a syncline structure of NE–SW structural strike formed in the mid Cretaceous with Jurassic and Lower Cretaceous formations in the central zone while the formations progressively get older towards the limbs, ranging in age from Early Palaeozoic to Late Triassic (e.g., Haas et al. 2013).

The Triassic formations in the TR reach a total thickness of 3–4 km (Haas & Budai 1995). In the study area, Late Permian alluvial plain and the evaporitic lagoonal-coastal sabkha deposits are covered by Early Triassic shallow carbonate ramp and a fine-grained siliciclastic ramp facies (e.g., Haas et al. 2012, 2013). During the middle Anisian, the extensional tectonic movements in the western end of the eastward progressing Neotethys (e.g., Haas et al. 2013) resulted in the differentiation of the shelf and the former carbonate ramp became dissected (e.g., Budai & Vörös 2006). The depositional environment with the hemipelagic basins divided by isolated carbonate platforms prevailed until the early Carnian (e.g., Budai & Vörös 2006). In a higher part of the Julian a drastic increase in the clastic input resulted in a thick (up to 800 m) succession composed of fine-grained, mixed carbonate–clastic sediments, mainly marls of the Veszprém Marl Formation (e.g., Haas et al. 2013) which filled up the deep troughs and intraplatform basins. By the late Julian, the basins had already been filled-up and in the remaining shallow, isolated basins bituminous limestone was deposited (Sándorhegy Limestone Formation) alternating with marl units depending on the amount of the terrestrial influx (Budai et al. 1999; Haas et al. 2012). The final stage of the intraplatform basin infilling ended by the late Tuvalian. The extremely levelled topography resulting from the upfilling of the larger basins established the basis for the development of the extensive Dachstein platform in the latest Carnian-early Norian leading to the depositions of the Main

Dolomite and subsequently the Dachstein Limestone (Budai & Haas 1997). The mixed carbonate-clastic deposits of the Carnian Veszprém Marl Formation have been interpreted as the local representative of the Carnian Pluvial Episode recorded elsewhere in the Alpine Tethys realm (Rostási et al. 2011; Haas et al. 2012; Dal Corso et al. 2015a). The age of the Veszprém Marl Formation and the underlying Füred Limestone Formation is constrained by ammonoids and conodonts. Ammonoids (*Frankites* sp. and *Trachyceras aon*) and conodonts (*Gladigondollela tethydis, Paragondolella foliata, Paragondolella foliate inclinata*) suggest early Julian age corresponding to the *Aon* zone in the underlying Füred Limestone (Dosztály et al. 1989; Kovács et al. 1991; Budai et al. 1999). However, *Neoprotrachyceras* spp. and *Sirenites* sp. from the uppermost part of the Füred Limestone indicate already the *Austriacum* ammonoid zone and Julian 2 age (Dal Corso et al. 2015a). In the upper part of the VMF *Austrotrachyceras austriacum* and *Neoprotrachyceras baconicum* indicate Julian 2 age (Budai et al. 1999; Dal Corso et al. 2015a). Recently, Dal Corso et al. (2015a) recorded a significant negative carbon isotope excursion in the lowermost part of Veszprém Marl form the Balatonfüred-1 borehole in the Balaton Highland area (southern part of the Transdanubian Range), which was correlated to the characteristic carbon isotope excursion marking the onset of the CPE and the Julian 1/2 boundary in the Tethyan realm. More recent carbon isotope analyses indicate the presence of multiple negative carbon isotope excursions within the late Julian (pers. comm. with Jacopo Dal Corso 2017).

In this study, we analysed borehole material from the Balaton Highland, Bakony Mountains area and one borehole succession from the Gerecse Hills northeast to the Bakony. The encountered Carnian succession of the Gerecse Hills is markedly different from the stratotypes in the Balaton Highland area (e.g., Haas & Budai 1999, 2014; Budai et al. 2015). Marl layers characteristic for the Veszprém Marl are present only in the lower part of the studied succession. Upsection the marl unit is followed by a cherty limestone unit with marls and subsequently by cherty dolomites of the Csákberény Formation spanning the Julian and early Tuvalian (Góczán et al. 1979; Góczán & Oravecz-Scheffer 1996a, b). Foraminifers, ostracods and conodont remains indicate a restricted basin environment and poorly oxygenated bottom water conditions for the Julian (Góczán et al. 1979; Góczán & Oravecz-Scheffer 1996b).

2.3 *Chinle geological setting*

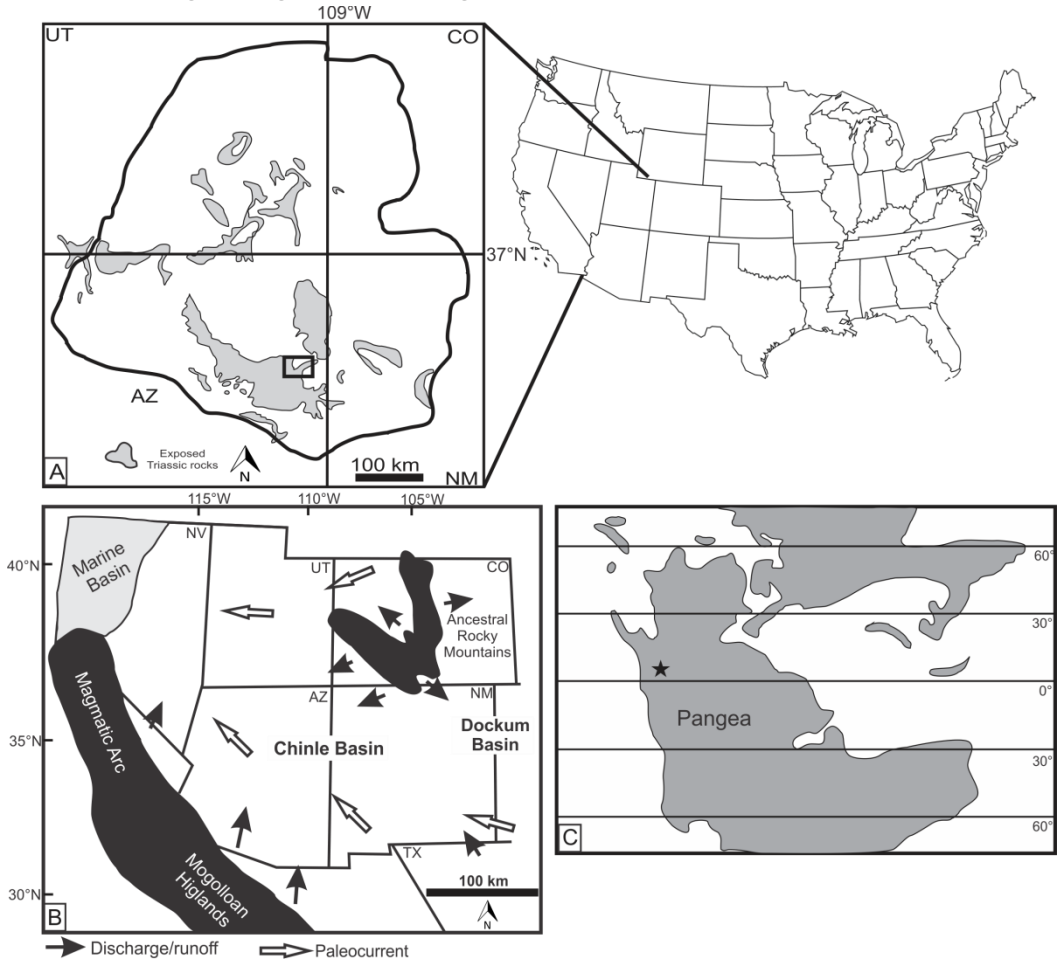

Figure 11 Geological setting and palaeogeographic reconstruction of the Chinle area. A: Map of the Petrified Forest National Park and its position on the Colorado Plateau in the SW USA, showing the exposure of Triassic rocks (grey area). Modified from Parker & Martz (2011). B: Palaeogeographic reconstruction of the Chinle sedimentary basin during the Norian and the general pattern of the Chinle fluvial system. Modified from Dubiel & Hasiotis (2011). C: Palaeogeographic position of the Chinle sedimentary basin in in western equatorial Pangea during the Late Triassic. Modified after Trendell et al. (2013a).

The Chinle Formation in the southwestern USA on the Colorado Plateau represents a complex system of fluvial, alluvial, lacustrine and eolian sediments deposited across Arizona, Utah, New Mexico and Colorado (Martz & Parker 2010) (Fig. 11). During the Late Triassic the area was situated 5°–10° north of the palaeoequator and *ca.* 400 km east of the western margin of the Pangea supercontinent (Bazard & Butler 1991; Dubiel et al. 1991; Kent & Tauxe 2005; Kent & Irving 2010) (Fig. 11) The Chinle depositional environment was located in a basin that drained north-westward into marine waters and received volcanic detritus from the southwest (Dickinson & Gehrels 2008; Martz & Parker 2010; Atchley et al. 2013; Howell & Blakey 2013; Riggs et al. 2013) (Fig. 11). The sedimentary evolution of the Chinle Formation depicts a cyclic depositional history starting with incision, filling of paleovalleys with fluvial

sediments and the subsequent development of floodplain environments (Martz & Parker 2010; Dubiel & Hasiotis 2011; Atchley et al. 2013; Trendell et al. 2013a, b). In the studied area at the Petrified Forest National Park (PEFO) in Arizona, the Chinle Formation can be divided into five members (Fig. 11). The lowermost conglomeratic and channel sandstones of the Shinarump/Mesa Redondo Member (Figs 11-12) represent primarily a braided rivers system overlying the Early to Middle Triassic Moenkopi Formation (Martz & Parker 2010). Subsequently, the Blue Mesa Member (Figs 11-12) is a large mudrock unit which was deposited in a predominantly suspended-load meandering river system with local lacustrine environments in the form of floodplain ponds and back-swamps (Trendell et al. 2013a, b). At the PEFO, the overlying Sonsela Member (Figs 11-12) is a semi-continuous sandstone complex interbedded with mudstones (Martz & Parker 2010). The depositional environment at the PEFO markedly changed between the deposition of the lower and upper Sonsela Member (e.g., Atchley et al. 2013; Howell & Blakey 2013; Nordt et al. 2015). The bedload-dominated fluvial style in the lower part of the Sonsela Member switched to a primarily suspended-load meandering river in the upper part. The rapid change in subsidence and fluvial style was interpreted to have been driven by changes in the subduction in the Cordilleran Arc, isostatic rebound of the arc and backarc aggradation (Howell & Blakey 2013). The stratigraphical boundary between the two disparate depositional styles is placed at a laterally persistent red silcrete horizon at the PEFO (Howell & Blakey 2013) that also marks the boundary between the Adamanian and Revueltian vertebrate biozones (Parker & Martz 2011). The fluvial sedimentation prevailed in the overlying Petrified Forest Member (Figs 11-12). The uppermost lithostratigraphical unit at the PEFO, the Owl Rock Member (Figs 11-12) was deposited in lacustrine, fluvial and floodplain settings and it contains (Martz & Parker 2010) calcretes and eolian deposits as well. An erosional surface terminates the Chinle Formation and it is overlain by the Early Jurassic Moenave Formation or Wingate Formation, but the exact relationship of these contacts is poorly understood (Martz & Parker 2010).

2.3.1. The age of the Chinle Formation

The Chinle Formation was thought to encompass the Carnian and Norian stages based on biostratigraphy (e.g., Litwin et al., 1991; Heckert et al. 2007), but palaeomagnetic correlations (Muttoni et al. 2004; Olsen et al. 2011) and recent radiometric dating (Riggs et al. 2003; Irmis et al. 2011; Ramezani et al. 2011, 2014) indicate a Norian-Rhaetian age (Fig. 12). Ramezani et al. (2011) dated the Black Forest Bed at the top of the Petrified Forest Member as 209.926 ± 0.072 Ma, which is close to the Norian-Rhaetian boundary age at 209.5 Ma according to the "Long-Rhaetian" age model (Muttoni et al. 2004; Ogg et al. 2014) implying that the topmost part of the Chinle formation is most likely Rhaetian (Riggs et al. 2003).

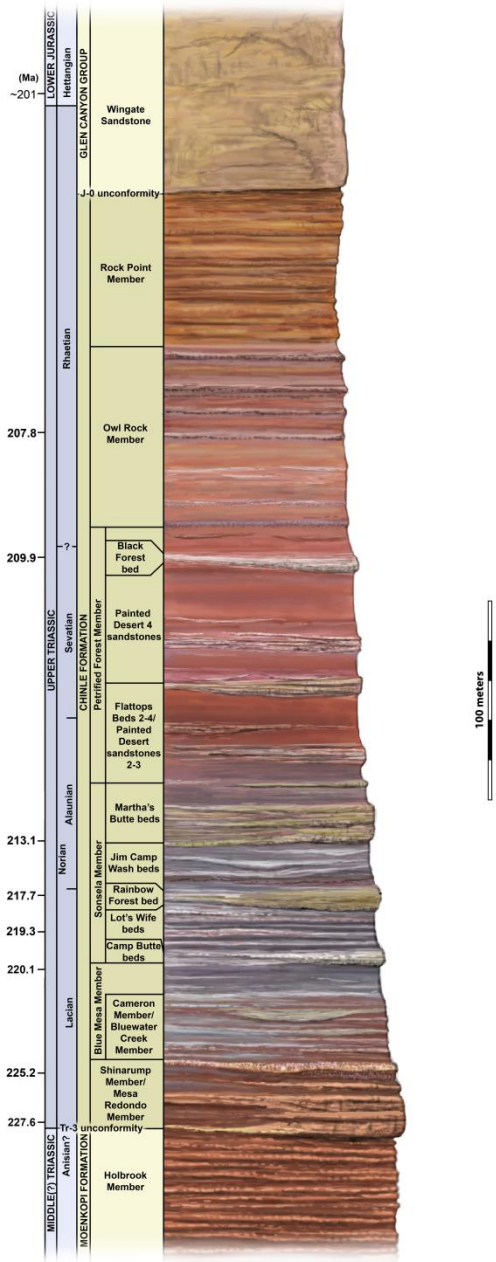

Figure 92 Composite lithostratigraphical model for the Chinle Formation at the PEFO in Arizona. Age model is after Ramezani et al (2011, 2014). Modified from Reichgelt et al. (2013).

3. Methodology

Sampling

The depositional setting and lithology have a great control over the likelihood of preservation of palynomorphs (Traverse 2007). Palynomorphs have the size range between silt-and fine sand (5-500 µm) and they tend to settle out in low energy depositional settings, in fine grained sediments (Traverse 2007). Therefore, the samples are collected preferably from siltstone or mudstone horizons. As the palynomorphs consist of organic molecules, their preservation may be affected by sub-aerial oxidation of organic matter, or a very basic environment. Rock types which are considered to bear rich palynomorph assemblages are deposited in reducing environments. Generally, they are very scarce in red beds (red-purple sediments with ferric oxides) or coarse-grained sediments (Traverse 2007).

From the Chinle Formation, 86 samples were collected from 12 outcrops at the PEFO. The samples were preferentially collected from mudstone or very fine sand intervals that were considered to bear rich palynomorph assemblages. Thirty-nine samples from the Sonsela Member had previously been analysed by Reichgelt et al. (2013). For the present study, an additional 47 samples were processed for palynological analyses. Additionally, the slides of Reichgelt et al. (2013) were re-investigated.

In the study on British Carnian successions a total of 104 samples were processed for palynological analysis from four successions within the Mercia Mudstone Group in South Devon and Somerset, SW England: 56 samples were collected from the Strangman's Cove outcrop located between Sidmouth and Seaton along the coastal cliff in Devon. Thirty-four samples were analysed from the Wiscombe Park-1 borehole located *ca.* 5 km inland from the Strangman's Cove coastal outcrop. Palynomorph assemblages of the Wiscombe Park-1 core were extracted from the same sample set as in Miller et al. (2017). In Somerset, three outcrops were sampled: Sutton Mallett (north of Bridgwater, four samples), Lipe Hill (between Taunton and Wellington, ten samples) and the Knapp Quarry locality (seven samples).

From the Alpine Tethys realm, 83 samples were collected from three boreholes (Mencshely-1, Veszprém-1 and Zsámbék-14) from the Transdanubian Range, western Hungary. Palynomorphs were extracted from the same samples set as in Rostási (2011) and Rostási et al. (2011).

Extraction of the palynomorphs

The standard technique for the extraction of palynomorphs from sedimentary rocks uses acid digestion of the mineral matrix followed by gravity separation of the organic particles and followed eventually by oxidative maceration (e.g., Wood et al. 1996). In the Palynological Laboratory of the University of Oslo the processing technique follows as described in Kuerschner et al. (2007). The outcrop samples were cleaned in order to remove the contamination and then dried in on oven at 60° overnight. Depending on the lithology, five to twenty grams of sediment were crushed. To calculate palynomorph concentration, one tablet containing *Lycopodium* spores (*ca.* 12000 grains per tablet) was added to each sample at the start of processing. All samples were treated with 10% HCl to dissolve the carbonate fraction. To dissolve the silicates, the samples were treated with concentrated HF and left in the acid

solution on a shaking table overnight. After decanting the supernascent liquid, 37% HCl was added to neutralize the HF. The HF step was repeated following neutralisation of each sample. In 2016, a water bath for hot acid treatment was installed in the Palynological Laboratory to accelerate the procedure. Subsequently, after the 10% HCl digestion and neutralisation, each sample was left in hot concentrated HF (65°C) in a water bath for two days.
To retrieve particles between 15 µm and 250 µm (the main size range of Mesozoic pollen and spores) the organic residue was sieved with a 250 µm and a 15 µm mesh. To separate mineral contaminants (e.g., pyrite) from the organic particles, heavy liquid $ZnCl_2$ (density 2.9 g/cm^3) was added to the organic residue between 250 µm and 15 µm and left overnight. The density (specific gravity) of pollen is less than that of clastic materials, so the heavy liquid with a higher specific gravity floats pollen and spores, while the clastics sink. As a result, the organic particles floated on top and could be extracted with a pipette. The organic residue was thoroughly neutralized and sieved before mounting. Slides were mounted using epoxy resin (Entellan). Many samples from the Hungarian Zsámbék-14 borehole were further treated with 10% sodium hypochlorite for 12 hours to decrease the high amount of amorphous organic matter (AOM) according to the method of Eshet & Hoek (1996). Unfortunately, the bleaching procedure was not successful and the amount of AOM didn't change a lot. The rock samples, organic residues and palynological slides are stored at the Department of Geosciences, University of Oslo (UiO), Norway. The final repository of the samples from the Chinle Formation will be the Petrified Forest National Park; they are temporally on loan at the UiO.

Microscopy analysis

Microscopy analysis was carried out at the UiO with a standard Zeiss trinocular No. 328883 type microscope connected to an AxioCam ERc5s camera and Zen 2011 software. In each sample, at least 300 terrestrial palynomorphs (spores and pollen) were identified (quantitative analysis). The relative abundances were plotted against depth with Tilia/TiliaGraph computer program (Grimm, 1991–2001) or C2 (Juggins 2007) and stratigraphically constrained cluster analysis CONISS built in Tilia was used to define palynomorph assemblages (Grimm 1987). For plotting the Tilia diagram, the counted abundance data of all identified taxa were used; unidentified forms and aquatics were excluded from the cluster analysis. *Lycopodium*, undetermined palynomorphs and aquatic palynomorphs were counted concomitantly but excluded from the palynomorph sum in each sample. Palynomorph concentration were calculated based on the counts of the identified palynomorphs, number of encountered Lycopodium grains, the dry weight of the sample, and the total number of grains in the Lycopodium tablet according to the equation of Maher (1981):

$$conc.per\ gram\ of\ sediment = Lycopodium_{total} \times particles_{counted} / Lycopodium_{counted} \times dry\ weight[g]$$

After encountering at least 300 terrestrial taxa all remaining slides were scanned for rare taxa (qualitative analysis). Spore Coloration Index (SCI) values follow those of Batten (2002).

Palynofacies

For palynofacies analysis different types of sedimentary organic matter (SOM) particles were distinguished in the samples. The subdivision of the different groups and terminology follows Oboh-Ikuenobe & de Villiers (2003). Approximately 300 SOM particles were counted in each sample. Variations in the amount of the various SOM group is illustrated in an abundance/depth plot with depth with Tilia/TiliaGraph computer program (Grimm, 1991–2001) or C2 (Juggins 2007). In **Paper 2**, variations in the amount of terrestrial input is shown using the phytoclasts=cuticles+plant tissues+wood fragments, AOM=amorphous organic matter and marine palynomorphs ternary diagram modified from Tyson (1995). The terrestrial/marine ratio represents the ratio of terrestrially derived palynomorphs (spores, pollen, freshwater algae) and marine palynomorphs (dinocysts, acritarchs, foraminiferal test linings, prasinophytes, scolecodonts) encountered during the palynofacies analysis.

Sedimentary organic Particles (SOM)	Description
Amorphous organic matter (AOM)	Structureless, irregularly shaped, fluffy yellowish-brown to black masses that can be derived from the degradation of terrestrial or marine organic matter
Charcoal/black debris	Totally opaque particles with variable shape and size. They are derived from highly oxidised wood or other plant debris.
Structured translucent plant debris	Structured transparent particles with yellow-green to brown colour. They may be derived from degraded plant tissues or wood. They are of various shape and size including lath-shaped and equidimensional particles.
Cuticles	Epidermal cells of higher plants, leaves and stems, often pale yellow to pale brown in colour. They typically possess rounded or polygonally-shaped cells.
Wood fragments	Structured lath-shaped or usually blocky particles, varying from pale yellow to brown in colour, often with cellular structure.
Spores	A general term for the spores of iso- and for the smaller spore for the heterosporous plants, from which the microgametophyte develops
Pollen grains	Male reproductive organs of the seed plants
Freshwater algae	*Botryococcus, Plaesiodictyon moesellanum*
Resin	Translucent, colourless or yellow to red, globular particles, angular fragments or bubbly masses, produced by higher land plants

Table 1: Summary of palynofacies terminology. The terminology used is from Oboh-Ikuenobe and de Villiers (2003).

Scanning and transmission electron microscopy (SEM and TEM)

SEM and TEM were applied in the morphological and ultrastructure study of *Froelichsporites traversei* tetrads (**Paper 4**). The tetrads were handpicked with an eyelash tool from the organic residue and dehydrated in a series of ethanol solutions with increasing concentration

(50%, 70%, 90%, and 100% ethanol solution). The tetrads stayed in each solution at least 30 minutes before being transferred into the next solution with a higher concentration. Plant remains must be preserved by dehydration for observation in an electron microscope because the coating system and the microscopes operate under high vacuum and most specimens cannot withstand water removal by the vacuum system without distortion. The dehydration procedure helps avoiding shrinkage during drying and preserves the morphology. The tetrads were placed on stubs and coated with gold with a Quorum Q150RS sputter-coater. SEM images were taken with a Hitachi SU5000 SEM at the Department of Geosciences, University of Oslo. Images were taken with an accelerating voltage at 5 kV.
For TEM studies, handpicked *F. traversei* tetrads were embedded in 0.1% agar (0.1 g of agar-agar powder dissolved in 10 mL of Milli-Q water) and dehydrated with 100% ethanol and propylene oxide. As embedding medium, Spurr replacement ERL 4221 was applied, and the infiltrated blocks were polymerized at 60°C for at least 48 h. Sectioning and preliminary TEM analyses were carried out at the Department of Animal and Plant Sciences, University of Sheffield. Approximately 85-nm-thick sections were cut by a diamond knife and a Leica UC-6 ultramicrotome. The sections were picked up on 400-mesh copper grids. Two additional blocks were sectioned at the Electron Microscopy Laboratory of the University of Oslo with a Leica ultracut UCT microtome. The sections were picked up on 75-mesh copper grids, and they were viewed on a JEOL 1400plus TEM. The sections have not been stained.

Bulk organic carbon isotopes ratios ($\delta^{13}C$)

The carbon isotope composition of bulk organic matter has been explored since the 1970s for carbon isotope stratigraphy, and to provide information on the history of the carbon cycle (Sharp 2007). The notation $\delta^{13}C$ expresses the ratio of the stable isotope ^{13}C to the lighter ^{12}C in relation to an international standard. The standard established for stable carbon isotope ratios was the Cretaceous Pee Dee Belemnite (PDB) with high $^{13}C/^{12}C$ ratio (Sharp 2007). The international standard was replaced with the Vienna PDB after the original reference material had been exhausted. Isotope ratios are reported in standard delta notation relative to the Vienna PDB ($\delta^{13}C$), calculated according to the following equation:

$$\delta^{13}\mathrm{Corg} = \left[\frac{\left(\frac{^{13}\mathrm{C}}{^{12}C_{sample}}\right) - \left(\frac{^{13}\mathrm{C}}{^{12}C_{standard}}\right)}{\left(\frac{^{13}\mathrm{C}}{^{12}C_{standard}}\right)} \right] \times 1000\ [‰]$$

The notation is expressed as parts per thousand.
During the fixation process (e.g., photosynthesis) organisms preferentially include the lighter carbon isotope (^{12}C) into their biomass (Arens & Jahren 2000). The $\delta^{13}C$ values associated with land plant-derived organic matter present in sedimentary rocks ($\delta^{13}C_{bulk}$) represents the average isotopic composition of plant components preserved in the sediments (Arens & Jahren 2000). Local environmental parameters like light, water availability, salinity and

global changes of atmospheric CO_2 concentration, are considered the primary factors affecting the carbon isotopic composition of vascular plants (e.g., Gröcke 1998).

From the Chinle Formation, the carbon isotopic composition of bulk organic matter was analysed for a total of 23 samples. Four to six grams of sediment was crushed and powdered then treated with 1 M HCl and left for 24 h to remove all inorganic carbon. Afterwards the samples were neutralized with water and dried at 60°C in an oven. The homogenised samples were analysed with Elemental Analyser- Isotope Ratio Mass Spectrometer (EA-IRMS). The measurements were carried out by Iso Analytical Ltd, The Quantum, United Kingdom. The analytical precision indicates a standard deviation of <0.08‰ based on the routine analysis of internal laboratory reference. IA-R001 wheat flour was used as reference material ($\delta^{13}C_{V\text{-}PDB}$=-26.43‰).

Isotope analysis of the British Carnian successions was performed at the GeoLab, University of Utrecht, Department of Earth Sciences. A total of 36 samples from the Strangman's Cove outcrop were homogenized and treated sequentially with 0.1M and 1M HCl for 24 hours, before being rinsed to neutrality with MilliQ water (18.2 MΩ cm) and drying at 40°C for 4 days. Each step, involving a change of reagent or water, was preceded by centrifugation (10 min at 1500 rpm) to prevent the loss of fine material in suspension. Samples were first measured for % TOC using a Fisons NA1500 NCS and then for isotopes using the Fisons NA1500 NCS coupled with a Thermo Delta plus IR-MS. Ratios were normalised using the laboratory standard GQ (a powdered Graphite-Quartzite). The precision obtained for repeat analysis was better than ± 0.19‰ (1σ).

Hygrophyte/xerophyte ratio

Dispersed palynomorphs can be classified as hygrophyte or xerophyte according to the concept of Visscher & van der Zwan (1981) which is based on the known or supposed botanical affinity and ecological needs of the parent plant. It can be regarded as the first approximation of climatic signal, yet it should be applied with caution as the exact botanical affinity and ecological needs of many Mesozoic dispersed spore and pollen are still uncertain. In addition it is more likely that plants cover the whole spectrum from arid to humid conditions and cannot simply classify as either hygrophytic or xerophytic (Muller et al. 2016b).

All spores are regarded as hygrophytes. The bisaccate *Alisporites* is considered as a transitional element in the sense of Visscher & van der Zwan (1981), but some works assign it to hygrophytes (e.g., Roghi et al. 2010; Whiteside et al. 2015; Mueller et al. 2016a). All other bisaccate pollen, monosaccate pollen and the members of the Circumpolles are in the xerophyte group (e.g., Hochuli & Vigran 2010; Roghi et al. 2010; Mueller et al., 2016a, b). Pollen of the cycads *Cycadopites* sp. and the Bennettitalean *Aulisporites astigmosus* are generally assigned to the hygrophyte pollen (Roghi 2004; Roghi et al. 2010). Gnetalean pollen grains (e.g., *Ephedripites* sp., *Cornetipollis*, *Equisetosporites chinleana*) are in the xerophyte group (Hochuli & Vigran 2010).

SEG method

The sporomorph ecogroup (SEG) method of Abbink (1998) and Abbink et al. (2004) was applied to distinguish plant communities based on dispersed palynomorphs in **Papers 1-2**. The method assigns the dispersed spores and pollen to various habitats based on the known or presumed parent plants and the transport mechanisms characteristic for palynomorph types. The original SEG method was established for Jurassic-Cretaceous assemblages, but several workers have applied the method to Triassic palynomorph assemblages (e.g., Götz et al. 2009, 2011; Kustatscher et al. 2012; Paterson et al. 2016). In the present study four terrestrial SEGs (habitats) are distinguished: river SEG, dry and wet lowland SEG and upland SEG. The upland SEG was modified by Kustatscher et al. (2012) to a more general hinterland SEG to incorporate pollen from plants growing permanently above groundwater level on well-drained terrains. The river SEG reflects riverbank communities that are periodically submerged, the dry lowland SEG reflects floodplain vegetation episodically submerged, wet lowland SEG represents marshes and swamps and the hinterland SEG reflects plant communities on well-drained terrains, above groundwater table. The coastal SEG incorporates coastal communities, never submerged but under constant influence of salt spray.

Multivariate ordination techniques

Paleontological data sets mainly based on fossil occurrences or morphology, often have high dimensionality. Multivariate ordination methods like principal components analysis (PCA) or correspondence analysis (CA) can simplify multivariate data into low dimensional graphical space (Kovach 1993; Hammer et al. 2001). Ordination groups multiple variables, so that variables with similar values are near each other and dissimilar objects are farther from each other. Their relationship, similarity-dissimilarity is characterized numerically and/or graphically and then usually plotted on several axes (Hammer et al. 2001).

PCA (**Paper 2**) is a standard method for reducing the dimensionality of morphometric and ecological data. It is produced for identifying the most important hypothetical gradients (components) that account for the variance in a multidimensional data set (Harper 1999). The PCA routine finds the eigenvalues and eigenvectors of the variance-covariance matrix. The eigenvalue gives the measure of the variance accounted for by the corresponding components (eigenvector), which is also displayed as the percentages of variance accounted for by each of these components (Harper 1999). The principal components are illustrated graphically on several axes with a scatter plot of the data point and variables (Harper 1999). The contribution of each of the original variables (e.g., species, taxa) to these trends can be determined by studying the component loadings i.e. species scores on each axis (Kovach 1993). Component scores i.e. sample scores, are derived from the component loadings and the original data, so that the highest and lowest scores indicate samples containing the most influential taxa for that axis (Kovach 1993). In palaeo-ecological studies, sample scores are often plotted against depth or time to study variations in the influence of the corresponding components i.e. trends in the environmental factor represented by the components (e. g., Kovach & Batten 1994; Bonis & Kürschner 2012).

Correspondence analysis (CA) in **Paper 3** compares associations containing counted data (Hammer et al. 2001). The primary goal of CA is to illustrate the most important relationships

among the variables in a contingency table (rows and columns of the data set) (Kovach 1993). It displays the data as points in a low dimensional space represented by the axes of the scatter plot.

4. Summary of the research articles

4.1. Paper 1

Baranyi, V., Miller, C.S., Ruffell, A., Hounslow, M.W. & Kürschner, W.M. A continental record of the Carnian Pluvial Episode (CPE) from the Mercia Mudstone Group: palynology and climatic implications *(submitted to the Journal of the Geological Society)*

The study analysis the palynological record of the Carnian Pluvial Episode (CPE) in a fully continental setting, from the Mercia Mudstone Group, SW UK. Quantitative palynological data revealed palaeoclimate trends, and palynostratigraphy integrated with bulk organic carbon isotope data enabled the correlation to other Carnian successions.

Four outcrops and the Wiscombe-Park 1 borehole were sampled for palynological analysis from the South Devon coastal area and Somerset (Wessex Basin, SW UK). A total of 104 samples were processed. The bulk organic carbon isotope composition was analysed for a total of 36 samples of the Strangman's Cove coastal outcrop (South Devon). Isotopic measurements for the Wiscombe Park-1 borehole were available from Miller et al (2017).

Major findings

- The palynological assemblages in South Devon and Somerset yield typical Carnian palynofloras and contain predominantly Circumpolles pollen, monosaccate and bisaccate pollen grains. *Aulisporites astigmosus* is recorded only sporadically and almost exclusively in the Sidmouth Mudstone Formation in South Devon.
- The palynological assemblages contain primarily the pollen related to the hinterland vegetation elements and reflect the regional pollen rain. Spore producing plants, pollen of cycads and the Bennettitales representing the local, or extra local vegetation are less abundant.
- In all studied sections, the xerophyte pollen types (in the sense of Visscher & van der Zwan 1981) are predominant. The hygrophyte/xerophyte ratios increase only in the samples from the isolated greenish grey mudstones of the Sidmouth and Branscombe Mudstone Formations.
- Three significant negative carbon isotope excursions are recorded in the Dunscombe Mudstone Formation in the Strangman's Cove Outcrop which could be correlated to the isotope excursions of the Wiscombe Park-1 borehole (Miller et al. 2017) based on palynostratigraphy and characteristic marker beds.

- In the Somerset outcrops, Lipe Hill and Sutton Mallett, several acritarchs are recorded. Some of them are clearly reworked indicated by dark wall and damaged body. However, some specimens show no sign of reworking.

Based on the palynological assemblages and the chemostratigraphy, the stratigraphical range of the Dunscombe Mudstone Formation in South Devon can be extended down into the Julian in contrast to the previous Tuvalian age assignment (e.g., Clarke 1965; Warrington 1970; Warrington et al. 1980; Barclay et al. 1997) while the assemblage from the overlying Branscombe Mudstone Formation is most likely Tuvalian based on the co-occurrence of *Brodispora striata* and *Partitisporites quadruplices*. In Somerset, the Lipe Hill locality contains Julian palynoflora. The presence of *Riccisporites tuberculatus* indicates already Tuvalian age for the Sutton Mallett section in Somerset.

Despite the evident lithological switch from red to greenish-grey mudstone into the base of the Dunscombe Mudstone Formation plausibly indicating climate change (Porter & Gallois 2008); a clear humidity signal related to the Carnian Pluvial Episode in the late Julian is missing in the palynological record. The quantitative palynological record suggests the predominance of xerophyte floral elements only with a few horizons of increased hygrophytes. The lack of humid signal might be related to the palaeogeographical setting of NW Europe during the Late Triassic. The study area was at *ca.* 30°N within the dry climate belt and with perhaps very little and highly seasonal annual rainfall (Kutzbach & Gallimore 1989; Parrish 1993; Sellwood & Valdes 2006; Vollmer et al. 2008). The strongly seasonal precipitation prohibited the development of extensive wetland vegetation and the preservation of spores and pollen grains. The wetter periods that developed regionally in the Carnian because of the CPE were perhaps still too short or dry in the UK to sustain the proliferation of "permanent" hygrophyte vegetation (e.g., ferns, Bennettitales). Secondly, the humid signal might be masked due to the overrepresentation of regional pollen rain and the predominance of xerophyte hinterland floral elements. The *Aulisporites*- and spore-dominated assemblages are confined to local wet habitats as suggested by Visscher et al. (1994) in the case of the Schilfsandstein. The isolated horizons from the Branscombe and Sidmouth Mudstone Formations likely represent these spatially restricted locally wet spots with higher representation of local pollen rain. The bias towards regional pollen rain is further enhanced by the possible increase in continental runoff related to regional seasonal moist pulses during the CPE. However, the prevailing "background" climate was probably drier. Evidence of

more humid climate can be perhaps inferred from the abundance of the *Alisporites* group. *Alisporites* species have been assigned to transitional and/or hygrophyte groups (e.g., Visscher & van der Zwan, 1981; Whiteside et al. 2015; Lindström et al. 2016; Mueller et al. 2016a, b). The increase in the total *Alisporites* and total spore abundance in the lower part of the DMF in the Strangman's Cove section coincides with a peak in freshwater algae (*P. mosellanum*) in the lacustrine facies of the Lincombe Member in South Devon. This increase in algae suggests expansion of the lacustrine facies, hence can be linked to a climatic interval with a relatively more humid season.

The acritarchs recorded in Somerset would indicate possible marine incursions, but the most plausible explanation is that the acritarchs are reworked and transported to the lakes during episodic flash floods or they have arrived in far-travelled eolian dust, in part sourced from marine aerosols, as occurs in modern desert settings as suggested by Hounslow & Ruffell (2006).

4.2. Paper 2

Baranyi, V., Rostási, Á., Raucsik, B., Kürschner, W.M. Climatic fluctuations during the Carnian Pluvial Episode (CPE) in marine successions from the Transdanubian Range (western Hungary) inferred from palynology *(to be submitted)*

The study analyses the palynological record of a CPE in marine successions of the Tethys realm from the Transdanubian Range (TR), western Hungary. During the Late Triassic the Transdanubian Range formed a segment of the passive western Neotethys margin and was situated between the Northern Calcareous Alps and the Southern Alpine units. In the late Julian a thick marl series (Veszprém Marl Formation) was deposited in the TR replacing a carbonate-dominated succession which has been related to the CPE. In order to reveal the vegetation changes and climate trends, three borehole sections have been selected for palynological analysis. A total of 83 samples were processed from the boreholes: Mencshely-1 (Met-1), Veszprém-1 (V-1) both in the Balaton Highland in the southern part of the TR, and the Zsámbék-14 (Zs-14) in the Gerecse Hills, NE part of the TR. To trace climatic variations on land, we compared the palynological data to the existing clay mineral record of Rostási et al. (2011) and geochemical weathering indices α^{Al}_{Ba}, α^{Al}_{K} and α^{Al}_{Na}.

Major findings

- Three local palynomorph assemblages are distinguished: *singhii-acutus-vigens* in the lowermost part of the studied succession, lower part of the Veszprém Marl Formation (Met-1/373.9–267.2 m, V-1/549-578, the *acutus-vigens-maljawkinae* (Met-1/215-69.8 m, V-1/541-485 m) and the *Aratrisporites-astigmosus-densus* in the uppermost part of the Veszprém Marl Formation (V-1/334.6-352-353 m). Dinocysts have never been found before in the Carnian of the TR. In the present study two dinocyst taxa are recorded: dinocyst indet and *Heibergella* sp (**Photoplate 12, see Appendix**).
- The application of the sporomorph ecogroup analysis (SEG method) reveals the overall dominance of the hinterland SEG and the dry lowland SEG. The abundance of wet lowland SEG and riverine SEG elements arises only in the lowert and uppermost part of the Veszprém Marl Formation.
- The humidity signal is described using the ratio of hygrophyte and xerophyte palynomorph groups and multivariate ordination method (PCA). The hygrophyte/xerophyte

ratio has a peak in the lowermost part of the Veszprém Marl Formation with very high values in the uppermost part of the studied section.

- The palynological data is compared to the clay mineral record of the same sections from Rostási et al. (2011) and weathering indices: α^{Al}_{Ba}, α^{Al}_{K} and α^{Al}_{Na}. The α indices have highly variable values in the studied sections. They suggest enhanced continental hydrolysis only in the lower part of the Veszprém Marl Formation.

In the lower part of the Veszprém Marl Formation in the early Julian 2, the increase in the hygrophyte vegetation elements is coincident with elevated kaolinite and partially higher α values indicating strong terrestrial runoff and intense chemical weathering. The upper marl unit of the Veszprém Marl formation in the late Julian 2 points to the renewal of the siliciclastic influx and the high amount of hygrophyte in the palynological assemblages would point to a second humid episode and the expansion of wet lowland and riverine habitats. However, the clay mineral profile and weathering indices indicate stronger seasonality and diminished continental weathering. The increase in the hygrophytes can be also linked to a sea level low stand, or the northward migration of the TR closer to the coastal areas in the Northern Calcareous Alps (e.g., Lunz). Alternatively, the established lowland vegetation (lowland, riverine, coastal SEG elements) trapped some of the sediment influx affecting also the clay mineralogical record. The palynological assemblage from the early Tuvalian Csákberény Formation consists of predominately xerophyte pollen types together with the low kaolinite values suggesting the return to drier climate during the early Tuvalian.

The distinct clastic pulses documented in other areas of the western Tethys during the CPE by Roghi et al. (2010) can be recognized in the TR as well. Three intervals are distinguished: the Mencshely Marl Member correlates to the first clastic episode known from the Dolomites and Julian Alps (Roghi et al. 2010), the top of the Mencshely Marl and the Csicsó Marl Member probably include both the second and third pulse, and they can not be separated in the TR. The last interval with enhanced terrestrial input is located in the upper part of the Sándorhegy Formation in the Balaton Highland and the upper part of the Csákberény Formation in the Gerecse Hills from the early Tuvalian which probably correlates to the fourth clastic pulse in the Dolomites and the third shale of the "Raibler Schichten". Although, the clastic pulses in the western Tethys were related primarily to more humid climate the comparison to clay mineralogy and weathering proxies suggest a more complicated scenario in the TR, Hungary.

The palynological and geochemical record is clearly influenced also by other environmental parameters e.g., sea level changes, currents or basin topography.

4.3. Paper 3

Baranyi, V., Reichgelt, T., Olsen, P.E., Parker, W.G. & Kürschner, W.M. 2017. Norian vegetation history and related environmental changes: New data from the Chinle Formation, Petrified Forest National Park (Arizona, SW USA). GSA Bulletin, Published Online First, https://doi.org/10.1130/B31673.1

In this study, palynological assemblages of the Chinle Formation were analysed from the Petrified Forest National Park (PEFO), Arizona to reconstruct the plant communities and vegetation changes. The emphasis was to evaluate floral turnover patterns during the Norian stage that is marked by a series of environmental perturbations in western equatorial Pangea including a shift to drier climate (Mid Norian Climate Shift), carbon cycle perturbation, volcanism, changes in the tectonic regime in the western part of the North American continent and a probable impact event.

Eighty-six samples were collected for palynological analysis from 12 outcrops at the PEFO spanning the Blue Mesa, Sonsela and Petrified Forest Members. The bulk organic carbon isotope composition was analysed for a total of 23 samples.

Major findings

- A palynological analysis of the Blue Mesa, Sonsela and Petrified Forest Members of the Norian Chinle Formation reveals four distinct palynofloras (assemblages 1-4).
- *Perinopollenites elatoides* is recorded the first time from the Sonsela Member, in the middle part of the Chinle Formation.
- The palynological assemblages contain predominantly pollen types with xerophyte affinity and only two distinct intervals are recorded with elevated hygrophyte/xerophyte ratio: The first is recognized in the middle of the Sonsela Member (Badlands section, samples BL 3-4). The second horizon with higher hygrophyte/xerophyte ratio is confined to the topmost part of the Sonsela Member (sample TH 10).
- Palynological analysis reveals that the floral turnover is followed by a severe drop in the diversity and abundance almost in all palynomorph groups except for *Klausipollenites gouldii*. After the turnover, the flora is associated with increased abundance of the *Patinasporites* pollen group (*Patinasporites*, *Daughertyspora chinleana*, *Enzonalasporites*), *Klausipollenites gouldii*, the enigmatic pollen *Froelichsporites traversei*, while the abundance of seed fern related bisaccate pollen (e.g., *Alisporites*, *Protodiploxypinus*, *Pityosporites*) strongly decreases.

- The turnover is also associated with a re-organisation of the lowland riparian plant communities. A seed fern–Gnetales-(cycadophytes) dominated riparian vegetation in the lower Sonsela Member is replaced by a new community with ferns, lycopsids, Araucariaceae and Cupressaceae in the upper Sonsela Member with less seed ferns and cycads.
- An interval with the occurrence of aberrant *Klausipolleniets gouldii* morphotypes (e.g., with three airbags, monosaccate forms, or grains with split sulcus), is confined to the Badlands and Mount Lion Mesa sections close to the floral/faunal turnover horizon. In several samples, the ratio of aberrant pollen grains exceeds 10% of the total abundance of *K. gouldii*. To date, aberrant pollen grains are only known from the Sonsela Member, at the PEFO, within the complete Chinle succession. No other pollen grains are recorded with similar morphological variability.

The predominance of xerophytic plants in the palynological record is consistent with the gradual aridification of the present western USA, due to the uplift of the Cordilleran Arc and the northward shift of North America. However, the palynological record suggests that the gradual aridification was interrupted by at least two short-lived wetter climatic periods during the deposition of the Sonsela Member inferred from increase in the hygrophyte vegetation elements. The presence of relatively more humid periods is also supported by the mean annual precipitation (MAP) variations from paleosols as shown by Atchley et al. (2013) and Nordt et al. (2015).

The floral reorganization of riparian plant communities is attributed primarily to changes in fluvial styles, possibly linked to changes in tectonic regime of the hinterland and gradual climate change. Their presence of a well-developed late-successional stage riparian plant community in the upper Sonsela Member was supported by a shift from braided to meandering fluvial style and the stabilisation of floodplain areas during the mid Norian (e.g., Howell & Blakey 2013; Trendell et al. 2013b).

The comparison of palynofacies and bulk $\delta^{13}C_{org}$ showed that the isotope variations at PEFO are most likely controlled by the depositional setting and local changes in the composition of sedimentary organic matter. The samples with relatively low $\delta^{13}C_{org}$ are very rich in cuticles and resin fragments. Cuticles and resin fragments are rich in plant lipids with generally lower $\delta^{13}C_{org}$ than wood which could explain the lower $\delta^{13}C_{org}$ of these samples (e.g., Tappert et al. 2013). However, the effect of Norian global carbon cycle perturbations cannot be excluded entirely. Muttoni et al. (2014) showed a negative excursion recorded at ~216 Ma close to the

age range of the floral and faunal turnover in the Chinle. However, there is no compelling evidence to correlate the local isotope variations and any global signal to date.

Comparison of the pollen record from PEFO to a younger succession from the Chinle Formation in the Chama Basin, New Mexico (Whiteside et al. 2015; Lindström et al. 2016) suggests that there were two distinct floral turnovers during the Norian. Floristically, the turnover events at PEFO and the Chama Basin are very similar with a general decrease in abundance and diversity of hygrophytes and an increase in wind-blown xerophytes, such as the *Patinasporites* group and *Klausipollenites*. However, the amplitude of floral turnover in the Chama Basin was higher, which may indicate that the severity of environmental perturbations, especially shift to dry climate and seasonality became more pronounced during the Norian.

The high proportion of aberrant pollen grains at the PEFO can be related to certain climatic stressors, e.g., drought, heat, frost, pCO_2 perturbations, or atmospheric pollution (aerosols and acid rain) related to volcanic activity (e.g., Foster & Afonin 2005). However, the single occurrence of aberrant pollen in *Klausipollenites* implies that the formation of these unusual pollen types might be a taxon-specific response of the parent plants to the ongoing climate change.

The climate change and the shift towards drier conditions seems to be the most plausible explanation for the floral turnover at the PEFO during the middle Norian, but a series of other environmental perturbations e.g., increase in the pCO_2 (e.g., Cleveland et al. 2008 a, b., Atchley et al. 2013; Nordt et al. 2015; Schaller et al. 2015; Whiteside et al. 2015), volcanism (Atchley et al. 2013; Nordt et al. 2015) could have contributed to the vegetation change. It is also tempting to link the floral turnover to the Manicouagan impact event due to their close age range, but the existing data are unable to prove direct causality.

4.4. Paper 4

Baranyi, V., Wellmann, C.H. & Kürschner, W.M. 2017. Ultrastructure and probable botanical affinity of the enigmatic sporomorph Froelichsporites traversei from the Norian (Late Triassic) of North America. International Journal of Plant Sciences, 179, 100–114, https://doi.org/10.1086/694762

The enigmatic playnomorph *Froelichsporites traversei* is primarily known from the Norian sedimentary succession of North America (Chinle Formation and Newark Supergroup). Its most striking morphological features are the occurrence as permanent tetrads, one well-developed distal pore (ulcus) on each grain and the annulus-like exine thickening around the pores. The abundance of the species arose during the mid Norian environmental perturbations recorded in the Chinle Formation (Reichgelt et al. 2013; Whiteside et al. 2015; **Paper 3**). Despite the significance of the species in the Late Triassic of North America and its peculiar morphological features, the botanical affinity is still unclear. In this study, the wall ultrastructure of *F. traversei* was analysed for the first time by transmission electron microscopy (TEM). Wall ultrastructure analyses of fossil dispersed spores and pollen grains can provide useful insight into the botanical affinity of dispersed palynomorphs and reveal relationships between plant groups (Doyle 2009).

Findings

- Three tetrads have been sectioned and studied in total.
- The wall *F. traversei* consists of two layers and an innermost faint discontinuous lamination (**Photoplate 4, see Appendix**). The outermost layer has a homogeneous texture, while the inner layer has a granular texture. The laminae below the granular layer are not continuous but directly contiguous with the granules.

The wall ultrastructure of *F. traversei* suggests that it represents a pollen type with gymnosperm affinity. The preserved layers of the wall can be interpreted as follows: the outer homogeneous and inner granular layer can be interpreted as the sexine. The homogeneous outer layer represents the tectum, and the granular layer is the infratectum. The faint lamination below the granular layer might be related to the nexine.

There is no other known gymnosperm pollen type with the same ultrastructure pattern, therefore the botanical affinity cannot be determined precisely based exclusively on the wall-

ultrastructure. Mesozoic gymnosperm pollen grains usually have stratified sporoderm with sexine and well-developed nexine. The lack of a real nexine in *F. traversei* might suggest early ontogenetic stage of the tetrad; however, the outer sporoderm layers indicate full development. The distal pore (ulcus) on each grain might represent a germinal aperture or a rehydration pore like that of the Cupressaceae pollen. The occurrence as permanent tetrads may be related to polyembryony or polyploidy, and they probably provided an adaptive advantage to the parent plant during the Norian environmental crisis in North America.

4.5 CPCP core (Colorado Plateau Drilling Project, core PF 1)

The original PhD project plan submitted in 2014 included the detailed palynological analysis of borehole material from the Chinle Formation at the Petrified Forest National Park, SW USA drilled in the framework of the Colorado Plateau Drilling Project (funded by the United States National Science Foundation and the International Continental Scientific Drilling Program) (Olsen et al. 2010 and *Olsen et al. submitted*). Two continuous (520 m and 253 m deep) cores have been drilled since 2013 through the entire Triassic succession that were going to be studied in the present project. These new cores provide new reference section in which magnetostratigraphic, geochronological, environmental, and palaeontological data can be registered to aim the correlation between the Chinle Formation and the astrochronologically tuned Newark Supergroup to facilitate evaluation of Late Triassic biotic changes. The cores were drilled in November and December of 2013. In April 2015 a total of 258 samples were collected for palynological analysis and organic geochemistry during a sampling party at the Rutgers University Core Repository. The 520 m-deep first core (CPCP PFNP13-1A) penetrated predominantly red, reddish brown sandstone, red-purple mudstone succession. Grey, greyish green, and purplish grey mudstone sequences were limited to a *ca.* 100 m thick interval within the Blue Mesa Member. Even these lithologies were characterized by frequent reddish-purple or yellow mottling and root halos. A total of 42 samples were processed, many from grey mudstones within the Blue Mesa Member. Unfortunately the rock samples did not yield any palynomorph assemblages and contained only scarce plant remains, charcoal particles and amorphous organic matter (Fig. 13). For the anticipated compound specific carbon isotope analysis, n-alkanes were found only in a very low amount in these samples possibly as the result of soil organic matter degradation. Furthermore, low concentrations *n*-alkanes were also in the bentonite additive and possibly in the drilling fluid additive that may have introduced organic contamination into any of the 1A core samples, although contamination should have been minimized because of standard sample preparation protocol. A contribution from migrated Paleozoic hydrocarbons is also possible as evidenced by common hydrocarbon shows in nearby exploratory wells (Heylmun 1997; Rauzi 2000; Schwab et al. 2017). The core materials turned out to be unsuitable for the planned palynological analysis and geochemistry which required the deviation from the original research plan (Figs 14-15).

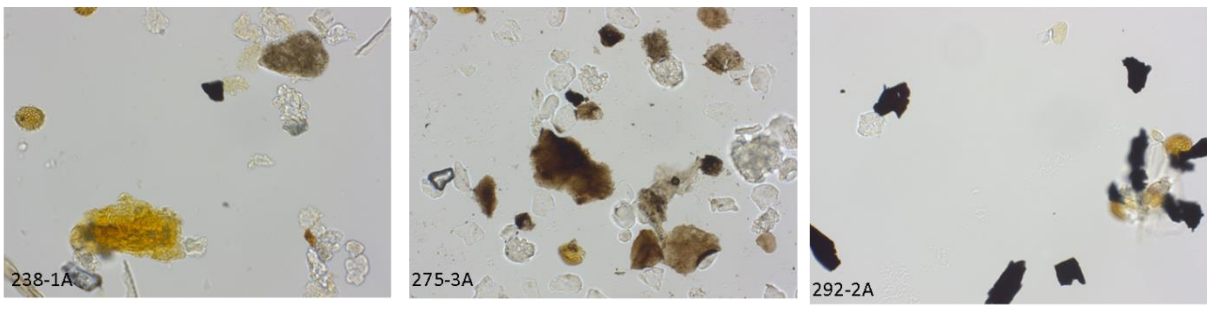

Figure 13: Microscopic images of the palynofacies from three sampels of the CPCP core 1.

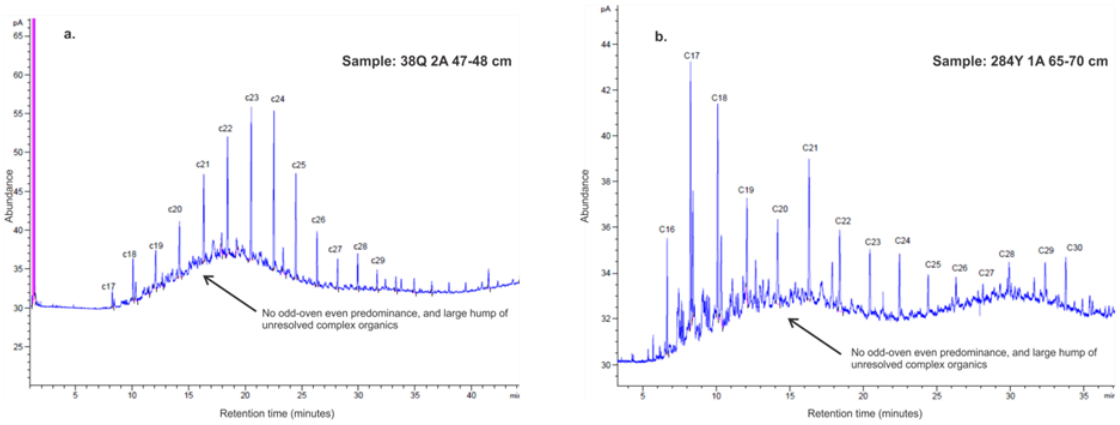

Figure 14 GC chromatogram traces for the ICDP core from PF National Park samples 38Q 2A 47-48 cm and 284Y 1A 65-70 cm. A) Trace of 38Q 2A 47-48 cm from detector 1, showing no odd over even predominance of n-alkanes and a large hump of unresolved organic compounds, possibly due to organic degradation. B) Trace of 284Y 1A 65-70 cm from detector 1, showing low abundance of organics, and mostly short chain n-alkanes. With the courtesy of C.S. Miller.

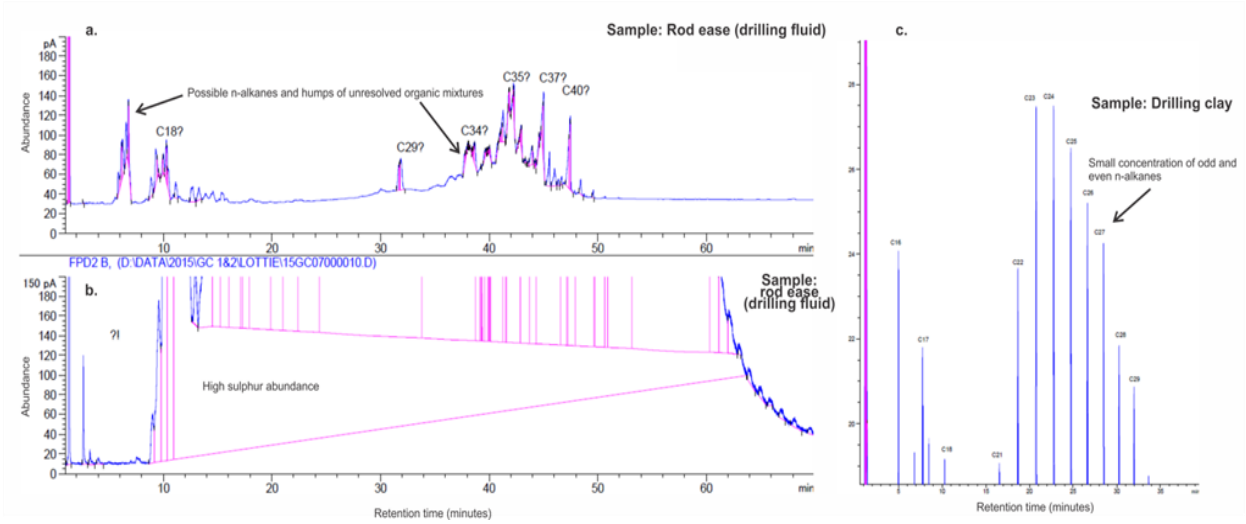

Figure 15 GC chromatogram traces for samples of the drilling materials used in the ICDP PF core extraction. A) Trace of rod ease (drilling additive) from detector 1, showing a high concentration of organics, possibly lipids. B) Trace of rod ease (drilling fluid) from detector 2, showing high concentration of elemental sulphur. C) Trace of bentonite additive from detector 1, showing small concentration of both long and short chained n-alkanes. With the courtesy of C.S. Miller.

Synthesis and concluding remarks

The research project aimed at reconstructing the impact of Late Triassic environmental changes and climate variations on the vegetation from palynological data. Two intervals have been chosen: the "mid Carnian" with the most pronounced humid episode throughout the entire Triassic termed as Carnian Pluvial Episode (CPE). The two CPE study sites represent completely different palaeoenvironmental settings and deposition in different climate regimes which allows the evaluation of the impact and the extent of this humid episode on a wide scale. The British Carnian represents a terrestrial succession which was deposited in the dry continental interior of Pangea in an arid, sabkha environment with lacustrine and fluvial facies. The Hungarian Carnian successions were deposited in a carbonate-dominated setting with intraplatform basin divided by reefs in a tropical sea on the western rim of the Neotethys.

The second studied interval is the mid Norian, the Mid Norian Climate Shift which was associated with a long-term gradual shift to drier climate in western equatorial Pangea (Nordt et al. 2015).

Palynostratigraphy was an important tool in the stratigraphical subdivision of the terrestrial successions as key marine index fossils are absent in them. The British palynological assemblages integrated with chemostratigraphy aided the correlation to other CPE successions and contributed to the biostratigraphical subdivision of the British Carnian formations (**Paper 1**). However, the palynostratigraphical correlation faced a significant challenge, as the range of many age-diagnostic palynomorphs in NW and Central Europe don't have independent age constraints and the ranges might differ in various climate belts. The effect of climate and environment on the temporal and spatial distribution of palynomorphs is well documented by different stratigraphical ranges between North American and the European palynofloras. Many typical Carnian taxa from Europe were still present in the Norian of North America (Litwin et al. 1991; Lindström et al. 2016; **Paper 3**). Perhaps in the seasonally wet climate of western equatorial Pangea the parent plants of some typically Carnian taxa from Europe thrived longer at least in the early Norian and disappeared only later. The different stratigraphic ranges highlight the need for independent means of correlation in the future such as radiometric dating and magnetostratigraphy.

The palynological results from the UK during the late Julian are not entirely in agreement with a pronounced shift to more humid conditions. The lack of the climate signal might be related to a taphonomic bias due to the overrepresentation of the regional pollen rain which is

primarily the wind-blown pollen of conifers with high pollen production rate and xerophyte affinity. Furthermore, permanent hygrophyte vegetation has not developed perhaps due to the predominantly arid climate in inner continental Pangea. The climate trends during the CPE were perhaps more likely manifested in moist pulses, fluctuations between drier and somewhat more humid conditions while the prevailing climate was generally arid. One humid episode can be inferred perhaps from the simultaneous increase in the *Alisporites* (with transitional to hygrophyte affinity) in the regional pollen rain and freshwater algae indicating the expansion of the lacustrine facies and a slight shift to wetter conditions (**Paper 1**).

In the Carnian successions of the Transdanubian Range (TR), Hungary the carbonate factory was interrupted by several clastic pulses during the late Julian-early Tuvalian (**Paper 2**). The siliciclastic input resulted from an increase in terrigenous input perhaps related to enhanced continental runoff and wetter climate. The siliciclastic pulses in the TR can be correlated to the clastic events in other localities of the Alpine Tethys (Southern Alps, Dolomites) with the help of palynostratigraphy and selected pollen and spore assemblages. The lithological changes and the increase in hygrophytes during the late Julian in the TR suggest a more humid climate during the Julian 2, while the mineralogical data (clay minerals, weathering indices) imply that the continental hydrolysis and chemical weathering increased only in the early stages of the CPE in the early part of the late Julian. Variations in clay mineral composition can be also influenced by sea level, ocean currents, basin topography and proximal-distal trends that can influence the mineralogical data. So far, there has been relatively few clay mineralogy and weathering studies on CPE successions. Further studies are needed which can shed light on the cause of the different results. Towards the early Tuvalian, the abundance of hygrophyte palynomorphs decreased in the last clastic interval indicating the return to more arid conditions as seen also in the Alpine sections in Italy (Roghi et al. 2010) or Austria (Muller et al. 2016b).

The results from the British and Hungarian CPE successions emphasize that although the CPE is considered to be a global phenomenon, the environmental and biotic changes do not necessarily follow a uniform pattern. Local factors and palaeogeography exerted significant control on the manifestation of the CPE in various regions. Even in the case of the ongoing climate change and global warming in the modern times, local differences are expected. For instance, the warming caused only a small increase in the global net precipitation, but it led to drastic differences in the distribution of precipitation (Zhang et al. 2007). Climate models estimate that anthropogenic forcing contributed significantly to increases in precipitation in

the Northern Hemisphere mid-latitudes, drying in the Northern Hemisphere subtropics and tropics, and moistening in the Southern Hemisphere subtropics and tropics by moving the ITCZ position (Rotstayn & Lohmann 2002; Zhang et al. 2007). In the present day zonal climate pattern, between 25° and 35° latitudes, the climate may shift to arid/semi-arid during warm periods and to humid/semi-humid during cold periods, but at higher or lower latitudes the opposite happens (Zhang et al. 2007). It is thus possible to record even opposite trends at different latitudes during the same climatic episode (Zhang et al. 2007). In the Carnian, the picture might be more complicated due to the non-zonal (or at least poorly defined zonal climate) pattern compared to the modern times and the presence of "azonal effects" e.g., the Wrangellia LIP volcanism.

The Mid Norian Climate Shift is a more regional climate change which affected mainly the terrestrial ecosystems in western equatorial Pangea (**Papers 3-4**). The shift to drier climate was also observed on the eastcoast in the Newark Supergroup (Olsen & Kent 2000). The floral changes are associated with a long-term increase in the abundance of xerophyte pollen types and successive peaks of certain palynomorphs e.g., *Klausipollenites gouldii,* the enigmatic *Froelichsporites traversei* and the *Patinasporites* group. The gradual climate change was interrupted at least by two relatively more humid episodes during the Norian suggested by the higher hygrophyte ratios and the comparison to the published mean annual precipitation values of Nordt et al. (2015). The climate deteriorated during the Norian, it became drier and the seasonality increased resulting in a younger more pronounced floral turnover *ca.* 4 Ma later recorded by Whiteside et al. (2015) and Lindström et al. (2016). Besides the climate change a series of other environmental perturbations affected the ecosystem from the mid-Norian on e.g., increase in the pCO_2 (e.g., Cleveland et al. 2008 a, b., Atchley et al. 2013; Nordt et al. 2015; Schaller et al. 2015; Whiteside et al. 2015), volcanism (Atchley et al. 2013; Nordt et al. 2015) and the Manicouagan impact event. Although it is very tempting to link the floral turnover to the Manicouagan impact event, the existing data are yet too incomplete to document a direct causality. The isotope ratios suggest that the recorded $\delta^{13}C_{org}$ variations are influenced by the local depositional setting and composition of sedimentary organic matter. Future studies might be able to demonstrate a potential a relationship with global carbon cycle perturbations. Within current sampling limits, the floral turnover happened roughly simultaneously with the Adamanian/Revueltian faunal turnover illustrating the strong relationship between flora and fauna. One possibility is that the loss of

wetland habitat space due to drier climate and the increase in coniferous xerophyte plants dwindled the supply of palatable vegetation for herbivores.

Potential for future work and limitations

The presented palynological and palaeobotanical data can be incorporated as a tool for comparison in future sedimentological, geochemical, or palaeoclimatological analyses that aim at reconstructing past environments during the Carnian-Norian. In order, to enhance our understanding on Carnian-Norian environmental perturbations further studies and new areas can be incorporated to gain a more comprehensive picture.

The palynological analysis of terrestrial succession represents a great challenge in terms of preservation potential and the problems regarding independent age constrains. The two floral turnovers during the Norian in the Chinle Formation raise the question about the possibility of further floral turnovers during the Norian. One of the main limitations is locating outcrops and sedimentary succession that can be systematically sampled and potentially bear palynomorphs. The preferable lithologies are often linked to distinct facies types (e.g., lacustrine, marsh, floodplain) which are spatially and temporally restricted in the Chinle. In these successions, magnetostratigraphy and radiometric dating provide the best age-control and the most reliable tool for correlation. Unfortunately, detailed radiometric dates of the Upper Triassic strata in the western United States are mainly confined to the Chinle Formation of Petrified Forest National (Parker & Martz 2017). Only a few beds have been dated elsewhere from the Chinle (e.g., Irmis et al. 2011; Ramezani et al. 2014), and high-resolution U-Pb zircon dates are not yet available for the age-equivalent Dockum Group in Texas, Dolores Formation in Colorado, or Popo Agie Formation in Colorado and Wyoming. The better age calibration could also reveal the relationship between the floral/faunal turnover and the Manicouagan impact event. To date, the palynological assemblages in the Badlands section contain the "stratigraphically closest" record of pollen assemblages only few metres above the turnover horizon placed at the "persistent red silcrete bed". However, the Badlands section is not dated by any independent methods which leave some uncertainty in the timing of the recorded palynological changes. Age constrains would also enable to link the biotic turnovers and environmental changes to orbital forcing and to shed light on the eventual cyclicity of the events. The study of two additional Petrified Forest cores (PFNP13-2A, PFNP13-2B) in the CPCP project might yiels palynological assemblages and also additional analysis of environmental changes will be possible in a continuous section. The primary advantage of the Petrified Forest core(s) is the numerous analyses (biostratigraphy, petrography, mineralogy, geochemistry, magnetostratigraphy) which are performed on the same sample set in

undoubted stratigrahic superposition. In this case, the main limitation for palynology is the lithology and the number of the potential pollen bearing horizons.

In our research, the bulk carbon isotope variations from the Chinle were interpreted as a function of the sedimentary organic matter composition, however, other factors e.g., global carbon cycle perturbation could not be excluded. Compound specific carbon isotope analysis of plant lipids could be a solution to reveal the atmospheric carbon isotope ratios. Dr. C.S. Miller attempted to extract n-alkanes from several samples from CPCP PFNP13-1A and outcrop samples from the PEFO. Most of them were unfortunately unsuitable, but new sample sets with more favourable lithologies could eventually provide better results.

The Newark Supergroup would be an excellent target for searching for the Mid Norian Climate Shift. Our preliminary studies based on several Norian samples from the Taylorsville Basin (Virginia, Maryland) revealed that organic matter is overmatured. Further test samples are required. Litwin & Ash (1993) studied few outcrop samples with well-preserved palynological assemblages from the Chatham Group, Deep River Basin, North Carolina which could be a potential target.

Froelichsporites traversei plays an important role during the floral turnovers in the Norian. Though the new TEM results (Paper 4) indicate that it was gymnosperm pollen, the botanical affinity could not be determined unambiguously. Especially the TEM study of the pore structure would be desirable. However, during our analysis we were unable to encounter it in the TEM sections although the orientation of the embedded tetrad was chosen accordingly in order to maximise the chance of hitting the pore during sectioning. In order to increase the chance of finding the pore structure, it is necessary to section a much greater number of tetrads. Eventually, different methods can help understanding the pore structure e.g., confocal laser scanning microscopy (CLSM), or focused ion beam scanning electron microscopy (FIB-SEM). Both methods would allow preparing a virtual section through the pore structure.

In order to improve our understanding of the climate change during the Carnian Pluvial Episode, the more widespread application of clay mineralogy and elemental analysis of the sedimentary rocks could be a useful attempt. The elemental ratios (e.g, Si/Al, Ti/Al, Zr/Al) and weathering proxies (CIA, CIW, α_i, $\alpha^{Al}{}_i$) (Nesbitt & Young 1982; Gaillardet et al. 1999; Cullers 2000; Garzanti et al. 2013) can be informative on weathering changes and terrestrial influx which can be then translated into potential climate variations. The two approaches together (palynology, elemental analysis) could provide a more robust interpretation of the

environmental changes. The clay mineral study and elemental composition of the Raibler Shales and Lunz in the Northern Calcareous Alps and in the sections in Dolomite (Dibona), Julian Alps (Cave del Perdil area) and the Schilfsandstein from the Germanic Realm would be of special interest as these successions had a significant influence on our views on the palynological record of the CPE. From the comparison of palynology to clay minerals and weathering proxies we could obtain more data on the variations between more arid and more humid periods.

To improve the knowledge on Carnian palynomorph assemblages from the north-western European realm, more sections can be studied from the UK. The main challenge there is the correlation of the often short and isolated successions. Palynofloras can have diachronous distributions and may be biased by local environmental and climatological conditions and the ranges may differ in the Alpine Tethys and north-western European realm. Therefore independent age correlations methods are crucial to enhance the correlation between the sections.

In Hungary, it would be interesting to include an additional borehole material e.g., Hévíz-1 borehole in the Keszthely Mts, Transdanubian Range, which could enable the detailed study of latest Julian-early Tuvalian assemblages, younger than those presented in this research. This borehole has already provided positive samples (Góczán et al. 1983) but a new systematic sampling can improve the temporal resolution of palynomorph assemblages. The unique geological features of Hungary enable to study Triassic successions of the Alpine Tethys and Germanic type facies realm as well. In south-west part of the country, the Mecsek Mts. exposed a mainly terrestrial, clastic, Keuper type Late Triassic succession. During the Triassic times, this area was located at the northern Tethyan shelf margin east of the dry lands of the Bohemian Massive and Vindelician High (Kovács et al. 2011). The facies evolution is characterized by a tripartite subdivision (Buntsandstein, Muschelkalk, Keuper) like in other areas of the Central European Germanic realm (Haas et al. 2013). The Ladian-Carnian Kanatavár Calcareous Marl Formation was deposited in a shallow lagoon then lacustrine environment. Subsequently, the Karolinavölgy Sandstone Formation (Carnian-Norian) represents a fluvial-alluvial-deltaic succession (Haas et al. 2013). The latter has already provided palynological assemblages (Bóna 1995). Although the Karolinavölgy Sandstone Formation comprises primarily sandstones of variegated colours but the presence of coal

seams and plant remains (Wéber 1984) might make the formation a potential target for further palynological studies.

The majority of the CPE research has focused on the central Pangean or western Tethys region. As Ruffell et al (2016, p. 8) pointed out "it's the data from beyond these 'central Pangaean' locations that will really provide further evidence as to what happened in the Carnian". Marine successions in Canada could also represent a potential target for further studies (pers. comm. with Jacopo Dal Corso in 2017). The Late Triassic Ludington and Baldonnel Formations are shallow marine mixed siliciclastic-carbonate successions in British Columbia spanning the Carnian. The formations in western Canada are located close to the Wrangellia LIP in the north eastern Pacific region (Greene et al. 2010) and the successions are expected to record the effect of the volcanism. The biostratigraphy of these units is also good due to detailed conodont zonation (Zonneveld & Orchard 2002), but the predominantly carbonate (limestone, dolomite) and sandstone units might be a challenge for palynological studies. In terms of lithology, the mainly siliciclastic units (silt, shale and sands) of the Sverdrup Basin in Arctic Canada (e.g., Embry 2011) are probably better suited for palynology.

References

Abbink, O.A.,1998. Palynological investigations in the Jurassic of the North Sea region.PhD thesis, University of Utrecht, LPP Contribution Series 8

Abbink, O.A., van Konijnenburg-van Cittert, J.H.A., Visscher, H., 2004. A sporomorph ecogroup model for the Northwest European Jurassic - Lower Cretaceousi: concepts and framework. Neth. J. Geosci. - Geol. En Mijnb, 83, 17-31. https://doi.org/10.1017/S0016774600020436

Adabi, M.H., 2004. A re-evaluation of aragonite versus calcite seas. Carbonates and Evaporites, 19, 133, https://doi.org/10.1007/BF03178476

Arche, A., López-Gómez, J., 2014. The Carnian Pluvial Event in Western Europe: New data from Iberia and correlation with the Western Neotethys and Eastern North America–NW Africa regions. Earth-Sci. Rev, 128, 196-231. https://doi.org/10.1016/j.earscirev.2013.10.012

Arens, N., Hope Jahren, A., 2000. Carbon isotope excursion in atmospheric CO_2 at the Cretaceous-Tertiary boundary: evidence from terrestrial sediments. PALAIOS, 15, 314-322, https://doi.org/10.2307/3515539

Ash, S.R., 1969. Ferns from the Chinle Formation (Upper Triassic) in the Fort Wingate area, New Mexico, Technical report 613D

Ash, S.R., 1972. Late Triassic plants from the Chinle Formation in northeastern Arizona: Palaeontology, 15, 598-618.

Ash, S.R., 2001. The fossil ferns of Petrified Forest NationalPark, Arizona, and their paleoclimatological implications, in Santucci, V.L., and McClelland, L.,eds., Proceedings of the 6th Fossil Resource Conference:National Park Service Geologic Resources Division, Technical Report NPS/NRGRD/GRDTR-01/01, 3–10.

Ash, S., 2005. Synopsis of the Upper Triassic flora of Petrified Forest National Park and vicinity. In: Nesbitt, S.J., Parker, W.G., Irmis, R.B. Guidebook to the Triassic formations of the Colorado Plateau in northern Arizona: Geology, Paleontology, and History, 9, 53-61.

Ash, S.R., Creber, G.T., 1992. Palaeoclimatic interpretationof the wood structures of the trees in the Chinle Formation (Upper Triassic), Petrified Forest NationalPark, Arizona, U.S.A.: Palaeogeography, Palaeoclimatology, Palaeoecology, 96, 299-317, https://doi.org/10.1016/0031-0182(92)90107-G

Ash, S.R., Creber, G.T., 2000. The Late Triassic Araucarioxylon Arizonicum trees of the Petrified Forest National Park, Arizona, USA. Palaeontology 43, 15-28, https://doi.org/10.1111/1475-4983.00116

Atchley, S.C., Nordt, L.C., Dworkin, S.I., Ramezani, J., Parker, W.G., Ash, S.R., and Bowring, S.A., 2013,A linkage among Pangean tectonism, cyclic alluviation, climate change, and biologic turnover in the Late Triassic: The record from the Chinle Formation, southwestern Unites States: Journal of Sedimentary Research, 83, 1147-1161, https://doi.org/10.2110/jsr.2013.89

Bachmann, G.H., Geluk, M.C., Warrington, G., Becker-Roman, A., Beutler, G., Hagdorn, H., Hounslow, M.W., Nitsch, E., Röhling, H.-G., Simon, T. & Szulc, A. 2010. Triassic. In: Doornenbal, J.C., Stevenson, A.G., (eds) Petroleum Geological Atlas of the Southern Permian Basin Area, EAGE Publications, 149-173, Hounten, 1–342.

Barclay, W.J., Ambrose, K.,Chadwick, R.A., Pharoah, T.C., 1997. Geology of the country around Worcester. Memoir of the Geological Survey of Great Britain, British Geological Survey, London, 1–157.

Batten, D.J., 2002. Palynofacies and petroleum potential. In: Jansonius, J. &McGregor D.C. (eds) Palynology: Principles and Applications, American Association of Stratigraphic Palynologists Foundation, 3, 1065-1084.

Bazard, D.R., Butler, R.F., 1991. Paleomagnetism of the Chinle and Kayenta Formations, New Mexico and Arizona. J. Geophys. Res. Solid Earth, 96, 9847-9871. https://doi.org/10.1029/91JB00336

Benton, M.J., 1995. Diversification and extinction in the history of life. Science 268, 52-58. https://doi.org/10.1126/science.7701342

Benton, M.J., Forth, J., Langer, M.C., 2014. Models for the Rise of the Dinosaurs. Curr. Biol. 24, 87-95, https://doi.org/10.1016/j.cub.2013.11.063

Berra, F., Jadoul, F., Anelli, A., 2010. Environmental control on the end of the Dolomia Principale/Hauptdolomit depositional system in the central Alps: Coupling sea-level and climate changes. Palaeogeogr. Palaeoclimatol. Palaeoecol., 290, 138-150, https://doi.org/10.1016/j.palaeo.2009.06.037

Bialik, O.M., Korngreen, D., Benjamini, C., 2013. Carnian (Triassic) aridization on the Levant margin: evidence from the M1 member, Mohilla Formation, Makhtesh Ramon, south Israel. Facies, 59, 559-581, https://doi.org/10.1007/s10347-012-0321-5

Birks, H., Seppä, H., 2004. Pollen-based reconstructions of late-Quaternary climate in Europe - Progress, problems, and pitfalls. Acta Palaeobotanica, 44, 317-334.

Blendinger, E., 1988. Palynostratigraphy of the late Ladinian and Carnian in the Southeastern Dolomites. Rev. Palaeobot. Palynol. 53, 329-348. https://doi.org/10.1016/0034-6667(88)90038-3

Bolli, H.M., Saunders, J.B., Perch-Nielsen, K. 1989. Plankton Stratigraphy Vol. 2, Cambridge Earth Science Series, Cambridge University Press.

Bóna, J. 1995. Palynostratigraphy of the Upper Triassic formations in the Mecsek Mts (Southern Hungary). Acta Geologica Hungarica, 38, 319-354.

Bonis, N.R., Kürschner, W.M., 2012. Vegetation history, diversity patterns, and climate change across the Triassic/Jurassic boundary. Paleobiology 38, 240-264. https://doi.org/10.1666/09071.1

Breda, A., Preto, N., Roghi, G., Furin, S., Meneguolo, R., Ragazzi, E., Fedele, P., Gianolla, P., 2009. The Carnian Pluvial Event in the Tofane area (Cortina d'Ampezzo, Dolomites, Italy). GeoAlp, 6, 80-115.

Bryant, V.M., Holloway, R.G., 1983. The role of palynology in archaeology. Adv. Archaeol. Method Theory, 6, 191-224.

Budai, T., Császár, G., Csillag, G., Dudko, A., Koloszár, L., Majoros, Gy., 1999. Geology of the Balaton Highland (Explanation to the Geological Map of the Balaton Highland, 1:50000). Special Publications of the Geological Institute of Hungary, 197, 171-257.

Budai, T., Haas, J., 1997. Triassic sequence stratigraphy of the Balaton Highland, Hungary. Acta Geol. Hung. 40, 307-335.

Budai, T., Haas, J., Olga, P., 2015. New stratigraphic data on the Triassic basement of the Zsámbék basin-tectonic inferences, 145, 247-257, in Hungarian with English abstract

Budai, T., Vörös, A., 2006. Middle triassic platform and basin evolution of the Southern Bakony mountains (Transdanubian Range, Hungary). Rivista Italiana di Paleontologia e Stratigrafia 112, 359-371, https://doi.org/10.13130/2039-4942/6346

Buratti, N., Cirilli, S., 2007. Microfloristic provincialism in the Upper Triassic Circum-Mediterranean area and palaeogeographic implication. Geobios, 40, 133-142, https://doi.org/10.1016/j.geobios.2006.06.003

Césari, S.N., Colombi, C.E., 2013. A new Late Triasssic phytogeographical scenario in westernmost Gondwana. Nat. Commun. 4, 1889. https://doi.org/10.1038/ncomms2917

Chaloner, W.G. & Muir, M. 1968. Spores and floras. In: Murchison, D.G. & Westoll, T.S. (eds) Coal and coal-bearing strata. Oliver and Boyd, Edinburgh, 122-146.

Cirilli, S., 2010. Upper Triassic–lowermost Jurassic palynology and palynostratigraphy: a review. In: Lucas, S.G., (ed.) The Triassic Timescale, Geological Society, London, Special Publications, 334, 285-314, https://doi.10.1144/SP334.12

Clarke, R.F.A. 1965. Keuper miospores from Worcestershire, England. Palaeontology, 8, 294-321.

Cleveland, D.M., Nordt, L.C., Atchley, S.C., 2008a. Paleosols, trace fossils, and precipitation estimates of the uppermost Triassic strata in northern New Mexico. Palaeogeogr. Palaeoclimatol. Palaeoecol. 257, 421-444, https://doi.org/10.1016/j.palaeo.2007.09.023

Cleveland, D.M., Nordt, L.C., Dworkin, S.I., Atchley, S.C., 2008b. Pedogenic carbonate isotopes as evidence for extreme climatic events preceding the Triassic-Jurassic boundary: Implications for the biotic crisis? Pedogenic carbonate isotopes as evidence for Late Triassic climate changes. GSA Bulletin, 120, 1408-1415, https://doi.org/10.1130/B26332.1

Clutson, M.J., Brown, D.E., Tanner, L.H., 2018. Distal processes and effect of multiple Late Triassic terrestrial bolide impacts: insights from the Norian Manicouagan Event, northeastern Quebec, Canada. In: Tanner, L.H., (ed.) The Late Triassic World Earth in a time of transition, Springer, Topics in Geobiology, 46, 127-187.

Colombi, C.E., Parrish, J.T., 2008. Late Triassic Environmental Evolution in Southwestern Pangea: Plant Taphonomy of the Ischigualasto Formation. PALAIOS, 23, 778-795, https://doi.org/10.2110/palo.2007.p07-101r

Cornet, B., 1977. The palynostratigraphy and age of the Newark Supergroup. PhD Thesis, Pennsylvania State University, University Park.

Cornet, B., 1993. Applications and limitations of palynology in age, climatic and paleoenvironmental analyses of Triassic sequences in North America. Pages 75–93 in SG Lucas, M Morales, eds. The nonmarine Triassic. New Mexico Museum of Natural History and Science Bulletin 3, Albuquerque.

Crowley, J.T., Hyde, W.T., Short, D.A., 1989. Seasonal cycle variations on the supercontinent Pangea. Geology, 17, 457-460, https://doi.org/10.1130/0091-7613(1989)017<0457:SCVOTS>2.3.CO;2

Csontos, L., Nagymarosy, A., Horváth, F., Kovác, M., 1992. Tertiary evolution of the Intra-Carpathian area: A model. Tectonophysics, 208, 221-241, https://doi.org/10.1016/0040-1951(92)90346-8

Csontos, L., Vörös, A., 2004. Mesozoic plate tectonic reconstruction of the Carpathian region. Palaeogeogr. Palaeoclimatol. Palaeoecol. 210, 1-56, https://doi.org/10.1016/j.palaeo.2004.02.033

Cullers, R.L., 2000. The geochemistry of shales, siltstones and sandstones of Pennsylvanian–Permian age, Colorado, USA: implications for provenance and metamorphic studies. Lithos, 51, 181-203, https://doi.org/10.1016/S0024-4937(99)00063-8

Dal Corso, J., Gianolla, P., Newton, R.J., Franceschi, M., Roghi, G., Caggiati, M., Raucsik, B., Budai, T., Haas, J., Preto, N., 2015a. Carbon isotope records reveal synchronicity between carbon cycle perturbation and the “Carnian Pluvial Event” in the Tethys realm (Late Triassic). Glob. Planet. Change 127, 79-90, https://doi.org/10.1016/j.gloplacha.2015.01.013

Dal Corso, J., Mietto, P., Newton, R., D. Pancost, R., Preto, N., Roghi, G., Wignall, P., 2012. Discovery of a major negative $\delta^{13}C$ spike in the Carnian (Late Triassic) linked to the eruption of Wrangellia flood basalts. Geology, 40, 79-82, https://doi.org/10.1130/G32473.1

Dal Corso, J., Roghi, G., Kustatscher, E., Preto, N., Gianolla, P., Manfrin, S., Mietto, P., 2015b. Ammonoid-calibrated sporomorph assemblages reflect a shift from hygrophytic to xerophytic elements in the late Anisian (Middle Triassic) of the Southern Alps (Italy). Review of Palaeobotany and Palynology, 218, 15-27, https://doi.org/10.1016/j.revpalbo.2014.02.010

Daugherty, L.H. 1941. The Upper Triassic flora of Arizona. Carnegie Institute Washington Publication, 526, 108 p.

Demko, T.M., Dubiel, R.F., Totman Parrish, J., 1998. Plant taphonomy in incised valleys: Implications for interpreting paleoclimate from fossil plants. Geology, 26, 1119-1122, https://doi.org/10.1130/0091-7613(1998)026<1119:PTIIVI>2.3.CO;2

Dettmann, E. 1963. Upper Mesozoic microfloras from South-Eastern Australia. Proc. Royal Soc. Victoria, New Series, 77, 1-148.

Dickinson, W.R., Gehrels, G.E., 2008. U-Pb Ages of Detrital Zircons in Relation to Paleogeography: Triassic Paleodrainage Networks and Sediment Dispersal Across Southwest Laurentia. J. Sediment. Res. 78, 745-764, https://doi.org/10.2110/jsr.2008.088

Dolby, J.H., Balme, B.E., 1976. Triassic palynology of the Carnarvon Basin, Western Australia. Rev. Palaeobot. Palynol. 22, 105–168. https://doi.org/10.1016/0034-6667(76)90053-1

Dosztály, L., S. Kovács, and T. Budai, 1989. Pécsely, Meggy hegy quarry. In XXI European Micropalaeontological Colloquium, Guidebook.

Doyle, J.A. 2009. Evolutionary significance of granular exine structure in the light of phylogenetic analyses. Rev Palaeobot Palynol, 156, 198-210, https://doi.org/10.1016/j.revpalbo.2008.08.001

Dubiel, R.F., Hasiotis, S.T., 2011. Deposystems, paleosoils and climatic variability in a continental system: the Upper Triassic Chinle Formation, Colorado Plateau, U.S.A. In: Davidson, S.K., Leleu, S., North, C.P.,(eds) From River To Rock Record: The Preservation Of Fluvial Sediments And Their Subsequent Interpretation, SEPM Special Publication 97, 393-421.

Dubiel, R.F., 1987. Sedimentology of the Upper Triassic Chinle Formation, Southeastern Utah: Paleoclimatic Implications. J. Ariz.-Nev. Acad. Sci. 22, 35-45.

Dubiel, R.F., Parrish, J.T., Parrish, J.M., Good, S.C., 1991. The Pangaean Megamonsoon: Evidence from the Upper Triassic Chinle Formation, Colorado Plateau. PALAIOS 6, 347-370. https://doi.org/10.2307/3514963

Dunay, R.E. & Fisher, M.J. 1978. The Karnian palynofloral succession in the Northern Calcareous Alps, Lunz-am-See, Austria. Pollen et Spores, 20, 177-187.

Dunlavey, M.G., Whiteside, J.H., Irmis, R.B., 2009. Ecosystem instability during the rise of dinosaurs: Evidence from the Late Triassic in New Mexico and Arizona, Geological Society of America Abstracts with Programs 41, 477.

Embry, A., 2011. Chapter 36 Petroleum prospectivity of the Triassic–Jurassic succession of Sverdrup Basin, Canadian Arctic Archipelago. Geol. Soc. Lond. Mem. 35, 545-558, https://doi.org/10.1144/M35.36

Eshet, Y., Hoek, R., 1996. Palynological processing of organic-rich rocks, or: How many times have you called a palyniferous sample “barren”? Rev. Palaeobot. Palynol. 94, 101-109, https://doi.org/10.1016/S0034-6667(96)00008-5

Falcon-Lang, H.J., 2003. Growth interruptions in silicified conifer woods from the Upper Cretaceous Two Medicine Formation, Montana, USA: implications for palaeoclimate and dinosaur palaeoecology. Palaeogeogr. Palaeoclimatol. Palaeoecol. 199, 299-314. https://doi.org/10.1016/S0031-0182(03)00539-X

Feist-Burkhardt, S., Götz, A., Szulc, J., Borkhataria, R., Geluk, M., Haas, J., Hornung, J., Jordan, P., Kempf, O., Jozef, M., Nawrocki, J., Reinhardt, L., Ricken, W., Röhling, H.-G., Rüffer, T., Török, Á., Zuehlke, R., 2008. Chapter 13: Triassic. In: McCann, T., (ed.) The Geology of Central Europe - Volume 2 Mesozoic and Cenozoic, Geological Society of London, 749-821.

Fijałkowska, A., 1994. Palynostratigraphy of the Lower and Middle Buntsandstein in NW part of the Holy Cross Mountains, Poland. Geological Quarterly, 38, 59-96.

Fijałkowska-Mader, A., Heunisch, C., Szulc, J., 2015. Palynostratigraphy and palynofacies of the Upper Silesian Keuper (southern Poland). Ann. Soc. Geol. Pol. 85, 637-661, https://doi.10.14241/asgp.2015.025

Fodor, L., Csontos, L., Bada, G., Győrfi, I., Benkovics, L., 1999. Tertiary tectonic evolution of the Pannonian Basin System and neighbouring orogens: a new synthesis of palaeostress data. In: Durand, B., Jolivet, L., Horváth, F., Séranne, M., (eds) The Mediterranean Basins: Tertiary Extension within the Alpine Orogen, Geological Society, London, Special Publications, 156, 295-334, https://doi.org/10.1144/GSL.SP.1999.156.01.15

Foster, C.B., Afonin, S.A., 2005. Abnormal pollen grains: an outcome of deteriorating atmospheric conditions around the Permian–Triassic boundary: Journal of the Geological Society, London, 162, 653-659, https://doi:10.1144/0016-764904-047

Fowell, S.J., 1993. Palynology of Triassic/Jurassic Boundary Sections from the Newark Supergroup of Eastern North America: Implications for Catastrophic ExtinctionScenarios. Ph.D. thesis, Columbia University

Fowell, J.S., Cornet, B., Olsen, P., 1994. Geologically rapid Late Triassic extinctions: Palynological evidence from the Newark Supergroup. Geological Society of America Special Papers, 288, 197-206, https://doi.org/10.1130/SPE288-p197

Frakes, L., Francis, J.E., 1988. A guide to Phanerozoic cold polar climates from high-latitude ice-rafting in the Cretaceous. Nature, 333, 547-549, https://doi.org/10.1038/333547a0

Fraser, W.T., Watson, J.S., Sephton, M.A., Lomax, B.H., Harrington, G., Gosling, W.D., Self, S., 2014. Changes in spore chemistry and appearance with increasing maturity. Rev. Palaeobot. Palynol. 201, 41-46. https://doi.org/10.1016/j.revpalbo.2013.11.001

Furin, S., Preto, N., Rigo, M., Roghi, G., Gianolla, P., L. Crowley, J., A. Bowring, S., 2006. High-precision UPb zircon age from the Triassic of Italy: Implications for the Triassic time scale and the Carnian origin of calcareous nannoplankton and dinosaurs. Geology, 34, 1009-1012, https://doi.org/10.1130/G22967A.1

Fægri, K. & van der Pijl, L. 1966. The principles of pollination ecology. Pergamon Press, London.

Gaillardet, J., Dupré, B., Allègre, C.J., 1999. Geochemistry of large river suspended sediments: Silicate weathering or recycling tracer? Geochimica et Cosmochimica Acta, 63, 4037-4051, https://doi.org/10.1016/S0016-7037(99)00307-5

Gallois, R.W., 2001. The lithostratigraphy of the Mercia Mudstone Group (mid-late Triassic) of the south Devon coast. Geosci. South-West Engl. - Proc. Ussher Soc. 10, 195-204.

Gallois, R.W., 2007. The stratigraphy of the Mercia Mudstone Group succession (mid to late Triassic) proved in the Wiscombe Park boreholes, Devon. Geoscience in south-west England, 11, 280-286.

Gallois, R.W., Porter, R.J., 2006. The stratigraphy and sedimentology of the Dunscombe Mudstone Formation (late Triassic) of south-west England. Geosci. South-West Engl. - Proc. Ussher Soc. 11, 174-182.

Garzanti, E., Padoan, M., Setti, M., Peruta, L., Najman, Y., Villa, I.M., 2013. Weathering geochemistry and Sr–Nd isotope fingerprinting of equatorial upper Nile and Congo muds. Geochemistry, Geophysics, Geosystems, 14, 292-316, https://doi.org/10.1002/ggge.20060

Góczán, F., Csalagovics, I., Fügedi, P., Földvári, M., Detre, Cs., Haas, J., Kovács, S., Oravecz, J., Ravaszné Baranyai, L., Vető, I., 1979. A Zsámbék Zs–14 fúrás kútfúrási jegyzőkönyve és földtani naplója. Geological Institute of Hungary, data repository number: 1656/29, in Hungarian

Góczán, F., Haas, J., Lőrincz, H., Oravecz-Scheffer, A. 1983. Faciological and strtigtraphic evaluation of a Carnian key section (borehole Hévíz 6, Keszthely Mts, Hungary). Magyar Állami Földtani Inézet Évi Jelentése 1981-ről, 263-293, in Hungarian with English abstract

Góczán, F., Oravecz–Scheffer, A., 1996a. Tuvalian sequences of the Balaton Highland and the Zsámbék Basin, Part I: Litho-, bio- and chronostratigraphic subdivision. Acta Geol. Hung. 39, 1-31.

Góczán, F., Oravecz–Scheffer, A., 1996b. Tuvalian sequences of the Balaton Highland and the Zsámbék Basin, Part II: Characterization of sporomorph and foraminifer assemblages, biostratigraphic, palaeogeographic and geohistoric conclusions. Acta Geol. Hung. 39, 33-101.

Golonka, J., 2007. Late Triassic and Early Jurassic palaeogeography of the world. Palaeogeogr. Palaeoclimatol. Palaeoecol., Triassic-Jurassic Boundary events: problems, progress, possibilities 244, 297–307, https://doi.org/10.1016/j.palaeo.2006.06.041

Gorin, G.E., Steffen, D., 1991. Organic facies as a tool for recording eustatic variations in marine fine-grained carbonates—example of the Berriasian stratotype at Berrias (Ardèche, SE France).

Palaeogeogr. Palaeoclimatol. Palaeoecol. 85, 303–320, https://doi.org/10.1016/0031-0182(91)90164-M

Gottesfeld, A.S. 1972. Palynology of the Chinle Formation. Museum Northern Arizona Bulletin, 47, 13-18.

Götz, A., Ruckwied, K., Pálfy, J., Haas, J., 2009. Palynological evidence of synchronous changes within the terrestrial and marine realm at the Triassic/Jurassic boundary (Csővár section, Hungary). Rev. Palaeobot. Palynol. 156, 401-409, https://doi.org/10.1016/j.revpalbo.2009.04.002

Götz, A.E., Ruckwied, K., Barbacka, M., 2011. Palaeoenvironment of the Late Triassic (Rhaetian) and Early Jurassic (Hettangian) Mecsek Coal Formation (south Hungary): implications from macro- and microfloral assemblages. Palaeobiodiversity Palaeoenvironments 91, 75-88, https://doi.org/10.1007/s12549-010-0048-7

Gradstein, F.M., Ogg, J.G., 2012. Chapter 2 - The Chronostratigraphic Scale, in: The Geologic Time Scale. Elsevier, Boston, 31-42, https://doi.org/10.1016/B978-0-444-59425-9.00002-0

Greene, A.R., Scoates, J.S., Weis, D., Katvala, E.C., Israel, S., Nixon, G.T., 2010. The architecture of oceanic plateaus revealed by the volcanic stratigraphy of the accreted Wrangellia oceanic plateau. Geosphere 6, 47-73, https://doi.org/10.1130/GES00212.1

Gregory, W.A., Hart, G.F., 1992. Towards a Predictive Model for the Palynologic Response to Sea-Level Changes. PALAIOS 7, 3–33. https://doi.org/10.2307/3514794

Grimm, E.C. 1987. CONISS: a FORTRAN 77 program for stratigraphically constrained cluster analysis by the method of incremental sum of squares. Computers & Geosciences, 13, 13-35.

Grimm, E.C. 1991–2001. Tilia, TiliaGraph and TGView Software. Illinois State Museum, Springfield, Illinois, USA.

Gröcke, D.R., 1998. Carbon-isotope analyses of fossil plants as a chemostratigraphic and palaeoenvironmental tool. Lethaia 31, 1-13, https://doi.org/10.1111/j.1502-3931.1998.tb00482.x

Haas, J.,Budai, T., 1995. Upper Permian-Triassic facies zones in the Transdanubian Range. Riv. Ital. Paleontol. E Stratigr. Res. Paleontol. Stratigr, 101, 249-266, https://doi.org/10.13130/2039-4942/8587

Haas, J., Budai, T., 1999. Triassic sequence stratigraphy of the Transdanubian Range (Hungary). Geologica Carpathica, 50, 459-475.

Haas, J., Budai, T., Raucsik, B., 2012. Climatic controls on sedimentary environments in the Triassic of the Transdanubian Range (Western Hungary). Palaeogeogr. Palaeoclimatol. Palaeoecol. 353-355, 31-44, https://doi.org/10.1016/j.palaeo.2012.06.031

Haas, J., Hámor, G., Áron, J., Kovács, S., Nagymarosy, A., Szederkényi, T., 2013. Geology of Hungary, Springer, https://doi.org/10.1007/978-3-642-21910-8

Hallam, A., 2002. How catastrophic was the end-Triassic mass extinction? Lethaia 35, 147-157, https://doi.org/10.1111/j.1502-3931.2002.tb00075.x

Hallam, A. & Wignall, P., 1999. Mass extinctions and sea-level changes. Earth-Sci. Rev. 48, 217-250. https://doi.org/10.1016/S0012-8252(99)00055-0

Hammer, Ø., Harper, D.A.T., and Ryan, P.D., 2001, PAST: Palaeontological statistics software package for education and data analysis: Palaeontologia Electronica, 4, 1-9.

Harper, D.A.T. 1999. Numerical palaeobiology, John Wiley & Sons, New York

Heckert, A.B., Lucas, S.G., Hunt, A.P., Spielmann, J.A. 2007. Late Triassic aetosaur biochronology revisited: New Mexico Museum of Natural History and Science Bulletin, 41, 49-50.

Helenes, J., Somoza, D., 1999. Palynology and sequence stratigraphy of the Cretaceous of eastern Venezuela. Cretac. Res. 20, 447-463, https://doi.org/10.1006/cres.1999.0160

Heunisch, C. 1999. Die Bedeutung der Palynologie für Biostratigraphie und Fazies in der Germanischen Trias. In: Hauschke, N. & Wilde, V. (eds) Trias - Eine ganze andere Welt Mitteleuropa im frühen Erdmittelalter, Dr. Friedrich Pfeil, Munich, 207-262

Heylmun, E.B., 1997. Arizona's Holbrook salt basin holds oil, gas opportunities, Oil and Gas Journal, 95, http://www.ogj.com/articles/print/volume-95/issue-18/in-this-issue/exploration/exploration-arizona39s-holbrook-salt-basin-holds-oil-gas-opportunities.html

Hochuli, P., Frank, S.M., 2000. Palynology (dinoflagellate cysts, spore-pollen) and stratigraphy of the Lower Carnian Raibl Group in the Eastern Swiss Alps.

Hochuli, P.A., Vigran, J.O., 2010. Climate variations in the Boreal Triassic — Inferred from palynological records from the Barents Sea. Palaeogeogr. Palaeoclimatol. Palaeoecol., Triassic climates 290, 20–42, https://doi.org/10.1016/j.palaeo.2009.08.013

Hounslow, M.W., McKie, T., & Ruffell, A.H. 2012. Permian to late Triassic post orogenic collapse and rifting, arid deserts, evaporating seas and mass extinctions. In: Woodcock, N.H. & Strachan, R.A. (eds) The Geological History of Britain and Ireland, Second revised edition, John Wiley & Sons, Ltd, Chichester, 301-321, https://doi.10.1002/9781118274064.ch16

Hounslow, M.W., Muttoni, G., 2010. The geomagnetic polarity timescale for the Triassic: linkage to stage boundary definitions. Geol. Soc. Lond. Spec. Publ. 334, 61-102, https://doi.org/10.1144/SP334.4

Hounslow, M.W. & Ruffell, A. 2006. Triassic-Seasonal Rivers, Dusty Deserts and Salty Lakes. In: Brenchly, P.J., Rawson, P. F. (eds) Geology of England and Wales, Geological Society of London Publication, 295-324.

Hornung, T., Brandner, R., 2005. Biochronostratigraphy of the Reingraben Turnover (Hallstatt Facies Belt): Local black shale events controlled by regional tectonics, climatic change and plate tectonics. Facies, 51, 460-479. https://doi.org/10.1007/s10347-005-0061-x

Hornung, T., Brandner, R., Krystyn, L., Joachimsky, M.M. & Keim, L. 2007a. Multistratigraphic constraints on the NW Tethyan “Carnian Crisis”. In: Lucas, S.G., Spielmann, J.A., (eds) The Global Triassic, New Mexico Museum of Natural History and Science Bulletin, 41, 59-67.

Hornung, T., Krystyn, L. & Brandner, R. 2007b. A Tethys-wide mid-Carnian (Upper Triassic) carbonate productivity decline: evidence for the Alpine Reingraben Event from Spiti (Indian Himalaya). Journal of Asian Earth Sciences, 30, 285-230, https://dx.doi.org/10.1016/j.jseaes.2006.10.001

Howard, A.S., Warrington, G., Ambrose, K., Rees, J.G., 2008. A formational framework for the Mercia Mudstone Group (Triassic) of England and Wales. British Geological Survey, Keyworth, Nottingham, Research Report RR/08/04.

Howell, E.R., Blakey, R.C., 2013. Sedimentological constraints on the evolution of the Cordilleran arc: New insights from the Sonsela Member, Upper Triassic Chinle Formation, Petrified Forest National Park (Arizona, USA). GSA Bulletin, 125, 1349-1368, https://doi.org/10.1130/B30714.1

Irmis, R.B., Mundil, R., Martz, J.W., Parker, W.G., 2011. High-resolution U–Pb ages from the Upper Triassic Chinle Formation (New Mexico, USA) support a diachronous rise of dinosaurs. Earth Planet. Sci. Lett. 309, 258-267, https://doi.org/10.1016/j.epsl.2011.07.015

Iversen, J., 1944. *Viscum, Hedera* and *Ilex* as climate indicators. Geol. Fören. Stockh. Förh. 66, 463-483, https://doi.org/10.1080/11035894409445689

Jacobson, G.L., Bradshaw, R.H.W., 1981. The selection of sites for paleovegetational studies. Quat. Res. 16, 80-96. https://doi.org/10.1016/0033-5894(81)90129-0

Jacoby, G.C., 1989. Overview of Tree-Ring Analysis in Tropical Regions. IAWA J. 10, 99-108. https://doi.org/10.1163/22941932-90000478

Jardine, P.E., Abernethy, F.A.J., Lomax, B.H., Gosling, W.D., Fraser, W.T., 2017. Shedding light on sporopollenin chemistry, with reference to UV reconstructions. Rev. Palaeobot. Palynol. 238, 1-6, https://doi.org/10.1016/j.revpalbo.2016.11.014

Jeans, C.V., 1978. The Origin of the Triassic Clay Assemblages of Europe with Special Reference to the Keuper Marl and Rhaetic of Parts of England. Philos. Trans. R. Soc. Lond. Ser. Math. Phys. Sci. 289, 549-636.

Jourdan, F., Renne, P.R., Reimold, W.U., 2009. An appraisal of the ages of terrestrial impact structures. Earth Planet. Sci. Lett. 286, 1-13. https://doi.org/10.1016/j.epsl.2009.07.009
Juggins, S., 2007. C2 Version 1.5 User guide Software for ecological and palaeoecological data analysis and visualisation, Newcastle University, Newcastle upon Tyne
Kavary, E., 1972. Significant Upper Triassic microspores from Bleiberg, Austria. Jahrbuch der Geologischen Bundesanstalt, 19, 87-105.
Kázmér, M., Kovács, S. 1985. Permian-Paleogene paleogeography along the eastern part of the Insubric-Periadriatic lineament system: Evidence for continental escape of the Bakony-Drauzug unit. Acta Geologica Hungarica 28, 71-84.
Keim, L., Spötl, C. & Brandner, R. 2006. The aftermath of the Carnian carbonate platform demise: a basinal perspective (Dolomites, Southern Alps). Sedimentology, 53, 361-386, https://doi.10.1111/j.1365-3091.2006.00768.x
Kent, D.V., Irving, E., 2010. Influence of inclination error in sedimentary rocks on the Triassic and Jurassic apparent pole wander path for North America and implications for Cordilleran tectonics. J. Geophys. Res. Solid Earth 115, B10103, https://doi.org/10.1029/2009JB007205
Kent, D.V., Tauxe, L., 2005. Corrected Late Triassic latitudes for continents adjacent to the North Atlantic. Science, 307, 240-244. https://doi.org/10.1126/science.1105826
Kiessling, W., Aberhan, M., Brenneis, B., Wagner, P., 2007. Extinction trajectories of benthic organisms across the Triassic-Jurassic boundary, Palaeogeography Palaeoclimatology Palaeoecology, 244, 201-222 https://doi.org/10.1016/j.palaeo.2006.06.029
Klaus, W. 1960. Sporen der karnischen Stufe der ostalpinen Trias. Jahrbuch der Geologischen Bundesanstalt Sonderbände, 5, 107-184.
Kovach, W.L., 1993. Multivariate techniques for biostratigraphical correlation. J. Geol. Soc. 150, 697-705, https://doi.org/10.1144/gsjgs.150.4.0697
Kovach, W. L., Batten, D.J., 1994. Association of playnomorphs and palynodebris with depositional environments: quantitative approaches. In: Traverse, A. (ed.) Sedimentation of organic particles, Cambridge University, Press, Cambridge, 391-407.
Kovács, S., L. Krystyn, S. Szabó, L. Dosztály, and T. Budai, 1991. The Ladinian/Carnian boundary in the Balaton Upland, Hungary. Symp. Trias. Strat. Abstratcs
Kovács, S., Sudar, M., Gradinaru, E., Gawlick, H.-J., Karamata, S., Haas, J., Péró, C., Gaetani, M., Mello, J., Polák, M., Alj inović, D., Ogorelec, B., Kolar-Jurkovšek, T., Jurkovšek, B., Buser, S., 2011. Triassic Evolution of the Tectonostratigraphic Units of the Circum-Pannonian Region. Jahrb. Geol. Bundesanst. 151, 199-280.
Kozur, H., 1991. The evolution of the Meliata-Hallstatt ocean and its significance for the early evolution of the Eastern Alps and Western Carpathians. Palaeogeogr. Paleoceanogr. 87, 109-135. https://doi.org/10.1016/0031-0182(91)90132-B
Kozur, H.W., Bachmann, G.H., 2010. The Middle Carnian Wet Intermezzo of the Stuttgart Formation (Schilfsandstein), Germanic Basin. Palaeogeogr. Palaeoclimatol. Palaeoecol., 290, 107-119, https://doi.org/10.1016/j.palaeo.2009.11.004
Kuerschner, W.M., Bonis, N.R., Krystyn, L., 2007. Carbon-isotope stratigraphy and palynostratigraphy of the Triassic–Jurassic transition in the Tiefengraben section — Northern Calcareous Alps (Austria). Triassic-Jurass. Bound. Events Probl. Prog. Possibilities 244, 257-280, https://doi.org/10.1016/j.palaeo.2006.06.031
Kürschner, W.M., Herngreen, G.F.W., 2010. Triassic palynology of central and northwestern Europe: a review of palynofloral diversity patterns and biostratigraphic subdivisions. Geol. Soc. Lond. Spec. Publ. 334, 263-283, https://doi.org/10.1144/SP334.11
Kustatscher, E., R. Ash, S., Karasev, E., Pott, C., Vajda, V., Yu, J., Mcloughlin, S., 2018. Flora of the Late Triassic. In: Tanner, L.H., The Late Triassic World Earth in a Time of Transition, 545-622. https://doi.org/10.1007/978-3-319-68009-5_13

Kustatscher, E., Heunisch, C & Van Konijnenburg-Van Cittert, J.H.A. 2012. Taphonomical implications of the Ladinian megaflora ans palynoflora of Thale (Germany). Palaios, 27, 753-764, https://doi.10.2110/palo.2011.p11-090r

Kustatscher, E., van Konijnenburg-van Cittert, J.H.A., Roghi, G., 2010. Macrofloras and palynomorphs as possible proxies for palaeoclimatic and palaeoecological studies: A case study from the Pelsonian (Middle Triassic) of Kühwiesenkopf/Monte Prà della Vacca (Olang Dolomites, N-Italy). Palaeogeogr. Palaeoclimatol. Palaeoecol., Triassic climates 290, 71-80, https://doi.org/10.1016/j.palaeo.2009.07.001

Kutzbach, J.E., Gallimore, R.G., 1989. Pangaean climates: Megamonsoons of the megacontinent. J. Geophys. Res. Atmospheres 94, 3341–3357. https://doi.org/10.1029/JD094iD03p03341

Lindström, S., Irmis, R.B., Whiteside, J.H., Smith, N.D., Nesbitt, S.J., Turner, A.H., 2016. Palynology of the upper Chinle Formation in northern New Mexico, U.S.A.: Implications for biostratigraphy and terrestrial ecosystem change during the Late Triassic (Norian–Rhaetian). Rev. Palaeobot. Palynol. 225, 106-131, https://doi.org/10.1016/j.revpalbo.2015.11.006

Litwin, R.J., Ash, S.R., 1993. Revision of the biostratigraphy of the Chatham Group (Upper Triassic), Deep River basin, North Carolina, USA. Rev. Palaeobot. Palynol. 77, 75-95, https://doi.org/10.1016/0034-6667(93)90057-2

Litwin, R.J., Smoot, J.P., Weems, R.E., 1993. *Froelichsporites* gen. nov. — a biostratigraphic marker palynomorph of Upper Triassic continental strata in the conterminous U. S. Palynology, 17, 157-168, https://doi.org/10.1080/01916122.1993.9989425

Litwin, R.J., Traverse, A., Ash, S.R., 1991. Preliminary palynological zonation of the Chinle formation, southwestern U.S.A., and its correlation to the Newark supergroup (eastern U.S.A.). Rev. Palaeobot. Palynol. 68, 269-287, https://doi.org/10.1016/0034-6667(91)90028-2

Loope, D.B., Steiner, M.B., Rowe, C.M., Lancaster, N., 2004. Tropical westerlies over Pangaean sand seas. Sedimentology 51, 315-322, https://doi.org/10.1046/j.1365-3091.2003.00623.x

López-Gómez, J., Escudero-Mozo, M.J., Martín-Chivelet, J., Arche, A., Lago, M., Galé, C., 2017. Western Tethys continental-marine responses to the Carnian Humid Episode: Palaeoclimatic and palaeogeographic implications. Glob. Planet. Change 148, 79-95, https://doi.org/10.1016/j.gloplacha.2016.11.016

Louveaux, J., Maurizio, A., Vorwohl, G., 1970. Methods of Melissopalynology. Bee World 51, 125-138, https://doi.org/10.1080/0005772X.1970.11097312

Lukeneder, S., Lukeneder, A., Harzhauser, M., İslamoğlu, Y., Krystyn, L., Lein, R., 2012. A delayed carbonate factory breakdown during the Tethyan-wide Carnian Pluvial Episode along the Cimmerian terranes (Taurus, Turkey). Facies 58, 279-296, https://doi.org/10.1007/s10347-011-0279-8

Mackenzie, G., Boa, A.N., Diego-Taboada, A., Atkin, S.L., Sathyapalan, T., 2015. Sporopollenin, the least known yet toughest natural biopolymer. Front. Mater. 2, Article 66, https://doi.org/10.3389/fmats.2015.00066

Maher, L.J., 1981. Statistics for microfossil concentration measurements employing samples spiked with marker grains. Rev. Palaeobot. Palynol. 32, 153-191, https://doi.org/10.1016/0034-6667(81)90002-6

Mander, L., Kürschner, W.M., McElwain, J.C., 2013. Palynostratigraphy and vegetation history of the Triassic–Jurassic transition in East Greenland. J. Geol. Soc. 170, 37-46, https://doi.org/10.1144/jgs2012-018

Mander, L., Kürschner, W.M., McElwain, J.C., 2010. An explanation for conflicting records of Triassic–Jurassic plant diversity. Proc. Natl. Acad. Sci. U. S. A. 107, 15351-15356, https://doi.org/10.1073/pnas.1004207107

Mander, L., Twitchett, R.J., Benton, M.J., 2008. Palaeoecology of the Late Triassic extinction event in the SW UK. J. Geol. Soc. 165, 319-332, https://doi.org/10.1144/0016-76492007-029

Mao, K., Milne, R.I., Zhang, L., Peng, Y., Liu, J., Thomas, P., Mill, R.R., S. Renner, S., 2012. Distribution of living Cupressaceae reflects the breakup of Pangea. Proc. Natl. Acad. Sci. 109, 7793-7798, https://doi.org/10.1073/pnas.1114319109

Márton, E., Fodor, L., 2003. Tertiary paleomagnetic results and structural analysis from the Transdanubian Range (Hungary): rotational disintegration of the Alcapa unit. Tectonophysics 363, 201-224, https://doi.org/10.1016/S0040-1951(02)00672-8

Martz, J.W., Parker, W.G., 2010. Revised Lithostratigraphy of the Sonsela Member (Chinle Formation, Upper Triassic) in the Southern Part of Petrified Forest National Park, Arizona. PLOS ONE, 5, e9329, https://doi.org/10.1371/journal.pone.0009329

Marzoli, A., Jourdan, F., Puffer, J.H., Cuppone, T., Tanner, L.H., Weems, R.E., Bertrand, H., Cirilli, S., Bellieni, G., De Min, A., 2011. Timing and duration of the Central Atlantic magmatic province in the Newark and Culpeper basins, eastern U.S.A. Lithos, 122, 175-188, https://doi.org/10.1016/j.lithos.2010.12.013

McElwain, J.C., Wagner, P.J., Hesselbo, S.P., 2009. Fossil Plant Relative Abundances Indicate Sudden Loss of Late Triassic Biodiversity in East Greenland. Science 324, 1554-1556. https://doi.org/10.1126/science.1171706

McHone, J.G., 2000. Non-plume magmatism and rifting during the opening of the central Atlantic Ocean. Tectonophysics, 316, 287-296, https://doi.org/10.1016/S0040-1951(99)00260-7

McKie, T., Williams, B., 2009. Triassic palaeogeography and fluvial dispersal across the northwest European Basins. Geol. J. 44, 711-741, https://doi.org/10.1002/gj.1201

Mildenhall, D.C., Wiltshire, P.E.J., Bryant, V.M., 2006. Forensic palynology: Why do it and how it works. Forensic Palynol. 163, 163-172, https://doi.org/10.1016/j.forsciint.2006.07.012

Miller, C., Peterse, F., Da Silva, A.-C., Baranyi, V., J. Reichart, G., Kürschner, W., 2017. Astronomical age constraints and extinction mechanisms of the Late Triassic Carnian crisis. https://doi.org/10.1038/s41598-017-02817-7

Moore, P.D., Webb, J.A., Collinson, M.E. 1991. Pollen analysis, second edition, Blackwell Scientific Publications, Oxford.

Mueller, S., Hounslow, M.W., Kürschner, W.M., 2016a. Integrated stratigraphy and palaeoclimate history of the Carnian Pluvial Event in the Boreal realm; new data from the Upper Triassic Kapp Toscana Group in central Spitsbergen (Norway). J. Geol. Soc. 173, 186-202, https://doi.org/10.1144/jgs2015-028

Mueller, S., Krystyn, L., Kürschner, W.M., 2016b. Climate variability during the Carnian Pluvial Phase — A quantitative palynological study of the Carnian sedimentary succession at Lunz am See, Northern Calcareous Alps, Austria. Impact Volcanism Glob. Chang. Mass Extinctions 441, 198-211, https://doi.org/10.1016/j.palaeo.2015.06.008

Mutti, M., Weissert, H., 1995. Triassic monsoonal climate and its signature in Ladinian-Carnian carbonate platforms (Southern Alps, Italy). J. Sediment. Res. 65, 357-367, https://doi.org/10.1306/D4268252-2B26-11D7-8648000102C1865D

Muttoni, G., Kent, D.V., Olsen, P.E., Stefano, P.D., Lowrie, W., Bernasconi, S.M., Hernández, F.M., 2004. Tethyan magnetostratigraphy from Pizzo Mondello (Sicily) and correlation to the Late Triassic Newark astrochronological polarity time scale. GSA Bull. 116, 1043-1058, https://doi.org/10.1130/B25326.1

Muttoni, G., Mazza, M., Mosher, D., Katz, M.E., Kent, D.V., and Balini, M., 2014., A Middle–Late Triassic (Ladinian–Rhaetian) carbon and oxygen isotope record from the Tethyan Ocean: Palaeogeography, Palaeoclimatology, Palaeoecology, 399, 246-259, https://doi.org/10.1016/j.palaeo.2014.01.018

Nakada, R., Ogawa, K., Suzuki, N., Takahashi, S., Takahashi, Y., 2014. Late Triassic compositional changes of aeolian dusts in the pelagic Panthalassa: Response to the continental climatic change. Palaeogeogr. Palaeoclimatol. Palaeoecol. 393, 61-75, https://doi.org/10.1016/j.palaeo.2013.10.014

Nesbitt, H.W., Young, G.M., 1982. Early Proterozoic climates and plate motions inferred from major elemental chemistry of lutites. Nature, 199, 715-717, https://doi.10.1038/299715a0

Nordt, L., Atchley, S., Dworkin, S., 2015. Collapse of the Late Triassic megamonsoon in western equatorial Pangea, present-day American Southwest. GSA Bull. 127, 1798–1815. https://doi.org/10.1130/B31186.1

Oboh-Ikuenobe, E.F., de Villiers, S.E., 2003. Dispersed organic matter in samples from the western continental shelf of Southern Africa: palynofacies assemblages and depositional environments of Late Cretaceous and younger sediments. Palaeogeogr. Palaeoclimatol. Palaeoecol. 201, 67-88, https://doi.org/10.1016/S0031-0182(03)00510-8

Ogg, J., Huang, C., Hinnov, L., 2014. Triassic timescale status: a brief overview. Albertiana, 41, 3-30.

Ogg, J.G., 2015. The mysterious Mid-Carnian "Wet Intermezzo" global event. J. Earth Sci. 26, 181-191, https://doi.org/10.1007/s12583-015-0527-x

Olsen, P., Kent, D., 2000. High-resolution Early Mesozoic Pangean climatic transect in lacustrine environments. Zentralblatt für Geologie und Paläontologie, 11, 1475-1496.

Olsen, P.E., Kent, D.V., Geissman, J.W., Bachmann, G., Blakey, R.C., Gehrels, G., Irmis, R.B., Kuerschner, W., Molina-Garza, R., Mundil, R., Sha, J.G. 2010. The Colorado Plateau Coring Project (CPCP): 100 million years of Earth system history. Earth science Frontiers, 17, 55-63.

Olsen, P.E., Kent, D.V., Sues, H.-D., Koeberl, C., Huber, H., Montanari, A., Rainforth, E.C., Fowell, S.J., Szajna, M.J., Hartline, B.W., 2002. Ascent of Dinosaurs Linked to an Iridium Anomaly at the Triassic-Jurassic Boundary. Science 296, 1305-1307, https://doi.org/10.1126/science.1065522

Olsen, P.E., Kent, D.V., Whiteside, J.H., 2011. Implications of the Newark Supergroup-based astrochronology and geomagnetic polarity time scale (Newark-APTS) for the tempo and mode of the early diversification of the Dinosauria. Earth Environ. Sci. Trans. R. Soc. Edinb. 101, 201-229, https://doi.org/10.7916/D87W6NT2

Orłowska-Zwolińska, T. 1983. Palynostratigraphy of the upper part of Triassic epicontinental sediments in Poland. Prace Instytutu Geologicznego, 54, 1-89.

Orłowska-Zwolińska, T. 1985. Palynological zones of the Polish epicontinental Triassic. Bulletin Academy of Sciences, Earth Sciences, 33, 107-119.

Pálfy, J., Demény, A., Haas, J., Carter, E.S., Görög, Á., Halász, D., Oravecz-Scheffer, A., Hetényi, M., Márton, E., Orchard, M.J., Ozsvárt, P., Vető, I., Zajzon, N., 2007. Triassic–Jurassic boundary events inferred from integrated stratigraphy of the Csővár section, Hungary. Triassic-Jurass. Bound. Events Probl. Prog. Possibilities 244, 11-33, https://doi.org/10.1016/j.palaeo.2006.06.021

Planderová, E. 1972. A contribution to palynological research of Lunz Beds in West-Carpathian region. Geologické práce, Správy, 58, 57-77.

Planderová, E. 1980. Palynomorphs from Lunz Beds and from black clayey shales in basement of Vienna Basin (borehole LNV-7). Geologica Carpathica, 31, 267-294.

Parker, W.G., Martz, J.W., 2011. The Late Triassic (Norian) Adamanian–Revueltian tetrapod faunal transition in the Chinle Formation of Petrified Forest National Park, Arizona. Earth Environ. Sci. Trans. R. Soc. Edinb. 101, 231-260, https://doi.org/10.1017/S1755691011020020

Parker, W.G., Martz, J.W., 2017. Building Local Biostratigraphic models for the Upper Triassic of Western North America: methods and considerations. In: Terrestrial Depositional Systems. Elsevier, 1-38. https://doi.org/10.1016/B978-0-12-803243-5.00001-7

Parrish, J.T., 1993. Climate of the Supercontinent Pangea. The Journal of Geology, 101, 215-233, http://dx.doi.org/10.1086/648217

Parrish, J., Peterson, F., 1988. Wind directions predicted from global circulation models and wind directions determined from Eolian Sandstones of the Western United States - A comparison. Sedimentary Geology, 56, 261-282, https://doi.org/10.1016/0037-0738(88)90056-5

Paterson, N.W., Mangerud, G., 2015. Late Triassic (Carnian– Rhaetian) palynology of Hopen, Svalbard. Rev. Palaeobot. Palynol. 220, 98-119, https://doi.org/10.1016/j.revpalbo.2015.05.001
Paterson, N.W., Mangerud, G., Mørk, A., 2016. Late Triassic (early Carnian) palynology of shallow stratigraphical core 7830/5-U-1, offshore Kong Karls Land, Norwegian Arctic. Palynology, 41, 230-254, https://doi.org/10.1080/019161 22.2016.1163295
Porter, R.J., Gallois, R.W., 2008. Identifying fluvio–lacustrine intervals in thick playa-lake successions: An integrated sedimentology and ichnology of arenaceous members in the mid–late Triassic Mercia Mudstone Group of south-west England, UK. Biot. Interact. 270, 381-398, https://doi.org/10.1016/j.palaeo.2008.07.020
Potonié, R., Kremp, G. 1954. Die Gattungen der palaozoischen Sporae dispersae und ihre Stratigraphie. Geololgisches Jahrbuch, 69, 111-194.
Prentice, I.C., 1986. Vegetation responses to past climatic variation. Vegetatio 67, 131-141. https://doi.org/10.1007/BF00037363
Preto, N., Kustatscher, E., Wignall, P.B., 2010. Triassic climates — State of the art and perspectives. Palaeogeogr. Palaeoclimatol. Palaeoecol. 290, 1-10, https://doi.org/10.1016/j.palaeo.2010.03.015
Preto, N., Willems, H., Guaiumi, C., Westphal, H., 2013. Onset of significant pelagic carbonate accumulation after the Carnian Pluvial Event (CPE) in the western Tethys. Facies, 59, 891-914, https://doi.org/10.1007/s10347-012-0338-9
Prochnow, S.J., Nordt, L.C., Atchley, S.C., Hudec, M.R., 2006. Multi-proxy paleosol evidence for middle and late Triassic climate trends in eastern Utah. Palaeogeogr. Palaeoclimatol. Palaeoecol. 232, 53-72, https://doi.org/10.1016/j.palaeo.2005.08.011
Punt, W., Hoen, P.P., Blackmore, S., Nilsson, S., Le Thomas, A., 2007. Glossary of pollen and spore terminology. Rev. Palaeobot. Palynol. 143, 1-81, https://doi.org/10.1016/j.revpalbo.2006.06.008
Ramezani, J., Bowring, S. A., Pringle, M. S., Winslow, F. D., Rasbury, E.T., 2005. The Manicouagan impact melt rock: A proposed standard for the intercalibration of U–Pb and 40Ar/39Ar isotopic systems. Geochimica et Cosmochimica Acta Supplemen, 69, A321.
Ramezani, J., Fastovsky, D.E., Bowring, S.A., 2014. Revised chronostratigraphy of the Lower Chinle Formation strata in Arizona and New Mexico (USA): High-precision U-Pb geochronological constraints on the Late Triassic evolution of dinosaurs. Am. J. Sci. 314, 981-1008, https://doi.org/10.2475/06.2014.01
Ramezani, J., Hoke, G.D., Fastovsky, D.E., Bowring, S.A., Therrien, F., Dworkin, S.I., Atchley, S.C., Nordt, L.C., 2011. High-precision U-Pb zircon geochronology of the Late Triassic Chinle Formation, Petrified Forest National Park (Arizona, USA): Temporal constraints on the early evolution of dinosaurs. GSA Bull. 123, 2142-2159, https://doi.org/10.1130/B30433.1
Raup, D.M., Sepkoski, J.J., 1982. Mass extinctions in the marine fossil record. Science 215, 1501-1503.
Rauzi, S.L., 2000. Permian Salt in the Holbrook Basin, Arizona. AZ Geol. Sur. Open File Rept., OFR-00-03, 1-20
Reichgelt, T., Parker, W.G., Martz, J.W., Conran, J.G., van Konijnenburg-van Cittert, J.H.A., Kürschner, W.M., 2013. The palynology of the Sonsela member (Late Triassic, Norian) at Petrified Forest National Park, Arizona, USA. Rev. Palaeobot. Palynol. 189, 18-28, https://doi.org/10.1016/j.revpalbo.2012.11.001
Retallack, G.J. 2009. Greenhouse crises of the past 300 million years. Geological Society of America Bulletin, 121, 1441-1455, https://doi.org/10.1130/B26341.1
Riggs, N.R., Ash, S.R., Barth, A.P., Gehrels, G.E., Wooden, J.L., 2003. Isotopic age of the Black Forest Bed, Petrified Forest Member, Chinle Formation, Arizona: An example of dating a continental sandstone. GSA Bull. 115, 1315-1323, https://doi.org/10.1130/B25254.1
Riggs, N.R., Reynolds, S.J., Lindner, P.J., Howell, E.R., Barth, A.P., Parker, W.G., Walker, J.D., 2013. The Early Mesozoic Cordilleran arc and Late Triassic paleotopography: The detrital record in

Upper Triassic sedimentary successions on and off the Colorado Plateau. Geosphere 9, 602-613, https://doi.org/10.1130/GES00860.1

Rigo, M., Preto, N., Roghi, G., Tateo, F., Mietto, P., 2007. A rise in the Carbonate Compensation Depth of western Tethys in the Carnian (Late Triassic): Deep-water evidence for the Carnian Pluvial Event. Palaeogeogr. Palaeoclimatol. Palaeoecol. 246, 188-205, https://doi.org/10.1016/j.palaeo.2006.09.013

Roghi, G., 2004. Palynological investigations in the Carnian of the Cave del Predil area (Julian Alps, NE Italy). Rev. Palaeobot. Palynol. 132, 1-35, https://doi.org/10.1016/j.revpalbo.2004.03.001

Roghi, G., Gianolla, P., Minarelli, L., Pilati, C., Preto, N., 2010. Palynological correlation of Carnian humid pulses throughout western Tethys. Palaeogeogr. Palaeoclimatol. Palaeoecol., Triassic climates 290, 89-106, https://doi.org/10.1016/j.palaeo.2009.11.006

Rostási, Á. 2011 Palaeoenvironmental reconstruction of the Carnian (Late Triassic) of the Gerencse and Bakony Basins, based on mineralogy and petrology. PhD thesis, University of Pannonia, Veszprém, (in Hungarian with English abstract).

Rostási, Á., Raucsik, B., Varga, A., 2011. Palaeoenvironmental controls on the clay mineralogy of Carnian sections from the Transdanubian Range (Hungary). Palaeogeogr. Palaeoclimatol. Palaeoecol. 300, 101-112. https://doi.org/10.1016/j.palaeo.2010.12.013

Rotstayn, L.D., Lohmann, U., 2002. Tropical Rainfall Trends and the Indirect Aerosol Effect. J. Clim. 15, 2103-2116, https://doi.org/10.1175/1520-0442(2002)015<2103:TRTATI>2.0.CO;2

Rozema, J., Broekman, R.A., Blokker, P., Meijkamp, B.B., de Bakker, N., van de Staaij, J., van Beem, A., Ariese, F., Kars, S.M., 2001. UV-B absorbance and UV-B absorbing compounds (para-coumaric acid) in pollen and sporopollenin: the perspective to track historic UV-B levels. Impacts Ultrav. Radiat. Aquat. Terr. Ecosyst. 62, 108-117, https://doi.org/10.1016/S1011-1344(01)00155-5

Ruffell, A., Shelton, R., 1999. The control of sedimentary facies by climate during phases of crustal extension: examples from the Triassic of onshore and offshore England and Northern Ireland. J. Geol. Soc. 156, 779-189, https://doi.org/10.1144/gsjgs.156.4.0779

Ruffell, A., Simms, M.J., Wignall, P.B., 2016. The Carnian Humid Episode of the late Triassic: a review. Geol. Mag. 153, 271-284, https://doi.org/10.1017/S0016756815000424

Schaller, M.F., Wright, J.D., Kent, D.V., 2015. A 30 Myr record of Late Triassic atmospheric pCO2 variation reflects a fundamental control of the carbon cycle by changes in continental weathering. GSA Bull. 127, 661-671. https://doi.org/10.1130/B31107.1

Schlager, W. & Schöllnberger, W. 1974. Das Prinzip stratigraphischer Wenden in der Schichtenfolge der Nordlichen Kalkalpen. Mitteilungen der Geologischen Gesellschaft Wien, 66/67, 165-193.

Schwab, K.W., Miller, H.W., Smith, M.A., 2017. Source-rock potential of the Lower Permian Supai Formation in the Blackstone. Exploration Company Rocking Chair Ranch No. 4 well, Navajo County, Arizona, Search and Discovery, Article #80601

Schweingruber, F.H., 1996. Tree Rings and Environment Dendroecology: Bern, Switzerland, Swiss Federal Institute for Forest

Scotese, C.R., 2001. Atlas of Earth History, PALEOMAP Project, Arlington, Texas

Sellwood, B.W., Valdes, P.J., 2006. Mesozoic climates: General circulation models and the rock record. Sediment. Geol., Sedimentology and Sequence Stratigraphy of Fluvial Deposits 190, 269-287, https://doi.org/10.1016/j.sedgeo.2006.05.013

Sharp, Z. 2007. Principles of Stable Isotope Geochemistry, Prentice Hall

Shukla, U.H., Bachmann, G.H. & Singh, I.B. 2010. Facies architecture of the Stuttgart Formation (Schilfsandstein, Upper Triassic), central Germany, and its comparison with modern Ganga system, India. Palaeogeography Palaeoclimatology Palaeoecology, 297, 110–128, https://doi.10.1016/j.palaeo.2010.07.019

Simms, M.J., Ruffell, A.H., 1990. Climatic and biotic change in the late Triassic. J. Geol. Soc. 147, 321-327, https://doi.org/10.1144/gsjgs.147.2.0321

Simms, M.J., Ruffell, A.H., 1989. Synchroneity of climatic change and extinctions in the Late Triassic. Geology 17, 265-268. https://doi.org/10.1130/0091-7613(1989)017<0265:SOCCAE>2.3.CO;2

Sluijs, A., Pross, J., Brinkhuis, H., 2005. From greenhouse to icehouse; organic-walled dinoflagellate cysts as paleoenvironmental indicators in the Paleogene. Earth-Sci. Rev. 68, 281-315, https://doi.org/10.1016/j.earscirev.2004.06.001

Sun, Y.D., Wignall, P.B., Joachimski, M.M., Bond, D.P.G., Grasby, S.E., Lai, X.L., Wang, L.N., Zhang, Z.T., Sun, S., 2016. Climate warming, euxinia and carbon isotope perturbations during the Carnian (Triassic) Crisis in South China. Earth Planet. Sci. Lett. 444, 88-100, https://doi.org/10.1016/j.epsl.2016.03.037

Tappert, R., McKellar, R.C., Wolfe, A.P., Tappert, M.C., Ortega-Blanco, J., and Muehlenbachs, K., 2013, Stable carbon isotopes of C3 plant resins and ambers record changes in atmospheric oxygen since the Triassic: Geochimica et Cosmochimica Acta, 121, 240-262, https://doi.org/10.1016/j.gca.2013.07.011

Traverse, A. 2007. Paleopalynology,second edition, Springer.

Trendell, A.M., Atchley, S.C., Nordt, L.C., 2013. Facies Analysis of A Probable Large-Fluvial-Fan Depositional System: The Upper Triassic Chinle Formation at Petrified Forest National Park, Arizona, U.S.A. J. Sediment. Res. 83, 873-895, https://doi.org/10.2110/jsr.2013.55

Trendell, A.M., Nordt, L.C., Atchley, S.C., Leblanc, S.L., Dworkin, S.I., 2013. Determining floodplain plant distributions and populations usin paleopedology and fossil root traces: Upper Triassic Sonsela Member of the Chinle Formation at Petrified Forest National Park, Arizona. PALAIOS 28, 471-490, https://doi.org/10.2110/palo.2012.p12-065r

Trotter, J.A., Williams, I.S., Nicora, A., Mazza, M., Rigo, M., 2015. Long-term cycles of Triassic climate change: a new δ18O record from conodont apatite. Earth Planet. Sci. Lett. 415, 165-174, https://doi.org/10.1016/j.epsl.2015.01.038

Tyson, R. 1995 Sedimentary Organic Matter Organic gacies and palynofacies, Springer.

van der Eem, J.G.L.A., 1983. Aspects of middle and late triassic palynology. 6. Palynological investigations in the Ladinian and lower Carnian of the Western Dolomites, Italy. Rev. Palaeobot. Palynol. 39, 189-300, https://doi.org/10.1016/0034-6667(83)90016-7

van de Schootbrugge, B., Quan, T.M., Lindström, S., Püttmann, W., Heunisch, C., Pross, J., Fiebig, J., Petschick, R., Röhling, H.-G., Richoz, S., Rosenthal, Y., Falkowski, P.G., 2009. Floral changes across the Triassic/Jurassic boundary linked to flood basalt volcanism. Nat. Geosci. 2, 589-594, https://doi.org/10.1038/ngeo577

van Veen, P.M. 1985. Stratigraphy of the Triassic in the Troms area. Oljedirektoratet technical report 0D-85-36.

Visscher, H., Brugman, W.A., 1981. Ranges of selected palynomorphs in the alpine triassic of Europe. Late Palaeoz. Early Mesoz. Stratigr. Palynol. 34, 115-128, https://doi.org/10.1016/0034-6667(81)90069-5

Visscher, H., Looy, C.V., Collinson, M.E., Brinkhuis, H., van Konijnenburg-van Cittert, J.H.A., Kürschner, W.M., Sephton, M.A., 2004. Environmental mutagenesis during the end-Permian ecological crisis. Proc. Natl. Acad. Sci. U. S. A. 101, 12952-12956, https://doi.org/10.1073/pnas.0404472101

Visscher, H., van der Zwan, C.J., 1981. Palynology of the circum-mediterranean triassic: Phytogeographical and palaeoclimatological implications. Geol. Rundsch. 70, 625-634, https://doi.org/10.1007/BF01822140

Visscher, H., van Houte, M., Brugman, W.A., Poort, R.J., 1994. Rejection of a Carnian (Late Triassic) “pluvial event” in Europe. Rev. Palaeobot. Palynol. 83, 217-226, https://doi.org/10.1016/0034-6667(94)90070-1

Vigran, J.O., Mangerud, G., Mørk, A., Bugge, T. and Weitschat, W. (1998) Biostratigraphy and sequence stratigraphy of the Lower and Middle Triassic deposits from the Svalis Dome, Central Barents Sea, Norway. Palynology, 22, 89-141.

Vigran, J.O., Mangerud, G., Mørk, A., Worsley, D. & Hochuli, P.A., 2014. Palynology and geology of the Triassic succession of Svalbard and the Barents Sea. NGU Special Publication, 14, Geological Survey of Norway, https://doi.10.5167/uzh-99116

Vollmer, T. Werner, R., Weber, M., Tougiannidis, N., Röhling, H-G. & Hambach, U. 2008. Orbital control on Upper Triassic Playa cycles of the Steinmergel-Keuper (Norian): A new concept for ancient playa cycles. Palaeogeography, Palaeoclimatology, Palaeoecology, 267, 1-16, https://doi.org/10.1016/j.palaeo.2007.12.017

Walkden, G., Parker, J., Kelley, S., 2002. A Late Triassic Impact Ejecta Layer in Southwestern Britain. Science 298, 2185, https://doi.org/10.1126/science.1076249

Warrington, G., 1967. The correlation of the Keuper by miospores. Nature, 214, 323-324, https://doi.10.1038/2141323a0

Warrington, G., 1970. The stratigraphy and palaeontology of the 'Keuper' Series of the central Midlands of England. Quarterly Journal of the Geological Society, 126, 183-223, https://doi.org/10.1144/gsjgs.126.1.0183

Warrington, G., Audley-Charles, M. G., Elliott, R. E., Evans, W. B., Ivemey-Cook, H. C., Kent, P. E., Robinson, P.L., Shotton, F. W., and Taylor, F. M., 1980. A correlation of Triassic rocks in the British Isles. Geological Society of London, Special Report, 13, 1-78.

Wéber, B., 1984. Kohlenserie in der Obertrias des Mecsek-Gebirges. Földtani Közlöny, 114, 225-230, (in Hungarian with German abstract).

Whiteside, J.H., Lindström, S., Irmis, R.B., Glasspool, I.J., Schaller, M.F., Dunlavey, M., Nesbitt, S.J., Smith, N.D., Turner, A.H., 2015. Extreme ecosystem instability suppressed tropical dinosaur dominance for 30 million years. Proc. Natl. Acad. Sci. 112, 7909-7913, https://doi.org/10.1073/pnas.1505252112

Willis, K.J & McElwain, J.C., 2002. The evolution of plants. Oxford University Press

Wilson, K.M., Pollard, D., Hay, W.W., Thompson, S.L., Wold, C.N., 1994. General circulation model simulations of Triassic climates: Preliminary results. In: Klein, G.O. (ed.), Pangea: Paleoclimate, tectonics, and sedimentation during accretion, zenith, and breakup of a supercontinent. Geological Society of America, Geological Society Special Paper, 288, 91-116.

Wood, G.D., Gabriel, A.M., Lawson, J.C., 1996. Chapter 3. Palynological techniques – processing and microscopy. In: Jansonius, J., McGregor, D.C., (eds), Palynology: principles and applications. American Association of Stratigraphic Palynologists Foundation, Dallas 1, 29-50.

Xu, G., Hannah, J.L., Stein, H.J., Mørk, A., Vigran, J.O., Bingen, B., Schutt, D.L., Lundschien, B.A., 2014. Cause of Upper Triassic climate crisis revealed by Re–Os geochemistry of Boreal black shales. Palaeogeogr. Palaeoclimatol. Palaeoecol. 395, 222-232, https://doi.org/10.1016/j.palaeo.2013.12.027

Zeigler, K.E., Geissman, J.W., 2011. Magnetostratigraphy of the Upper Triassic Chinle Group of New Mexico: Implications for regional and global correlations among Upper Triassic sequences. Geosphere 7, 802-829. https://doi.org/10.1130/GES00628.1

Zhang, X., W Zwiers, F., Hegerl, G., Hugo Lambert, F., P Gillett, N., Solomon, S., Stott, P., Nozawa, T., 2007. Detection of human infuence on twentieth-century precipitation trends. Nature,448, 461-465, https://doi.org/10.1038/nature06025

Zhang, Y., Li, M., Ogg, J.G., Montgomery, P., Huang, C., Chen, Z.-Q., Shi, Z., Enos, P., Lehrmann, D.J., 2015. Cycle-calibrated magnetostratigraphy of middle Carnian from South China: Implications for Late Triassic time scale and termination of the Yangtze Platform. Palaeogeogr. Palaeoclimatol. Palaeoecol. 436, 135-166, https://doi.org/10.1016/j.palaeo.2015.05.033

Ziegler, A., Eshel, G., Rees, P.M., Rothfust, T., Rowley, D., Sunderlin, D., 2003. Tracing the tropics across land and sea: Permian to present. Lethaia 36, 227-254, https://doi.org/10.1080/00241160310004657

Ziegler, A.M., Parrish, M.J., Jiping, Y., Gyllenhaal, E.D., Rowley, D.B., Parrish, J.T., Shangyou, N., Bekker, A., Hulver, M.L., 1993. Early Mesozoic phytogeography and climate. Phil. Trans. R. Soc. Lond. B, 341, 297-305, https://doi.10.1098/rstb.1993.0115

Zonneveld, J.-P., Orchard, M., 2002. Stratal relationships of the Upper Triassic Baldonnel Formation, Williston Lake, northeastern British Columbia. Geological Survey of Canada Current Research 2002-A8, 1-13.

Systematic palynology

This chapter contains a short description of selected terrestrial palynomorph taxa. A complete systematic study of the whole palynoflora has not been performed, as many of the identified taxa have been sufficiently described elsewhere. List of the identified taxa with full author citation in Papers 1-2 can be found in the two chapters respectively. In the systematic part on fossil dispersed spores and pollen the morphology-based artificial classification system is applied, as it was proposed by e.g., Potonié & Kremp (1954) and Dettmann (1963). The references to the photo plates are indicated by bold font. Morphological description follows the terminology of Punt et al. (2007).

Anteturma SPORITES H. Potonié 1893

Turma TRILETES Reinsch ex Schopf emend. Dettmann 1963

Suprasubturma ACAVATITRILETES Dettmann 1963

Subturma AZONOTRILETES Luber emend. Dettmann 1963

Infraturma LAEVIGATI Bennie & Kidston emend. R. Potonié 1956

Form genus *Laevigatisporites* (Bennie & Kidston 1886) Ibrahim 1933

Laevigatisporites robostus Leschik 1956 **(Plate 13/10)**

Description. Trilete spores with circular or subtriangular equatorial outline. The trilete mark is usually distinct, the laesurae extend about to 3/4 of the spore radius. The laesure are bordered by a thin exine thickening on the proximal face. The exine thickening does not reach the margin. The exine is smooth, unsculptured, 2-3 µm thick.

Remarks. It differs from the other laevigate species in its size, being much bigger compared to *Dictyophyllidites harrisii* or *Deltoidospora* and the thin exine thickening along the trilete rays.

Formagenus *Paraconcavisporites* Klaus 1960

Paraconcavisporites lunzensis Klaus 1960 **(Plate 13/11)**

Description. Trilete spores with circular or subtriangular equatorial outline. The sides of the outline are usually straight, sometimes slightly concave or convex. On the proximals surface, along the sutures of the trilete mark the exine is thickened and connected forming a kyrtome. The contact areas of the kyrtome around the termination of the trilete rays are rounded. The exine is smooth, unsculptured, 2-3 µm thick.

Remarks. It differs from *Dictyophyllidites harrisii* in having real kyrtome. *Deltoidospora* sp. has no thickening, or folded exine. *Concavisporites toralis* has usually a more concave outline.

Formagenus *Todisporites* Couper, 1958

Todisporites rotundiformis (Maljavkina, 1943) Pocock, 1970 **(Plate 1/W, Plate 9/1)**

Description. Trilete spores with circular equatorial outline. The trilete mark is usually distinct, the laesurae extend about to 2/3 of the spore radius. The exine is smooth and thin; the grains are often folded, crumpled or broken.

Remarks. It differs from *Todisporites major* in the size being much smaller than *T. major*. *Todisporites minor* is a junior synonym of *T. rotundiformis*-

Infraturma APICULATI Bennie & Kidston 1896 emend. Potonié, 1956
Subinfraturma GRANULATI Dybova & Jachowicz, 1957

Formagenus *Granulatisporites* (Ibrahim, 1933) Potonié & Kremp, 1954

Granulatisporites infirmus (Balme, 1957) Cornet & Traverse, 1975 **(Plate1/F)**

Description. Trilete spore with triangular-subtriangular outline and rounded apices. The sides are convex or slightly concave. Laesurae extend almost to the equatorial margin but only rarely reaching it. The exine is sparsely to densely sculptured with grana, a few bacula and coni. The ornamentation is usually moderately densely packed. The exine is thin less than 1 µm.

Subinfraturma VERRUCATI Dybova & Jachowicz, 1957

Genus *Converrucosisporites* Potonié & Kremp, 1954

Converrucosiporites tumolosus (Leschik, 1956) Roghi, 2004 **(Plate 11/25, Plate 13/20)**

Description. Trilete spore with subtriangular outline. The exine is *ca.* 2 µm thick. It is densely ornamented with coalescent and elongate verrucae proximally and distally giving the exine a rugulate appearance. The trilete laesurae extend almost to the equator.

Formagenus *Trilites* Cookson 1947 ex Couper, 1953

Trilites klausii Bharadwaj & Singh, 1964 **(Plate 1/AA)**

Description. Trilete spore with circular-subtriangular outline. The trilete mark is usually not visible due to the unfavourable orientation of the grains. The exine is thick, dark brown. It is densely packed with verrucae and papillae. The sculptural elements extend to the equatorial margin resulting in an undulating equatorial margin.

Remarks. *Triletes tubercoliformis* Cookson 1947 has similar appearance but the undulation of the thickened exine is much more developed in the case of the *T. klausii*.

Genus *Uvaesporites* Döring, 1965

Uvaesporites argenteaeformis (Bolkhovitina, 1953) Schulz, 1967 **(Plate 1/N-O)**

Description. Trilete spores with subtriangular outline. The trilete mark is distinct extending to about 3/4 of the spore radius. The laesurae are straight. The exine is 1-1.5 µm thick. The proximal side is smooth and unsculptured, the distal side is verrucate. The warts (2-3 µm high and 3-5 µm in diameter) are fused together to form a reticulum.

Uvaesporites gadensis Praehauser-Enzenberg 1970 (**Plate 5/8, Plate 13/4)**

Description. Trilete spore with triangular outline. The trilete mark is distinct extending to about 3/4 of the spore radius. The laesurae are undulating. The exine is 1-1,5 µm thick. The proximal side is smooth and unornamented, the distal side is verrucate. The warts (2-3 µm high and 3-5 µm in diameter) are fused together to form a reticulum. The verrucae extend over the equatorial margin of each grain.

Remarks. *Uvaesporites gadensis* differs from *U. argentaeformis* in its smaller size and the undulating laesurae.

Formagenus *Verrucosisporites* (Ibrahim, 1933) Potonié & Kremp, 1954

Verrucosisporites morulae Klaus 1960 (Plate 5/9-10, 25)

Description. Trilete spores with circular, subcircular or oval outline. The exine is densely packed with warts (*ca.* 2-5 µm high, 2 µm wide) forming a distinct verrucate surface proximally and distally. The trilete mark is extending to about 2/3 of the spore radius. The laesurae are often not visible due to the dense ornamentation.

Remarks. Klaus (1960) classifies verrucate spores of relatively large size (50-70 µm), with big (5-6 µm high) but relatively few warts.

Infraturma APICULATI Bennie & Kidston, 1896 emend. Potonié, 1956

Formagenus *Anapiculatisporites* Potonié & Kremp, 1954

Anapiculatisporites telephorus (Pautsch 1958) Klaus 1960 (Plate 13/16)

Description. Trilete spores with circular outline. The laesurae of the trilete mark are extending ca. 2/3 of the spore radios. The wall is thin it and has usually very pale yellow-green colour. The surface of the spore is packed by spines. The spines are mainly confined to the distal side. On the proximal side the spines extend only until the termination of the trilete rays.

Remarks. The genus *Carnisporites* is a junior synonym for *Anapiculatisporites*.

Formagenus *Neoraistrickia* Potonié, 1956

Neoraistrickia taylorii Playford & Dettmann, 1965 (Plate 13/17)

Description. Trilete spores with triangular outline. The sides are slightly concave. The laseurae of the trilete mark extend to equator or occasionally only ¾ of the spore radius. The exine is thin 1-2 µm and densely packed with bacula and spines with rounded tips of 2-3 µm height

Remarks. *Neoraistrickia taylorii* differs from the other *Neoraistrickia* species in having a distinct triangular outline and densely packed ornamentation.

Infraturma MURORNATI Potonié & Kremp, 1954

Formagenus *Cristatitriletes* Mädler, 1964

Cristatitriletes baculatus Mädler, 1964 (Plate 1/D)

Description. Trilete spores with triangular-subtriangular outline. The trilete mark is distinct; the length of the laesurae is approx. ½ of the spore radius. The exine is ornamented with an incomplete reticulum of fused bacula which extend over the equatorial margin. The bacula are 4-5 µm long.

Formagenus *Klukisporites* Couper, 1958

Klukisporites granosifenestellatus Fisher& Dunay, 1984 (Plate 1/M)

Description. Trilete spore with triangular–subtriangular outline. Laesurae extend almost to the equatorial margins. The spore is ornamented with distinct reticulation, the lumina are polygonal.

Formagenus *Lycopodiacidites* (Couper, 1953) R. Potonié, 1956

Lycopodiacidites kuepperi Klaus, 1960 (Plate 13/1)

Description. Trilete spore with subtriangular outline. The laseurae of the trilete mark extend to the equator. The prixmal sides is smooth, unornamented, the distal side is densely packed with warts forming a heavily ornamented rugulate surface. The rugulae are often hook-shaped or bent. The exine is *ca.* 3 µm thick.

Remarks. *Lycopodiacidites kuepperi* differs from the other *Lycopodiacidites* speices in having hook-shaped rugulae. *Lycopodiacodtes kokenii* van der Eem is very similar in appearance to *L. kuepperi*, but the former has an ornamented proximal and distal side as well.

Formagenus *Reticulatisporites* Leschik 1955

Reticulatisporites dolomiticus Blendinger, 1988 (Plate 13/13)

Description. Trilete spore with circular to subcircular outline. The spore is heavily ornamented with large muri on both the distal and proximal sides (ca. 5 µm high and 3 µm wide) giving the exine a reticulate surface. The outline of the spore is irregular due to the large muri. The lumina are mostly pentagonal and up to 10 µm wide. Within the lumina one or several bacula or spinae (up to 2-4 µm high) may occur. The trilete rays are often invisible due to the ornamentation. The laesurae extend up to 1/3 to 1/2 of the spore radius.

Infraturma AURICULATI (Schopf, 1944) Potonié & Kremp, 1954

Formagenus *Kyrtomisporis* (Mädler, 1964) van der Eem, 1983

Kyrtomisporis erveii van der Eem 1983 (Plate 13/19)

Description. Trilete spore with triangular, subtriangular outline. The sides are slightly convex. The proximal exine is smooth and thickened in the equatorial interradial regions to form a prominent kyrtome. The kyrtome extends to 2/3 of spore radius or up to the equator. The kyrtome is sometimes slightly protruding beyond the equator and interconnected at the apices. On the distal side, the exine is ornamented with elongated rugulae (*ca.* 2.5-6 µm long). The laesurae of the trilete mark almost extend to the equator.

Remarks. *Kyrtomisporis laevigatus* lacks rugulae on the distal sides and the kyrtome of *Kyrtomisporis speciosus* does not extend beyond the equator.

Kyrtomisporis speciosus Mädler, 1964 (Plate 1/Y)

Description. Trilete spore with triangular outline. The sides are straight, or slightly convex. The trilete mark is distinct. The laesurae extend almost to the periphery. The proximal face is ornamented with distinct kyrtome, enclosing laesurae and forming prominent apices. The distal face is ornamented with ridges; the cingulum is 3-5 µm thick.

Infraturma CINGULATI Potonié & Klaus, 1954

Formagenus *Striatella* Mädler, 1964

Striatella seebergensis Mädler 1964 (Plate 1/P, Plate 13/21)

Description. Trilete spore with subtriangular, subcircular outline and convex sides. The exine is 2 µm thick. It is ornamented both on the distal and proximal sides and packed densely with muri (*ca.* 4-6 µm wide). The trilete mark is not always distinct due to the orientation of compression. It is surrounded by a 4–5 µm wide cingulum.
Remarks. *Contignisporites problematicus* (Couper 1958) Döring 1965, *Duplexisporites gyratus* (Playford & Dettmann 1964); de Jersey & Paten 1964; *Asseretospora gyrata* (Playford & Dettmann 1964) Schuurman 1977, *Corrugatisporites klausi* Kavary 1972, *Corrugatisporites scanicus* Nilsson 1978 can be considered as synonyms of *S. seebergensis*.

Subturma ZONOTRILETES Waltz, 1935
Infraturma TRICRASSATI Dettmann, 1963

Genus *Camarozonosporites* Pant 1954 ex Potonié, 1965 emend. Klaus, 1960
Camarazonosporites rudis (Leschik, 1956) Klaus, 1960 (Plate 13/2)
Description. Trilete spore with subtriangular outline. The laseurae of the trilete mark extend to the equator. The exine is slightly thickened along the rays of the trilete mark. The proximal sides is smooth, unornamented, the distal side is densely packed with warts forming a heavily ornamented rugulate surface. A thin cingulum surrounds the spore.
Remarks. It differs from *Lycopodiacidites kuepperi* in having a cingulum.

Infraturma ZONATI Potonié & Kremp, 1954

Genus *Kraeuselisporites* Leschik & Jansonius, 1962
Kraeuselisporites cooksonae (Klaus 1960) Dettmann 1963 (Plate 13/6)
Description. Trilete, zonate spore with triangular, subtriangular outline. The distal side is punctate, reticulate and covered with coni, echini and grana. The zona is 5-10 µm wide. On the proximal face, there is a distinct trilete mark, the trilete rays extend to the inner edge of the zona. The exine is often folded due to compression.

Formagenus *Thomsonisporites* Leschik, 1955
Thomsonisporites punctatus Leschik, 1955 (Plate 5/12)
Description. Trilete spores with subtriangular, subcircular outline. The lasurae of the trilete mark are distinct and they extend to the equator. The exine is thick and punctate. The zone is thin and often folded due to compression. The trilete mark was not visible because of the folds. The inner body is surrounded by a *ca.* 5-10 µm wide zona.

Suprasubturma PERINOTRILETES Erdtman, 1947
Genus *Guthoerlisporites* Bhardwaj, 1954
Guthoerlisporites cancellosus Playford & Dettmann, 1965 (Plate 1/J-K)
Description. Trilete spore with circular outline and distinct monosaccus like perine. A central part when present has a distinct, circular to oval outline and dark, thickened exine. The trilete

rays are very thin and short approx. ¾ of the radius of the inner part and 1/10 of the total spore radius. The perine is finely reticulate with relatively indistinct radial folds.

Turma MONOLETES Ibrahim, 1933
Subturma ZONOMONOLETES Luber, 1935

Genus *Aratrisporites* (Leschik, 1955) Playford & Dettmann, 1965

Aratrisporites crassitectatus Reinhardt, 1964 (Plate 5/4-6)

Description. Monolete and zonate spores with oval outline. The monolete mark extends the whole length of the spore; it is usually marked by an exine thickening. The mark can be straight or sinuous. The exine is covered with warts.
Remarks. It differs from the other *Aratrisporites* species by having warts.

Aratrisporites palettae (Klaus, 1960) Schulz, 1967 (Plate 13/14)

Description. Monolete and zonate spores with oval outline surrounded by a wide pseudozona. Width of the zona is 3-11 µm, the zona is covered by hairs of up to 7 µm in length. The monolete mark is distinct, the exine is slightly thickened along the monolete mark.

Anteturma VARIEGERMINANTES Potonié, 1970
Turma ALETES Ibrahim, 1933
Subturma AZONALETES Potonié & Kremp, 1954

Genus *Gibeosporites* Leschik, 1959

Gibeosporites lativerrucosus Leschik, 1959 (Plate 11/14, Plate 13/3)

Description. Trilete spore with circular outline and robust appendages. The trilete mark is not observable, it is usually covered by the ornamentation. The exine is sculptured with long thorn-like bacula, or appendages with more rounded tips. Basal width of bacula is 5-6 µm, height 2-5 µm.
Remarks. *Gibeosporites lativerrucosus* is a junior synonym of *Apiculatasporites lativerrucosus* Leschik, 1955.

Anteturma POLLENITES Potonié, 1931
Turma SACCITES Erdtman, 1947
Subturma DISACCITES Cookson, 1947
Infraturma DISACCIATRILETI Leschik, 1956

Genus *Alisporites* (Daugherty, 1941) Nilsson 1958

Alisporites aequalis Mädler, 1964 (Plate 14/1)

Description. Bisaccate alete haploxylonoid pollen grains of large size with distinct ellipsoidal outline. The outline of the pollen grain is bilaterally symmetrical and ellipsoidal, much broader than long. Distal sulcus defined by inner margins of sacci. The sacci are symmetrical, their greatest breadth is at their roots, the roots form a straight line. The sacci are slightly darker

than the corpus. The exine of the sacci is reticulate with indistinct lumina. The exine of the corpus is scabrate. The exine of the sacci is reticulate with indistinct lumina. The exine of the corpus is scabrate.

Alisporites giganteus (Danzé-Corsin & Laveine 1963) Cornet, 1977 (Plate 2/A)

Description. Bisaccate alete haploxylonoid pollen grains of large size with distinct ellipsoidal outline. The outline of the pollen grain is bilaterally symmetrical and ellipsoidal, much broader than long. Distal sulcus defined by inner margins of sacci. The sacci are symmetrical, their greatest breadth is at their roots, the roots form a straight line. The sacci are slightly darker than the corpus. The exine of the sacci is reticulate with indistinct lumina. The exine of the corpus is scabrate.

Remarks. *Alisporites giganteus* differs from the other *Alisporites* species in its greater size and characteristic ellipsoidal outline and the straight saccus bases. *A. giganteus* is most likely a synonym to *Alisporites aequalis* Mädler 1964 but the former name has been applied to this type of *Alisporites* in the North American taxonomy.

Alisporites grandis (Cookson, 1953) Dettmann, 1963 (Plate 2/B, Plate 9/12)

Description. Bisaccate alete haploxylonoid pollen grains of large size with distinct oval-rectangular outline. The outline of the pollen grain is oval-rectangular, width and height are often around the same length, sometimes longer than broad. Distal sulcus defined by inner margins of sacci. The sacci are symmetrical, their greatest breadth is at their roots, the root bases form a straight line. The sacci are darker than the corpus. The exine of the sacci are reticulate with indistinct lumina. The exine of the corpus is scabrate.

Remarks. *Alisporites grandis* differs from *A. giganteus* in its shape.

Alisporites grauvogeli Mädler, 1964 (Plate 11/10)

Description. Bisaccate alete haploxylonoid pollen grains of large size. The outline is oval, with slightly greater height than width. Distal sulcus defined by inner margins of sacci. The exine is thickened and often folded along the sulcus margins. The sacci are symmetrical, their greatest breadth is at their roots. They overlap almost with the whole corpus. The sacci are reticulate. The sacci root bases form a straight line.

Alisporites opii (Daugherty, 1941) Jansonius, 1962 (Plate 2/C, Plate 6/1)

Description. Bisaccate alete haploxylonoid pollen grains of large size. The ouline is oval, with slightly greater width than height. The sulcus is a single fusiform furrow. This relatively narrow germinal groove is covered by thin exine and bordered by the parallel straight bladder bases. The exine of the corpus and the sacci is laevigate with no distinct reticulum or ornamentation. The exine in rather thick. Sacci have always significant intramarginal overlapping.

Remarks. It differs from the other *Alisporites* species in the investigated material in its greater size, thick exine and the characteristic narrow germinal groove the exinal thickenings parallel to it.

Genus *Angustisaccus* Fisher & Dunay, 1984

Angustisaccus sp. (Plate 2/Q)

Description. Alete bisaccate pollen: outline haploxylonoid; somewhat kidney shaped. Corpus is almost circular in outline; the corpus exine is punctate, up to 3 µm thick. The sacci are small, less than ¼ of corpus size; distally attached and pendent. The sacci bases are well defined forming a narrow ellipse. The sacci are reticulate.

Genus *Falcisporites* (Leschik, 1956) Klaus, 1960

Falcisporites gottesfeldi (Stone, 1978) Fisher & Dunay, 1984 (Plate 2/D)

Description. Sulcate, non-striate bisaccate grain. Outline haploxylonoid, corpus circular-elliptical with the transverse axis greater than the longitudinal. The sulcus is distal and distinct. The sulcus has a characteristic dumbbell shape with rounded ends and with greatest width attained at those ends.

Remarks. The shape of the sulcus differentiates *F. gottesfeldi* from the other *Falcisporites* species.

Genus *Klausipollenites* Jansonius, 1962

Klausipollenites gouldii Dunay & Fisher, 1979 (Plate 2/AA-AB, AD-AE)

Description. Alete bisaccate pollen grain with haploxylonoid outline. The corpus is finely reticulate, circular to elliptical with the transverse axis greater than the longitudinal axis. The sacci are crescent-shaped, more coarsely reticulate than the corpus, proximally attached near the equator. The saccus bases are not sharply delineated, the sacci are occasionally connected by a thin equatorial strip of exine. The distal germinal aperture is a leptoma which is indistinctly defined but possesses a thinner exine than the remainder of the corpus. Normally no sulcus is present.

Remarks. In the Chinle Formation several xenomorphic (aberrant) morphotypes were recorded: with sulcus, three sacci or sacci grown together to form a monosaccate pollen grain.

Klausipollenites schaubergeri (Potonié & Klaus, 1954) Jansonius, 1962 (Plate 2/AC)

Description. Alete, bisaccate grains pollen grains with haploxylonoid, bean-shaped outline. The sacci show clear displacement towards distal pole, they are proximally attached near the equator. The germinal area is not distinct generally thinner than rest of the wall. The sacci have variable shape, crescent and half-circular. On the proximal side the exine may show some thickening interconnecting the sacci.

Genus *Minutosaccus* Mädler, 1964

Minutosaccus crenulatus (Dolby & Balme, 1976) (Plate 2/P)

Description. Bisaccate and diploxylonoid pollen grains. The corpus is transversely elongate oval or almost circular. The cappa is convex, 1-3 µm thick, finely reticulate. The sacci are distally detached, rounded to sub-triangular, the line of saccus detachment bordering the cappula is straight, slightly curved or irregular. In some specimens the sacci are united sub-equatorially to enclose an elongate oval, slightly depressed, thin unstructured, cappula. The surface of sacci is radially or irregularly crenulated.

Genus *Microcachryidites* (Cookson, 1947) Couper, 1953

Microcachryidites doubingeri Klaus 1964 (Plate 2/AD)

Description. Usually small, bisaccate pollen grains with diploxylonoid outline. The corpus is round with thick wall and punctate exine. The sacci are spherical, subequatorially attached and strongly distally pendent. The sacci are reticulate.

Genus Platysaccus Naumova, 1939 ex Ischenko, 1952

Platysaccus triassicus (Maljavkina, 1964) Dunay & Fisher, 1979 (Plate 2/M)

Description. Bisaccate pollen grain. The corpus is circular to elliptical, with the transvers axis longer than the longitudinal axis. The corpus exine is finely rugulate, a thick cappa is present. The sacci are crescent-shaped, slightly distally pendent, always larger than corpus. The saccus attachment is distinctly curved. The surface of the sacci is finely reticualte. On the distal side sharply delimited sulcus is present.

Remarks. It differs from *Platysaccus queenslandi* in having a bigger corpus and the curved saccus attachment.

Genus *Plicatisaccus* Pautsch, 1971

Plicatisaccus badius Pautsch, 1971 (Plate 2/K)

Description. Alete, bisaccate pollen grains with thick, brown exine. The corpus is oval, much longer than broad. The exine of the corpus is granulate. The sacci are brown with thick exine, with radially disposed plicae forming a reticulum. The sacci are often secondarily and centripetally brought together, so that a narrow parallel-sided space is formed distally between them. This space has undulate margins on account of the ridges of radial exine folds.

Genus *Pityosporites* (Seaward, 1914) Manum, 1960

Pityosporites oldhamensis Dunay & Fisher, 1979 (Plate 2/F)

Description. Bisaccate pollen grain with elliptical outline and a circular corpus. The corpus exine is finely reticulate; a weakly developed cappa is present. The sacci are semi-circular, reticulate. The sacci are proximally attached at the equator, distally strongly pendent. The saccus bases are distinct, generally straight to slightly curved. A broad, weakly developed cappula occurs between the saccus bases.

Genus *Protodiploxypinus* (Samoilovich, 1953) emend. Scheuring, 1970

Protodiploxypinus americus Dunay & Fisher, 1979 (Plate 2/N)

Description. Bisaccate pollen grain with elliptical outline and a circular to elliptical corpus. The longitudinal axis is usually greater than the transverse axis. The corpus exine is double-layered, reticulate. The sacci are semi-circular, always smaller than the corpus, rugulate and transparent. The sacci are proximally attached, subequatorially and distally pendent; the distal saccus bases are straight. A sharply delimited, prominent lens-shaped sulcus is present on the distal face of the corpus and extends the full height of the corpus; the greatest width being 1/8 to 1/3 of the corpus diameter.

Protodiploxypinus fastidiosus Jansonius, 1962) Warrington, 1974 (Plate 2/L)

Description. Medium-large sized bisaccate pollen grain with round corpus. The sacci are semi-circular with straight distal bases. The sacci are always smaller than the central body, usually ½ of it. The sacci are proximally attached with considerable distal displacement. The corpus exine is moderately thick, reticulate

Protodiploxypinus ujhelyi Dunay & Fisher, 1979 (Plate 2/I)

Description. Usually small-sized bisaccate pollen grains with circular to elliptical corpus. The corpus exine is thin, two-layered, faintly reticulate. The sacci are semi-circular, always smaller than the corpus, finely rugulate with individual elements radially oriented. Breadth of sacci 1/2 to 2/3 of corpus diameter. No distinct sulcus is present.

Genus *Schizosaccus* Mädler, 1964

Schizosaccus keuperi Mädler, 1964 (Plate 2/Z)

Description. Bisaccate pollen grain with oval ouline. The longitudinal axis is greater than the transversal. The corpus is almost spherical to oval, distally frequently somewhat inclined. A clear distal sulcus can reach the equator. The exine is on all sides up to 3 µm thick and punctate. The sacci are relatively small

Genus *Staurosaccites* Dolby, 1976

Staurosaccites quadrifidus Dolby, 1976 (Plate 14/5)

Description. Bisaccate pollen grain with haploxylonoid, or slightly diploxylonoid, circular or sub-circular ouline. The corpus is circular; it is dissected into two equal halves by a narrow furrow. Corpus and sacci are punctate, reticulate. The sacci are semi-circular and only little inflated,

Genus *Voltziaceasporites* Klaus, 1964

Voltziaceasporites heteromorpha Klaus, 1964 (Plate 2/H)

Description. Alete, bisaccate pollen grain with haploxylonoid outline. The shape and size of the sacci are largely variable. The exine of the corpus is smooth to finely punctate, granulate it is usually oval. The sacci extend over the proximal side of the corpus and the saccus bases are not clearly separated from the corpus exine. The sacci are finely reticualte, equatorially attached, and somewhat distally inclined.

Infraturma STRIATITI Pant, 1954

Genus *Lueckisporites* (Potonié & Klaus, 1954) emend. Klaus, 1963

Luecksporites singhii Balme, 1970 (Plate 14/4)

Description. Alete, bisaccate, taeniate pollen grain with elliptical haploxylonoid outline. The corpus is elliptical or sub-circular, the corpus exine is punctate faintly reticulate. The corpus is trnasected by a longitudinal furrow forming two taeniae (*ca.* 20 µm wide). The sacci are crescent shaped, finely reticulate.

Genus *Infernopollenites* Scheuring, 1970

Infernopollenites sulcatus (Pautsch 1958) Scheuring 1970 (Plate 14/6)

Description. Alete, bisaccate, large-sized pollen grains with elliptical outline. The exine is thick, dark brown. Two-four taeniae cross the whole corpus. Taeniae reach the body margin. The corpus exine is granulate, or smooth. The sacci are finely reticulate.

Remarks. *Infernopollenites sulcatus* differs from *I. parvus* mainly in its large size.

Genus *Striatoabietites* (Sedova, 1956) Hart, 1964

Striatoabietites aytugii Visscher, 1966 (Plate 14/10)

Description. Alete, bisaccate, taeniate pollen grain with elliptical haploxylonoid, or slightly diploxylonoid outline. The corpus is strongly elliptical. Proximally the exine is structurally differentiated to form 10-14 irregularly developed longitudinal taeniae separated by narrow sutures r monolete mark. The sacci are more or less diploxylonoid, distally inclined, finely reticulate.

Infraturma DISACCITRILETI Leschik, 1956

Genus *Triadispora* Klaus, 1964

Triadispora aurea Scheuring, 1970 (Plate 6/3, 6)

Description. Bisaccate pollen grain with diploxylonoid outline and a trilete mark. The corpus is oval-ellipsoidal, the exine is granulate-punctate. The longitudinal axis of the corpus is usually longer than the sacci. On the proximal side the corpus is exine is folded parallel to the saccus roots. The sacci are reticulate.

Remarks. It differs from other Triadispora species by having a diploxylonoid ouline, oval corpus and the exine thickening on the proximal side of the corpus. The size of *T. aurea* is much large compared to the other *Triadispora* species.

Triadispora crassa Klaus, 1964 (Plate 6/7, Plate 7/14, Plate 14/11)

Description. Bisaccate pollen grain with haploxylonoid, oval outline and a trilete mark. The corpus is round, the exine is granulate. The sacci are narrow.

Remarks. *Triadispora crassa* and *T. obscura* have similar ornamentation. As both species have a wide range of morphological variability, transitional forms between the two species can be present.

Triadispora dockumensis Dunay & Fisher, 1979 (Plate 2/T-U)

Description. Bisaccte, often monosaccate pollen grain with a trilete mark. The corpus is circular. The corpus exine is rugulate, dark, always thicker than that of the sacci. The trilete mark usually small, indistinct. The sacci are finely reticulate, filamentous usually connected equatorially by a narrow strip of exine.

Remarks. *Triadispora dockumenis* differs from *T. obscura* in the darker color, and denser ornamentation of the corpus.

Triadispora epigona (Klaus, 1964) Scheuring, 1970 (Plate 7/5)

Description. Small, bisaccte pollen grains with circular, oval outline and a small trilete mark. Corpus exine is granulate. The sacci are only little inflated, crescent-shaped.

Remarks. It differs from the other *Triadispora* species mainly in its small size.

Triadispora fallax (Fisher & Dunay, 1984) (Plate 2/X)

Description. Bisaccate pollen grain with diploxylonoid outline tending towards haploxylonoid. The corpus is oval, sub-rounded with longitudinal axis barely greater than transverse axis. The corpus exine is punctate, *ca.* 2 µm thick. The sacci are slightly smaller than the corpus, weakly distally inclined, the saccus bases often indistinct. The sacci are finely reticulate.

Triadispora modesta Scheuring, 1970 (Plate 6/14, Plate 7/6)

Description. Bisaccate pollen grain with haploxylonoid oval outline and a trilete mark. The corpus is oval with a longitudinal axis longer than the transversal. The corpus exine is darker, thick and rugulate. The sulcus on the distal side is bordered by parallel running exine thickening on both sides. The sacci are narrow, crescent shaped. The trilete mark on the proximal side is indistinct.

Remarks. It differs from the other *Triadispora* species by having the exine thickening parallel to the sulcus on the distal side.

Triadispora suspecta Scheuring, 1970 (Plate 6/11)

Description. Bisaccate pollen grain with haploxylonoid dipoloxylonoid, oval outline and a trilete mark. The sacci are equatorially attached and extending over the corpus periphery. The sacci are crescent-shaped, reticulate with radial ornamentation. The transition between the corpus exine and saccus exine is continuous. The corpus is circular with reticulate exine. The trilete mark is usually distinct.

Triadispora plicata Klaus 1964 (Plate 6/12, Plate 7/13, plate 11/2)

Description. Bisaccte, often monosaccate pollen grain with a trilete mark and haploxylonoid ouline. The corpus is oval or subcircular. The corpus exine is punctate, finely granulate. The exine is folded on the proximal side forming a plicate surface. The trilete mark is often indistinct because of the exinal folds. Length of the corpus approx. equals the length of the sacci. The sacci are crescent-shaped, equatorially attached and slightly distally pendent. The sacci are reticulate.

Remarks. It differes from the other *Triadispora* species by having a procate-ornamented proximal side.

Triadispora staplini (Jansonius, 1962) Klaus, 1964

Description. Bisaccate pollen grain with haploxylonoid, oval outline and a trilete mark. The corpus is round or oval. The saccus and corpus exine is granulate. The sacci are equatorially attached. Corpus and sacci are of equal length. There is a narrow exine thickening along the saccus roots.

Triadispora verrucata (Schulz, 1966) Scheuring, 1970 (Plate 6/13)

Description. Bisaccte, often monosaccate pollen grain with a trilete mark and haploxylonoid ouline. The corpus is oval or subcircular. The corpus exine is punctate, finely granulate. The corpus exine is folded resulting in warts on the proximal side and a verrucate ornamentation. The sacci are crescent-shaped, equatorially attached. The trilete mark is often indistinct because of the verrucate ornamentation.

Remarks. It differs from the other *Triadispora* species by having a verrucate corpus.

Subturma MONOSACCITES (Chitaley, 1951) Potonié & Kremp, 1954

Infraturma ALETESACCITI Leschik, 1955

Genus *Cordaitina* (Samoilovich, 1953) Balme, 1970

Cordaitina minor (Pautsch, 1971) Pautsch, 1973 (Plate 3/J)

Description. Monosaccate pollen grain with circular outline and circular central body. The central body is moderately ornamented, finely reticulate without secondary folds. The saccus outline is regular without undulations, the bladder roots are circular covering one another.

Genus *Daughertyspora* Dunay & Fisher, 1979

Daughertyspora chinleana (Daugherty, 1941) Dunay & Fisher, 1979 (Plate 3/N)

Description. Monosaccate pollen grain with circular outline and circular central body. The exine is two-layered, the layers are smooth or punctate. The saccus is circular and rugulate with radially oriented sculptural elements.

Remarks. It differs from the other observed monosaccate pollen grains in its significantly smaller size.

Genus *Pachysaccus* Lele & Maithy 1969

Pachysaccus ferroccidentalis Fisher & Dunay, 1984 (Plate 3/D)

Description. Monosaccate pollen grain with subcircular-circular outline. The exine is two-layered; the endexine is smooth, the ectexine is plicate. The saccus has irregular, undulating outline and often many folds and it has diaphanous appearance. The trilete mark is not distinct.

Remarks. *Pachysaccus* differs from *Patinasporites* in the irregular, undulating outline of the saccus and broader saccus and smaller central body.

Genus *Patinasporites* (Leschik, 1955) Klaus, 1960

Patinasporites explanatus (Leschik 1956) Góczán & Oravecz-Scheffer 1996 (Plate 9/18, Plate 14/15)

Description. Monosaccate pollen grains with circular-subcircular outline. The contour of the central body is distinct; the exine has a darker colour compared to the monosaccus due to thickening. The corpus is smaller compared to the broad monosaccus. The saccus is often folded and it has diaphanous appearance.

Remarks. Patinasporites explanatus differs from the other PAtinapsorites species in the small copus/monosaccus ratio.

Patinasporites iustus Klaus, 1960 (Plate 3/C, Plate 9/15)

Description. Monosaccate pollen grains with circular-subcircular outline. The contour of the central body is distinct; the exine has a darker colour compared to the monosaccus due to thickening. The saccus is often folded and it has diaphanous appearance.

Remarks. It differs from *Patinasporites densus* and *Patinasporites toralis* in the characteristic dark central body.

Patinasporites toralis Scheuring, 1970

Description. Monosaccate pollen grains with oval-subcircular outline. The contour of the central body is indistinct. There is a darker ring-like exine thickening around the corpus. The saccus is often folded and it has diaphanous appearance.

Remarks. It differs from *Patinasporites densus* in having a dark ring-like thickening of the exine around the central body and a more oval equatorial outline.

Genus *Tulesporites* Dunay & Fisher, 1979

Tulesporites briscoensis Dunay & Fisher, 1979 (Plate 3/I)

Diagnosis: Monosaccate pollen grain with triangular outline. A faint trilete mark is present, extending at least to the periphery of the corpus. The trilete marks reflected by the intersection of the four contact areas. The monosaccus is rugulate; the sculptural elements are radially aligned.

Remarks. Dunay & Fisher (1979) and Fisher & Dunay (1984) described the *Tulesporites* species as zonate palynomorphs. In this contribution they are considered as monosaccate pollen grain. Roghi et al. (2010) listed them also as monosaccate pollen grains,

Tulesporites terraruberae Fisher & Dunay, 1984 (Plate 3/H)

Diagnosis: Monosaccate pollen grain with triangular outline. The corpus is circular, the copi exie is reticulte-rugulate and much thicker and darker than that of the monosaccus. A fain trilete mark is present which extends to the copis periphery, and occasionally onto the monosaccus. The monosaccus is rugulate.

Remarks. It differs from *Tulesporitrs briscoensis* in the surface ornamentation of the corpus.

Turma KRYPTOAPERTURATES Potonié, 1966

Subturma CIRCUMPOLLES Pflug, 1953 emend. Klaus, 1960

Genius *Duplicisporites* (Leschik, 1955) Scheuring, 1970

Duplicisporites continuus Praehauser-Enzenberg, 1970 (Plate 14/22-23)

Description. Pollen grains are circular to subtriangular in outline. A small trilete mark with simple laesurae is often visible at the proximal pole. In the equatorial zone a ring-like exine thinning forms a rimula. On the proximal side the exine is thickened forming a fold parallel to the equatorial outline. The exine seems to be smooth, unornamented in light microscopy.

Remarks. It differs from other Duplicisporites species in the proximal exine fold and the smooth surface.

Duplicisporites mancus Klaus, 1960 (Plate 8/5-6, Plate 10/4, Plate 14/20)

Description. Pollen grains are circular to subtriangular in outline. A small trilete mark with simple laesurae is often visible at the proximal pole. In the equatorial zone a rimula is present. The exine is vermiculate and verrucate.

Remarks. It differs from the other *Duplicisporites* species in its sculptured exine.

Genus *Partitisporites* Leschik, 1956

Partitisporites scurrilis Scheuring, 1970 (Plate 6/26-28, Plate 8/22-24)

Description. Pollen grains are circular to oval in outline. A small trilete mark with simple laesurae is often visible at the proximal pole. In the equatorial zone a ring-like exine thinning forms a rimula. The exine is granulate, punctate.

Remarks. It differs from other *Partitisporites* species by the oval outline and punctate, granulate ornamentation. *Duplicisporites granulatus* has a clear triangular outline.

cf. *Partitisporites tenebrosus* (Scheuring, 1970) van der Eem, 1983 (Plate 10/1-2, 6, Plate 14/17, 19, 25)

Pollen grains are circular to oval in outline. A small trilete mark with simple laesurae is often visible at the proximal pole. In the equatorial zone a ring-like exine thinning forms a rimula. The exine is generally thick and smooth, occasionally finely rugulate.

Remarks. It differs from the other *Partitisporites* species by its thick and smooth or rugulate exine. Van der Eem (1983) assigned *Duplicisporites continuus* to this species, but in the case *of*

P. tenebrosus there is no exine thickening and folds on the proximal side and the outline is clearly oval-circular.

Turma PLICATES Naumova 1939 emend. Potonié 1960
Subturma POLYPLICATES Erdtman, 1952

Genus *Equisetosporites* Daugherty, 1941

Equisetosporites chinleana (Daugherty, 1941) Scott, 1960 (Plate 3/S, Plate 14/12)

Description. Ellipsoidal pollen grains comprising a series of alternating exinal bands and furrows. The bands are usually radially symmetrical, but deviation can be present. Deviation from radial symmetry is exemplified by the diagonal orientation of the bands. The bands typically are wider (3-5 µm) than the intervening furrows (*ca*. 1 µm)

Genus *Cornetipollis* Pocock & Vasanthy, 1988

Cornetipollis reticulata Pocock & Vasanthy, 1988 (Plate 3/R)

Description. Ellipsoidal pollen grains comprising an almost smooth central body encased in a banded exterior. Exinal bands alternate with narrowfurrows. The exine of the bands is reticulate or foveo-reticulate, perforate. The bands are straight to distinctly twisted around the longitudinal axis toward the two points of convergence.

Remarks. Diagonal symmetry which is characteristic for E. chinleana is very rare or absent in the case of C. reticulata. The reticulate-perforate bands differentiate it from the other polyplicate pollen grains.

NOT ASSIGNED

Genus *Brodispora* Clarke, 1965

Brodispora striata Clarke 1965 (Plate 1/AC, Plate 7/4, Plate 9/4-5, Plate 11/11)

Description. Palynomorphs with elliptical-oval outline and thin wall. The wall consists of 7-14 striations. The striations occasionally have a fingerprint-like pattern.

Remarks. *Brodispora* has unknown affinity.

Genus *Froelichsporites* Litwin, Smoot, Weems, 1993

Froelichsporites traversei (Dunay & Fisher, 1979) Litwin, Smoot, Weems, 1993 (Plate 3/W, Plate 4/A-K)

Description. The specimens are obligate tetrahedral tetrads with slightly to moderately thickened and fused contact areas. The specimens are permanently united in tetrads. The proximal face of each sporomorph is in complete contact with all others and they are joined at an oblique angle (in polar view). Two wall layersare distinguished, but the outermost layer (l1, fig.2A) is not always present. The tetrads occasionally exhibit only the inner wall-layer on the distal hemisphere of each member, and the remnant of the outermost layer is visible only along the sutures between the members. The outer wall layer is thin, psilate, and diaphanous. This layer is thickened towards the contact area of the grains to form a thick contact area. The inner layer is thin and scabrate. On the distal face of each member a distinct pore structure,

ulcus is present. The ulcus is rimmed by a slight thickening of the inner wall layer to form an annulus-like structure, and it is usually 2-4 µm in diameter (observed range 1-7 µm). On the proximal face of the spores a distinct (but perhaps non-functional) trilete scar is present.

Photoplates

Plate 1

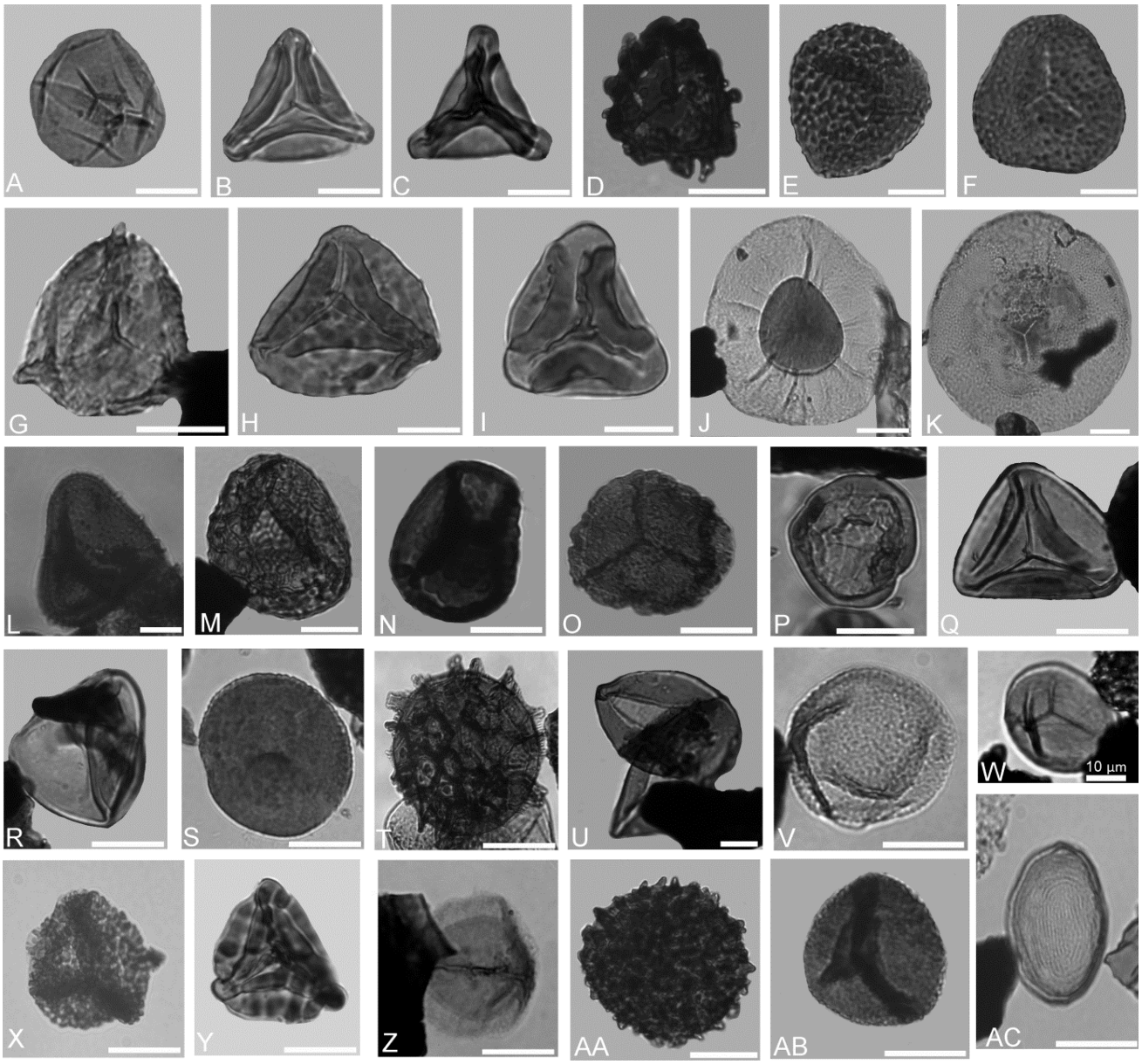

Plate 1 (Chinle Formation)

Images of selected spores from the Chinle Formation at the PFNP. The scale bar is 20 µm. Sample codes and slide numbers are in brackets.

A *Calamospora tener* [TH 10/3], B *Concavisporites toralis* [TH 10/1], C *Concavisporites toralis* [TH 10/1], D *Cristatitriletes baculatus* [MLM 1/2], E *Ischyosporites* sp. [TH 10/1], F *Granulatisporites infirmus* [TH 10/1], G *Kyrtomisporis sp. A* [BL 2/2], H *Kyrtomisporis gracilis* [BL 3/1], I *Gleicheniidites senonicus* [BL 3/1], J *Guthoerlisporites cancellosus* [BL 5/1], K *Guthoerlisporites cancellosus* [MLM 1/1], L *Converrucosisporites cameronii* [MLM 1/1], M *Klukisporites granosifenestellatus* [BL 2/1], N *Uvaesporites argentaeformis* [MLM 2/1], O *Uvaesporites argentaeformis* [DPG 3/2], P *Striatella seebergensis* [BL 5/1], Q *Dictyophyllidites harrisii* [BL 3/1], R *Dictyophyllidites harrisii* (triplane position) [BL 3/2], S *Cyclogranulatisporites* sp. [BL 3/2], T *Retitriletes* sp. [DPG 5/2], U *Todisporites major* [BL 3/1], V *Osmundacidites wellmanii* [TH 10/1], W *Todisporites rotundiformis* [TH 10/1], X *Conbaculatisporites* sp. [BL 1/2], Y *Kyrtomisporis speciosus* [BL 3/1], Z *Aratrisporites* sp. [TH 10/1], AA *Trilites klausii* [BL 2/1], AB *Foveolatisporites* sp. [BL 3/2], AC *Brodispora striata* [BL 2/1]

Plate 2

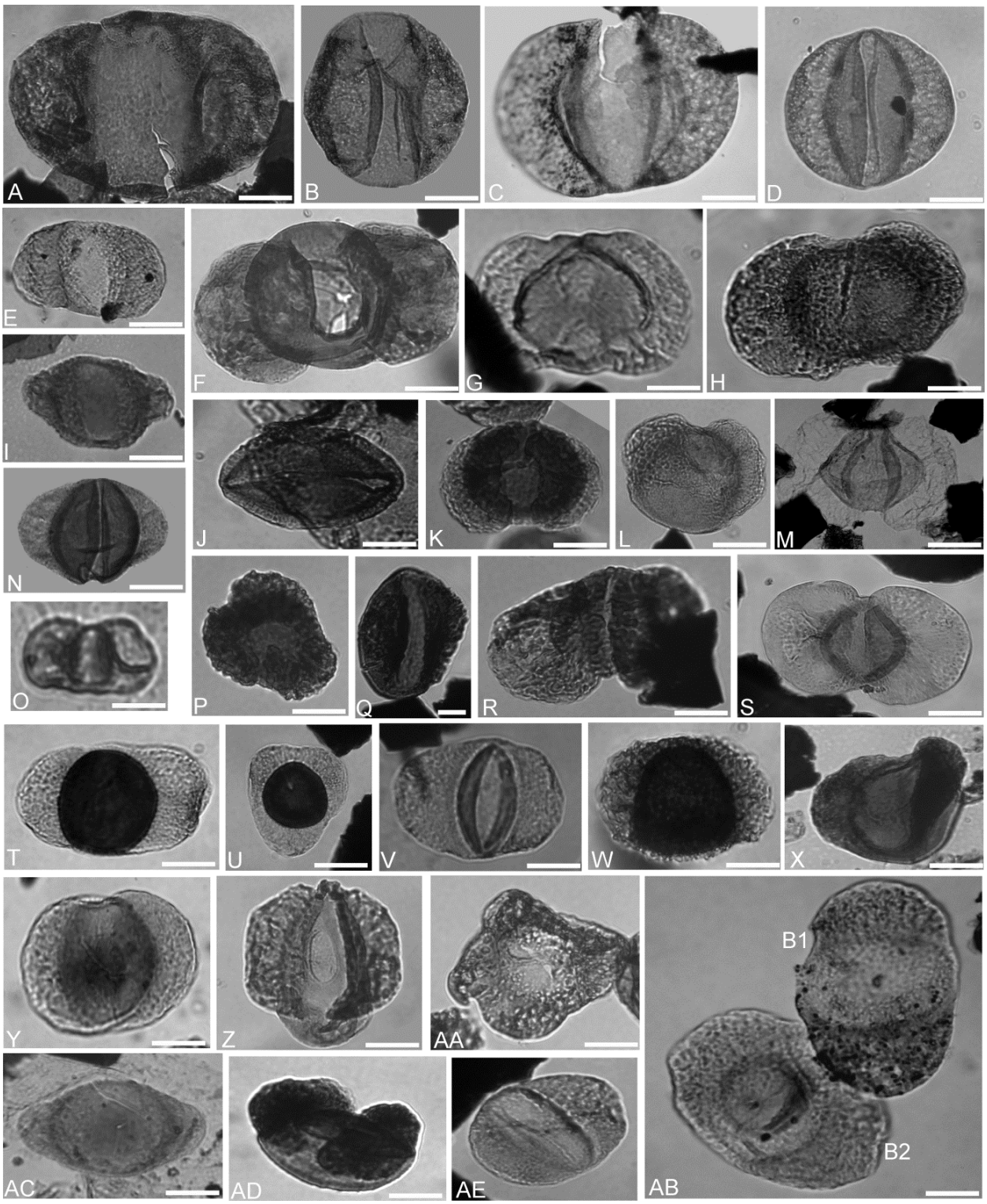

Plate 2 (Chinle Formation)

Images of selected bisaccate pollen grains from the Chinle Formation at the PFNP. The scale bar is 20 µm. Sample code and slide number are in brackets.

A *Alisporites giganteus* [OL 1/3], B *Alisporites grandis* [OL 2/1], C *Alisporites opii* [TH 10/1], D *Falcisporites gottesfeldi* [OL 3/4], *E Alisporites parvus* [BL 3/1], F *Pityosporites oldhamensis* [DPG 1/2], G *Colpectopollis singulisinus* [MLM 3/2], H *Voltziaceasporites heteromorpha* sensu Klaus 1964 [DPG 5/2], I *Protodiploxypinus ujhelyi* [OB/2], J *Ovalipollis lunzensis* [MLM 3/2], K *Plicatisaccus badius* [BL 2/1], L *Protodiploxypinus fastidiosus* [MLM 1/2], M *Platysaccus triassicus* [TH 10/1], N *Protodiploxypinus americus* [OL 2/1], O *Vitreisporites pallidus* [BH/5], P *Minutosaccus crenulatus* [BL 6/1] with three airbags, Q *Angustisaccus* sp. [OL 1/1], R *Pseudoillinites crassus* [BL 6/1], S *Platysaccus queenslandi* [DPG 4/1], T *Triadispora dockumensis* [MLM 3/2], U *Triadispora dockumensis* [MLM 3/2], V *Triadispora sulcata* [MLM 3/2], W *Triadispora verrucata* [MLM 2/2], X *Triadispora fallax* [BH/2], Y *Triadispora crassa* [BL 3/1], Z *Schizosaccus keuperi* [BL 7/1], AA *Klausipollenites gouldii* aberrant morphotype with three airbags [BL 7/1], AB *Klausipollenites gouldii* [MLM 3/2], normal morhotypes (2013), AC *Klausipollenites schaubergeri* [OL 1/1], AD *Microcachrydites doubingeri* [OL 1/1], AE *Klausipollenites gouldii* aberrant morphotype with split sulcus [MLM 3/2]

Plate 3

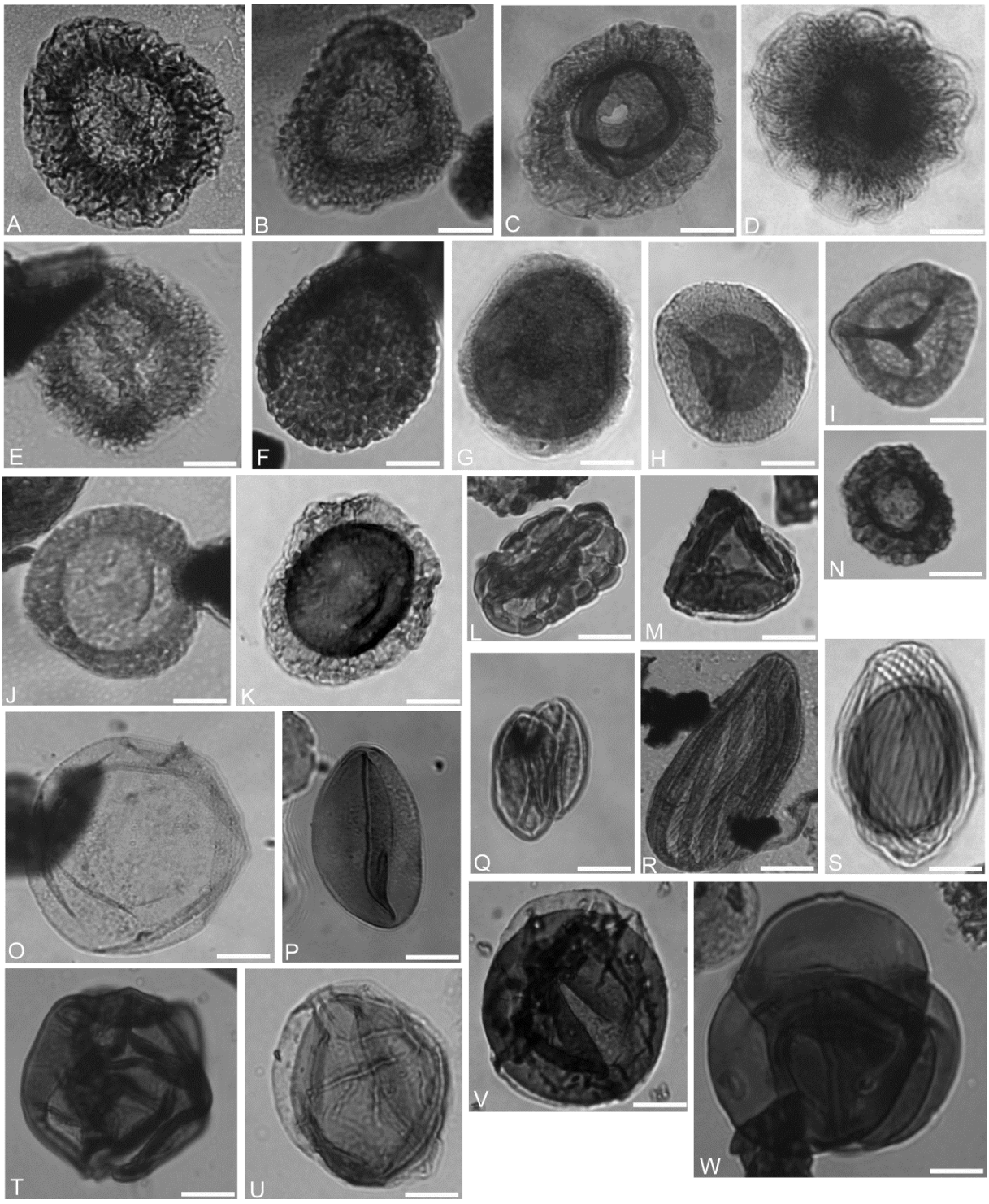

Plate 3 (Chinle Formation)

Images of selected monosaccate, non-saccate pollen grains and *Froelichsporites traversei* from the Chinle Formation at the PFNP. The scale bar is 20 µm. Sample code and slide number are in brackets.

A *Patinasporites densus* [TH 10/1], B *Patinasporites densus* [MLM 2/1] triangular morphotype, C *Patinasporites iustus* [LS/1], D *Pachysaccus feroccidentalis* [LS/1], E *Vallasporites ignacii* [OL 3/3], F *Pseudoenzonalasporites summus* [MLM 1/2], G *Enzonalasporites vigens* [FT 1/1], H *Tulesporites terraruberae* [DPG 5/2], I *Tulesporites briscoensis* [FT 3/2], J *Cordaitina minor* [OL 1/1], K *Kuglerina meieri* [MLM 3/2], L *Camerosporites secatus* [BL 5/2], M *Duplicisporites* sp. [BL 4/2], N *Daughertyspora chinleana* [MLM 1/2], O *Inaperturopollenites* sp. [BL 4/1], P *Cycadopites follicularis* [DPG 3/1], Q *Cycadopites fragilis* [DPG 41/], R *Cornetipollis reticulata* [OB/1], S *Equisetosporites chinleana* [TH 10/1], T *Araucariacites australis* [BL 3/1], U *Perinopollenites elatoides* [BL 4/2], V *Perinopollenites elatoides* [BL 3/2], W *Froelichsporites traversei* [BL 2/2]

Plate 4

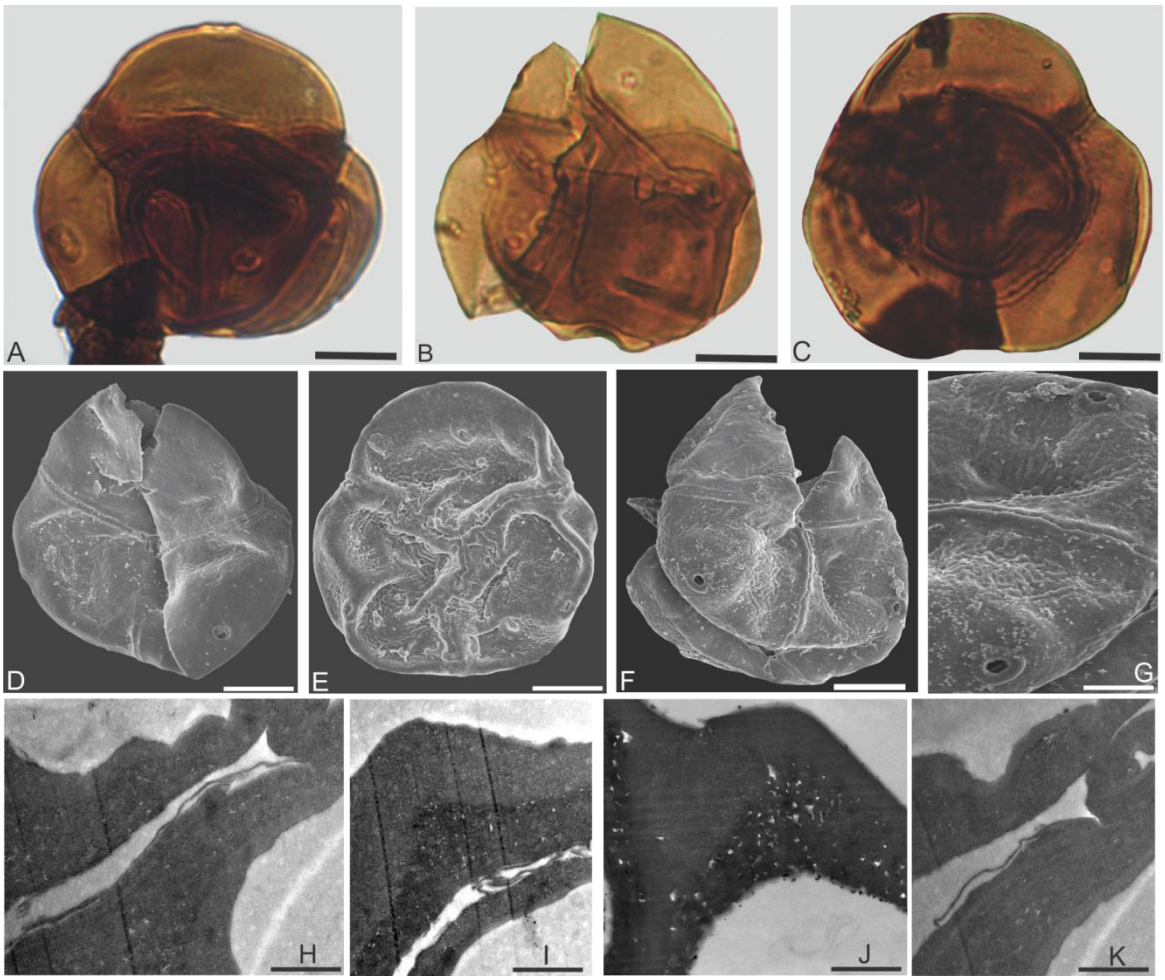

Plate 4 (Chinle Formation)

Light microscopy, scanning electron microscopy and transmission electron microscopy images of *Froelichsporites traversei*. Specimen location is given with sample and slide or stub, or block and grid numbers together. For scale see A-K.

A *Froelichsporites traversei* tetrad in polar view BL 2/2, B tetrad in oblique polar view BL 3/2, C tetrad in polar view BL 4/2, Scale bar = 20µm A-C. D-G SEM images of *Froelichsporites traversei* tetrads from sample BL 7, D polar view, Stub 1, scale bar=15 µm, E polar view, stub 1, scale bar=15 µm, F polar view, stub 2, scale bar=15 µm, G Enlargement of F showing the ulci, stub 2, scale bar=5µm, H-K TEM images of *Froelichsporites traversei* showing the ultrastructure of the palynomorph wall, H shows the wall-ultrastructure in a segment close to the junction between the individual grains, block 1/grid H1, scale=1µm, the innermost layer is running parallel with the granular layer, I segment of the exine showing the outer electron-dense, homogenous and inner granular wall layers with faint lamination below the inner layer, block 1/grid H5, scale=1µm, J segment of the exine showing the outer electron-dense, homogenous and the inner granular wall layers, block 3/grid 8A, scale=1 µm, K segment of the exine shows that the innermost laminae are directly contiguous with granules in the granular layer, block 1/grid H2, scale=1 µm.

Plate 5 (Mercia Mudstone Group, Sidmouth Mudstone Formation)

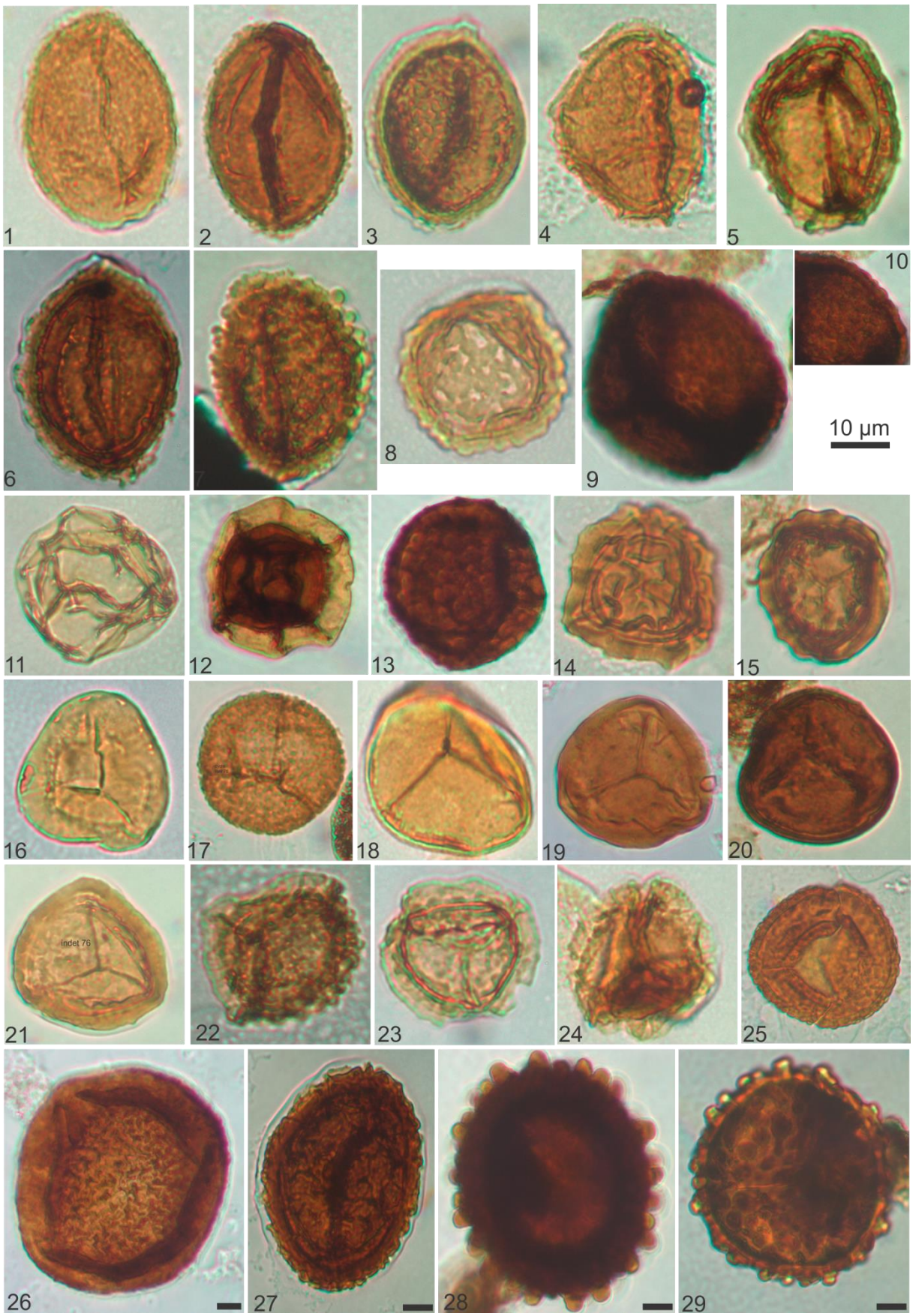

Plate 5 (Mercia Mudstone Group, Sidmouth Mudstone Formation)

Spores from the Sidmouth Mudstone Formation with the indication of sample name, or code and slide number. Scale bar 10 µm.

1 *Aratrisporites granulatus* (111.98 m/1), 2 *Aratrisporites granulatus* (111.98 m/1), 3 *Aratrisporites* sp. (111.98 m/2), 4 *Aratrisporites crassitectatus* (109.11 m/1), 5 *Aratrisporites crassitectatus* (111.98 m/1), 6 *Aratrisporites crassitectatus* (111.98 m/1), 7 *Aratrisporites* sp. (111.98 m/1), 8 *Uvaesporites gadensis* (111.98 m/1), 9 *Verrucosisporites morulae* (111.98 m/1), 10 *Verrucosisporites morulae* high resolution same as 10, (111.98 m/1), 11 *Calamospora tener* (111.98 m/1), 12 *Thomsonisporis punctatus* (109.11 m/1), 13 *Lycopodiacidites* sp. (109.11 m/1), 14 *Uvaesporites* sp. (111.98 m/1), 15 *Uvaesporites* sp. (111.98 m/1), 16 *Rogalskaiasporites* sp. (111.98 m/1), 17 *Cyclogranisporites* sp. (111.98 m/1), 18 *Punctatisporites* (111.98 m/1), 19 spore indet B (111.98 m/1), 20 *Punctatisporites* (111.98 m/1), 21 spore indet B (111.98 m/1), 22 cf. *Kraeuselisporites* sp. (111.98 m/1), 23 cf.s *Kraeuselisporites* sp. (111.98 m/1), 24 cf. *Kraeuselisporites* sp. (111.98 m/1), 25 *Verrucosisporites morulae* (111.98 m/1), 26 *Cyclotriletes* sp. (111.98 m/1), 27 *Aratrisporites* sp. (111.98 m/1), 28 megaspore indet (111.98 m/1), 29 megaspore indet (109.11 m/1).

Plate 6 (Mercia Mudstone Group, Sidmouth Mudstone Formation)

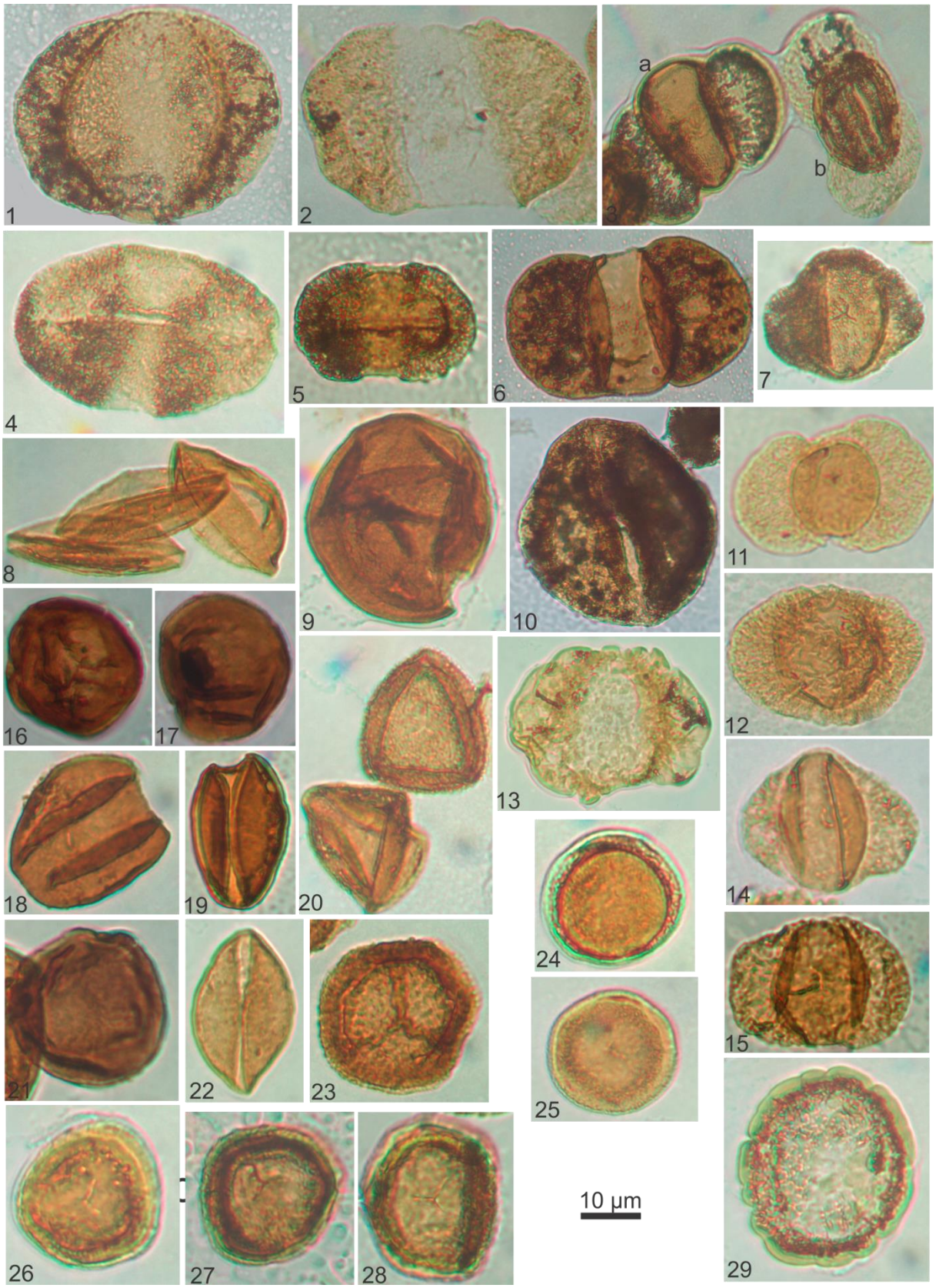

Plate 6 (Mercia Mudstone Group, Sidmouth Mudstone Formation)

Pollen grains from the Sidmouth Mudstone Formation with the indication of sample name, or code and slide number. Scale bar 10 µm. WP refers to samples from the Wiscombe Park 1

1 *Alisporites opii* (WP-1 111.98 m/1), 2 *Alisporites robostus* (WP-1 111.98 m/1), 3 a) *Triadispora aurea* b) *Lunatisporites acutus* (WP-1 111.98 m/1), 4 *Ovalipollis ovalis* (WP-1 111.98 m/1), 5 *Ovalipollis notabilis* (WP-1 109.11 m/1), 6 *Triadispora aurea* (WP-1 111.98 m/1), 7 *Triadispora crassa* (WP-1 111.98 m/2), 8 *Cycadopites* sp. (WP-1 111.98 m/1), 9 *Araucariacites australis* (WP-1 111.98 m/1), 10 *Brachysaccus neomundanus* (WP-1 109.11 m/1), 11 *Triadispora suspecta* (WP-1 111.98 m/1), 12 *Triadispora plicata* (WP-1 111.98 m/1), 13 *Triadispora verrucata* (WP-1 111.98 m/1), 14 *Triadispora modesta* (WP-1 111.98 m/1), 15 *Triadispora staplini* (WP-1 109.11 m/1), 16 *Aulisporites astigmosus* (WP-1 111.98 m/1), 17 *Aulisporites astigmosus* (WP-1 111.98 m/1), 18 *Aulisporites astigmosus* (WP-1 111.98 m/1), 19 cf. *Aulisporites astigmosus* (WP-1 109.11 m/1), 20 *Duplicisporites granulatus* (WP-1 111.98 m/1), 21 *Aulisporites astigmosus* (WP-1 111.98 m/1), 22 *Cycadopites* sp. (WP-1 111.98 m/2), 23 *Vallasporites ignacii* (WP-1 111.98 m/2), 24 *Partitisporites novimundanus* (WP-1 109.11 m/2), 25 *Partitisporites novimundanus* (WP-1 111.98 m/1), 26 *Partitisporites scurrilis* (WP-1 111.98 m/1), 27 *Partitisporites scurrilis* (WP-1 109.11 m/1), 28 *Partitisporites scurrilis* (WP-1 109.11 m/1), 29 *Camerosporites secatus* (WP-1 111.98 m/1)

Plate 7 (Mercia Mudstone Group, Dunscombe Mudstone Formation)

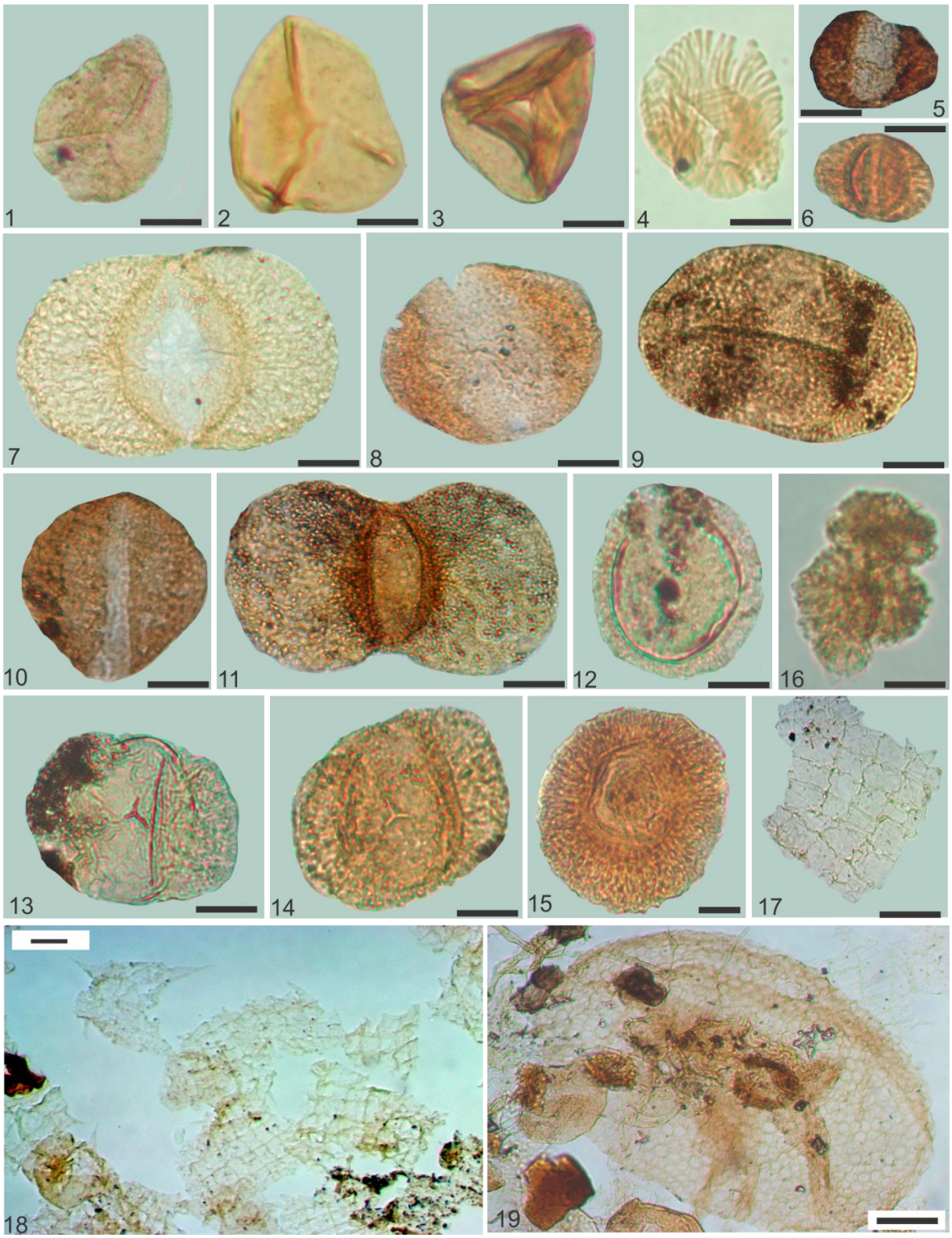

Plate 7 (Mercia Mudstone Group, Dunscombe Mudstone Formation)

Palynomorphs in the Dunscombe Mudstone Formation with the indication of sample name, or code and slide number, scale bar 1-6, 16-17: 10 µm; 7-15, 18-19: 20 µm, WP refers to samples from the Wiscombe Park 1, WE from the Strangman`s Cove outcrop.

1 *Deltoidospora* sp. (WE016/A), 2 *Deltoidospora* sp. (WE213/A), 3 *Concavisporites toralis* (WE016/A), 4 *Brodispora striata* (WE111/A), 5 *Triadispora epigona* (WE017/A), 6 *Triadispora modesta* (WE201/A1), 7 *Platysaccus* sp. (WP-1 57.86 m/1), 8 *Alisporites* sp. (WE017/A), 9 *Ovalipollis ovalis* (WE305/B), 10 *Brachysaccus neomundanus* (WE017/A), 11 *Platysaccus* sp. (WE015/A), 12 *Enzonalasporites vigens* (WP-1 56.15 m/1), 13 *Triadispora plicata* (WE103/A), 14 *Triadispora crassa* (WE305/C), 15 *Patinasporites densus* (WE305/C), 16 *Botryococcus braunii* (WE018/A), 17 *Plaesiodictyon mosellanum* (WE017A), 18 *Plaesiodictyon mosellanum* (WE017A), 19 insect egg or wing (WE017/A)

Plate 8 (Mercia Mudstone Group, Dunscombe Mudstone Formation)

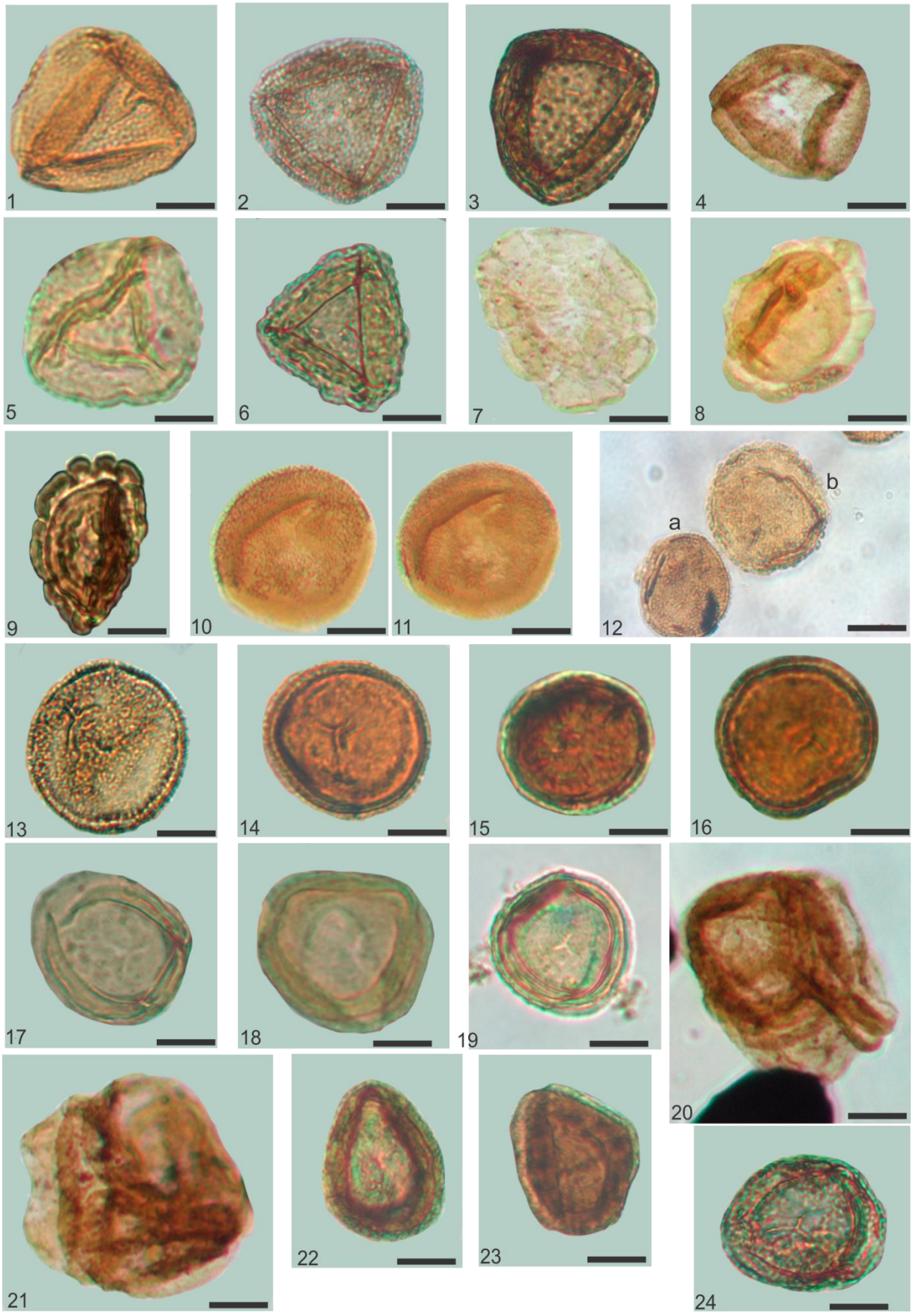

Plate 8 (Mercia Mudstone Group, Dunscombe Mudstone Formation)

Circumpolles pollen in the Dunscombe Mudstone Formation with the indication of sample name, or code and slide number, scale bar 10 µm, WP refers to samples from the Wiscombe Park 1 borehole, WE from the Strangman`s Cove outcrop.

1 *Duplicisporites granulatus* (WE003/A), 2 *Duplicisporites granulatus* (WE103/A), 3 *Duplicisporites granulatus* (WE305/B), 4 *Duplicisporites granulatus* (WE213/A), 5 *Duplicisporites mancus* (WE302/B), 6 *Duplicisporites mancus* (WE103/A), 7 *Camerosporites secatus* (WE213/A), 8 *Camerosporites secatus* (WE21/3A), 9 *Camerosporites secatus* (WE305/B), 10 *Praecirculina granifer* (WE001/A), 11 same as 10 *Praecirculina granifer* (WE001/A), different focus, 12 a *Praecirculina granifer*, b *Camerosporites pseudoverrucosus* (WE015/A), 13 *Praecirculina granifer* (WE015/A), 14 *Partitisporites novimundanus* (WE003/A), 15 *Partitisporites novimundanus* (WP-1 49.8 5m/1), 16 *Partitisporites novimundanus* (WE201/A), 17 *Partitisporites maljawkinae* (WE302/A), 18 *Partitisporites maljawkinae* (WP-1 50.99 m/1), 19 *Partitisporites maljawkinae* (WP-1 55.65 m/1), 20 *Partitisporites quadruplices* (WE213/A), 21 *Partitisporites quadruplices* (WE213/A), 22 *Partitisporites scurrilis* (WE016/A), 23 *Partitisporites* scurrilis (WP-1 48.94 m/1), 24 *Partitisporites scurrilis* (WE103/A).

Plate 9 (Mercia Mudstone Group, Branscombe Mudstone Formation)

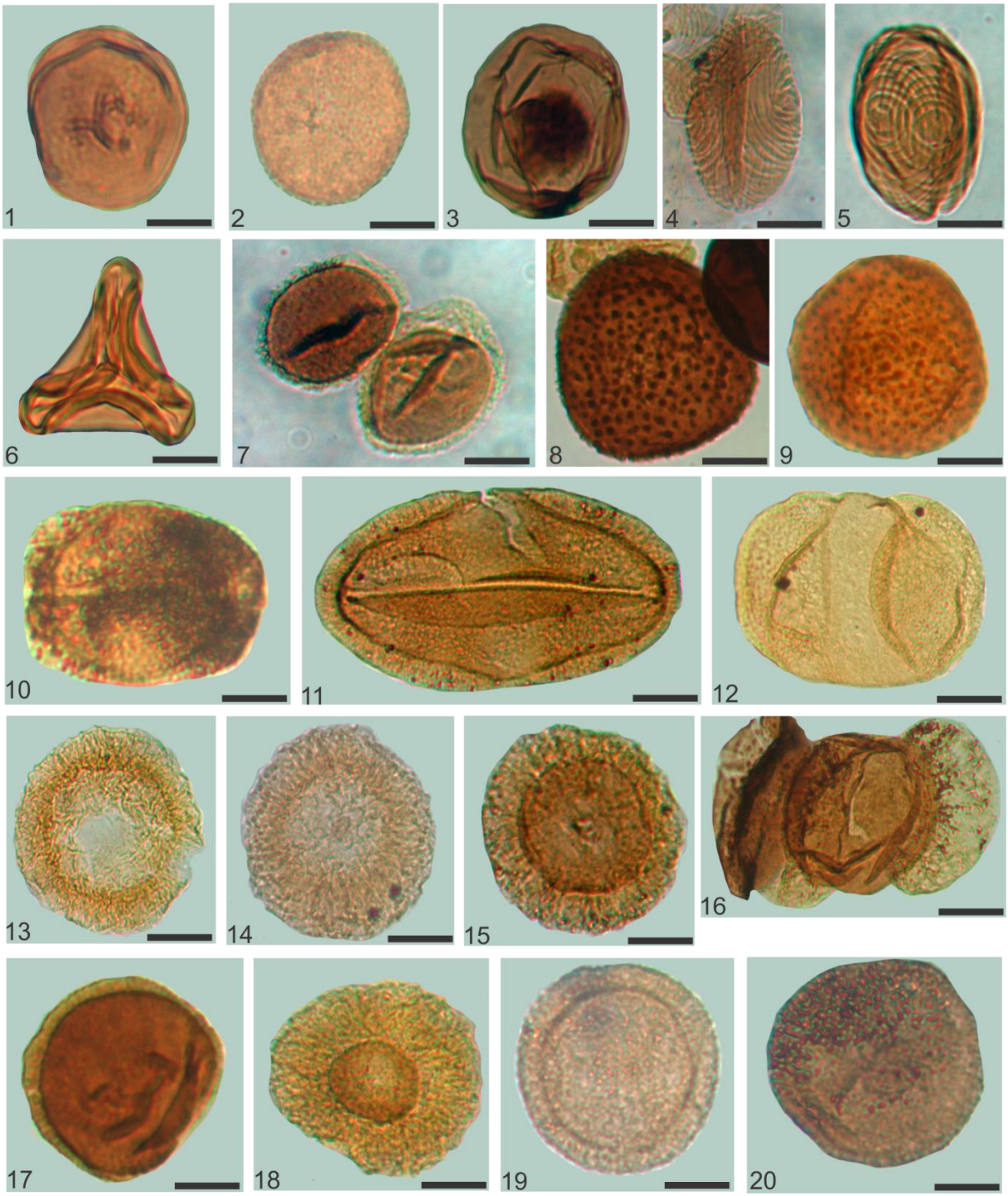

Plate 9 (Mercia Mudstone Group, Branscombe Mudstone Formation)

Palynomorphs in the Branscombe Mudstone Formation I with the with the indication of sample name, or code and slide number, scale bar 10 µm, WE refers to samples from the Strangman`s Cove outcrop.

1 *Todisporites rotundiformis* (WE203/C), 2 *Cyclogranisporites* sp. (WE203/B), 3 *Calamospora tener* (WE203/A), 4 *Brodispora striata* WE203/A), 5 *Brodispora striata* (WE203/A), 6 *Concavisporites toralis* (WE203/A), 7 a, b *Aratrisporites granulatus* (WE203/A), 8 *Porcellispora longdonensis* (WE203/A), 9 *Porcellispora longdonensis* (WE203/A), 10 *Ovalipollis minimus* (WE203/A), 11 *Ovalipollis lunzenis* (WE203/A), 12 *Alisporites grandis* (WE203/A), 13 *Patinasporites densus* (WE203/A), 14 *Patinasporites densus* (WE203/A), 15 *Patinasporites iustus* (WE203/A), 16 *Pityosporites* sp. (WE203/A), 17 *Enzonalasporites vigens* (WE203/A), 18 *Patinasporites explanatus* (WE203/A), 19 *Enzonalasporites manifestus* (WE203/B), 20 *Pseudoenzonalasporites summus* (WE203/A)

Plate 10 (Mercia Mudstone Group, Branscombe Mudstone Formation)

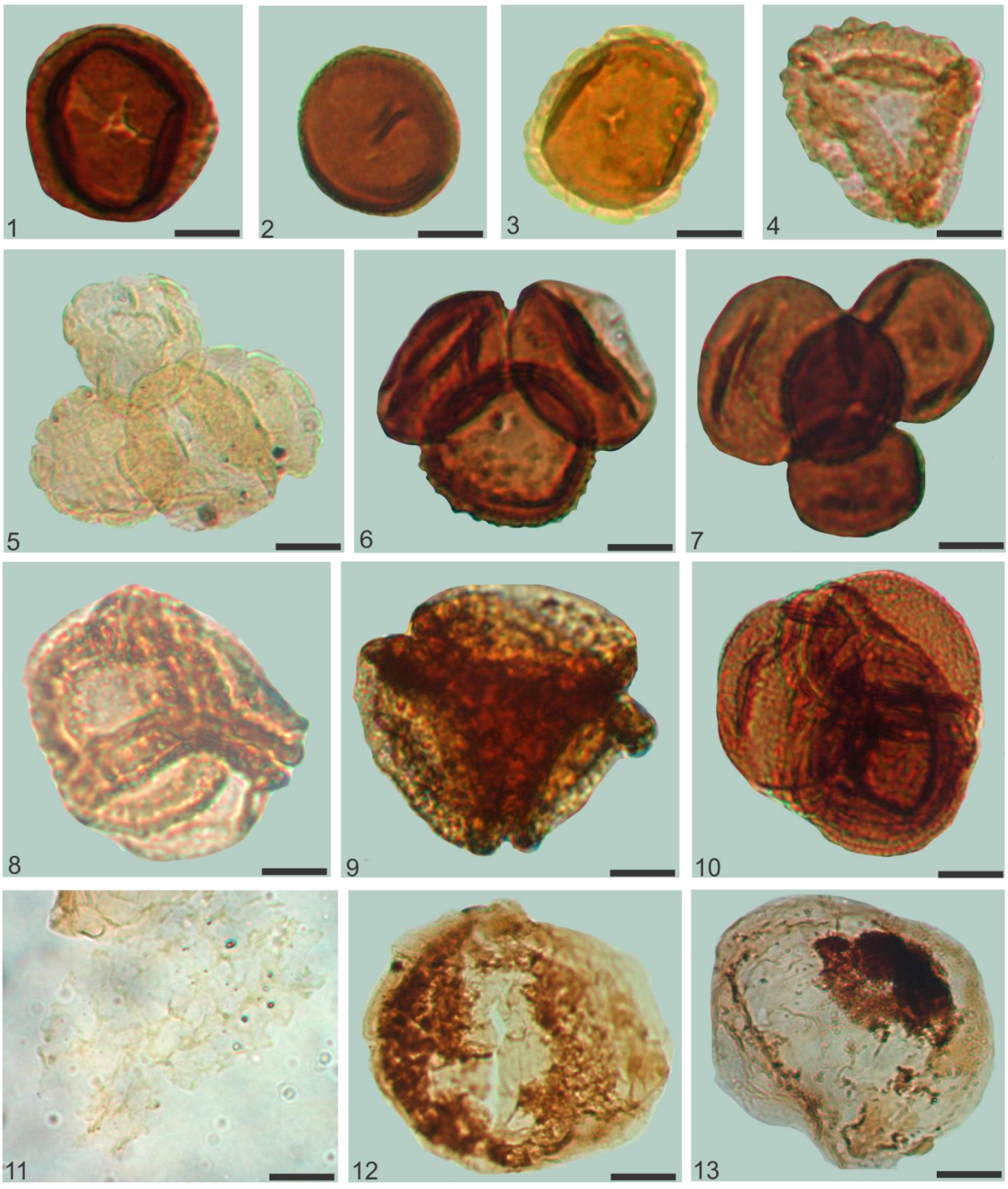

Plate 10 (Mercia Mudstone Group, Branscombe Mudstone Formation)

Palynomorphs in the Branscombe Mudstone Formation II with the indication of sample name, or code and slide number, scale bar 10 µm, *WE refers to samples from the Strangman`s Cove outcrop.*

1 cf. *Partitisporites tenebrosus*(WE203/A), 2 cf. *Partitisporites tenebrosus*? (WE203/A), 3 *Camerosporites secatus* (WE203/A), 4 *Duplicisporites mancus* (WE203/A), 5 *Camerosporites secatus* (WE203/A), 6 cf. *Partitisporites tenebrosus* (WE203/B), 7 cf. *Partitisporites tenbrosus* (WE203/B), 8 *Partitisporites quadruplices* (WE203/B), 9 *Partitisporites quadruplices* (WE203/B), 10 *Partitisporites* sp. (WE203/C), 11 *Plaesiodictyon mosellanum* (WE203/B), 12 *Schizosporis* sp. (WE203/A), 13 *Schizosporis* sp. (WE203/A)

Plate 11 (Mercia Mudstone Group, Somerset Lipe Hill and Sutton Mallett)

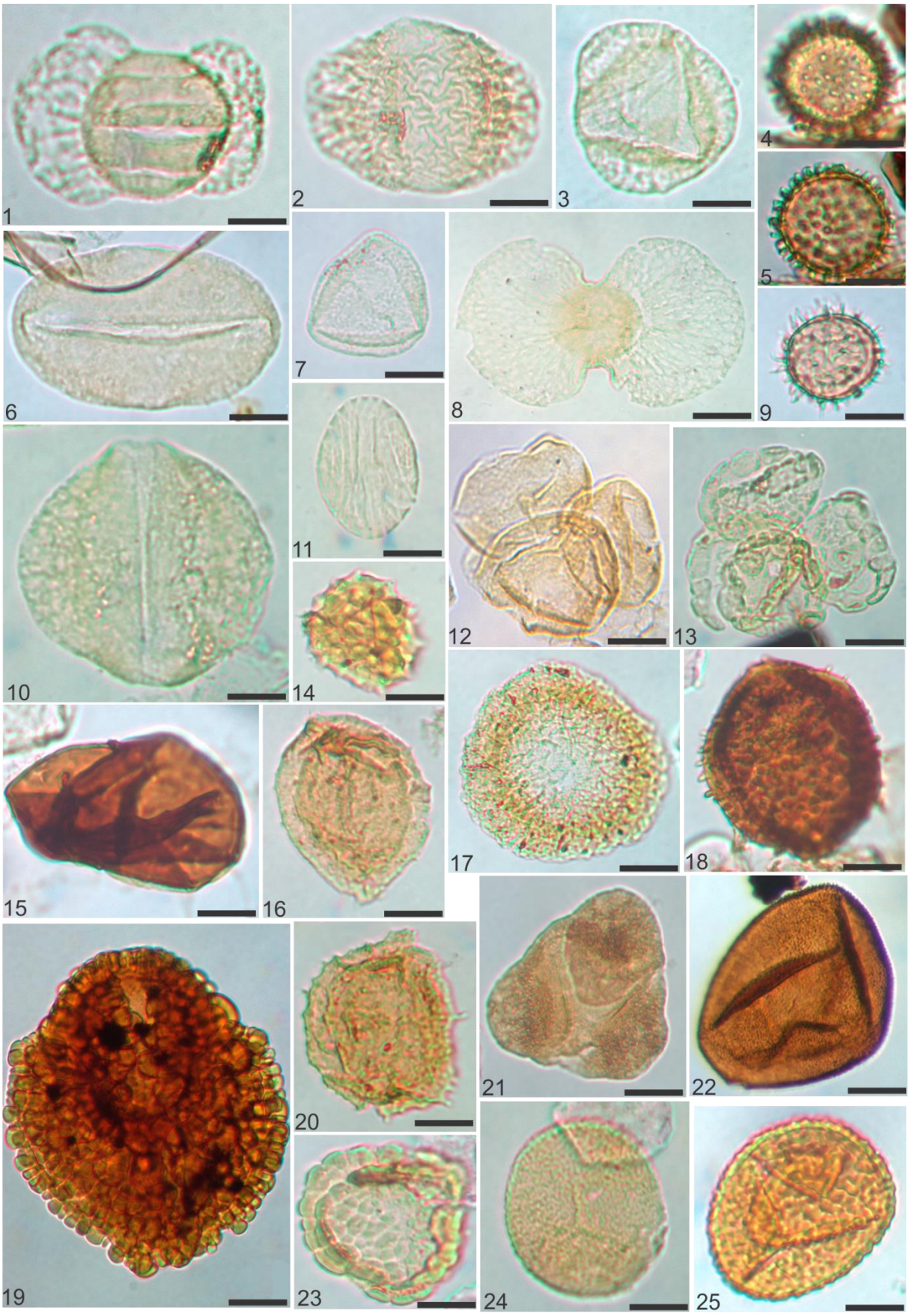

Plate 11 (Mercia Mudstone Group, Somerset Lipe Hill and Sutton Mallett)

Somerset palynomorphs with the indication of sample name, or code and slide number, scale bar 10 µm, SM refers to samples from Sutton Mallet, LH from Lipe Hill.

1 *Lunatisporites acutus* (LH 2/2), 2 *Triadispora plicata* (LH 2/2), 3 Bisaccate indet with three airbags (LH 2/2), 4 acritach indet (LH 2/2), 5 acritarch indet same as 4 with different focus (LH 2/2), 6 *Ovalipollis ovalis* (LH 2/2), 7 *Duplicisporites granulatus* (LH 4/1), 8 *Platysaccus* sp. (LH 5/1), 9 *Micrhystridium* sp. (LH 2/2), 10 *Alisporites grauvogeli* (LH 7/1), 11 *Brodispora striata* (LH 9/1), 12 *Duplicisporites granulatus* tetrad (LH 8/1), 13 *Camerosporites secatus* tetrad (LH 7/1), 14 *Gibeosporites lativerrucosus* (SM 2/1), 15 cf. *Aulisporites astigmosus* (SM 3/1), 16 *Aratrisporites scabratus* (SM 3/1), 17 *Patinasporites densus* (SM 2/1), 18 *Porcellispora longdonensis* (SM 3/1), 19 *Riccisporites tuberculatus* (SM 2/1), 20 *Aratrisporites paraspinosus* (SM 2/1), 21 bisaccate indet with three airbags (SM 4/1), 22 *Cyclotriletes* sp. (SM 4/1), 23 *Camerosporites secatus* (SM 2/1), 24 *Cyclogranisporites* sp. (SM 4/1), 25 *Converrucosisporites tumolosus* (SM 4/1)

Plate 12 (Veszprém Marl Formation, Transdanubian Range)

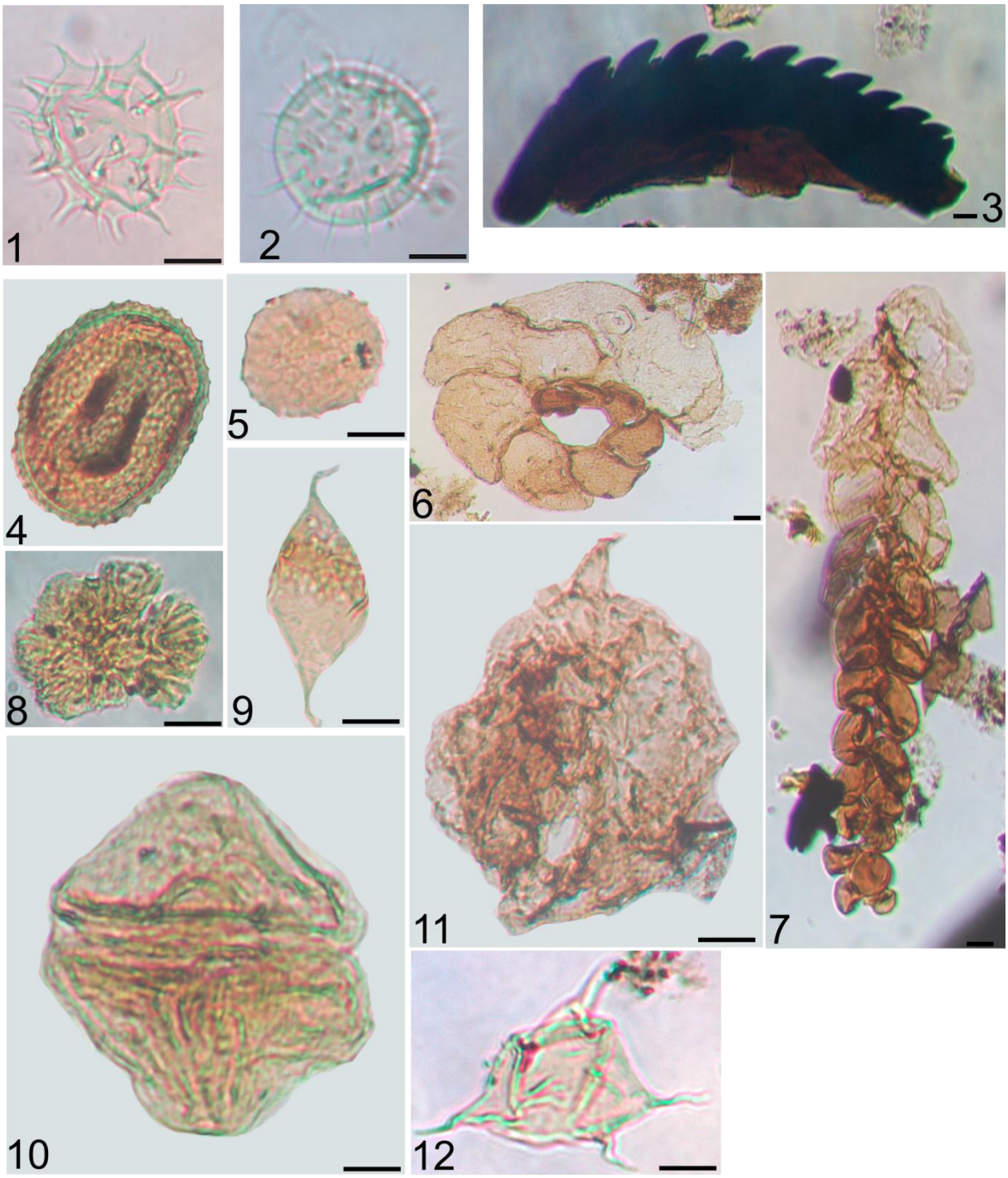

Plate 12 (Veszprém Marl Formation, Transdanubian Range)

Aquatic palynomorphs from the Veszprém Marl Formation, with the indication of sample code, sample code refers to the depth in meters; scale 10 µm, Met refers to samples from borehole Mencshely-1, V from Veszprém-1.

1 *Mirchystridium* sp. 2. V-1/578, 2 *Mirchystridium* sp. 1. V-1/573, 3 scolecodont V-1/532, *4 Tasmanites* sp. Met-1/122.9, 5: *Cymatiosphaera* sp. V-1/343, 6: foraminiferal test lining A Met-1/150, 7:foraminiferal test lining B V-1/485, 8: *Botryococcus braunii* Met-1/81, 9: *Leiofusa* sp. V-1/549, 10: *Heibergella* sp. Met-1/325, 11: dinocyst indet. Met-1/122.9, 12: *Verychachium* sp. Met-1/69.8.

Plate 13

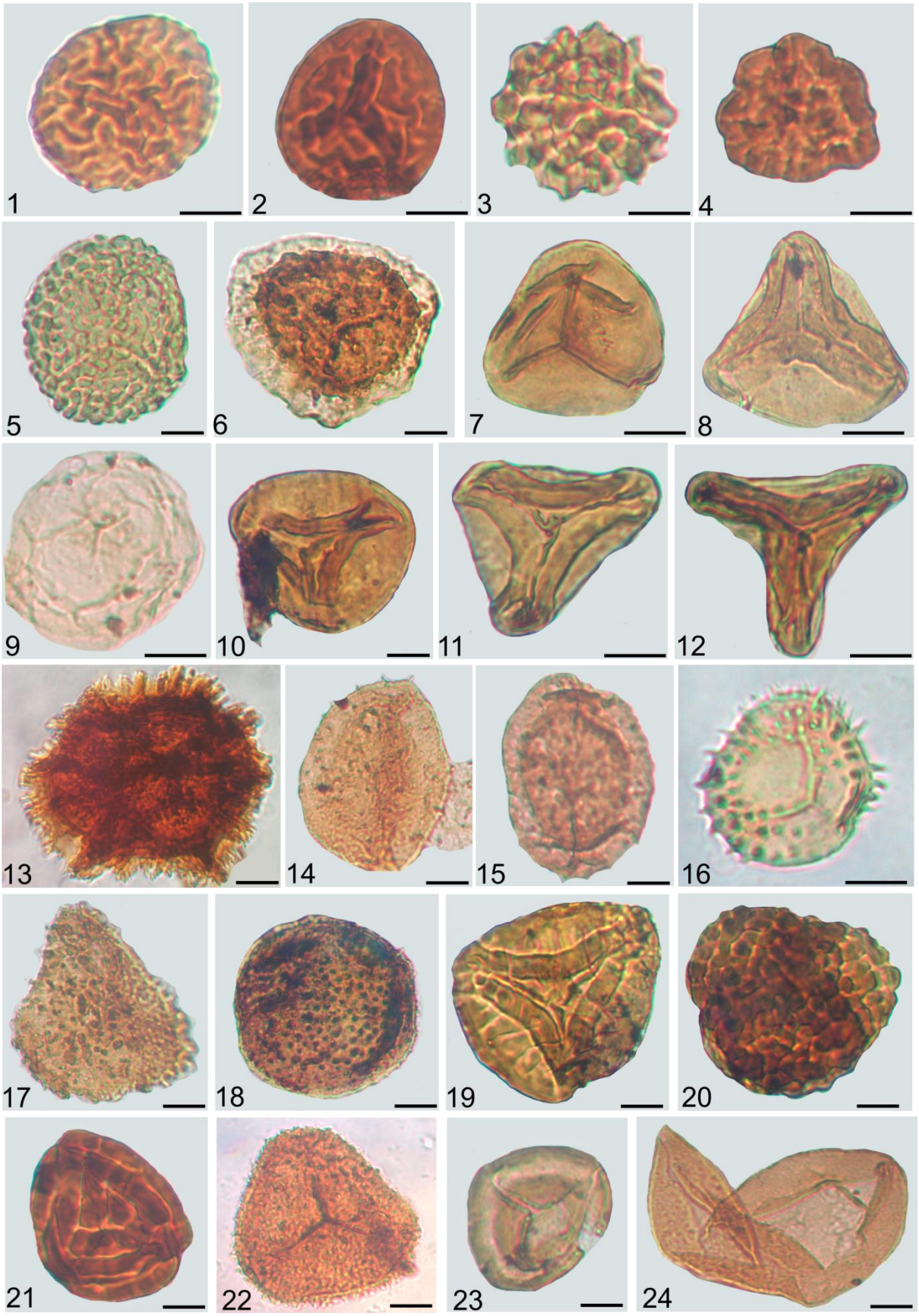

Plate 13

Spores from the Veszprém Marl Formation and Csákberény Formation, with the indication of sample code and slide number, sample code refers to the depth in meters; scale 10 µm, Met refers to samples from borehole Mencshely-1, V-1 from Veszprém-1, Zs from Zsámbék-14.

1 *Lycopodiacidites kuepperi* V-1 334.6/1, 2 *Camarazonosporites rudis* V-1 343/2, 3 *Gibeosporites lativerrucosus* V-1 335/1, 4 *Uvaesporites gadensis* V-1 343/2, 5 *Verruocisporites moroluae* V-1 350/1, 6 *Kraeuselisporites cooksonae* V-1 532/1, 7 *Deltoidospora* sp. Met-1 299.5/1, 8 *Dictyophillidites harrisii* V-1 491-492/1, 9 *Calamospora tener* V-1 578/1, 10 *Laevigatisporites robostus* Met-1 199.4/1, 11 *Paraconcavisporites lunzensis* Met-1 87/1, 12 *Concavisporites toralis* Met-1 135/1, 13 *Reticulatisporites dolomiticus* V-1 334.6/1, 14 *Aratrisporites palettae* V-1 573/2, 15 *Aratrisporites scabratus* V-1 343/2, 16 *Anapiculatisporites telephorus* Met-1 177.4/1, 17 *Neoraistrickia taylorii* Met-1 252/1, 18 *Porcellispora longdonensis* Met-1 135/1, 19 *Kyrtomisporits erveii* Zs 329.7/1, 20 *Converrucosisporites tumolosus* tetrad Zs 329.7/1, 21 *Striatella seebergensis* Met-1 91/1, 22 *Conbaculatisporites mesozoicus* V-1 343/1, 23 *Rogalskaisporites* sp. V-1 334.6/1, 24: *Todisporites major* V-1 493/2.

Plate 14

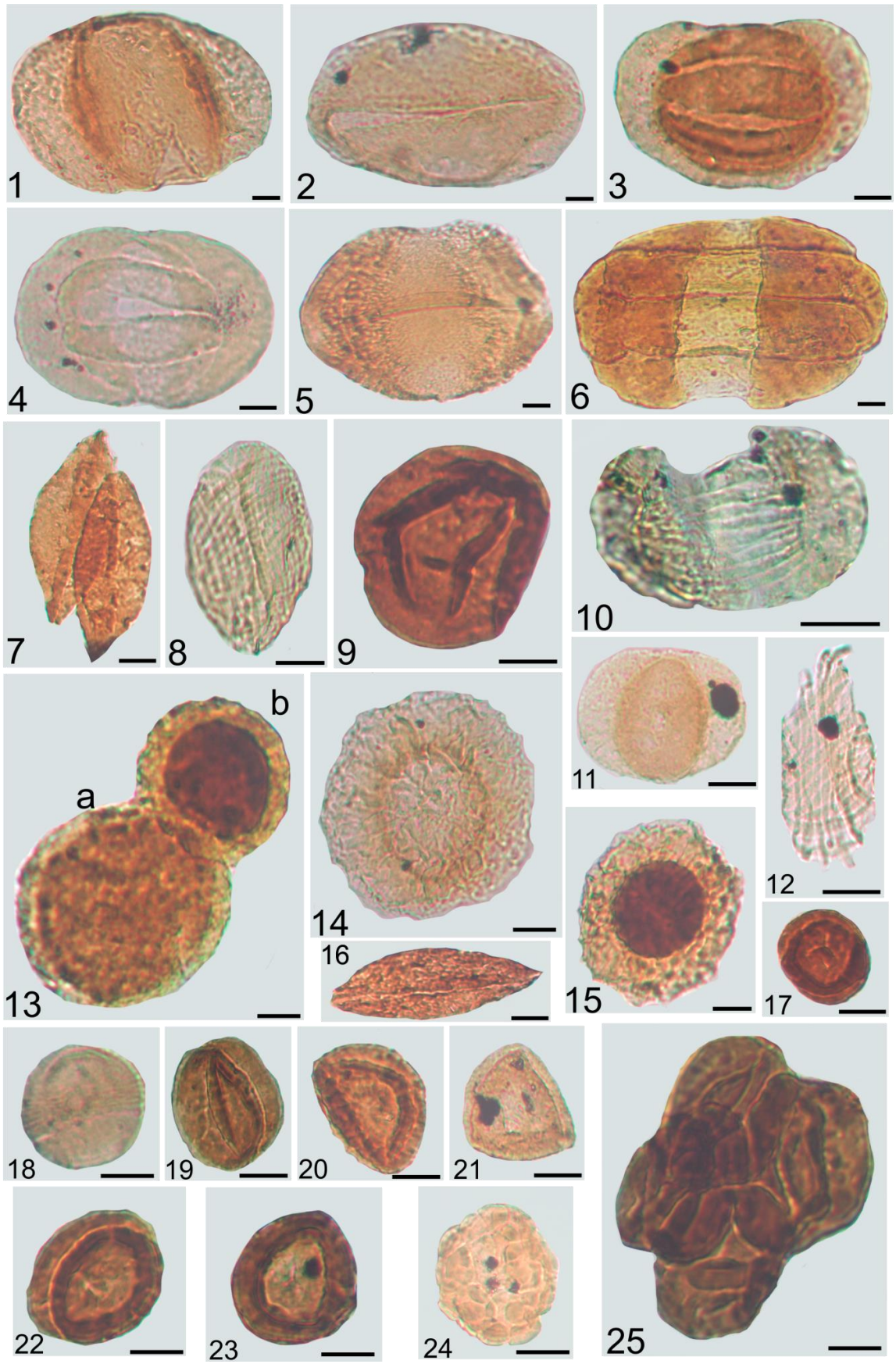

Plate 14

Pollen grains from the Veszprém Marl Formation and Csákberény Formation*, with the indication of sample code and slide number,* sample code refers to the depth in meters; *scale 10 µm, Met refers to samples from borehole Mencshely-1, V-1 from Veszprém-1, Zs from Zsámbék-14.*

1 *Alisporites aequalis* Met-1 122.9/1, 2 *Ovalipollis ovalis* V-1 343/2, 3 *Lunatisporites acutus* V-1 343/1, 4 *Lueckisporites singhii* V-1 573/1, 5 *Staurosaccites quadrifidus* V-1 343/2, 6 *Infernopollenites sulcatus* Met-1 101.4/1, 7 *Cycadopites* sp. V-1 493/1, 8 *Lagenella martinii* Met-1 299.5/1, 9 *Aulisporites astigmosus* V-1 335/1, 10 *Striatoabietites aytugii* Zs 373.2/1, 11 *Triadispora crassa* V-1 573/1, 12 *Equisetosporites chinleana* V-1 506/1, 13 a) *Enzonalasporites vigens* b) *Enzonalasporites tenuis* Met-1 252/1, 14 *Patinasporites densus* V-1 343/2, 15: *Patinasporites explanatus* V-1 343/2, 16 Cycadopites sp. V-1 493/2, 17 cf. *Partitisporites tenebrosus* Met-1 122.9/1, 18 *Partitisporites maljawkinae* Met-1 81/2, 19 cf. *Partitisporites tenebrosus* V-1 491-492/1, 20 *Duplicisporites mancus* Met-1 122.9/1, 21 *Duplicisporites granulatus* Met-1 122.9/1, 22 *Duplicisporites continuus* Met-1 252/1, 23 D*uplicisporites continuus* V-1 491-492/1 24 *Camerosporites secatus* V-1 335/1, 25 cf. *Partitisporites tenebrosus* tetrad V-1 343/2.

Scientific papers

PAPER 1

PAPER 2

PAPER 3

Published paper and supplementary data available at:
https://pubs.geoscienceworld.org/gsa/gsabulletin/article/519602/norian-vegetation-history-and-related

PAPER 4

Published paper and supplementary data available at:
http://www.journals.uchicago.edu/doi/abs/10.1086/694762

Int. J. Plant Sci. 179(2):000–000. 2018.

1058-5893/2018/17902-00XX$15.00 DOI: 10.1086/694762

ULTRASTRUCTURE AND PROBABLE BOTANICAL AFFINITY OF THE ENIGMATIC SPOROMORPH *FROELICHSPORITES TRAVERSEI* FROM THE NORIAN (LATE TRIASSIC) OF NORTH AMERICA

Viktória Baranyi,[1,*] Charles H. Wellman,† and Wolfram M. Kürschner*

*Department of Geosciences, University of Oslo, P.O. Box 1047, Blindern, Oslo 0316, Norway; and †Department of Animal and Plant Sciences, University of Sheffield, Western Bank, Sheffield S10 2TN, United Kingdom

Editor: Patrick S. Herendeen

Premise of research. *Froelichsporites traversei* is a prominent palynomorph in the Upper Triassic of North America that always occurs in tetrahedral permanent tetrads. It is an important regional biostratigraphic marker in the Norian of North America, and its abundance rises around 215 Ma, associated with a significant floral and faunal turnover. Its most striking morphological features are one well-developed distal pore (ulcus) on each grain and the annulus-like exine thickening around them. Previous works suggested that it was produced by spore-producing plants or Cheirolepidiaceae, but its botanical affinity is still unclear.

Methodology. The wall ultrastructure of *F. traversei* was analyzed by TEM in order to reveal more information on the botanical affinity of the palynomorph.

Pivotal results. The sporoderm consists of two layers and an inner faint discontinuous lamination. The outermost exine layer has a homogeneous texture (tectum), while the inner layer has a granular texture (infratectum). The laminae below the granular layer are not continuous but directly contiguous with the granules.

Conclusions. The ultrastructure studies have ambiguous results, and the botanical affinity could not be revealed with certainty. It represents most likely a gymnosperm. The sporoderm layers indicate full development, and *F. traversei* was most likely dispersed as permanent tetrads at maturity. The ulcus might represent a germinal aperture or a rehydration pore similar to Cupressaceae pollen. The permanent tetrads may be related to polyembryony or polyploidy, and they probably provided an adaptive advantage to the parent plant.

Keywords: Froelichsporites traversei, ultrastructure, permanent tetrad, ulcus, Late Triassic.

Online enhancement: appendix figure and tables.

Introduction

Froelichsporites traversei is an enigmatic palynomorph in the Upper Triassic of North America that always occurs as tetrahedral permanent tetrads (Litwin et al. 1991, 1993; Litwin and Ash 1993; Reichgelt et al. 2013). It has a peculiar morphology, including occurrence as permanent tetrads, one distal pore on each grain, and an annulus-like thickening around each pore. These features are often but not exclusively associated with angiosperm pollen (Moore et al. 1991). Unambiguous remains of angiosperm pollen are known from the Early Cretaceous onward (Friis et al. 2011), but in the Late Triassic several pollen types of gymnosperm pollen show angiosperm-like features (e.g., *Afropollis*, Crinopollis group; Cornet 1989*a*; Doyle 2005, 2009; Hochuli and Feist-Burkhardt 2013).

[1] Author for correspondence; e-mail: viktoria.baranyi@geo.uio.no.

Manuscript received April 2017; revised manuscript received July 2017; electronically published December 4, 2017.

Permanent tetrads might represent a special reproductive strategy (e.g., polyemebryony; Mander et al. 2012) that provided adaptive advantages for the parent plant during environmental perturbations by increasing the chance for producing viable offspring. Dispersed spore tetrads can be associated with environmental stress (Graustein 1930), and the occurrence of these tetrads related to environmental perturbation are also known from fossil assemblages (Visscher et al. 2004; Looy et al. 2005).

Froelichsporites traversei was first described as *Pyramidosporites traversei* by Dunay and Fisher (1979) from the Dockum Group in Texas. Later Litwin et al. (1993) erected the new genus *Froelichsporites* to replace the generic assignment to *Pyramidosporites* because *Froelichsporites* possesses a double-layered wall and ulci; in addition, the proximal faces of the individual grains are closely adpressed, in contrast to *Pyramidosporites*.

The distribution of *F. traversei* is restricted to Upper Triassic formations of North America (Dunay and Fisher 1979; Fisher and Dunay 1984; Litwin et al. 1991, 1993; Cornet 1993; Fowell and Olsen 1993; Fowell et al. 1994; fig. 1; table 1), but similar forms have been described from Upper Triassic continental strata of Portugal (Adloff et al. 1974). *Froelichsporites traversei* has

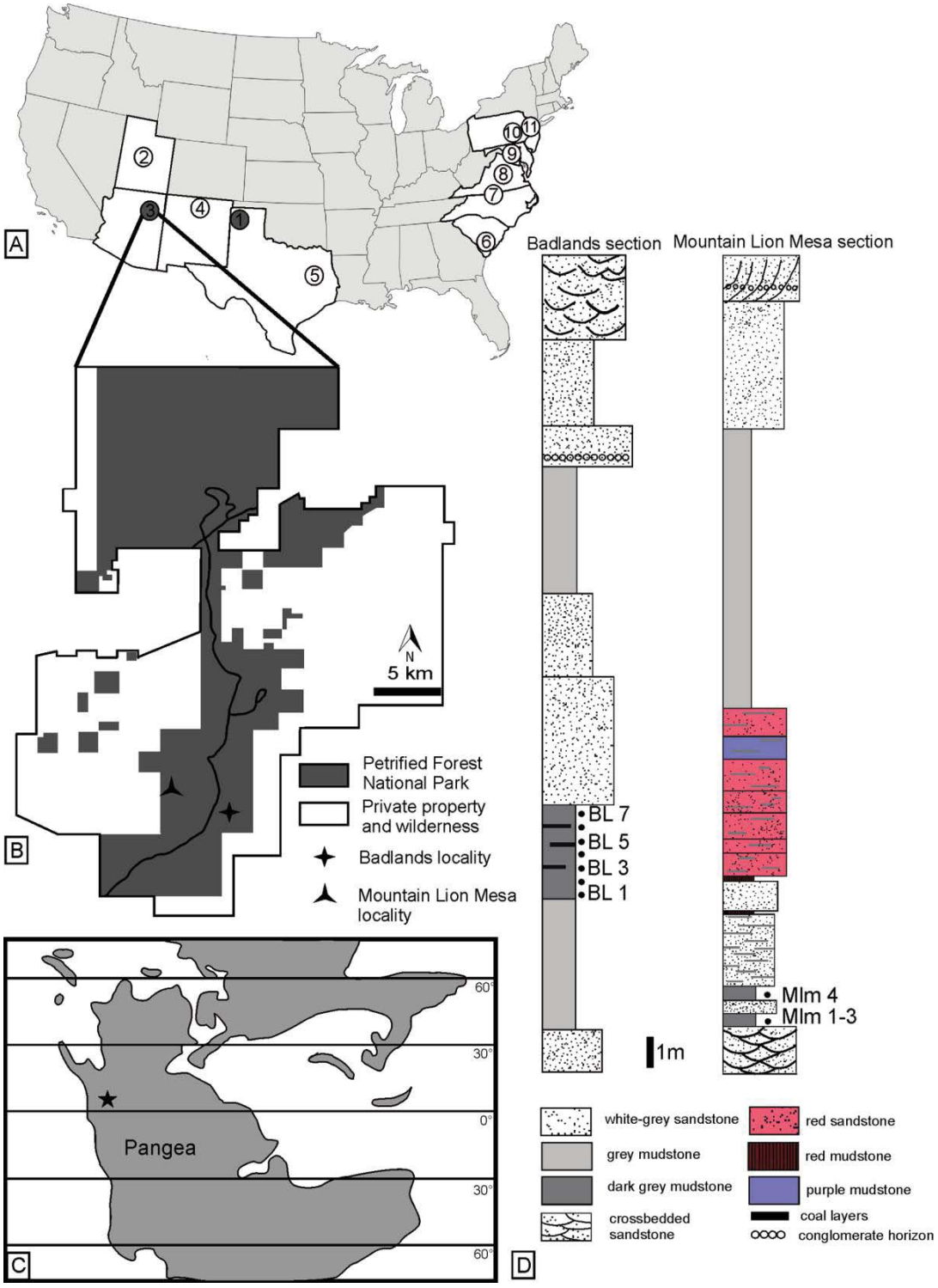

Fig. 1 *A*, Position of the Petrified Forest National Park within North America. Numbers indicate the *Froelichsporites traversei* occurrences: 1, Texas (Tecovas Formation) holotype locality; 2, Utah (Chinle Formation); 3, Arizona (Chinle Formation; this study); 4, New Mexico (Chinle Formation); 5, Texas (Eagle Mills Formation); 6, South Carolina (South Georgia Basin); 7, North Carolina (Deep River Basin); 8, Virginia (Culpeper Basin); 9, Maryland (Gettysburg Basin); 10, Pennsylvania (Gettysburg Basin); 11, New Jersey (Newark Supergroup). Modified from Litwin et al. (1993). *B*, Location of the sampling sites within the Petrified Forest National Park. Map modified from Parker and Martz (2011). *C*, Paleogeographic position of the Chinle sedimentary basin during the Late Triassic. Triassic map modified from Trendell et al. (2013). *D*, Stratigraphic position of the studied palynological samples. Logs modified from Reichgelt et al. (2013).

Table 1

Summary of Previous Studies on *Froelichsporites traversei*

Year	Taxa	References	Locality	Remarks
1972	New genus A	Dunay 1972	Dockum Group, Texas	Recorded
1975	*Tetrahedrosporites hechtii*	Gottesfeld 1972	Chinle Formation, Arizona	Informally described
1977	Genus A of Dunay	Cornet 1977	Newark Supergroup	Recorded
1979	*Pyramidosporites traversei*	Dunay and Fisher 1979	Dockum Group, Texas, New Mexico	Formally described
1984	*P. traversei*	Fisher and Dunay 1984	Chinle Formation, Arizona	Recorded
1986	*P. traversei*	Litwin 1986	Chinle Formation, Arizona, Utah, New Mexico	Recorded
1987	*P. traversei*	Traverse 1987	South Carolina	Recorded
1988	*P. traversei*	Robbins et al. 1988	North Carolina	Recorded
1991	*P. traversei*	Litwin et al. 1991	Chinle Formation, Arizona, Utah, New Mexico	Recorded
1993	*P. traversei*	Litwin and Ash 1993	Chatham Group, North Carolina	Recorded
1993	*P. traversei*	Cornet 1993	Newark Supergroup	Recorded
1993	*F. traversei*	Litwin et al. 1993	Chinle Formation, Arizona, Utah, New Mexico	Emended
1994	*P. traversei*	Fowell et al. 1994	Newark Supergroup	Recorded
2013	*F. traversei*	Reichgelt et al. 2013	Chinle Formation, Arizona	Recorded
2016	*F. traversei*	Lindström et al. 2016	Chinle Formation, New Mexico	Recorded

been recorded from the Chinle Formation in the southwestern United States (Arizona, Utah, New Mexico; Gottesfeld 1972; Dunay and Fisher 1979; Fisher and Dunay 1984; Litwin et al. 1991; Reichgelt et al. 2013; Lindström et al. 2016), the Dockum Group (Texas, New Mexico), the Chatham Group (North Carolina; Litwin and Ash 1993), and the Newark Supergroup (Cornet 1993; table 1). It can be considered as a regional biostratigraphy marker of the middle Norian in North America (Litwin et al. 1991; Reichgelt et al. 2013). In the Chinle Formation in Arizona and New Mexico, peaks of its abundance are associated with a floral and faunal turnover, and severe environmental perturbations including a shift toward arid climate and increased seasonality (Reichgelt et al. 2013; Whiteside et al. 2015; Lindström et al. 2016). The highest abundance of *F. traversei* is coeval with the maximum abundance of the *Patinasporites* group (*Patinasporites*, *Enzonalasporites*; Lindström et al. 2016) and *Klausipollenites gouldii*, which are probably associated with opportunistic voltzialean plants.

Despite the significance of the species in the Upper Triassic of North America and its peculiar morphological features, the botanical affinity is still unclear. Previous work suggested that it was produced by spore-producing plants or that it is a prepollen, or pollen related to Cheirolepidiaceae on the basis of the resemblance to *Classopollis* tetrads (Litwin et al. 1993).

In order to clarify its botanical affinity, we document its morphology using SEM and TEM. This is the first documentation of the wall ultrastructure of *F. traversei*. Exine ultrastructure analyses can provide useful insight into the botanical affinity of dispersed palynomorphs and reveal relationships between plant groups (Doyle 2009). The precise botanical assignment of *F. traversei* is also crucial in understanding the role of the taxon during the environmental perturbation recorded in the Norian of North America.

Material and Methods

The *Froelichsporites traversei* tetrads investigated here were collected from the Chinle Formation at the Petrified Forest National Park (PEFO), Arizona (fig. 1). Samples BL 1–BL 7 were taken from the Badlands section, in the upper Jim Camp Wash Beds, in the upper part of the Sonsela Member from the Badlands locality (34°50′36.3120″N, 109°47′59.0541″W) in the southeast corner of the PEFO (fig. 1*B*, 1*D*). Samples MLM 1–MLM 4 were collected from the Mountain Lion Mesa section from the upper part of the Sonsela Member, in a higher stratigraphic position compared with the BL samples (fig. 1*B*, 1*D*) at the Mountain Lion Mesa locality (34°51′51.75″N, 109°49′25 .3502″W). The SEM and TEM studies were carried out on tetrads from one palynological sample, BL 7, from the Badlands section (fig. 1*B*, 1*D*). Sample BL 7 is dark gray mudstone with high organic material content. The sample comes from a low-energy, possibly lacustrine or marsh-floodplain environment.

Preparation of the palynological samples follows the protocol of Kuerschner et al. (2007). About 10 g of sediment was crushed and the carbonates and silicates dissolved in 10% HCl and 40% HF. The organic residue was sieved with a 250- and a 15-µm mesh. In order to separate heavy minerals (e.g., pyrite) from the organic particles, heavy liquid ($ZnCl_2$) was added to the organic residue between 250 and 15 µm. Palynological slides were prepared using glycerine jelly. Spore coloration index (SCI) values follow those of Batten (2002). The organic residues are stored at the Department of Geosciences, University of Oslo. LM analysis was carried out with a Zeiss Standard Trinocular (328883) microscope connected to an AxioCam ERc5s camera and Zen 2011 software.

Additionally, a palynological slide of B. Cornet from the Newark Supergroup was studied in order to compare the morphological features of the *F. traversei* specimens between the PEFO and Newark. The studied sample comes from the Graters Member from a locality at the Nishisakawick Creek close to Frenchtown (New Jersey; 40°32′39″N, 75°02′47″W). The slides of B. Cornet are curated at the Lamont-Doherty Earth Observatory, Columbia University, but temporally stored at the Department of Geosciences, University of Oslo.

The *F. traversei* tetrads were handpicked with an eyelash from the organic residue and dehydrated in a series of ethanol solutions with increasing concentration (50%, 70%, 90%, and 100% ethanol solution). The tetrads stayed in each solution at least 30 min before being transferred into the next solution with

a higher concentration. The tetrads were placed on stubs and coated with gold with a Quorum Q150RS sputter-coater. SEM images were taken with a Hitachi SU5000 SEM at the Department of Geosciences, University of Oslo. Images were taken with an accelerating voltage at 5 kV.

For ultrastructure analysis, handpicked *F. traversei* tetrads were embedded in 0.1% agar (0.1 g of agar dissolved in 10 mL of Milli-Q water) and dehydrated with 100% ethanol and propylene oxide. As embedding medium, Spurr replacement ERL 4221 was applied, and the infiltrated blocks were polymerized at 60°C for at least 48 h. Sectioning and preliminary TEM analyses were carried out at the Department of Animal and Plant Sciences, University of Sheffield. Approximately 85-nm-thick sections were cut by a diamond knife and a Leica UC-6 ultramicrotome. The sections were picked up on 400-mesh copper grids. Two additional blocks were sectioned at the Electron Microscopy Laboratory of the University of Oslo with a Leica ultracut UCT microtome. The position of the tetrad documented in figures 6 and 7 within the agar block and embedding medium is shown in figure A1, available online. The sections were picked up on 75-mesh copper grids, and they were viewed on a JEOL 1400plus TEM. The sections have not been stained. Three tetrads have been sectioned and studied in total. TEM grids and SEM stubs are stored at the Department of Geosciences, University of Oslo. A complete list of all studied items (including palynological samples, SEM stubs, TEM blocks, grids, and the assigned PEFO catalog numbers) are listed in tables A1 and A2, available online.

Results

Systematics

In the morphological description, no interpretative terminology was applied to avoid premature conclusions.

Genus—Froelichsporites *Litwin, Smoot, Weems*

Species—Froelichsporites traversei *(Dunay and Fisher) Litwin, Smoot, Weems*

1979 *Pyramidosporites traversei* n. sp.; Dunay and Fisher (pl. 1, figs. 6–9).

1984 *P. traversei* Dunay and Fisher; Fisher and Dunay (pl. 2. fig. 4).

1991 *P. traversei* Dunay and Fisher; Litwin et al. (pl. 2, fig. 7).

1993 *F. traversei* (Dunay and Fisher) nov. comb. emend.; Litwin et al. (pl. 1, figs. 1–6; pl. 2, figs. 1–6; pl. 3, figs. 1–12).

2016 *F. traversei* (Dunay and Fisher) Litwin et al.; Lindström et al. (pl. VI, figs. 1–4).

Detailed Description

Froelichsporites traversei specimens are obligate tetrahedral tetrads with slightly to moderately thickened and fused contact areas (curvaturae perfectae; fig. 2*A*). The grains are permanently united in tetrads. The proximal face of each sporomorph is in complete contact with all others, and they are joined at an oblique angle (in polar view). Two wall layers (l1, l2; fig. 2*A*) are distinguished, but the outermost layer (l1; fig. 2*A*) is not always present. The tetrads occasionally exhibit only the inner wall layer (l2; fig. 2*A*) on the distal hemisphere of each member, and the remnant of the outermost layer is visible only along the sutures between the members. The outer wall layer is thin, psilate, and diaphanous. This layer is thickened toward the contact area of the grains to form a thick contact area (fig. 2*A*). The inner layer is thin and scabrate. A distinct pore structure (ulcus) is present on the distal face of each member (fig. 2*A*, u). The ulcus is rimmed by a slight thickening of the inner wall layer to form an annulus-like structure that is usually 2–4 µm in diameter (observed range, 1–7 µm; fig. 3*H*). On the proximal face of the grains, trilete rays are present (fig. 2*B*, r), which are the inner junction areas of the individual grains and probably nonfunctional. The rays extend to the margins of each grain. The individual members of the *F. traversei* tetrads cannot be separated; they are firmly bonded. Specimens from the PEFO are well preserved. The color of the palynomorphs varies between yellow to golden brown, their SCI index ranges from 2 to 7. The color of the wall (SCI index) does not indicate significant thermal alteration. The specimens from the Newark Supergroup (fig. 2*K*, 2*L*) show increased thermal alteration, and their SCI index ranges between 8 and 9.

Dimensions. Thirty specimens of *F. traversei* tetrads were measured. The tetrad diameter ranges between 40 and 94 µm (average, 58 µm; fig. 4). Equatorial diameter of the single grains ranges between 29 and 48 µm (average, 30 µm; fig. 4). Unbalanced tetrads, where the individual grains within the tetrad differ in size, are not observed. The diameter of the ulcus is between 3 and 10 µm (average, 5.6 µm; fig. 4). The width of the contact area (curvatura perfecta) is 2–7 µm (average, 4 µm; fig. 4). There is no difference in size range between the specimens from the PEFO and those from the Newark Supergroup.

Ultrastructure

The preserved sporoderm of *F. traversei* consists of two distinct layers and innermost faint discontinuous laminae (figs. 5*A*–5*H*, 7). The outermost layer (L1, fig. 5*A*–5*H*) is a thin electron-dense homogeneous layer, and it contains no discernible internal structures. It measures 0.2 µm and thickens gradually toward the contact areas (fig. 5*G*–5*I*). The boundary between the outer and inner layer is sharp, and no gradation is observed. The layer below (L2, fig. 5) has granular texture with small cavities. This layer is 0.4–0.6 µm thick, and similar to the outermost layer, it thickens gradually toward the triple junction areas of three individual grains (fig. 5*G*–5*I*). The tetrads are flattened because of compression; therefore, the granules and cavities in this layer might be bigger. Occasionally, the cavities seem to increase in size toward the boundary between L1 and L2 (fig. 5*G*, 5*H*). Below the granular layer, indication of faint lamination is observed (L3, figs. 5*B*–5*F*, 5*I*, 7); however, the lamellate layer is not continuous. The granules in L2 are directly contiguous with the underlying dark-staining laminae. The individual members of the tetrad are connected by the outer layer and the inner granular layer and they are firmly bonded (fig. 6).

Sporoderm Layers

The wall ultrastructure of *F. traversei* suggests that it represents a pollen type with gymnosperm affinity. The preserved layers of the sporoderm can be interpreted as follows: the outer

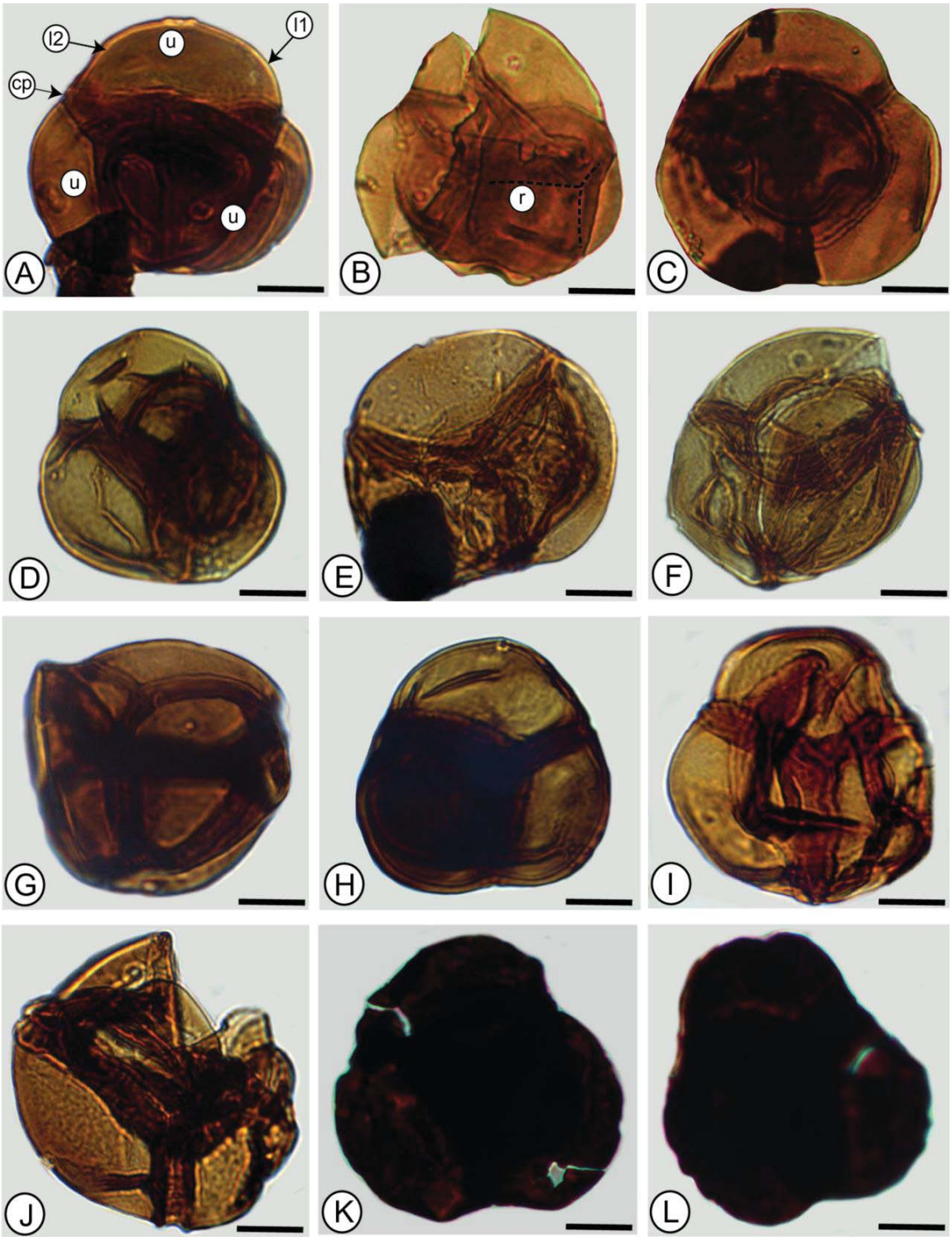

Fig. 2 *Froelichsporites traversei* tetrads seen in LM. Specimen location is given with sample and slide numbers together with the referring Petrified Forest National Park (PEFO) catalog numbers of the palynological slides from the Chinle Formation. *A*, Tetrad in polar view exhibiting double-layered wall (l1, l2), ulci (u), and thickened contact area (curvaturae perfectae [cp]), BL 2/2 (PEFO 39878). *B*, Tetrad in oblique polar view exhibiting the trilete rays (r), BL 3/2 (PEFO 39875). *C*, Tetrad in polar view, BL 4/2 (PEFO 39872). *D*, Tetrad in polar view, MLM 2/2 (PEFO 39845). *E*, Tetrad in polar view, BL 7/2 (PEFO 39863). *F*, Tetrad in oblique polar view, BL 7/1 (PEFO 39862). *G*, Tetrad in oblique view, BL 4/1 (PEFO 39871). *H*, Tetrad in polar view, MLM 2/2 (PEFO 39845). *I*, Tetrad in polar view, BL 6/1 (PEFO 39865). *J*, Broken tetrad in polar view, BL 7/2 (PEFO 39863). *K*, Polar view of a thermally altered specimen from the Newark Supergroup 1 sample, Graters Member, Frenchtown, New Jersey. *L*, Polar view of a thermally altered specimen from the Newark Supergroup 1 sample, Graters Member, Frenchtown, New Jersey. Scale bars = 20 μm.

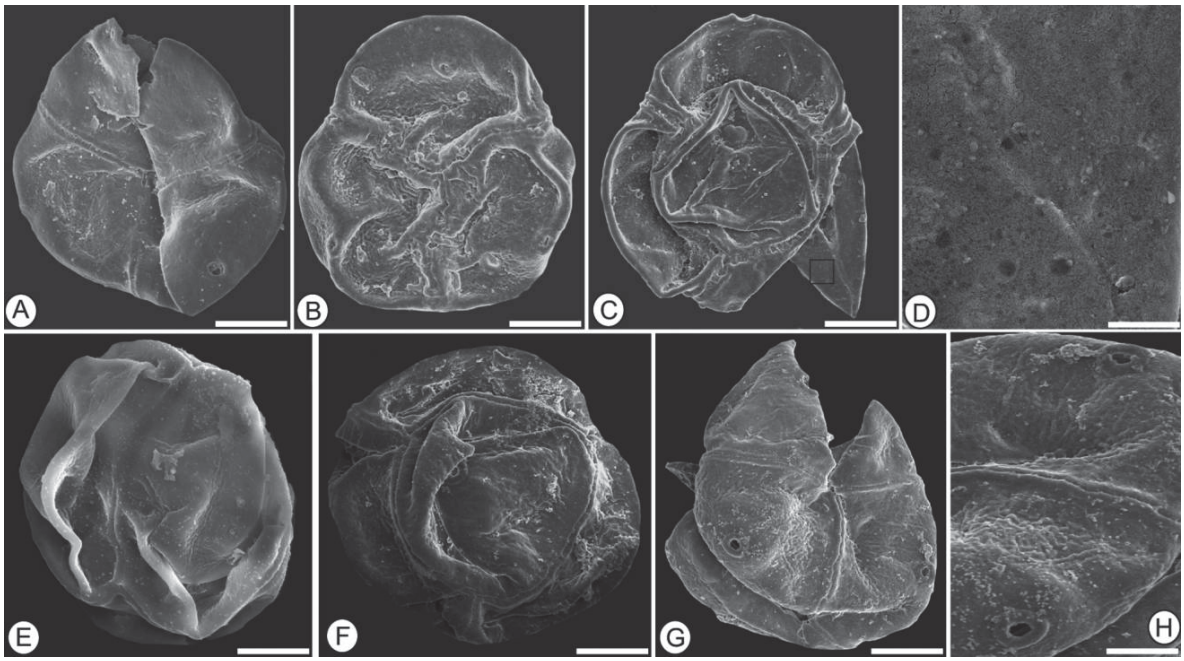

Fig. 3 SEM images of *Froelichsporites traversei* tetrads from sample BL 7 (PEFO 39861). *A*, Polar view, stub 1. *B*, Polar view, stub 1. *C*, Polar view, stub 1. *D*, Surface of *F. traversei*, same specimen as *C*; black square in *C* indicates the position of the imaged surface in *D*, stub 1. *E*, Oblique view, stub 2. *F*, Polar view, stub 2. *G*, Polar view, stub 2. *H*, Enlargement of *G* showing the ulci, stub 2. Scale bars = 15 μm (*A–C*, *E–G*), 2.5 μm (*D*), 5 μm (*H*).

homogeneous and inner granular layer can be interpreted as the sexine (fig. 7). The homogeneous outer layer represents the tectum, and the granular layer is the infratectum (fig. 7). The faint lamination below the granular layer might be related to the nexine (fig. 7).

Discussion

Botanical Affinity

Litwin et al. (1993) assigned the tetrads to spores on the basis of the presence of distinct but probably nonfunctional trilete rays on the proximal face of the tetrad members. However, the presence of a trilete scar is not necessarily an unambiguous feature of spores because there are several gymnosperm pollen grains in the Triassic that possess a trilete scar (e.g., *Triadispora*, certain *Circumpolles* grains). The affinity to spore-producing plants is challenged by its granular ultrastructure, the presence of a distal pore, and the permanent occurrence as tetrads. Various bryophyte groups disperse permanent tetrads (reviewed in Gray et al. 1985; Edwards et al. 1999). However, these all have very different wall ultrastructures compared with *Froelichsporites traversei* (e.g., in the Andreaopsida, as described in Brown and Lemmon 1984). In many Permian-Triassic transition sequences, lycopsid miospores regularly occur as tetrahedral tetrads (Visscher et al. 2004) that have been interpreted as an indication of environmental mutagenesis because of the destruction of the ozone layer (Visscher et al. 2004; Looy et al. 2005). Occurrences of unusual abundances of trilete spores dispersed as permanent tetrads have also been reported from the Devonian (Lavender and Wellman 2002). Their occurrence was assigned to the unusual reproductive strategies of the early land plants (Lavender and Wellman 2002). However, all these spores (both in the Devonian and at the Permian-Triassic transition) are all also known as individual grains in contrast to *F. traversei*, which has been found only in tetrad form. By contrast, permanent tetrads can normally occur among the gymnosperms (e.g., *Classopollis* spp. and *Riccisporites tuberculatus*; Mander et al. 2012; Kürschner et al. 2013, 2014; table 2). According to the observation of Litwin et al. (1993), *Froelichsporites* possesses a distal thinning similar to *Classopollis*, but they also noted that it differs from the members of the Circumpolles group by the lack of a ring tenuitas, the presence of the annulus, and the high degree of proximal contact of tetrad members.

Ultrastructure studies can help in identifying the botanical affinity of dispersed spores and pollen grains, but it should not be considered as the only basis for assigning sporomorphs to any botanical groups (Doyle 2005, 2009). The wall ultrastructure analysis of *F. traversei* provides ambiguous results because there is no well-developed nexine layer, while the homogeneous outer and the granular middle layer indicate an affinity within the gymnosperms. The homogeneous outer and granular middle layer observed in *F. traversei* occur in the Gnetales, Pentoxylales, Bennettitales, nonsaccate conifers such as the Araucariaceae and Cupressaceae, as well as certain angiosperms (Doyle 2009). The majority of Mesozoic gymnosperms have a stratified sporoderm (Kurmann 1992; Osborn and Taylor 1994; Osborn 2000) and possess a lamellate nexine, while nexine (or equivalent lamel-

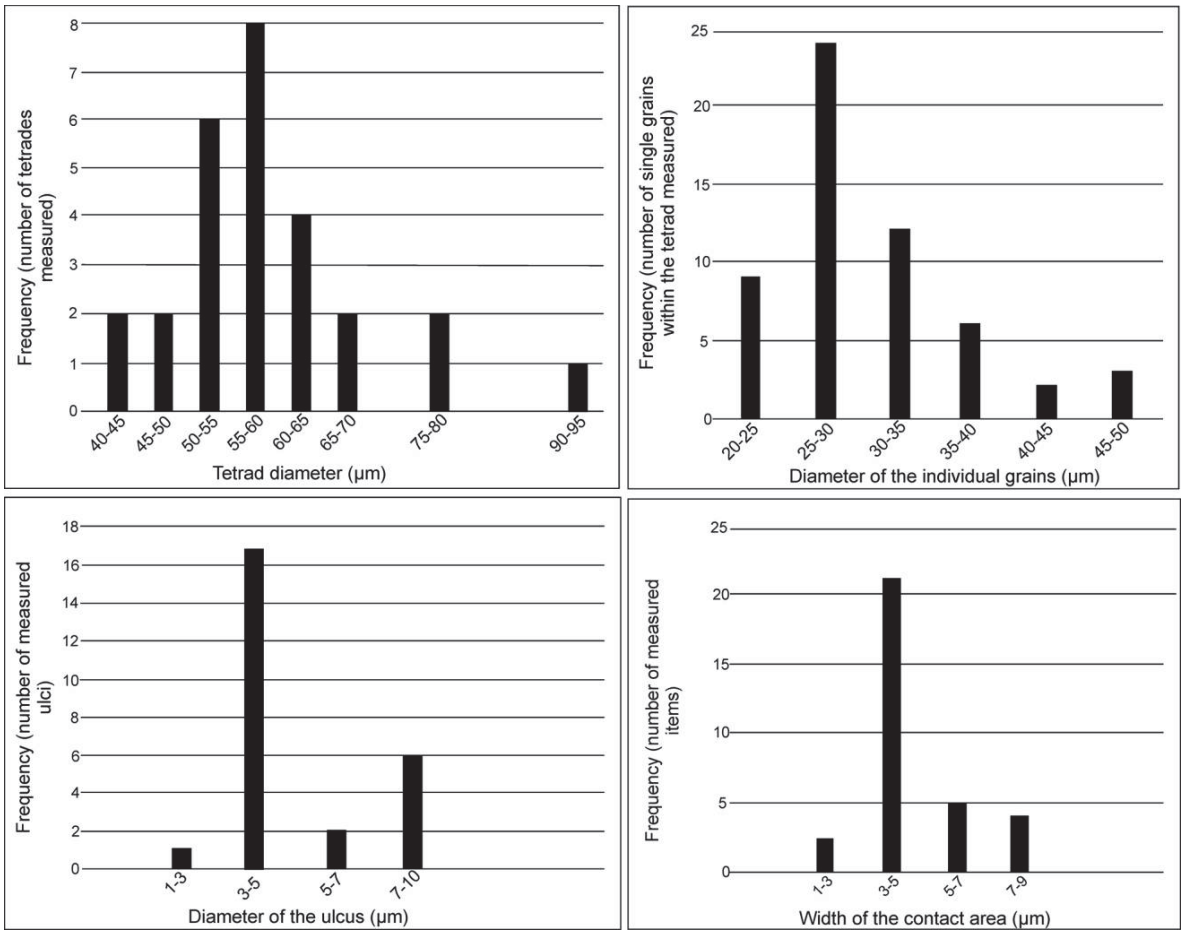

Fig. 4 Abundance distribution of the measured morphological characters based on 30 specimens.

lated inner layer of the sporoderm) might be reduced and discontinuous or absent in angiosperms (Doyle 2005). The outer and middle layers of *F. traversei* are most similar to the tectum and infratectum of the Gnetales (Kurmann 1992; Osborn et al. 1993; Osborn 2000; Tekleva and Krassilov 2009), although the pollen morphology of *F. traversei* is completely different from any modern or fossil Gnetalean pollen.

There are several Mesozoic pollen grains that show extraordinary ultrastructure patterns, such as bennettitalean pollen grains. They exhibit various ultrastructure patterns and in several cases deviate from the typical stratified pattern of the gymnosperm pollen grains (Zavada 1990; Zavialova et al. 2009). A thin lamellated inner layer is present in the bennettitalean pollen *Granamonocolpites luisae* from the Chinle Formation, while its ultrastructure is otherwise homogeneous (Zavada 1990). The pollen grains found in situ in *Williamsoniella coronata* (Zavialova et al. 2009) also have a homogeneous ultrastructure. The wall of the pollen found in situ in *Cycadeoidea dacotensis* possesses a stratified pattern characteristic for other gymnosperms (Osborn and Taylor 1995), with homogeneous tectum, granular infratectum, and a thick darker-staining homogeneous nexine with only faint indication of lamellae. Another exception is *Clusphaera psilata* (Taylor et al. 1987), a diporate pollen grain with affinity to Araucariaceae (Del Fueyo and Archangelsky 2005) that has columellar ultrastructure, which is unusual in the Araucariaceae.

The distal pore with annulus is a characteristic feature of Cupressaceae pollen (Bortenschlager 1990; Kurmann 1994), but the exine of mature modern Cupressaceae pollen grains possesses two wall layers: a granular ectexine and a clearly lamellated endexine without any homogeneous outer layer (Kurmann 1994). In the pore area, the exine becomes reduced and only one lamella covers the aperture (Kurmann 1994).

The reduction or absence of the nexine is a characteristic feature within the angiosperms (Doyle 2005, 2009). In addition to the reduced nexine, the ulcus and the dispersal as permanent tetrads make *F. traversei* comparable to the early angiosperm pollen *Walkeripollis gabonensis* (Doyle et al. 1990*a*, 1990*b*). However, the winteroid *W. gabonensis* has reticulate pollen and columellar exine, differing from *F. traversei* (Doyle et al. 1990*a*; Doyle and Hotton 1991).

On the basis of the results of the ultrastructure study, the precise botanical affinity still remains ambiguous, but at least the assignment to the Cheirolepidiaceae, as suggested previ-

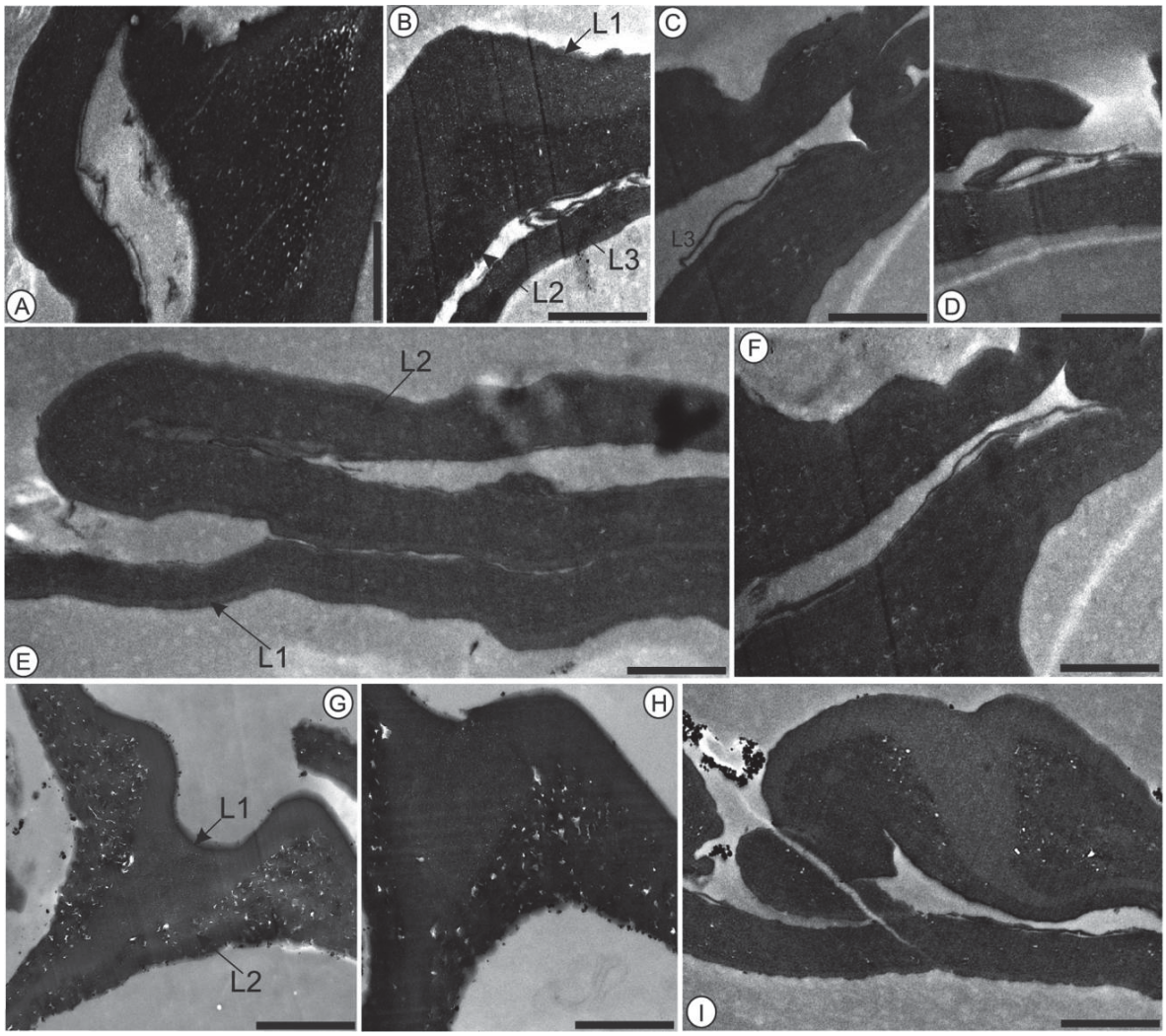

Fig. 5 TEM images of *Froelichsporites traversei* showing the ultrastructure of the palynomorph wall. *A*, Segment of the exine showing the outer electron-dense homogeneous layer and the inner granular wall layer, with a faint lamina below the inner layer, block 1/grid E2. *B*, Segment of the exine showing the outer electron-dense homogeneous layer (L1) and inner granular wall layer (L2), with faint lamination below the inner layer (L3), block 1/grid H5. *C*, Segment of the exine shows that the innermost laminae are directly contiguous with granules in the granular layer, block 1/grid H2. *D*, Innermost laminae, block 1/grid G3. *E*, Wall ultrastructure of one individual grain within the tetrad at greater distance from the junction areas, block 1/grid H1. Note that the outermost layer is very thin in this segment. *F*, Wall ultrastructure in a segment close to the junction between the individual grains, block 1/grid H1. The innermost layer is running parallel with the granular layer. *G*, Segment of the exine showing the outer electron-dense homogeneous layer and the inner granular wall layer, block 3/grid 8A. The cavities within the granular layer seem to increase in size toward the boundary between L1 and L2. *H*, Segment of the exine showing the outer electron-dense homogeneous layer and the inner granular wall layer, block 3/grid 8A. *I*, Segment of the junction area between the individual grains, block 2/grid E4. A thin lamina is running parallel to the granular layer below its inner boundary. The cavities within the granular layer seem to increase in size toward the boundary between L1 and L2. Scale bars = 1 μm (*A–D*, *F*, *H*), 2 μm (*E*, *G*, *I*).

ously by Litwin et al. (1993), can be excluded on the basis of the available ultrastructure information on Circumpolles pollen. Most of the members of the Circumpolles group possess completely different exine stratification and characteristic columellar or columellar-like infratectum (Taylor and Alvin 1984; Zavialova 2003; Zavialova et al. 2010) in contrast to the granular texture in *F. traversei*. *Duplicisporites* is the only Circumpolles pollen that possesses granular ultrastructure (Zavialova and Roghi 2005), but in this case the outer exine layer is granular and the inner exine layer is homogeneous, in contrast to *F. traversei*.

The Chinle Formation is the source of several enigmatic plant fossils unlike any known seed plant and with uncertain botanical affinity (Ash 1989, 2005). The pollen found in situ in the

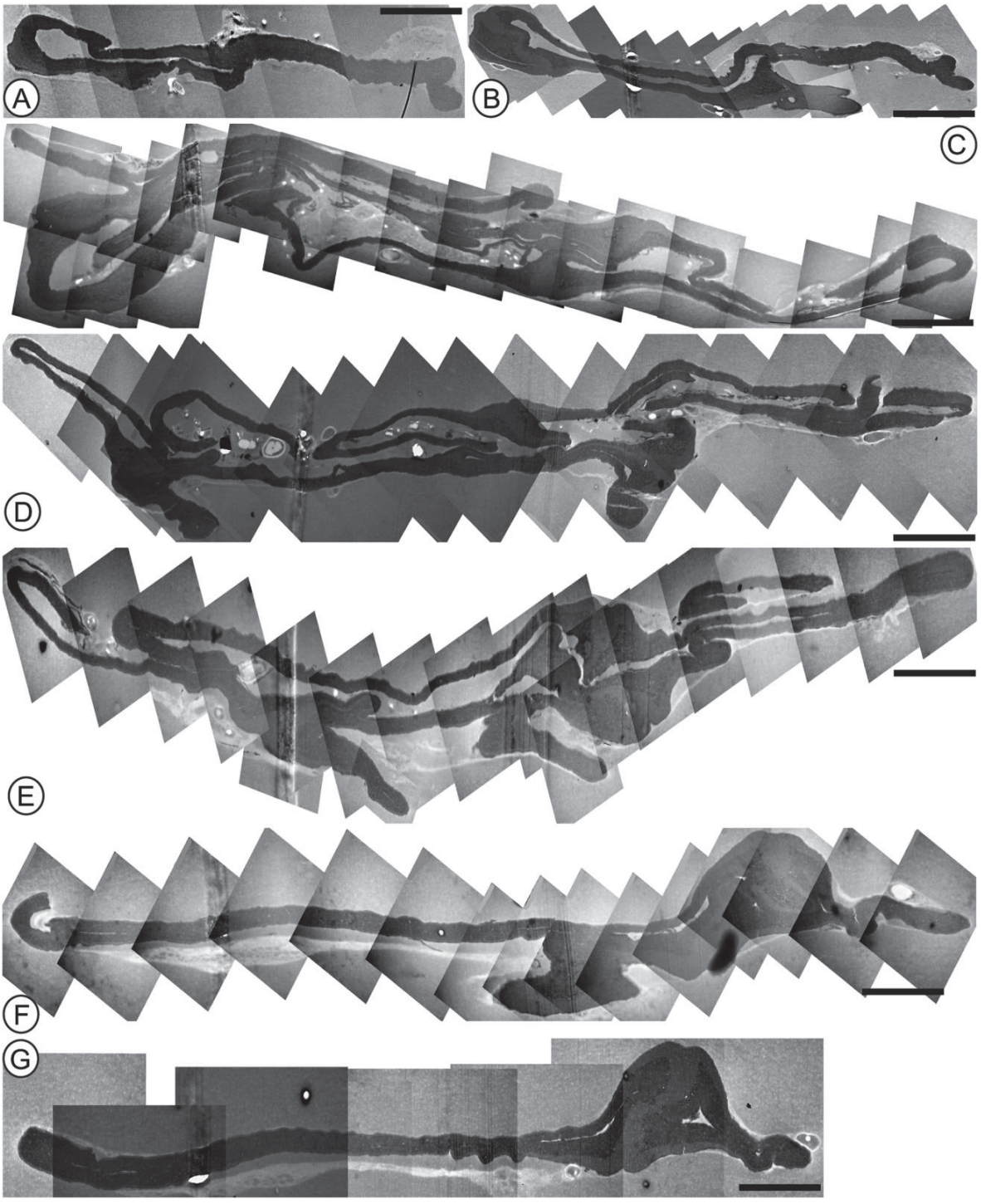

Fig. 6 TEM images showing the inner tetrad structure and the wall ultrastructure in a series of sections from the outside toward the center of the tetrad from block 1. Position of the section within the tetrad is marked in fig. 7. *A*, Grid E1. *B*, Grid E2. *C*, Grid F1. *D*, Grid G1. *E*, Grid H1. *F*, Grid H5. *G*, Grid I1. *A–G* were created by digitally stitching together several images taken at × 10,000 magnification. Scale bars = 10 μm.

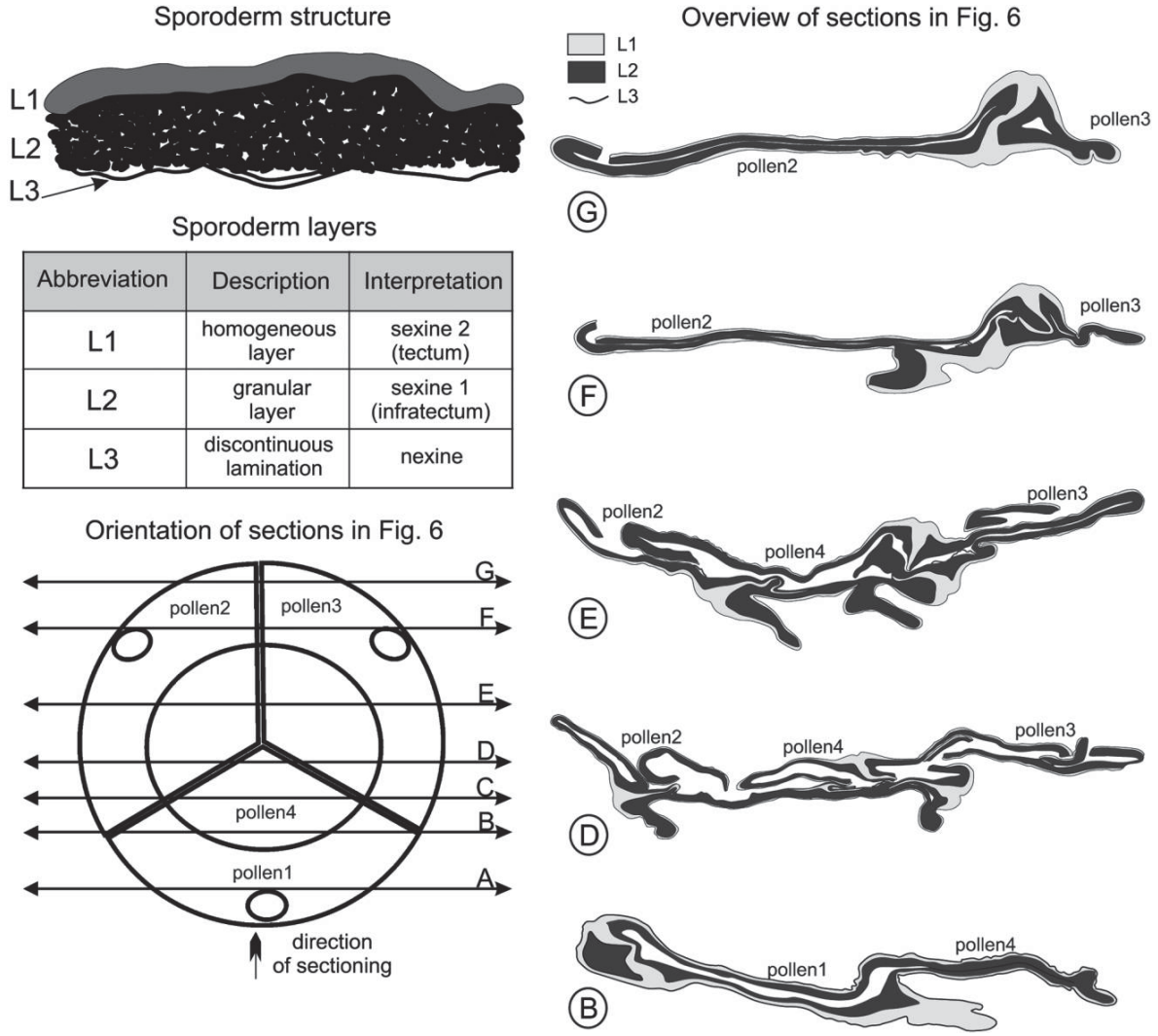

Fig. 7 Schematic interpretation of the sporoderm of *Froelichsporites traversei*. Overview of the sections shows the inner organization of selected segments of the tetrad with the indication of the individual tetrad members.

presumably pollen-producing organ of *Sanmiguelia* (*Synangispadixis*) from the Dockum Group in Texas is monocolpate, which differs from *F. traversei*, although they have similar granular ultrastructure (Cornet 1989*b*). *Dinophyton* combines gnetalean and pteridosperm features (Ash 1972; Krassilov and Ash 1988, 2007), but its pollen is bisaccate with alveolar ultrastructure (Tekleva 2015), differing from *F. traversei*. The differences in ultrastructure suggest that *F. traversei* represents a distinct taxon. The diversity of these enigmatic plants highlights that during the Late Triassic the morphological variety (e.g., pollen morphology, ultrastructure) of seed plants was extensive. Some of the combinations of features such as those observed in *F. traversei* have been lost among extant seed plants. The evaluation of their evolutionary significance and relationships needs further work.

Sporoderm Preservation and Maturity

A variety of both abiotic and biotic effects (such as preservation state and developmental stage) can influence the observed ultrastructure in spores and pollen grains (Osborn and Taylor 1995). Besides preservation and thermal maturity, palynomorph wall ultrastructure may also be obscured or damaged by the processes of embedding or sectioning during preparation for TEM examination (e.g., knife marks and chatter).

A well-developed nexine has not been found in *F. traversei* so far, although multiple grains were sectioned and all of them show only faint discontinuous laminae. It might be related to the taphonomic processes (transport, diagenesis) that affected the tetrads, or it has not been preserved during the preparation for TEM studies.

In the pollen of certain plants (e.g., Gnetales, cycads), the nexine forms in a later tetrad stage during ontogeny (Audran 1981; Doores et al. 2007). In the case of *F. traversei* tetrads, both sexine layers are present in the contact areas, which suggests that the tetrad members are likely to be fully developed according to Mander et al. (2012). In addition, no individual pollen grains of *F. traversei* have been found in the samples from the Chinle Formation or the Newark Supergroup. Therefore, the specimens of *F. traversei* investigated here can be most likely considered as fully developed and dispersed as tetrads at maturity from the parent plant.

The Reproductive Biology of the Parent Plant of Froelichsporites traversei

The parent plant of *F. traversei* and its pollination mechanism are unknown, but the morphology of pollen grains and some aspects of exine organization may be relevant to pollination mechanism (Bolinder et al. 2015). Dispersal of mature pollen grains as tetrads or other compound units is widespread among angiosperms (e.g., Cyperaceae, Juncaceae) but very rare in extant gymnosperms (Shukla et al. 1998). However, during the Mesozoic permanent tetrads among gymnosperms may have been more frequent, considering the common occurrence of Circumpolles tetrads in the fossil record (Kürschner et al. 2013). Compound units are often an adaptation to insect pollination among angiosperms (Pacini and Franchi 1996). The granular exine with no or very thin endexine is considered as an early specialization trend in some Magnoliales in order to reduce exine thickness (Doyle 2009), which has been related to an adaptation to beetle pollination (Doyle 2009) in addition to the dispersal as compound units, Among the candidates for the parent plant of *F. traversei*, the Bennettittales are considered to be primarily insect pollinated on the basis of the large pollen size and thick granular infratectum (Crane 1986; Bolinder 2014). In the case of fossil Gnetales, entomophily was suggested to be the primitive pollination mechanism (Bolinder et al. 2015, 2016). Conifers are primarily wind pollinated and wind transported (Fægri and Van der Pijl 1966).

In the angiosperms, the dispersal of pollen grains as permanent compound units (tetrads, dyads) is a common phenomenon in order to fertilize several ovules during one pollination event (Shukla et al. 1998). In the case of the gymnosperm pollen species *Riccisporites tuberculatus*, Mander et al. (2012) suggested that simple polyembryony (Webber 1940) is the explanation for dispersal as permanent tetrads. Polyembryony is the formation of more than one embryo within a single ovule caused by the fertilization of more than one archegonium by different pollen grains (Shukla et al. 1998). This type of fertilization is present in the life cycle of several conifers (e.g., *Picea*, *Larix*, *Pseudotsuga*, *Pseudolarix*), and in *Gnetum* (Gnetales) the process is especially common (Sporne 1974; Williams 2007). Mander et al. (2012) argued that the simple polyembryony provided the parent plant of *R. tuberculatus* an adaptive strategy to avoid self-fertilization and increase the chances of producing viable offspring.

In the original description, Litwin et al. (1993) reported the occurrence of *F. traversei* triads, but in the present material only tetrads were documented. The presence of aberrant uneven-sized tetrads among permanent tetrads and the occurrence as triads as well as dyads indicated unreduced 2n pollen in the case of *Classopollis* (Kürschner et al. 2013). The formation of

Table 2

Summary of Morphological and Ultrastructure Features of *Froelichsporites traversei* and Comparison to Potentially Related Groups

Plant groups	Permanent tetrads	Perine/perispore	Granular exine	Exine/exospore layers	Nexine lamellae	Ulcus	Reference
F. traversei	Present	Present	Present	Three	Discontinuous	Present	This study
Andreaopsida, bryophyte	Present	Present	Present	Three	Absent	Absent	Brown and Lemmon 1984
Pteridophytes	Absent	Present	Present	Three	Present	Absent	Tryon and Lugardon 1990
Gnetales	Absent	Absent	Present	Three	Present	Absent	Kurmann 1992; Osborn et al. 1993; Osborn 2000; Tekleva and Krassilov 2009
Bennettitales	Absent	Absent	Present	Two or three	Not always present	Absent	Zavada 1990; Osborn and Taylor 1995; Zavialova et al. 2009
Riccisporites tuberculatus	Present	Absent	Present	Three	Present	Absent	Mander et al. 2012
Cupressaceae	Absent	Present	Present	Three	Present	Present	Kurmann 1992; Doyle 2009
Cheirolepidiaceae	Present	Absent	Absent	Three	Present	Absent	Taylor and Alvin 1984; Zavialova 2003; Zavialova et al. 2010
Crinopollis group	Absent	Absent	Absent	Two	Absent	Absent	Cornet 1989*a*; Doyle and Hotton 1991
Walkeripollis gabonensis	Present	Absent	Absent	Two	Absent	Present	Doyle et al. 1990*a*; Doyle 2009
Sanmiguelia lewisii	Absent	Absent	Present	Absent	Not determined	Absent	Cornet 1989*b*; Friis et al. 2011
Dinophyton	Absent	Absent	Absent	Absent	Absent	Absent	Tekleva 2015

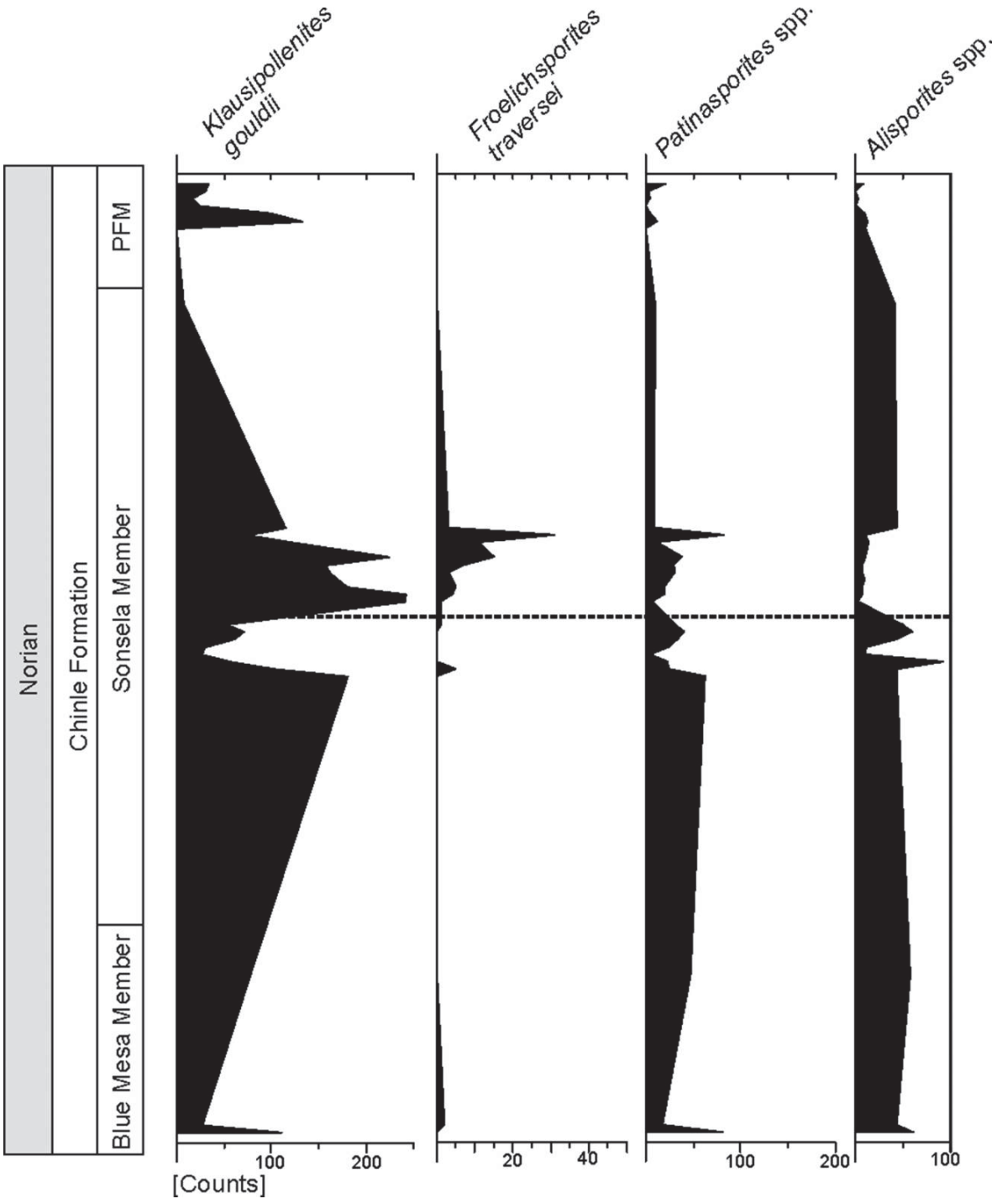

Fig. 8 Simplified pollen diagram with the abundance distribution of *Froelichsporites traversei* and selected ecologically important pollen taxa in the Chinle Formation at the Petrified Forest National Park during the Norian. Dashed line indicates the horizon of the faunal and floral turnover, after Parker and Martz (2011) and Reichgelt et al. (2013).

unreduced 2n pollen is linked to polyploidization among land plants, which frequently results in better adaptation capabilities than the diploid parent plants (Comai 2005). This process is common in flowering plants but a rare phenomenon in extant gymnosperms (Li et al. 2015), with the exception of *Ephedra* (Gnetales), where it can be prevalent (Ahuja 2005).

The distal ulcus is a conspicuous feature of the morphology of *F. traversei*. It might be the germinal aperture. Alternatively, the ulcus might represent a rehydration pore that facilitates the expansion of the pollen grain and exine shedding before pollen grain germination, as observed in the Cupressaceae (Duhoux 1982; Takaso and Owens 2008; Danti et al. 2011). In Cupressaceae, the pollen reaches the pollination drop secreted by the ovule. The pollen is hydrated as water penetrates through the distal pore. The intine swells and the exine sheds, and afterward the expanded pollen grain enters the micropyle and micropylar canal before reaching the nucellus (Takaso and Owens 2008). Ruptures with similar position and orientation to the one recorded in modern Cupressaceae pollen (Duhoux 1982) are also observed in several *F. traversei* specimens (fig. 3*A*, 3*G*), but they might be simply broken specimens, and the ruptures might be related to mechanical degradation.

Paleoenvironmental Significance

Froelichsporites traversei has a long stratigraphic range in the Chinle Formation, where it is present in zones II and III of Litwin et al (1991). Lindström et al. (2016) found it in the topmost part of the Petrified Forest Member in New Mexico (zone III), and it is also present in the Norian successions of the Newark Basin (Cornet 1993; Fowell and Olsen 1993; Fowell et al. 1994).

Its abundance considerably increases after a faunal and floral turnover in the Sonsela Member in the PEFO around 215 Ma (Reichgelt et al. 2013; Baranyi et al. 2017; fig. 8) and at the floral turnover in the upper part of the Petrified Forest Member in New Mexico about 4 million years later (ca. 211.9 Ma ago; Whiteside et al. 2015; Lindström et al. 2016). During both palynofloral turnovers, the high abundance of *F. traversei* is accompanied by an increase in *Klausipollenites* (which is a bisaccate pollen with *Voltzialean* affinity) and the *Patinasporites* group (*Patinasporites* spp., *Enzonalasporites vigens*, *Daughertyspora chinleana*; fig. 8). The pollen grains in the *Patinasporites* group were produced most likely by the Majonicaceae, a group within the Voltziales (Axsmith et al. 1998). They are considered to be indicative of dry paleoclimates (Roghi et al. 2010). Whiteside et al. (2015) explained the abundance of these palynomorphs as a consequence of a shift toward drier climate, harsh environmental conditions, and climatic extremities. Most likely *F. traversei* belonged to a plant group that had greater stress tolerance and thrived in disturbed areas or during arid periods. The unusual morphological features together with the proposed reproductive biology provided most likely adaptive advantages for the parent plant of *F. traversei* that made it successful during the environmental perturbation.

Conclusions

The enigmatic palynomorph *Froelichsporites traversei* from the Norian of North America exhibits a number of peculiar morphological features, such as a distal pore (ulcus) with annulus-like thickening and a simple granular wall ultrastructure with discontinuous nexine lamination. The sporoderm structure suggests that the *F. traversei* pollen grains were most likely mature at dispersal and shed as permanent tetrads. The wall ultrastructure and the palynomorph morphology provided ambiguous results, and the botanical affinity of *F. traversei* could not be determined precisely. The prevailing information suggests that the parent plant was most likely a gymnosperm. Dispersal as permanent tetrads probably provided adaptive advantage of the parent plant of *F. traversei*. The morphological features of *F. traversei* most likely represent a lost pathway of gymnosperm evolution. During the Late Triassic, the morphological variety (e.g., pollen morphology, ultrastructure) of extant plant groups could have been different compared with modern equivalents explaining the extraordinary morphology and ultrastructure of *F. traversei*.

Acknowledgments

V. Baranyi and W. M. Kürschner acknowledge the financial support of the Department of Geosciences, University of Oslo. We are grateful to Johanna H. A. Van Konijnenburg-van Cittert (Utrecht University) and Henk Visscher (Utrecht University) for useful suggestions that improved the manuscript. We thank Margaret Collinson (Royal Holloway University of London) for her advice during an early stage of the research and Wilson A. Taylor (University of Wisconsin) for useful comments. Two anonymous reviewers are thanked for the thorough reviews and constructive comments in order to improve an early version of the manuscript. Chris J. Hill (University of Sheffield) is gratefully thanked for providing training in the embedding procedure and help with the sectioning. Antje Hofgaard (University of Oslo) helped with the sectioning at the Electron Microscopy Laboratory of the University of Oslo.

Literature Cited

Adloff MC, J Doubinger, C Palain 1974 Contribution à la palynologie du Trias et du Lias inférieur du Portugal "Grès de Silves" du Nord du Tage. Comun Serv Geol Port 58:91–143.

Ahuja MR 2005 Polyploidy in gymnosperms. Rev Silvae Genet 54: 59–69.

Ash SR 1972 Late Triassic plants from the Chinle Formation in northeastern Arizona. Palaeontology 15:598–618.

——— 1989 A catalog of Upper Triassic plant megafossils of the western United States through 1988. Pages 189–222 *in* SG Lucas, AP Hunt, eds. Dawn of the age of dinosaurs in the American Southwest. New Mexico Museum of Natural History, Albuquerque.

——— 2005 Synopsis of the Upper Triassic flora of Petrified Forest National Park and vicinity. Pages 53–61 *in* SJ Nesbitt, WG Parker, RB Irmis, eds. Guidebook to the Triassic formations of the Colorado Plateau in northern Arizona: geology, palaeontology and history. Mesa Southwest Museum Bulletin 9.

Audran JC 1981 Pollen and tapetum development in *Ceratozamia mexiana* (Cycadaceae): sporal origin of the exinic sporopollenin in cycads. Rev Palaeobot Palynol 33:315–346.

Axsmith BJ, TN Taylor, ELTaylor 1998 A new fossil conifer from the Triassic of North America: implications for models of ovulate cone scale evolution. Int J Plant Sci 159:358–366.

Baranyi V, T Reichgelt, PE Olsen, WG Parker, WM Kürschner 2017 Norian vegetation history and related environmental changes: new data from the Chinle Formation, Petrified Forest National Park (Arizona, SW USA). Geol Soc Am Bull, doi:10.1130/B31673.1.

Batten DJ 2002 Palynofacies and petroleum potential. Pages 1065–1084 *in* J Jansonius, DC McGregor, eds. Palynology: principles and applications. Vol. 3. American Association of Stratigraphic Palynologists Foundation, Dallas.

Bolinder K 2014 Pollination in *Ephedra* (Gnetales). Licentiate diss. Stockholm University.

Bolinder K, AM Humphreys, J Ehrlén, R Alexandersson, SM Ickert-Bond, C Rydin 2016 From near extinction to diversification by means of a shift in pollination mechanism in the gymnosperm relict *Ephedra* (Ephedraceae, Gnetales). Bot J Linn Soc 180:461–477.

Bolinder K, KJ Niklas, C Rydin 2015 Aerodynamics and pollen ultrastructure in *Ephedra*. Am J Bot 102:457–470.

Bortenschlager S 1990 Aspects of pollen morphology in the Cupressaceae. Grana 29:129–137.

Brown RC, BE Lemmon 1984 Spore wall development in *Andreaea* (Musci: Andreaeopsida). Am J Bot 71:412–420.

Comai L 2005 The advantages and disadvantages of being polyploid. Nature 6:836–846.

Cornet B 1977 The palynostratigraphy and age of the Newark Supergroup. PhD diss. Pennsylvania State University, University Park.

——— 1989*a* Late Triassic angiosperm-like pollen from the Richmond Rift Basin of Virginia, USA. Palaeontogr Abt B 213:37–87.

——— 1989*b* The reproductive morphology and biology of *Sanmiguelia lewisii*, and its bearing on angiosperm evolution in the Late Triassic. Evol Trends Plant 3:1–40.

——— 1993 Applications and limitations of palynology in age, climatic and paleoenvironmental analyses of Triassic sequences in North America. Pages 75–93 *in* SG Lucas, M Morales, eds. The nonmarine Triassic. New Mexico Museum of Natural History and Science Bulletin 3, Albuquerque.

Crane PR 1986 Form and function in wind dispersed pollen. Pages 179–202 *in* S Blackmore S, IK Ferguson, eds. Pollen and spores: form and function. Academic Press, London.

Danti R, G Fella Rocca, R Calamassi, B Mori, M Mariotti Lippi 2011 Insights into a hydration regulating system in *Cupressus* pollen grains. Ann Bot 108:299–306.

Del Fueyo G, S Archangelsky 2005 A new araucarian pollen cone with in situ *Cyclusphaera* Elsik from the Aptian of Patagonia, Argentina. Cretac Res 26:757–768.

Doores AS, JM Osborn, G El-Ghazaly 2007 Pollen ontogeny in *Ephedra americana* (Gnetales). Int J Plant Sci 168:985–997.

Doyle JA 2005 Early evolution of angiosperm pollen as inferred from molecular and morphological phylogenetic analyses. Grana 44:227–251.

——— 2009 Evolutionary significance of granular exine structure in the light of phylogenetic analyses. Rev Palaeobot Palynol 156:198–210.

Doyle JA, CL Hotton 1991 Diversification of early angiosperm pollen in a cladistics content. Pages 169–195 *in* S Blackmore, SH Barnes, eds. Pollen and spores. Clarendon, Oxford.

Doyle JA, CL Hotton, JV Ward 1990*a* Early Cretaceous tetrads, zonasulculate pollen, and Winteraceae. I. Taxonomy, morphology, and ultrastructure. Am J Bot 77:1544–1557.

——— 1990*b* Early Cretaceous tetrads, zonasulculate pollen, and Winteraceae. II. Cladistic analysis and implications. Am J Bot 77:1558–1568.

Duhoux E 1982 Mechanisms of exine rupture in hydrated taxoid type of pollen. Grana 27:1–7.

Dunay RE 1972 The palynology of the Triassic Dockum Group of Texas, and its application to stratigraphic problems of the Dockum Group. PhD diss. Pennsylvania State University.

Dunay RE, MJ Fisher 1979 Palynology of the Dockum group (Upper Triassic), Texas, U.S.A. Rev Palaeobot Palynol 28:61–92.

Edwards D, CH Wellman, L Axe 1999 Tetrads in sporangia and spore masses from the Upper Silurian and Lower Devonian of the Welsh Borderland. Bot J Linn Soc 130:11–155.

Fægri K, L Van der Pijl 1966 The principles of pollination ecology. Pergamon, London.

Fisher MJ, RE Dunay 1984 Palynology of the Petrified Forest member of the Chinle Formation (Upper Triassic), Arizona, U.S.A. Pollen Spores 26:241–284.

Fowell SJ, B Cornet, PE Olsen 1994 Geologically rapid Late Triassic extinctions: palynological evidence from the Newark Supergroup. Geol Soc Am Spec Pap 288:197–206.

Fowell SJ, PE Olsen 1993 Time calibration of Triassic/Jurassic microfloral turnover, eastern North America. Tectonophysics 222:361–369.

Friis EM, PR Crane, KR Pedersen 2011 Early flowers and angiosperm evolution. Cambridge University Press, Cambridge.

Gottesfeld AS 1972 Paleoecology of the lower part of the Chinle Formation. Mus North Ariz Bull 47:59–73.

Graustein JE 1930 Evidence of hybridism in Selaginella. Bot Gaz 90: 46–74.

Gray J, WG Chaloner, TS Westoll 1985 The microfossil record of early land plants: advances in understanding of early terrestrialization, 1970–1984. Philos Trans R Soc B 309:167–195.

Hochuli PA, S Feist-Burkhardt 2013 Angiosperm-like pollen and *Afropollis* from the Middle Triassic (Anisian) of the Germanic Basin (Northern Switzerland). Front Plant Sci 4:344.

Krassilov VA, SR Ash 1988 On Dinophyton–protognetalean Mesozoic plant. Palaeontogr Abt B 208:33–38.

——— 2007 Order Dinophytonales Krassilo and Ash nov. Page 206 *in* JM Anderson, HM Anderson, CJ Cleal, eds. Brief history of the gymnosperms: classification, biodiversity, phytogeography and ecology. Vol 20. South African National Biodiversity Institute, Pretoria.

Kuerschner WM, NR Bonis, L Krystyn 2007 Carbon-isotope stratigraphy and palynostratigraphy of the Triassic–Jurassic transition in the Tiefengraben section—Northern Calcareous Alps (Austria). Palaeogeogr Palaeoclimatol Palaeoecol 244:257–280.

Kurmann MH 1992 Exine stratification in extant gymnosperms: a review of published transmission electron micrographs. Kew Bull 47:25–39.

——— 1994 Pollen morphology and ultrastructure in the Cupressaceae. Acta Bot Gall 141:141–147.

Kürschner WM, SJ Batenburg, L Mander 2013 Aberrant *Classopollis* pollen reveals evidence for unreduced (2n) pollen in the conifer family Cheirolepidiaceae during the Triassic–Jurassic transition. Proc R Soc B 280:20131708.

Kürschner WM, L Mander, JC McElwain 2014 A gymnosperm affinity for *Ricciisporites tuberculatus* Lundblad: implications for vegetation and environmental reconstructions in the Late Triassic. Palaeobiodivers Palaeoenviron 94:295.

Lavender K, CH Wellman 2002 Lower Devonian spore assemblages from the Arbuthnott Group at Canterland Den in the Midland Valley of Scotland. Rev Palaeobot Palynol 118:157–180.

Li Z, AE Baniaga, EB Sessa, M Scascitelli, SW Graham, LH Rieseberg, MS Barker 2015 Early genome duplications in conifers and other seed plants. Sci Adv 1:e1501084.

Lindström S, RB Irmis, JH Whiteside, NS Smith, SJ Nesbitt, AH Turner 2016 Palynology of the upper Chinle Formation in northern New Mexico, U.S.A.: implications for biostratigraphy and terrestrial ecosystem change during the Late Triassic (Norian–Rhaetian). Rev Palaeobot Palynol 225:106–131.

Litwin RJ 1986 The palynostratigraphy and age of the Chinle and Moenave Formations, southwestern U.S.A. PhD diss. Pennsylvania State University, University Park.

Litwin RJ, SR Ash 1993 Revision of the biostratigraphy of the Chatham Group (Upper Triassic), Deep River basin, North Carolina, USA. Rev Palaeobot Palynol 77:75–95.

Litwin RJ, JP Smoot, RE Weems 1993 *Froelichsporites* gen. nov.: a biostratigraphic marker palynomorph of Upper Triassic continental strata in the conterminous U. S. Palynology 17:157–168.

Litwin RJ, A Traverse, SR Ash 1991 Preliminary palynological zonation of the Chinle Formation, southwestern U.S.A., and its correlation to the Newark Supergroup. Rev Palaeobot Palynol 68:269–287.

Looy CV, ME Collinson, JHA Van Konijnenburg-van Cittert, H Visscher, APR Brain 2005 The ultrastructure and botanical affinity of end-Permian spore tetrads. Int J Plant Sci 166:875–887.

Mander L, ME Collinson, WG Chaloner, APR Brain, DG Long 2012 The ultrastructure and botanical affinity of the problematic mid-Mesozoic palynomorph *Ricciisporites tuberculatus* Lundblad. Int J Plant Sci 173:429–440.

Moore PD, JA Webb, ME Collinson 1991 Pollen analysis. Blackwell Scientific, Oxford.

Osborn JM 2000 Pollen morphology and ultrastructure of gymnospermous antophytes. Pages 163–185 *in* MM Harley, CM Morton, S Blackmore, eds. Pollen and spores: morphology and biology. Royal Botanic Gardens, Kew.

Osborn JM, TN Taylor 1994 Comparative ultrastructure of fossil gymnosperm pollen and its phylogenetic implications. Pages 99–121 *in* MH Kurmann, JA Doyle, eds. Ultrastructure of fossil spores and pollen. Royal Botanic Gardens, Kew.

——— 1995 Pollen morphology and ultrastructure of the Bennettitales: in situ pollen of Cycadeoidea. Am J Bot 82:1074–1081.

Osborn JM, TH Taylor, MR de Lima 1993 The ultrastructure of fossil ephedroid pollen with gnetalean affinities from the Lower Cretaceous of Brazil. Rev Palaeobot Palynol 77:171–184.

Pacini E, GG Franchi 1996 Some cytological, ecological and evolutionary aspects of pollination. Acta Soc Bot Pol 65:11–16.

Parker WG, JW Martz 2011 The Late Triassic (Norian) Adamanian-Revueltian tetrapod faunal transition in the Chinle Formation of Petrified Forest National Park, Arizona. Earth Environ Sci Trans R Soc Edinb 101:231–260.

Reichgelt T, WG Parker, JW Martz, JC Conran, JHA Van Konijnenburg-van Cittert, WM Kürschner 2013 The palynology of the Sonsela member (Late Triassic, Norian) at Petrified Forest National Park, Arizona, USA. Rev Palaeobot Palynol 89:18–28.

Robbins EI, GP Wilkes, DA Textoris 1988 Coal deposits of the Newark rift system. Pages 649–682 *in* W Manspeizer, ed. Triassic-Jurassic rifting: North America and North Africa. Elsevier, Amsterdam.

Roghi G, P Gianolla, L Minarelli, C Pilati, N Preto 2010 Palynological correlation of Carnian humid pulses throughout western Tethys. Palaeogeogr Palaeoclimatol Palaeoecol 290:89–106.

Shukla AK, MR Vijayaraghavan, B Chaudhry 1998 Biology of pollen. 1st ed. APH, New Delhi.

Sporne KR 1974 The morphology of gymnosperms. 2nd ed. Hutchinson, London.

Takaso T, JN Owens 2008 Significance of exine shedding in Cupressaceae-type pollen. J Plant Res 121:83–85.

Taylor TN, KL Alvin 1984 Ultrastructure and development of Mesozoic pollen: *Classopollis*. Am J Bot 71:575–587.

Taylor TN, MS Zavada, S Archangelsky 1987 The ultrastructure of *Cyclusphaera psilata* from the Cretaceous of Argentina. Grana 26: 74–80.

Tekleva MV 2015 Bisaccate pollen of probable Gnetalean species and pollen diversity in Gnetophytes. Botanica Pacifica 4:117–126.

Tekleva MV, VA Krassilov 2009 Comparative pollen morphology and ultrastructure of modern and fossil gnetophytes. Rev Palaeobot Palynol 156:130–138.

Traverse A 1987 Pollen and spores date origin of rift basins from Texas to Nova Scotia as early Late Triassic. Science 236:1469–1471.

Trendell AM, SC Atchley, LC Nordt 2013 Facies analysis of probable large-fluvial-fan depositional system: the Upper Triassic Chinle Formation at Petrified Forest National Park, Arizona, U.S.A. J Sediment Res 83:873–895.

Tryon AF, B Lugardon 1990 Spores of the Pteridophyta. Springer, New York.

Visscher H, CV Looy, ME Collinson, H Brinkhuis, JHA Van Konijnenburg-van Cittert, WM Kürschner, M Sephton 2004 Environmental mutagenesis during the end-Permian ecological crisis. Proc Natl Acad Sci USA 101:12952–12956.

Webber JM 1940 Polyembryony. Bot Rev 6:575–598.

Whiteside JH, S Lindström, RB Irmis, IJ Glasspool, MF Schaller, M Dunlavey, SJ Nesbitt, ND Smith, AH Turner 2015 Extreme ecosystem instability suppressed tropical dinosaur dominance for 30 million years. Proc Natl Acad Sci USA 112:7909–7913.

Williams CG 2007 Re-thinking the embryo lethal system within the Pinaceae. Can J Bot 85:667–677.

Zavada MS 1990 The ultrastructure of three monosulcate pollen grains from the Triassic Chinle Formation, Western United States. Palynology 14:41–51.

Zavialova NE 2003 On the ultrastructure of *Classopollis* exine: a tetrad from the Jurassic of Siberia. Acta Palaeontol Sin 42:1–7.

Zavialova N, B Buratti, G Roghi 2010 The ultrastructure of some Rhaetian Circumpolles from southern England. Grana 49:281–299.

Zavialova NE, G Roghi 2005 Exine morphology and ultrastructure of *Duplicisporites* from the Triassic of Italy. Grana 44:337–342.

Zavialova N, JHA Van Konijnenburg-van Cittert, M Zavada 2009 The pollen ultrastructure of *Williamsoniella coronata* Thomas (Bennettitales) from the Bajocian of Yorkshire. Int J Plant Sci 171:1195–1200.

Supplements